

**THE PURIFICATION AND CHARACTERISATION OF A  
MUTANT FORM OF PYRUVATE KINASE FROM  
*SACCHAROMYCES CEREVISIAE* PRODUCED  
BY SITE-DIRECTED MUTAGENESIS**

**RICHARD A. COLLINS**

BSc (Hons), MSc, CChem.MRSC

THESIS PRESENTED FOR THE DEGREE OF DOCTOR OF PHILOSOPHY  
UNIVERSITY OF EDINBURGH  
1993



## DECLARATION

I HEREBY DECLARE THAT THIS THESIS HAS BEEN COMPOSED BY ME, THAT IT HAS NOT BEEN ACCEPTED IN ANY PREVIOUS APPLICATION FOR A DEGREE, AND THAT THE WORK OF WHICH IT IS A RECORD HAS BEEN CARRIED OUT BY ME.

RICHARD A. COLLINS



## ACKNOWLEDGEMENTS

I would like to thank my supervisors Dr. L. A. Fothergill-Gilmore and Dr. I. R. Bowman for advice and encouragement. I would also like to thank various colleagues who have provided help and useful discussions throughout the course of this project, particularly Dr. Malcolm White, Dr. Fiona Stuart, Dr. Gary Paterson, Dr. Jacqueline Nairn and Dr. Teresa McNally. I would also like to thank Dr. Simon Potter, Daniel Rigden, Nantana Fugtong, Rebecca Walter and Thalles Rocha for friendship and support.

Particular thanks to Gillian Smith at the Student Advice Place, Professor C. Edwards and Professor A. Miller. The author was in receipt of a William Thynne Centenary Fellowship Award and is grateful to the family and trustees for financial assistance.

I would like to thank Douglas Lamont, Shona Cunningham and Stella Bury for technical assistance. Thanks are due to Prof. W. C. Plaxton, Dr. S. Blakeley and Dr. P. Michels for supplying me with the DNA and protein sequences of several plant, bacterial and protozoa pyruvate kinases and allowing me to use them ahead of publication. Sequence analysis and construction of phylogenetic trees was performed by I. Ernest at the International Institute of Cellular and Molecular Pathology, Research Unit of Tropical Disease, Brussels, Belgium. CD spectroscopy facilities were provided by Dr. N. C. Price and S. M. Kelly at the University of Stirling. I would like to express my thanks to members of other labs who have helped me with various aspects of my project particularly Dr. A. Boyd and Dr. N. Bryant, Dr. D. Apps and Dr. A. Ryle and Prof. Al. Matheson.

I would like to thank Kay Bowles and Katrina Pfahlsberger for their friendship in troubled times.

To my parents whose love and hard cash has kept me going-words are not enough.

## TABLE OF ABBREVIATIONS AND SYMBOLS

A	absorbance
Ab	antibody
ADP	adenosine 5'-diphosphate
Ag	antigen
Ap	ampicillin
ATP	adenosine 5'-triphosphate
bis	N, N'-methylenebisacrylamide
bp	base pairs
BSA	bovine serum albumin
c	centi ( $10^{-2}$ )
°C	degree Celsius
Da	Dalton
DEAE	diethylaminoethyl
dH <sub>2</sub> O	distilled water
DMSO	dimethylsulphoxide
ds	double-stranded
DTNB	5,5'-dithiobis (2-nitrobenzoic acid)
DTT	dithiothreitol
E64	trans-epoxysuccinyl-L-leucylamido-(4-guanido)-butane
EC	Enzyme Commission number
EDTA	ethylenediaminetetraacetic acid
<i>E.coli</i>	<i>Escherichia coli</i>
EtBr	ethidium bromide
Fru-1,6-P <sub>2</sub> / FBP	fructose-1,6-bisphosphate
Fru-2,6-P <sub>2</sub>	fructose-2,6-bisphosphate
g	gramme
<i>g</i>	gravitational force
HPLC	high performance (pressure) liquid chromatography
HRP	horseradish peroxidase
hr	hour
id	internal diameter
IgG	immunoglobulin G
$k_{cat}$	catalytic constant ( $s^{-1}$ )
K <sub>m</sub>	kanamycin
K <sub>M</sub>	Michaelis constant
k	kilo ( $10^3$ )
l	litre
LB	Luria-Bertani media

$\mu$	micro ( $10^{-6}$ )
m	milli ( $10^{-3}$ ), metre
M	molar ( $\text{mol l}^{-1}$ )
MES	2-[N-morpholino] ethanesulphonic acid
MES-TPA	buffered mixture of MES and TPA
min(s)	minute(s)
mol	amount of substance
$M_r$	relative molecular mass
n	nano ( $10^{-9}$ )
$n_H$	Hill coefficient
$\text{NAD}^+$	$\beta$ -nicotinamide adenine dinucleotide (oxidized)
NADH	$\beta$ -nicotinamide adenine dinucleotide (reduced)
NEM	N-ethylmaleimide
OD	optical density
PCR	polymerase chain reaction
PEG	polyethylene glycol
PEP	phosphoenolpyruvate
$\text{PK}_r$	rabbit muscle pyruvate kinase
PMSF	phenylmethylsulphonyl fluoride
p	pico ( $10^{-12}$ )
rpm	revolutions per minute
S384P	serine 384 mutated to proline
SDS	sodium dodecyl sulphate
SDS-PAGE	polyacrylamide gel electrophoresis in the presence of sodium dodecyl sulphate
SDW	sterile distilled water
$S_{0.5}$	substrate concentration at half-maximal velocity
<i>S.cerevisiae</i>	<i>Saccharomyces cerevisiae</i>
sec(s)	second(s)
ss	single-stranded
SSC	NaCl-sodium citrate
TBE	Tris-borate-EDTA
TBS	Tris -buffered saline
TE	Tris-EDTA
TEMED	N, N, N', N'-tetramethylethylenediamine
TPA	Tetrapropylammonium hydroxide
Tris	Tris[hydroxymethyl] aminomethane
Tween 20	polyoxyethylenesorbitan monolaurate
v	initial velocity

Ve	elution volume
V <sub>m</sub>	maximal velocity
v/v	volume in volume
w/v	weight in volume
WT	wild type

## AMINO ACIDS

NAME	3-letter abbreviation	Single letter abbreviation
Alanine	Ala	A
Asparate	Asp	D
Asparagine	Asn	N
Arginine	Arg	R
Cysteine	Cys	C
Glycine	Gly	G
Glutamine	Gln	E
Glutamate	Glu	Q
Histidine	His	H
Isoleucine	Ile	I
Leucine	Leu	L
Lysine	Lys	K
Methionine	Met	M
Phenylalanine	Phe	F
Proline	Pro	P
Serine	Ser	S
Threonine	Thr	T
Tryptophan	Trp	W
Tyrosine	Tyr	Y
Valine	Val	V

## LIST OF FIGURES

Fig.1	Number of references to pyruvate kinase versus year of publication
Fig.2	Cat muscle pyruvate kinase tetramer
Fig.3	Domain structure of the cat muscle pyruvate kinase subunit
Fig.4	Schematic illustration of pyruvate kinase active site
Fig.5	Hypothetical active site ternary complexes
Fig.6	Formation of binary complex in the pyruvate kinase reaction
Fig.7	Postulated ternary complexes in the pyruvate kinase reaction
Fig.8	Mechanism of conversion of substrate complex to product complex in the pyruvate kinase reaction
Fig.9	Comparison of primary and secondary reactions of pyruvate kinase
Fig.10	Schematic drawing of the rabbit muscle enzyme active site
Fig.11	Pyruvate kinase reaction mechanism as determined from X-ray crystallographic work
Fig.12	Schematic presentation of the functional thiol groups of one subunit of pyruvate kinase
Fig.13	Ternary complexes in the rabbit muscle enzyme active site determined from NMR data
Fig. 14	Conformational states of <i>E.coli</i> pyruvate kinase
Fig.15A	Hyperbolic and sigmoidal substrate saturation curves
Fig.15B	Typical Hill plot
Fig.16	Rabin's model to explain substrate cooperativity
Fig.17	Change in hexokinase tertiary structure upon substrate binding
Fig.18	Difference in conformation of phosphofructokinase R and T states
Fig.19	Schematic representation of expression of the pyruvate kinase L gene
Fig.20	Schematic representation of expression of the pyruvate kinase M gene
Fig.21	<i>S.cerevisiae</i> chromosome 1 showing location of <i>PYK1</i>
Fig.22	<i>PYK1</i> upstream and downstream regulatory signals
Fig.23	Occurrence of amino acids in proteins of known sequence
Fig.24	Plasmid maps of pAYE434 and pK19pyk
Fig.25	Plasmid maps of pPYK20 and pMA91pyk
Fig.26	Removal of plasmid DNA from CsCl gradient
Fig.27	Growth of parental and transformed yeast cells
Fig.28	Growth of <i>pyk1::ura3</i> on different carbon sources
Fig.29	Morphology of parent and transformed yeast analysed by EM
Fig.30	Effect of KCN on growth of parent and transformed yeast
Fig.31	Intracellular Fru-1,6-P <sub>2</sub> levels in parent and transformed yeast
Fig.32	HPLC chromatogram of CNBr digest products
Fig.33	Calibration chromatogram of derivatised amino acid residues and by-products

Fig.34	Chromatogram produced following first cycle of Edman degradation
Fig.35	Comparison of most prominent peptide with sequence database
Fig.36	DNA amplification strategy
Fig.37	Secondary structure analysis of oligonucleotide primers
Fig.38	LDMS chromatogram of oligonucleotide primers
Fig.39	Amplification of PYK1 DNA by PCR
Fig.40	Calibration curve of DNA markers
Fig.41	HPLC chromatogram of PCR product
Fig.42	LDMS chromatogram of PCR product
Fig.43	DNA sequence of wild type and S384P mutant
Fig.44	Chromatogram of wild type and S384P mutant pyruvate kinase from Sephacryl S200 column
Fig.45	Chromatogram of wild type and S384P mutant pyruvate kinase from ion-exchange column
Fig.46	Purification of wild type pyruvate kinase
Fig.47	Rate of reaction versus enzyme concentration
Fig.48	Effect of Fru-1,6-P <sub>2</sub> on wild type and S384P mutant pyruvate kinase
Fig.49	Rate of reaction versus [PEP] for wild type and S384P mutant pyruvate kinase
Fig.50	Hill plot of data produced in Fig.49
Fig.51	Rate of reaction versus [ADP] for wild type and S384P mutant pyruvate kinase
Fig.52	Hill plot of data produced in Fig.51
Fig.53	Rate of reaction versus [KCl] for wild type and S384P mutant pyruvate kinase
Fig.54	Hill plot of data produced in Fig.53
Fig.55	Monovalent cation specificity of wild type and S384P mutant pyruvate kinase
Fig.56	Divalent cation specificity of wild type and S384P mutant pyruvate kinase
Fig.57	Effect of monovalent and divalent cations on lactate dehydrogenase
Fig.58	pH curve for wild type and S384P mutant pyruvate kinase
Fig.59	Effect of 5mM PEP on the fluorescence emission spectra of wild type and S384P mutant pyruvate kinase
Fig.60	Effect of 2mM ADP on the fluorescence emission spectra of wild type and S384P mutant pyruvate kinase
Fig.61	Effect of Fru-1,6-P <sub>2</sub> on the fluorescence emission spectra of wild type and S384P mutant pyruvate kinase
Fig.62	Far uv CD spectra of wild type and S384P mutant pyruvate kinase
Fig.63	Effect of 5mM PEP on the far uv CD spectrum of wild type pyruvate kinase

Fig.64	Effect of 2mM ADP on the far uv CD spectrum of wild type pyruvate kinase
Fig.65	Effect of 1mM Fru-1,6-P <sub>2</sub> on the far uv CD spectrum of wild type pyruvate kinase
Fig.66	Effect of 5mM PEP on the far uv CD spectrum of S384P mutant pyruvate kinase
Fig.67	Effect of 2mM ADP on the far uv CD spectrum of S384P mutant pyruvate kinase
Fig.68	Effect of 1mM Fru-1,6-P <sub>2</sub> on the far uv CD spectrum of S384P mutant pyruvate kinase
Fig.69	Effect of ligands on the susceptibility of wild type pyruvate kinase to trypsin digestion
Fig.70	Effect of ligands on the susceptibility of S384P mutant pyruvate kinase to trypsin digestion
Fig.71	Effect of ligands on the susceptibility of wild type pyruvate kinase to inhibition by NEM
Fig.72	Effect of ligands on the susceptibility of S384P mutant pyruvate kinase to inhibition by NEM
Fig.73	Thermal denaturation of wild type, S384P mutant and rabbit muscle pyruvate kinase
Fig.74	Effect of temperature on the absorbance at 280nm of wild type pyruvate kinase in the presence and absence of Fru-1,6-P <sub>2</sub>
Fig.75	Western blot
Fig.76	Immunotitration of wild type pyruvate kinase
Fig.77	PEPLOT of wild type pyruvate kinase
Fig.78	PEPLOT of S384P mutant pyruvate kinase
Fig.79	PLOTSTRUCTURE of wild type pyruvate kinase
Fig.80	PLOTSTRUCTURE of S384P mutant pyruvate kinase
Fig.81	PREDICT plot of wild type pyruvate kinase
Fig.82	PREDICT plot of S384P mutant pyruvate kinase
Fig.83	Phylogenetic tree constructed by the program FITCH
Fig.84	Consensus phylogenetic tree constructed after bootstrap analysis
Fig.85	Location of trypsin cleavage sites in pyruvate kinase subunit
Fig.86	Location of cysteine residues in pyruvate kinase subunit

## LIST OF TABLES/SCHEMES

TABLE 1	Primary sequence alignment of all known pyruvate kinases sequenced to date
TABLE 2	Primary sequence alignment of yeast and vertebrate helices C $\alpha$ 1, C $\alpha$ 2 and putative effector binding sites
TABLE 3	Cooperativity between substrates and effectors in <i>S.cerevisiae</i> pyruvate kinase
TABLE 4	Theoretical CNBr fragments from pyruvate kinase
TABLE 5	Yield of PTH-derivatised amino acids after each cycle of Edman degradation
TABLE 6	Peptide sequences detected following Edman degradation
TABLE 7	Properties of oligonucleotide primers 961Y and 962Y
TABLE 8	Purification of wild type pyruvate kinase
TABLE 9	Purification of S384P mutant pyruvate kinase
TABLE 10	Kinetic parameters of wild type and S384P mutant pyruvate kinase determined by enzyme assay
TABLE 11	Binding parameters of wild type and S384P mutant pyruvate kinase determined by fluorimetry
TABLE 12	Secondary structure content of wild type, S384P mutant and cat muscle pyruvate kinase
TABLE 13	Effect of ligands on the susceptibility of wild type and S384P mutant pyruvate kinases to trypsin digestion
TABLE 14	Effect of ligands on the susceptibility of wild type and S384P mutant pyruvate kinase to inhibition by NEM
TABLE 15	Immunisation protocol
TABLE 16	Percentage identities between pyruvate kinase sequences
TABLE 17	Previous pyruvate kinase assay conditions
TABLE 18	Alignment of plant pyruvate kinase N-termini sequences

SCHEME 1 Alternative glucose metabolism pathways in yeast

SCHEME 2 Pyruvate kinase purification protocol



## **CONTENTS**

### **1.0 INTRODUCTION**

### **PAGE**

1.1	Importance of pyruvate kinase.	1
1.2	Importance of phosphoenolpyruvate and pyruvate.	11
1.3	A comparison of yeast and vertebrate pyruvate kinases.	13
1.4	The reaction mechanism.	19
1.5	The active site.	36
1.6	Substrate specificity.	47
1.7	The divalent cation.	48
1.8	The monovalent cation.	50
1.9	Binding of fructose-1,6-bisphosphate.	52
1.10	Conformational changes in pyruvate kinase.	54
1.11	Allostery.	67
1.12	Cooperativity in pyruvate kinase.	77
1.13	Allostery and conformational changes in the glycolytic pathway.	86
1.14	Isoenzymes of pyruvate kinase.	93
1.15	Gene structure of pyruvate kinase.	103
1.16	Cloning and overexpression strategy.	109
1.17	Aims of the project.	113

### **2.0 MATERIALS AND METHODS**

2.1	Materials.	115
2.2	Plasmids and strains.	115
2.3	Pyruvate kinase assay.	116
2.4	Measuring intracellular metabolites.	118
2.5	Protein determination.	119
2.6	Purification of pyruvate kinase.	120
2.7	Confirmation of homogeneity.	123
2.8	Western blotting/immunodiffusion/immunotitration.	126
2.9	Immunisation.	130
2.10	DNA purification.	132
2.11	Bacterial transformation.	138
2.12	Yeast transformation.	140
2.13	Growth and maintenance of yeast strains.	142
2.14	Plotting a growth curve.	143
2.15	Plasmid rescue.	144
2.16	Restriction enzyme digest.	145
2.17	Agarose gel electrophoresis.	145
2.18	Southern blotting.	146
2.19	Sequencing of DNA.	151
2.20	Fluorescence measurements.	158

2.21	Protein sequencing.	159
2.22	Electron microscopy.	160
2.23	Alignment and phylogenetic analysis of pyruvate kinase sequences.	162

### 3.0 RESULTS

3.1	Morphological and biochemical studies on the parent and transformed yeast cells.	164
3.2	Peptide sequencing.	171
3.3	DNA sequencing.	180
3.4	Purification and kinetic characterisation of the wild type and mutant pyruvate kinases.	190
3.5	Fluorescence and CD spectroscopic studies.	211
3.6	Trypsin digestion studies.	223
3.7	NEM inhibition studies.	223
3.8	Thermal stability studies.	230
3.9	Antibody studies.	233
3.10	Computer prediction studies of the secondary structure of the wild type and mutant enzymes.	237
3.11	Alignment and phylogenetic analysis of pyruvate kinase sequences.	244

### 4.0 DISCUSSION

4.1	Purification of pyruvate kinase.	250
4.2	Enzyme assay conditions.	258
4.3	Morphological and biochemical studies of the parent and transformed cells.	264
4.4	Peptide sequencing.	267
4.5	DNA sequencing.	269
4.6	Purification and kinetic characterisation of the wild type and mutant enzymes.	272
4.7	Fluorescence and CD studies.	281
4.8	Trypsin digestion of wild type and mutant enzymes.	296
4.9	The effect of NEM on pyruvate kinase activity.	301
4.10	Thermal stability studies.	306
4.11	Antibody studies.	310
4.12	Computer predictions of secondary structure.	313
4.13	Sequence comparison of pyruvate kinases.	317
4.14	Alignment and phylogenetic analysis of pyruvate kinase sequences.	326

<b>5.0</b>	<b>CONCLUSIONS</b>	<b>329</b>
<b>6.0</b>	<b>REFERENCES</b>	<b>333</b>
<b>7.0</b>	<b>PUBLICATIONS</b>	<b>344</b>

## ABSTRACT

A variant form of the glycolytic enzyme pyruvate kinase (E.C 2.7.1.40) in which the serine residue at position 384 of the polypeptide chain has been mutated to proline has been overexpressed in the yeast *Saccharomyces cerevisiae*. The mutant protein has been purified to homogeneity and has been characterised by a number of physical, kinetic and chemical techniques. The properties of the mutant enzyme have been compared to those of the native wild type enzyme overexpressed from the same organism. The wild type enzyme is activated by the allosteric effector fructose-1,6-bisphosphate. The mutant enzyme was found to be dependent upon the presence of this effector for catalytic activity and was inactive in its absence. The mutant enzyme became 50% activated at  $1.9 \pm 0.1 \text{ mM Fru-1,6-P}_2$ . In the absence of the effector the  $k_{\text{cat}}$  of the mutant enzyme was reduced by a factor of 250. The fully activated mutant enzyme had a  $k_{\text{cat}}$  68% of that of the wild type enzyme. The mutation introduced into the enzyme was proposed to be at a site critical for the transfer of the allosteric effect across the enzyme upon effector binding. This hypothesis is demonstrated to be correct, and can be extended to invoke additional conformational changes at the active site, as the mutant enzyme displayed different kinetic properties to the wild type enzyme in the presence of the allosteric effector fructose-1,6-bisphosphate. The  $S_{0.5\text{PEP}}$  and  $S_{0.5\text{ADP}}$  of the wild type enzyme were 0.15mM and 0.39mM respectively. In the mutant enzyme, these kinetic parameters increased to 0.69 and 0.94mM respectively. The cooperativity between binding sites also increased significantly in the mutant enzyme. The mutant also displayed altered monovalent and divalent cation specificities and an altered pH profile in the presence and absence of saturating concentrations of effector. In the presence of effector, the mutant enzyme had a narrower pH profile than the wild type enzyme although both enzymes displayed maximal activity at pH 6.5.

The conformations of the mutant and wild type enzymes were examined by circular dichroism (CD) spectroscopy and fluorimetry in the presence and absence of a number of ligands. The secondary structure of the mutant appeared to be little different from that of the wild type enzyme indicating that they both

adopt the same overall conformation in solution. The addition of substrates and effectors did not alter the CD spectrum of either enzyme. The tertiary and quaternary structures of the wild type and mutant enzymes appear to be significantly different when thermostability, tryptophan fluorescence, susceptibility to trypsin digestion and thiol group reactivity were examined.

An improved purification procedure has been devised that allows large quantities of enzyme to be prepared rapidly. The enzyme produced in this manner is essentially homogeneous, as analysed by SDS-PAGE, and free from contaminating proteins. The enzyme is produced in a high yield and exhibits a specific activity comparable to recent, more laborious, techniques. The reproducibility of the improved protocol was maintained throughout the duration of the project.

The amino acid sequences of 31 pyruvate kinases from a number of organisms have been collected and compared. This represents the most comprehensive set of sequences yet analysed and provides interesting data on residues essential for catalysis and regulation. Likely targets for future mutagenesis experiments can be identified. Available secondary structure prediction programs have been used to compare the predicted structure of the wild type and mutant enzymes and to reconcile the different properties of the enzymes observed during the various studies undertaken throughout this project.

## **1.0 INTRODUCTION**

### **1.1 THE IMPORTANCE OF PYRUVATE KINASE**

Pyruvate kinase is ubiquitous to all living organisms yet studied from the Archeae to higher eukaryotes. Its expression is regulated according to tissue type and cellular requirements by a variety of means. The enzyme activity can also be regulated in a variety of ways from phosphorylation/dephosphorylation, allosteric interactions and by association/dissociation of subunits. Its overexpression has been detected in carcinomas from a variety of tissue types indicating that it may have a primary role in other cellular functions such as cell division and tumorigenesis. Further investigation may determine whether pyruvate kinase expression in this situation is diagnostically useful.

An indication of the importance of pyruvate kinase can be obtained by examining the number of nucleotide and protein sequences available and the variety of their sources. As can be seen from Table 1, thirty-one complete protein sequences are known (four bacterial, five fungal, three trypanosomal, nine plant and ten vertebrate), making pyruvate kinase one of the most studied enzymes.

A further indicator of the importance of pyruvate kinase in an active research environment can be determined from a database search of the number of research publications in which pyruvate kinase is mentioned (Fig 1). As can be seen, the number of publications has remained consistently high over the past decade, indicating that study of the enzyme is still yielding important information on all aspects of its biochemistry.

Yeast pyruvate kinase can be considered as a model enzyme for studying allosteric interactions in eukaryotes. Its nucleotide and protein sequence are known. Its three-dimensional structure has been interpolated, by computer analysis, by superimposing its polypeptide chain on to the coordinates of the cat muscle enzyme which were determined by X-ray crystallography (Clayden, 1987; Murcott, 1990). From detailed analysis of these structures, important residues involved in both catalysis and intersubunit communication can be inferred. The growing application of molecular biological techniques to protein structure-function problems can be used to test these inferences. This is the basis of the work described in this thesis.



castA		SQ	SLHFSPLNLT	AKQPFPKLPL	PFPTNSRYP	VNNYKSLSIK
tobacA	SQALNFFVSS	SSRSPATFTI	SRPSVFPSTG	SLRLLVKKSL	RTLVEASSA	
brasG		LSP	NGGSASTRSD	KFLKPASFRV	KVLGNEAKKS	
tobacG			ATMNLPTGLH	VAAKPASLNR	L...SSAKNV	
ratR				MSVQENTLPQ	QLMPWIFRSQ	
humanR				MSIQENISSL	QLRSWVSKSQ	

castA	ASTSPSSSSD	PQVLVADNGT	GN..SGVLYN	NNKSVTVSD	PSSIEVDAVT	aaaaa
castB				AVVVKD	.....L	
tobacA	AASDLDEPQS	SPVLVSENGS	GGVLSSATQE	YGRNAAPGTD	SSSIEVDVT	
brasG	GRVSVRGGR.	..KVDTTVRS	ARVET.EVIP	VSP*DVPNRE	EQLERFLEMQ	
tobacG	QDLFFSDSRH	RKRVTNSNQI	MAVQSLEHIH	GVNNVYANY	VNFNVPSSGY	
bras1					SN	
bras2					SN	
potat					MAN	
tobacc					A	
asnig				MAASSS	LDHLSNRMKL	
asnid				MAASSS	LDHLSNRMKL	
trire			MSQIS	RTQSIMATTA	QEHLETGGRI	
Scere					SRL(3)	
yarli				MIY	TANSSPSTNL	
tryb1					MSQ..L	
tryb2					MSQ..L	
leish					MSQ..L	
ratL		MEGPAGYLR	RASVAQLTQE	LGTAFFQQQQ	LPAAMADTFL	
ratR	KDLAKSALSG	APGGPAGYLR	RASVAQLTQE	LGTAFFQQQQ	LPAAMADTFL	
humanL		MEGPAGYLR	RASVAQLTQE	LGTAFFQQQQ	LPAAMADTFL	
humanR	RDLAKSILIG	APGGPAGYLR	RASVAQLTQE	LGTAFFQQQQ	LPAAMADTFL	
humanM1			SKPHSE	AGTAFIQTOQ	LHAAMADTFL	
humanM2			SKPHSE	AGTAFIQTOQ	LHAAMADTFL	
catM1			SKPHSD	VGTAFIQTQQ	LHAAMADTFL	(26)
ratM1			PKPDSE	AGTAFIQTOQ	LHAAMADTFL	
ratM2			PKPDSE	AGTAFIQTOQ	LHAAMADTFL	
chickM1			SKHHD	AGTAFIQTOQ	LHAAMADTFL	

aaa	bb	bbbbbb			
castA	ETELKENGFR	ST...RRTK	LVCTIGPAT.	.....	.....
castB	EEAVRVVLA	VL...RDME	VVVVLVTAV.	.....	.....
tobacA	EAELKENGFR	ST...RRTK	LICTIGPAT.	.....	.....
brasG	KFSDTSVEMW	SKPTVRRKTK	IVCTVGPST.	.....	.....
tobacG	SLGQESVYLN	S....PRKTK	IVCTIGPST.	.....	.....
ecoli	.....	....MKRKT	IVCTIGPKTE	.....	.....
bacste	.....	....MKRKT	IVCTIGPASE	.....	.....
lactolac	.....	....MNKRVK	IVSTLGPAVE	IRGGKKFGES	GYWGESLDVE
bras1	IDIEGILKEL	PNDGRIPKTK	IVCTLGPASR	.....	.....
bras2	IDIEGILKEL	PNDGRTPKTK	IVCTLGPASR	.....	.....
potat	IDIAGIMKDL	PNDGRIPKTK	IVCTLGPSSR	.....	.....
tobacc	IENNNINGVNF	CTVKR.PKTK	IVCTLGPASR	.....	.....
asnig	EWHSKLNTEM	VPSKNFRRTS	IIGTIGPKTN	.....	.....
asnid	EWHSKLNTEM	VPAKNFRRTS	IICTIGPKTN	.....	.....
trire	NWLASLNTAF	TPARNFRRTS	IICTIGPKTN	.....	.....
Scere	ERLTSLN..V	VAGSDLRRTS	IIGTIGPKTN	.....	.....
yarli	QGPSTLNTDD	IPTKNYRKSS	IIGTI.....	.....	.....
tryb1	EHNIGLSIFE	PVAKH.RANR	IVCTIGPSTQ	.....	.....
tryb2	EHNIGLSIFE	PVAKH.RANR	IVCTIGPSTQ	.....	.....
leish	AHNLTLSIFD	PVANY.RAAR	IICTIGPSTQ	.....	.....
ratL	EHLCLLDIDS	QPVA..RSTS	IIATIGPASR	.....	.....
ratR	EHLCLLDIDS	QPVA..RSTS	IIATIGPASR	.....	.....
humanL	EHLCLLDIDS	EPVA..RSTS	IIATIGPASR	.....	.....
humanR	EHLCLLDIDS	EPVA..RSTS	IIATIGPASR	.....	.....
humanM1	EHMCRLDIDS	PPITA.RNTG	IICTIGPASR	.....	.....
humanM2	EHMCRLDIDS	PPITA.RNTG	IICTIGPASR	.....	.....
catM1	EHMCRLDIDS	PPITA.RNTG	IICTIGPASR	.....	.....
ratM1	EHMCRLDIDS	APITA.RNTG	IICTIGPASR	.....	.....
ratM2	EHMCRLDIDS	APITA.RNTG	IICTIGPASR	.....	.....
chickM1	EHMCRLDIDS	EPTIA.RNTG	IICTIGPASR	.....	.....
ecoliI	.....	..SRRLRRTK	IVTTLGPATD	RD.....	.....



	aaaaaaaa	aaa	bbbbbb	b	aaaaa	aaaaaaaaaaaa	aaaaa
castA	CGFEELEALA	VGGMNVARIN	MCHGTREWHK	SVIERVRLN	EE.KGF	....	
castB	MG.....V	VGDMNVARIN	MCHGTREWHK	SVIERVRLN	EE.KGF	....	
tobacA	CGFEQLERLA	EGGMNVARIN	MCHGTREWHK	MVIERLRLN	EE.KGF	....	
brasG	NTREMIWKVA	EAGMNVARMN	MSHGDHASHK	KVIDLVKEYN	AQSKDN	....	
tobacG	SSREMIWKLA	EAGMNVARLN	MSHGDHASHQ	RTIDLVKEYN	AQFEDK	....	
ecolI	.SEEMLAKML	DAGMNVMLN	FSHGDYAEHG	QRIQNLRLNM	SKTG	....	
bacste	.SVDKLVQLM	EAGMNVARLN	FSHGDHEEHG	RRIANIREAA	KRTG	....	
lactolac	ASAKNIAALI	EEGANVFRFN	FSHGDHPEQG	ARMATVHRAE	EIAG	....	
bras1	.TVPMIEKLL	RAGMNVARFN	FSHGSHEYHQ	DTLNNLRAM	QNTGILA	....	
bras2	.SVPMIEKLL	KAGMNVARFN	FSHGSHEYHQ	ETLDNLRAAM	QNTGILA	....	
potat	.TVPMLEKLL	RAGMNVARFN	FSHGTHEYHQ	ETLDNLKIAM	QNTQILC	....	
tobacc	.SVPMIEKLL	RAGMNVARFN	FSHGSHDYHQ	ETIDNLQAM	ESTGILC	....	
asnig	.SVEKINSLR	TAGLNVVRMN	FSHGSYEYHQ	SVIDNAREAA	KTOVG	....	
asnid	.SVEKINALR	RAGLNVVRMN	FSHGSYEYHQ	SVIDHAREAE	KQAAG	....	
trire	.SVEALNKLK	DAGLNVARMN	FSHGSYEYHQ	SVIDNVRASV	AAHPG	....	
Scere	.NPETLVALR	KAGLNVVRMN	FSHGSYEYHK	SVIDNARKSE	ELYPG	.... (75)	
yarli	.....	.AGLNVVRMN	FSHGSYEYHQ	SVIENARESE	QRFRG	....	
tryb1	.SVEALKNLM	KSGMSVARMN	FSHGSHEYHQ	TTINNVRAAA	AELGLH	....	
tryb2	.SVEALKNLM	KSGMSVARMN	FSHGSHEYHQ	TTINNVRAAA	AELGLH	....	
leish	.SVEALKGLI	QSGMSVARMN	FSHGSHEYHQ	TTINNVRQAA	AELGVN	....	
ratL	.SVDRLKEMI	KAGMNIARLN	FSHGSHEYHA	ESIANIREAT	ESFATSPLSY		
ratR	.SVDRLKEMI	KAGMNIARLN	FSHGSHEYHA	ESIANIREAT	ESFATSPLSY		
humanL	.SVERLKEMI	KAGMNIARLN	FSHGSHEYHA	ETIANVREAV	ESFAGSPLSY		
humanR	.SVERLKEMI	KAGMNIARLN	FSHGSHEYHA	ETIANVREAV	ESFAGSPLSY		
humanM1	.SVETLKEMI	KSGMNVARLN	FSHGTHEYHA	ETIKNVRTAT	ESFASDPILY		
humanM2	.SVETLKEMI	KSGMNVARLN	FSHGTHEYHA	ETIKNVRTAT	ESFASDPILY		
catM1	.SVEILKEMI	KSGMNVARLN	FSHGTHEYHA	ETIKNVRAAT	ESFASDPILY (104)		
ratM1	.SVEMLKEMI	KSGMNVARLN	FSHGTHEYHA	ETIKNVRAAT	ESFASDPILY		
ratM2	.SVEMLKEMI	KSGMNVARLN	FSHGTHEYHA	ETIKNVRAAT	ESFASDPILY		
chickM1	.SVDKLKEMI	KSGMNVARLN	FSHGTHEYHE	GTIKNVREAT	ESFASDPITY		
ecolII	...NNLEKVI	AAGANVVRMN	FSHGSPEDHK	MRADKVREIA	AKLG	....	

\* \* \* \*

	bbbbbb	bbbbbb	bbbb	bbbb	bbbb	aaaaaa
castA	.AVAIMMDTE	GSEIHMGLD	.GGASSAKAE	DGEIWTFSVR	AYDSPRPRT	
castB	.AVAIMMDTE	GSEIHMGLD	.GGASSAKAE	DGEIWTFSVR	AYDSPRPRT	
tobacA	.AVAIMMDTE	GSEIHMGLD	.GGASSAKAE	DGEIWNFTVR	SFDPPILPERT	
brasG	.TIAIMLDTK	GPEVRSGDL	...PQPIMLD	PGQEFTFTIE	..RGVSTPTC	
tobacG	.VIAIMLDTK	GPEVISGDV	...PKPILLK	EGQEFNFSIK	..RGVSTEDT	
ecolI	KTAAILLDTK	GPEIRTMKLE	GGND..VSLK	AGQFTFTTDD	KSVIGNSEMV	
bacste	RTVAILLDTK	GPEIRTHNME	NG.A..IELK	EGSKLVISMS	E.VLGTPEKI	
lactolac	HKVGFLLDTK	GPEMRTEFLT	DGADS..ISVV	TGDKFRVATK	QGLKSTPELI	
bras1	...AVMLDTK	GPEIRTGFLK	DG..NPIQLK	EGQEITITTD	..YDIQDES	
bras2	...AVMLDTK	GPEIRTGFLK	DG..NPIQLK	EGQEITISTD	..YEIKGDEK	
potat	...AVMLDTK	GPEIRTGFLT	DG..KPIQLK	EGQEITVSTD	..YTIKGNEE	
tobacc	...AVMLDTK	GPEIRTGFLK	DA..KPVQLK	QGQEITISTD	..YSIKGDES	
asnig	RPLAIALDTK	GPEIRTG..N	TPDDKDIPK	QGHENITTD	EQYATASDDK	
asnid	RPVAIALDTK	GPEIRTG..N	TVGDKDIPK	AGHEMNISTD	EQYATASDDQ	
trire	RPVAIALDTK	GPEIRTG..N	TAGDVDIPIS	AGTVMNFTTD	EKYATACDTQ	
Scere	RPLAIALDTK	GPEIRTG..T	TTNDVDYPIP	PNHEMIFTTD	DKYAKACDDK (123)	
yarli	RPLAIALDTK	GPEIRTG..V	TKDDKDWDVK	AGHVMLFSTN	PKYKQCCDDK	
tryb1	..IGIALDTK	GPEIRTGFLK	DG...EVSFA	PGDIVCVTTD	PAYEKVGTK	
tryb2	..IGIALDTK	GPEIRTGFLK	DG...EVTFA	PGDIVCVTTD	PAYEKVGTK	
leish	..IAIALDTK	GPEIRTGQFV	GG...DAVME	RGATCYVTTD	PAFADKGTGD	
ratL	RPVAIALDTK	GPEIRTGVLQ	GGPESEVEIV	KGSQVLVTVD	PKFQTRGDAK	
ratR	RPVAIALDTK	GPEIRTGVLQ	GGPESEVEIV	KGSQVLVTVD	PKFQTRGDAK	
humanL	RPVAIALDTK	GPEIRTGILQ	GGPESEVELV	KGSQVLVTVD	PAFRTRGNAN	
humanR	RPVAIALDTK	GPEIRTGILQ	GGPESEVELV	KGSQVLVTVD	PAFRTRGNAN	
humanM1	RPVAIALDTK	GPEIRTGLIK	GGTAELVELK	KGATLKITLD	NAYMEKCDEN	
humanM2	RPVAIALDTK	GPEIRTGLIK	GGTAELVELK	KGATLKITLD	NAYMEKCDEN	
catM1	RPVAIALDTK	GPEIRTGLIK	GGTAELVELK	KGATLKITLD	NAYMEKCDEN (154)	
ratM1	RPVAIALDTK	GPEIRTGLIK	GGTAELVELK	KGATLKITLD	NAYMEKCDEN	
ratM2	RPVAIALDTK	GPEIRTGLIK	GGTAELVELK	KGATLKITLD	NAYMEKCDEN	
chickM1	RPVAIALDTK	GPEIRTGLIK	GGTAELVELK	KGAALKVTLD	NAFMENCDEN	
ecolII	RHVAIGDLQ	GPKIRVSTFK	EG...KVFLN	IGDKFLL..D	ANLGKGECDK	

\* \*

	aaa	aaaaaaaaa	bbbbbbb	bbbbbbbbb	bb
castA	I..NVNYDGF	AEDVKVDEL	LVDGGMVRFE	VIEKIGP..D	VKCRCTDPGL
castB	I..NVNYDGF	AEDVKVDEL	LVDGGMVRFE	VIEKIGP..D	VKCRCTDPGL
tobacA	V..TVNYDGF	AEDVKVDEL	LVDGGMVRFE	VIEKIGP..D	VKCLCTDPGL
brasG	V..SVNYDDF	VNDVEAGDML	LVDGGMMSFM	VKSKTKE..T	VICEVVDGGE
tobacG	V..SVNYDDF	INDVEPGDIL	LVDGGMMSLA	VKSKTSD..I	VKCEVIDGGE
ecolI	AVTYEG...F	TTDLISVGNV	LVDDGLIGME	VTAEI..GNK	VICKVLNNGD
bacste	SVTYP...L	IDDVSVGAKI	LLDDGLISLE	VNAVDKQAGE	IVTTVLNGGV
lactolac	ALNVAGGLDI	FDDVEIGQTI	LIDDGKLGSL	LTGKDAATRE	FEVEAQNDGV
bras1	TI..SMSYKKL	PLDVQPGNTI	LCADGSISLA	VVSCDPESGT	VRCRCENTAM
bras2	TI..SMSYKKL	PVDVQPGHTI	LCADGSISLA	VLSCDPKSGT	VRCRCENTAT
potat	MI..SMSYKKL	VMDLKPNTI	LCADGTITLT	VLSCDPPSGT	VRCRCENTAT
tobacc	MI..CMSYKKL	AEDVKPQSVI	LCADGQITFT	VLSCDKENGL	DRCRCENTAV
asnig	NM..YLDYKNI	TKVISPGKLI	YVDDGILSFE	VLEVVDK..T	IRVRCNLNGN
asnid	NM..YVDYKNI	TKVISAGKLI	YVDDGILSFE	VLEVVDK..T	LRVRCNLNGN
trire	NM..YVDYKNI	TKVIQPGRVI	YVDDGVLAFD	VLSIKDDQ..T	VEVRARNNGF
Scere	IM..YVDYKNI	TKVISAGRII	YVDDGVLFSFQ	VLEVVDK..T	LKVKALNAGK (171)
yarli	IM..YIDYTNL	VKQIDIGKII	FVDDGVLSFK	VLEKIDGE..T	LKVETLNGK
tryb1	KF..YIDYPQL	TNAVVPVGGSI	YVDDGVMTLR	VVSKEDDR..T	LKCHVNNHHR
tryb2	KF..YIDYPQL	TKAVPVGGSI	YVDDGVMTLR	VVSKEDDR..T	LKCHVNNHHR
leish	KF..YIDYQNL	SKVVRPGNYI	YIDDGILILQ	VQSHEDQ..T	LECTVTNSHT
ratL	TV..WVDYHNI	TRVAVVGRI	YIDDGLISLV	VQKIGPE..G	LVTEVEHGGI
ratR	TV..WVDYHNI	TRVAVVGRI	YIDDGLISLV	VQKIGPE..G	LVTEVEHGGI
humanL	TV..WVDYPNI	VRVVPVGGRI	YIDDGLISLV	VQKISPE..G	LVTQVENGGV
humanR	TV..WVDYPNI	VRVVPVGGRI	YIDDGLISLV	VQKISPE..G	LVTQVENGGV
humanM1	IL..WLDYKNI	CKVVEVGSKI	YVDDGLISLQ	VKQKGAD..F	LVTEVENGGG
humanM2	IL..WLDYKNI	CKVVEVGSKI	YVDDGLISLQ	VKQKGAD..F	LVTEVENGGG
catM1	VL..WLDYKNI	CKVVEVGSKV	YVDDGLISLL	VKEKGAD..F	LVTEVENGGG (201)
ratM1	IL..WLDYKNI	CKVVEVGSKI	YVDDGLISLQ	VKEKGAD..Y	LVTEVENGGG
ratM2	IL..WLDYKNI	CKVVEVGSKI	YVDDGLISLQ	VKEKGAD..Y	LVTEVENGGG
chickM1	VL..WVDYKNI	IKVIDVGSKI	YVDDGLISLL	VKEKGAD..F	VMTEVENGGM
ecolII	EKVGIDYKGL	PADVVPDIL	LLDDGRVQLK	VLEVQGMK..	VFTEVTVGGP

\*

	bbb bbb	bbbb	bbb	aaaaaaa	bbbb
castA	LLPRANLTFW	RDGSLVRERN	AMLPTISSKD	WLD.IDFGIA	E..GVDFIAI
castB	LLPRANLTFW	RDGSLVRERN	AMLPTISSKD	WLD.IDFGIA	E..GVDFIAI
tobacA	LLPRANLTFW	RDGSLVRERN	AMLPTISSKD	WLD.IDFGIA	E..GVDFIAV
brasG	LKSRRLHN..	....VRGKS	ATLPSITEKD	WED.IKFGVE	N..KVDFYAL
tobacG	LKSRRLHN..	....VRGKS	ATLPSITEKD	WDD.IKFGVN	N..QVDFYAV
ecolI	LGENKGVN..	....LPGVS	IAPALAEKD	KQD.LIFGCE	Q..GVDFVAA
bacste	LKNKKGVN..	....VPGVK	VNLPGITEKD	RAD.IIFGIR	Q..GIDFIAA
lactolac	IGKQKGVN..	....IPNTK	IPFPALAEKD	DAD.IRFGLS	QPGGINFIAI
bras1	LGERKGVN..	....LPGVV	VDLPTLTDKD	IEDILGWGP	N..GIDMIAL
bras2	LWERKGVN..	....LPGVV	VDLPTLTTEKH	VEDILKWGP	N..KIDMIAL
potat	LGERKGVN..	....LPGVV	VDLPTLTTEKH	KEDILEWGP	N..NIDMIAL
tobacc	LGERKGVN..	....LPGVI	VDLPTLTDKD	KDDILNWGP	N..HIDMIAL
asnig	ISSRKGVN..	....LPGTD	VDLPALSEKD	IAD.LKFGVR	N..KVDMVFA
asnid	ISSRKGVN..	....LPGTD	VDLPALSEKD	ISD.LKFGVK	N..KVDMVLA
trire	ISSRKGVN..	....LPNTD	VDLPALSEKD	KAD.LRFGVK	N..NVDMVFA
Scere	ICSHKGVN..	....LPGTD	VDLPALSEKD	KED.LRFGVK	N..GVHMFVA (211)
yarli	ISSRKGVN..	....LPGTD	VDLPALSEKD	KAD.LKFGVE	H..GVDMIFA
tryb1	LTDRRGIN..	....LPGCE	VDLPAVSEKD	RKD.LEFGVA	Q..GVDMIFA
tryb2	LTDRRGIN..	....LPGCE	VDLPAVSEKD	RKD.LEFGVA	Q..GVDMIFA
leish	ISDRRGVN..	....LPGCD	VDLPAVSAKD	RVD.LQFGVE	Q..GVDMIFA
ratL	LGSRKGVN..	....LPNTE	VDLPGLSEQD	LLD.LRFGVQ	H..NVDIIFA
ratR	LGSRKGVN..	....LPNTE	VDLPGLSEQD	LLD.LRFGVQ	H..NVDIIFA
humanL	LGSRKGVN..	....LPGAQ	VDLPGLSEQD	VRD.LRFGVE	H..GVDIVFA
humanR	LGSRKGVN..	....LPGAQ	VDLPGLSEQD	VRD.LRFGVE	H..GVDIVFA
humanM1	LGSKKGVN..	....LPGAA	VDLPAVSEKD	IQD.LKFGVE	Q..DVIDMVFA
humanM2	LGSKKGVN..	....LPGAA	VDLPAVSEKD	IQD.LKFGVE	Q..DVIDMVFA
catM1	LGSKKGVN..	....LPGAA	VDLPAVSEKD	IQD.LKFGVE	Q..DVIDMVFA (241)
ratM1	LGSKKGVN..	....LPGAA	VDLPAVSEKD	IQD.LKFGVE	Q..DVIDMVFA
ratM2	LGSKKGVN..	....LPGAA	VDLPAVSEKD	IQD.LKFGVE	Q..DVIDMVFA
chickM1	LGSKKGVN..	....LPGAA	VDLPAVSEKD	IQD.LKFGVE	Q..NVDMVFA
ecolII	LSNNKGIN..	....KLGGG	LSAEALTEKD	KAD...IKTA	ALIGVDYLAV

	aaaaaaa	aaaaa	bbbbbb	aaaaaa	aaaaaaa
castA	SFVKSAEVIN	HLKSYIAARS	RDSIDIAVIK	IESIDSL...	KNLEEIIIRAS
castB	SFVKSAEVIN	HLKSYIAARS	RDSIDIAVIK	IESIDSL...	KNLEEIIIRAS
tobacA	SFVKSAEVIK	HLKSYIQARA	RDSIDISVIK	IESIDSL...	KNLEEIIQAS
brasG	SFVKDAQVVH	ELKNYL..QG	CGADIHVIVK	IESADSI...	PKLHSIITAS
tobacG	SFVKDAKVH	ELKDYL..KS	CNADIHVIVK	IESADSI...	PNLHSIISAS
ecoli	SFIRKRSDVI	EIREHLKAHG	.GENIHIISK	IENQEGV...	NNFDEILEAS
bacste	SFVRRASDVL	EIRELLEAHD	.ALHIQIIAK	IENEEGV...	ANIDEILEAA
lactolac	SFVRTANDVK	EVRRICEETG	.NPHVQLLAK	IENQOGI...	ENLDEIIEAA
bras1	SFVRKGSIDL	NVRRVLGSHA	.K.SIMIMSK	VENQEGV...	VNFDEILRET
bras2	SFVRKGSIDL	NVTKVLGSHS	.K.SIMIMSK	VVYQEGV...	INFDEILRET
potat	SFVRKGSIDL	NVRKVLGPHA	.K.RIQIMSK	VENQEGV...	INFDEILRET
tobacc	SFVRKGSIDL	EVRRKLGEHA	.K.NILIMSK	VENQEGV...	ANFDDILINS
asnig	SFIRRGSDIR	HIREVLGEEG	.R.EIQIIAK	IENQOGV...	NNFDEILEET
asnid	SFIRRGSDIR	HIREVLGEEG	.R.EIQIIAK	IENQOGV...	NNFDEILEET
trire	SFIRRAQDIK	DIRDVLGPEG	.K.QIQIIAK	IENRQGL...	NNFAEILEET
Scere	SFIRTANDVL	TIREVLGEQG	.K.DVKIIVK	IENQOGV...	NNFDEILKVT (256)
yarli	SFVRTANDVQ	AIRDVLGEKG	.K.GIQVISK	IENQOGV...	NNFDEILKET
tryb1	SFIRTAEQVR	EVRAALGEKG	.K.DILIISK	IENHQGV...	QNIDSIIIEAS
tryb2	SFIRTAEQVR	EVRAALGEKG	.K.DILIISK	IENHQGV...	QNIDSIIIEAS
leish	SFIRSAEQVG	DVRKALGPKG	.R.DIMIICK	IENHQGV...	QNIDSIIIEES
ratL	SFVRKASDVL	AVRDALGPEG	.Q.NIKIISK	IENHEGV...	KKFDEILEVS
ratR	SFVRKASDVL	AVRDALGPEG	.Q.NIKIISK	IENHEGV...	KKFNEILEVS
humanL	SFVRKASDVA	AVRAALGPEG	.H.GIKIISK	IENHEGV...	KRFDEILEVS
humanR	SFVRKASDVA	AVRAALGPEG	.H.GIKIISK	IENHEGV...	KRFDEILEVS
humanM1	SFIRKASDVH	EVRRVLGEKG	.K.NIKIISK	IENHEGV...	RRFDEILEAS
humanM2	SFIRKASDVH	EVRRVLGEKG	.K.NIKIISK	IENHEGV...	RRFDEILEAS
catM1	SFIRKASDVH	EVRRVLGEKG	.K.NIKIISK	IENHEGV...	RRFDEILEAS (286)
ratM1	SFIRKAADVH	EVRRVLGEKG	.K.NIKIISK	IENHEGV...	RRFDEILEAS
ratM2	SFIRKAADVH	EVRRVLGEKG	.K.NIKIISK	IENHEGV...	RRFDEILEAS
chickM1	SFIRKAADVH	AVRRVLGEKG	.K.HIKIISK	IENHEGV...	RRFDEIMEAS
ecoliI	SFPRCGEDLN	YARR.LARDA	.GCDAKIVAK	VERAEAVCSQ	DAMDDIILAS

\*\*

\*

\*

	bbbb	aaaa	a	aaaaaa	aaaaaaaaa	a	bbbbbb
castA	DGAMVARGDL	GAQIPLEQVP	SAQQNIVQVC	RQINKPVIVA	SOLLESIMIEY		
castB	DGAMVARGDL	GAQIPLEQVP	SAQQNIVQVC	RQINKPVIVA	SOLLESIMIEY		
tobacA	DGAMVARGDL	GAQIPLEQVP	SEQQKIVQIC	RQINRPVIVA	SOLLESIMIEY		
brasG	DGAMVARGDL	GAELPIEEVP	ILQERIINLC	RSMEKPVIVA	TNMLESIMIVH		
tobacG	DGAMVARGDL	GAELPIEEVP	LLQEDIIRRC	QSMQKPVIVA	TNMLESIMIDH		
ecoli	DGIMVARGDL	GVEIPVEEVI	FAQKMMIEKC	IRARKVVITA	TQMLDSMIKN		
bacste	DGLMVARGDL	GVEIPAEVVP	LIQKLLIKKC	NMLGKPVITA	TQMLDSMORN		
lactolac	DGIMVARGDL	GIEVPFEMVP	VYQKLIISKV	NKAGKIVVTA	TNMLESMTYN		
bras1	DAFMVARGDL	GMEIPIEKIF	LAQKMMIYKC	NLAGKPVVTA	TQMLDSMIKS		
bras2	DAFMVARGDL	GMEIPIEKIF	LAQKMMIYKC	NLAGKPVVTA	TQMLDSMIKS		
potat	DSFMVARGDL	GMEIPVEKIF	LAQKMMIYKC	NLAGKAVVTA	TQMLDSMIKS		
tobacc	DAFMVARGDL	GMEIPIEKIF	LAQKMMIYKC	NIQKGPVITA	TQMLDSMIKS		
asnig	DGVMVARGDL	GIEIPAPKVF	IAQKMMIAKC	NIQKGPVICA	TQMLDSMTYN		
asnid	DGVMVARGDL	GIEIPAPKVF	IAQKMMIAKC	NIQKGPVICA	TQMLDSMTYN		
trire	DGVMVARGDL	GIEIPAAEVF	AAQKMMIAMC	NIAGKPVICA	TQMLDSMIKN		
Scere	DGVMVARGDL	GIEIPAPEVL	AVQKCLIACS	NLAGKPVICA	TQMLDSMTYN (306)		
yarli	DGVMVARGDL	GIEIPAPQVF	IAQKQLIAC	NLAGKPVICA	TQMLDSMTYN		
tryb1	NGIMVARGDL	GVEIPAECVC	VAQMCIIISC	NVVGKPVICA	TQMLDSMTSN		
tryb2	NGIMVARGDL	GVEIPAECVC	VAQMCIIISC	NVVGKPVICA	TQMLDSMTSN		
leish	DGIMVARGDL	GVEIPAECVV	VAQKILISK	NVAGKPVICA	TQMLDSMTYN		
ratL	DGIMVARGDL	GIEIPAECVF	LAQKMMIGRC	NLAGKPVVCA	TQMLDSMITK		
ratR	DGIMVARGDL	GIEIPAECVF	LAQKMMIGRC	NLAGKPVVCA	TQMLDSMITK		
humanL	DGIMVARGDL	GIEIPAECVF	LAQKMMIGRC	NLAGKPVVCA	TQMLDSMITK		
humanR	DGIMVARGDL	GIEIPAECVF	LAQKMMIGRC	NLAGKPVVCA	TQMLDSMITK		
humanM1	DGIMVARGDL	GIEIPAECVF	LAQKMMIGRC	NRAGKPVICA	TQMLDSMIKK		
humanM2	DGIMVARGDL	GIEIPAECVF	LAQKMMIGRC	NRAGKPVICA	TQMLDSMIKK		
catM1	DGIMVARGDL	GIEIPAECVF	LAQKMMIGRC	NRAGKPVICA	TQMLDSMIKK (336)		
ratM1	DGIMVARGDL	GIEIPAECVF	LAQKMMIGRC	NRAGKPVICA	TQMLDSMIKK		
ratM2	DGIMVARGDL	GIEIPAECVF	LAQKMMIGRC	NRAGKPVICA	TQMLDSMIKK		
chickM1	DGIMVARGDL	GIEIPAECVF	LAQKMMIGRC	NRAGKPIICA	TQMLDSMIKK		
ecoliI	DVVMVARGDL	GVEIGDPELV	GIQKALIRRA	RQINRAVITA	TQMLDSMITN		

\* \*\*\*\* \*

\*

\*

\*\*



	aaaaaaaa	aaa	bbb	bbb	aaaaaaaa	aaaaaaaa
castA	PTPTRAEVAD	VSEAVRQRAD	ALMLSGESAM	GQYPEKALAV	LRSVSVRIEK	
castB	PTPTRAEVAD	VSEAVRQRAD	ALMLSGESAM	GQYPEKALAV	LRSVSVRIEK	
tobacA	PIPTRAEVAD	VSEAVRQRGD	ALMLSGESAM	GQYPEKALT	LRSVSLRIER	
brasG	PTPTRAEVSD	IAIAVREGAD	AVMLSGETAH	GKFPLKAAGV	MHTVALRTEA	
tobacG	PTPTRAEVSD	ISIAVREGAD	AVMLSGETAH	GKYPLKAVKV	MHIVALRTES	
ecolI	PRPTRAEAGD	VANAILDGT	AVMLSGESAK	GKYPLEAVSI	MATICERTDR	
bacste	PRPTRAEASD	VANAIFDGT	AVMLSGETAA	GQYPVEAVKT	MHQIALRTEQ	
lactolac	PRATRSEISD	VFNAVIDGTD	ATMLSGESAN	GKYPRESVRT	MATVNKNAQT	
bras1	PRPTRAEATD	VANAVLDGTD	CVMLSGESAA	GAYPEIAVKV	MAKISIEAES	
bras2	PRPTRAEPRD	VANAVLDGTD	CVMLSGESAA	GAFPEIAVKT	MAKICIQAES	
potat	PAPTRAEATD	VANAVLDGTD	CVMLSGESAA	GAYPELAVKI	MSRICIEAES	
tobacc	PRPTRAEATD	VANAVLDGTD	CVMLSGETAA	GAYPDLAVGT	MAKICIEAES	
asnig	PRPTRAEVSD	VANAVLDGAD	CVMLSGETAK	GNYPNEAVKM	MSETCLLAEV	
asnid	PRPTRAEVSD	VANAVLDGAD	CVMLSGETAK	GNYPCEAVTM	MSETCLLAEV	
trire	PRPTRAEISD	VGNAVTDGAD	CVMLSGETAK	GNYPAESIHE	MHEASLKAEN	
Scere	PRPTRAEVSD	VGNAILDGD	CVMLSGETAK	GNYPINAVTT	MAETAVIAEQ (356)	
yarli	PRPTRAEVSD	VGNAILDGD	CVMLSGETAK	GTYPIESVKM	MHETCLVAEK	
tryb1	PRPTRAEVSD	VANAVLNGAD	CVMLSGETAK	GKYPNEVVQY	MARICVEAQS	
tryb2	PRPTRAEVSD	VANAVLNGAD	CVMLSGETAK	GKYPNEVVQY	MARICVEAQS	
leish	PRPTRAEVSD	VRNAVFGAD	CVMLSGETAK	GKYPNEVVQY	MARICLEAQS	
ratL	ARPTRAETSD	VANAVLDGAD	CIMLSGETAK	GSFPVEAVMM	QHAIAREAEA	
ratR	ARPTRAETSD	VANAVLDGAD	CIMLSGETAK	GSFPVEAVMM	QHAIAREAEA	
humanL	PRPTRAETSD	VANAVLDGAD	CIMLSGETAK	GNFPVEAVKM	QHRIAREAEA	
humanR	PRPTRAETSD	VANAVLDGAD	CIMLSGETAK	GNFPVEAVKM	QHAIAREAEA	
humanM1	PPPTRAEGSD	VANAVLDGAD	CIMLSGETAK	GDYPLEAVRM	QHAIAREAEA	
humanM2	PRPTRAEGSD	VANAVLDGAD	CIMLSGETAK	GDYPLEAVRM	QHAIAREAEA	
catM1	PRPTRAEGSD	VANAVLDGAD	CIMLSGETAK	GDYPLEAVRM	QHAIAREAEA (386)	
ratM1	PRPTRAEGSD	VANAVLDGAD	CIMLSGETAK	GDYPLEAVRM	QHAIAREAEA	
ratM2	PRPTRAEGSD	VANAVLDGAD	CIMLSGETAK	GDYPLEAVRM	QHAIAREAEA	
chickM1	PRPTRAEGSD	VANAVLDGAD	CIMLSGETAK	GDYPLEAVRM	QHAIAREAEA	
ecolII	PMPTRAEVMD	VANAVLDGTD	AVMLSAETAA	GQYPSETVAA	MARVCLGAEK	

\*\*\* \* \* \* \* \*\*\* \* \* \* \*

	aaaaaaaa	aaaaaaaa	aaaaaaaa	aaaa	bb	bbbbbb
castA	WWREEKHHEA	MELPAIGSTY	SDSISEEICN	SAAKMANNL	GVDAFVYTK	
castB	WWREEKHHEA	MELPAIGSTY	SDSISEEICN	SAAKMANNL	GVDAFVYTK	
tobacA	MWREQKRHEV	IELPSIASSF	SDSISEEICN	SAAKMANNL	GVDAFVYTK	
brasG	TITTSTEMP.	...PNLGQAF	KNHMSEMFAY	HATMMSNTL	G.TSTVVFTR	
tobacG	SLQKSTS.S.	...PSQSAAY	KSHMGEMFAF	HSSSMANTL	S.TPIIVFTR	
ecolI	VM...NSRLE	FNNDNRKLR.	.I...TEAVCR	GAVETAEKLD	A.PLIVVATQ	
bacste	AL...EHRDI	LSQRTKESQT	TI...TDAIGQ	SVAHTALNLD	V.AAIVTPTV	
lactolac	ML...KEYGR	L.HPERYDKS	TV...TEVVAA	SVKNAAEAMD	V.KLIVLALTE	
bras1	SL...DYNTI	FKEMIRATPL	PMSPLESLAS	SAVRTANKAH	A.KLIIVLTR	
bras2	SL...DYNTI	FKEMIRATPL	PMSTLESLS	SAVRTANKAR	A.KLIIVLTR	
potat	SL...DNEAI	FKEMIRCTPL	PMSPLESLAS	SAVRTANKAR	A.KLIVVLTR	
tobacc	TI...DYPDV	FKRIMSNAPV	PMSPLESLAS	SAVRTANSK	A.ALILVLTR	
asnig	AI...PHFNV	LDELRLNAPR	PTDTVESIAM	AAVSASLELN	A.GAIVVLTT	
asnid	AI...PHFNV	FDELRLNAPR	PTDTVESIAM	AAVSASLELN	A.GAIVVLTT	
trire	TI...PYVSH	FEEMCTLVKR	PVSTVESCAM	AAVRASLDLG	A.GGIIVLST	
Scere	AI...AYLPN	YDDMRNCTPK	PTSTTETVAA	SAVAAVFEQK	A.KAIIVLST (402)	
yarli	AI...AYAPL	FNEMRTLTVR	PTETVETIAI	SAVSASFQEQ	A.RAIIVLST	
tryb1	AT...HDTVM	FNSIKNLQKI	PMCPEEAVCS	SAVASAFEVQ	A.KAMLVLST	
tryb2	AT...HDTVM	FNSIKNLQKI	PMCPEEAVCS	SAVASAFEVQ	A.KAMLVLST	
leish	AL...NEYVF	FNSIKKLQHI	PMSADEAVCS	SAVNSVYETK	A.KAMVVLST	
ratL	AV...YHRQL	FEELRRAAPL	SRDPTEVTAI	GAVEASFQCC	A.AAIIVLTK	
ratR	AV...YHRQL	FEELRRAAPL	SRDPTEVTAI	GAVEASFQCC	A.AAIIVLTK	
humanL	AV...YHRQL	FEELRRAAPL	SRDPTEVTAI	GAVEASFQCC	A.AAIIVLTK	
humanR	AV...YHRQL	FEELRRAAPL	SRDPTEVTAI	GAVEASFQCC	A.AAIIVLTK	
humanM1	AI...YHLQL	FEELRLRLPI	TSDPTEATAV	GAVEASFQCC	S.GAIIVLTK	
humanM2	AI...YHLQL	FEELRLRLPI	TSDPTEATAV	GAVEASFQCC	S.GAIIVLTK	
catM1	AM...FHRKL	FEELVRGSSH	STDLMAMAM	GSVEASYKCL	A.AALIVLTK (432)	
ratM1	AV...FHRLL	FEELARASSQ	STDPLEAMAM	GSVEASYKCL	A.AALIVLTK	
ratM2	AI...YHLQL	FEELAAWRPL	PATPQKLPPW	VPWRPPSSAA	V.GPLSCSPS	
chickM1	AM...FHRQQ	FEEILRHSVH	HREPADAMAA	GAVEASFQCC	A.AALIVMTE	
ecolIII	I.....PSI	NVSKHRLDVQ	FDNVEEAIAM	SAMYAANHLK	GVTAIITMTE	

	aaaaaa	bbbb		aaaaaa	aaaaaa bbb
castA	DGHMASLLSR	CRPDCPIFAF	.....	...TTTTSVR	RRLNLQWGLI
castB	DGHMASLLSR	CRPDCPIFAF	.....	...TTTTSCR	RRLNLQWGLI
tobacA	NGHMASLLSR	CRPDCPIFAF	.....	...TTTTSVR	RRLNLQWGLM
brasG	TGFMAILLSH	YRPSGTIYAF	.....	...TNEKKIK	QRLALYQGV
tobacG	TGSMAILLSH	NRPSTTVFAF	.....	...TNNERVK	QRLALYHGV
ecolI	GGKSARAVRK	YFPDATILAL	.....	...TTNEKTA	HQLVLSKGV
bacste	SGKTPQMVAK	YRPKAPIIAV	.....	...TSNEAVS	RRLALVWGV
lactolac	SGNTARLISK	HRPDADILAI	.....	...TFDEKVE	RGLMINWGV
bras1	GGSTANLVAK	YRPVPIILSV	VVPVMTTDTF	DWSCTDESPA	RHSLTYRGLI
bras2	GGTTAKLVAK	YRPVPIILSV	VVPVFTSDTF	NWSCSDESPA	RHILTYRGLI
potat	GGSTAKLVAK	YRPVPIILSV	VVPVLTDTDF	DWSISDETPA	RHSLVYRGLI
tobacc	GGSTAKLVAK	YRPGMPIILSV	VVPEIKTDSF	DWTCSDSPA	RHSLIFRGLV
asnig	SGKTARYISK	YRPVCPIMV	.....	...TRNPAAS	RYSHLYRGV
asnid	SGNTARMISK	YRPVCPIMV	.....	...SRNPAAT	RYSHLYRGV
trire	SGDSARLLSK	YRPVCPIMV	.....	...TRNPPTS	RFSHLYRGV
Scere	SGTTPRLVSK	YRPNCPIILV	.....	...TRCPRAA	RFSHLYRGV (439)
yarli	SGTSARLCSK	YRPNCPIILV	.....	...TRNAQAA	RFSHLYRGV
tryb1	TGRSARLISK	YRPNCPIICV	.....	...TTRLQTC	RQLNVTRSV
tryb2	TGRSARLISK	YRPNCPIICV	.....	...TTRLQTC	RQLNVTRSV
leish	TGRSARLVAK	YRPNCPIICV	.....	...TTRLQTC	AQLNITQGV
ratL	TGRSAQLLSQ	YRPRAAVIAV	.....	...TRSAQAA	RQVHLSRGV
ratR	TGRSAQLLSQ	YRPRAAVIAV	.....	...TRSAQAA	RQVHLSRGV
humanL	TGRSAQLLSR	YRPRAAVIAV	.....	...TRSAQAA	RQVHLCRGV
humanR	TGRSAQLLSR	YRPRAAVIAV	.....	...TRSAQAA	RQVHLCRGV
humanM1	SGRSAHQVAR	YRPRAPIIAV	.....	...TRNPQTA	RQAHLYRGIF
humanM2	SGRSAHQVAR	YRPRAPIIAV	.....	...TRNPQTA	RQAHLYRGIF
catM1	SGRSAHQVAR	YRPRAPIIAV	.....	...TRNHQTA	RQAHLYRGIF (469)
ratM1	SGRSAHQVAR	YRPRAPIIAV	.....	...TRNPQTA	RQAHLYRGIF
ratM2	LARSAHQVAR	YRPRAPIIAV	.....	...TRNPQTA	RQAHLYRGIF
chickM1	SGRSAHLVSR	YRPRAPIIAV	.....	...TRNDQTA	RQAHLYRGV
ecolII	SGRTALMTSR	ISSGLPIFAM	.....	...SRHERTL	NLTALYRGV

	bb	aaaaa	aaaaaaaaa	aaaa	
castA	PFRLS.....	.....FADD	ESNLNKTFSL	LKARGMIKSG	DLVIAV....
castB	PFRLS.....	.....FADD	ESNLNKTFSL	LKARGMIKSG	DLVIAV....
tobacA	PFRLS.....	.....FSDD	ESNLNKTFSL	LKARGMIKSG	DLIIIV....
brasG	PIYME.....	.....FSDD	EDTFTKALAT	LLKQGMVKKG	EEIATVQSGS
tobacG	PIYME.....	.....FSDD	EETFSRAIKL	LLSKSLVKDG	QYVTLVQSGA
ecolI	PQLVKEIT..	.....ST	DDFYRLGKEL	ALQSGLAHKG	DVVVYGFWCT
bacste	TKEAPHVN..	.....TT	DEMDDVAVDA	AVRSGLVKHG	DLVVITAGVP
lactolac	PMMTEKPA..	.....ST	DDMFVAVK	ALASGLVEAG	DNIIIVAGVP
bras1	PMLAEGSAKA	TD....SEST	EVIEAALKS	ATQGRGNVG	DAVVALH...
bras2	PVLAEGSAKA	TD....NEST	EEIESALKQ	ATEKGLCNHG	DAVVALH...
potat	PLLGECSAKA	TD....SEST	EVILEAALKS	AVTRGLCKPG	DAVVALH...
tobacc	PVLHAGSARA	SH....EEST	EEALDFALQH	AKTKGLCKQG	DSVVALH...
asnig	PFLFPEKKPD	FNVKIQEDV	DRRLKWGINH	ALKLGIINKG	DNIVCVQGW
asnid	PFFYFPEKKPD	FNVKIQEDV	DRRLKWGINH	GLKLGIINKG	DNIVCVQGW
trire	PFLYPEQKPD	FDTVNWQEDV	DKRIKWAVTR	AIELKTLTAG	DTVVVVQGW
Scere	PFVF.EKEP.	..VSDWTDV	EARINFGIEK	AKEFGILKKG	DTYVSIQGF (485)
yarli	PFIY.HKARA	SNPAEWQHDV	EERLKWGMDE	AVAGLILNKG	DVVVAIQGW
tryb1	SVFY.DAAS	....GEDKD	EKRVLGLDF	AKKEYASTG	DVVVVHADH
tryb2	SVFY.DAAS	....GEDKD	EKRVLGLDF	AKKEYASTG	DVVVVHADH
leish	SVFF.DADKL	....GHDEG	EHRVAAGVEF	AKSKGYVQTG	DYCVVIHADH
ratL	PLLYREPPEA	....IWADD	DRRVQFGIES	GKLRGFLRVG	DLVIVVTGWR
ratR	PLLYREPPEA	....IWADD	DRRVQFGIES	GKLRGFLRVG	DLVIVVTGWR
humanL	PLLYREPPEA	....IWADD	DRRVQFGIES	GKLRGFLRVG	DLVIVVTGWR
humanR	PLLYREPPEA	....IWADD	DRRVQFGIES	GKLRGFLRVG	DLVIVVTGWR
humanM1	PVLCKDPVQE	....AWAED	DLRVNFAMNV	GKARGFFKKG	DVVIVLTGWR
humanM2	PVLCKDPVQE	....AWAED	DLRVNFAMNV	GKARGFFKKG	DVVIVLTGWR
catM1	PVVCCKDPVQE	....AWAED	DLRVNLMNV	GKARGFFKKG	DVVIVLTGWR (515)
ratM1	PVLCKDAVLD	....AWAED	DLRVNLMNV	GKARGFFKKG	DVVIVLTGWR
ratM2	PVLCKDAVLD	....AWAED	DLRVNLMNV	GKARGFFKKG	DVVIVLTGWR
chickM1	PVLCKQPAHD	....AWAED	DLRVNLMNV	GKARGFFKKG	DVVIVLTGWR
ecolIII	PVHFDSD....	.....ANDG	VAAASEAVNL	LRDKGYLMSG	DLVIVTQGDV

\*

castA	.....SDMLQ	SIQVMNVP	
castB	.....SDMLQ	SIQVMNVP	
tobacA	.....SDMLQ	SIQVMNVP	
brasG	QPIWRSQSTH	NIQVRKV	
tobacG	QPIWRRHSTH	HIQVRKVQS	
ecolI	GT..ERHY		
bacste	VG..ETGSTN	LMKVHVISDL	LAKGQGIGRK SAFGKAVVAK TAEERQKMV
lactolac	VG...TGRTN	TMRIRTVK	
bras1	.R...IGAAS	VIKICLVK	
bras2	.R...IGAAS	VIKICVVK	
potat	.R...IGSAS	VIKICVVK	
tobacc	.R...VGTAS	VIKIVTVK	
asnig	GG...MGHTN	TVRVVPAE.E	NLGLAEE
asnid	GG...MGHTN	TVRVVPAE.E	NLGLSEE
trire	GG...MGNTN	TLRIVRADPD	HLGIGQME
Scere	AG...AGHSN	TLQVSTV	(499)
yarli	GG...LA.TP	TLSEFSSVSK	LFNTNLLDYK TYSMVIKSVN GGVLYK
tryb1	SV...KGYPN	QTRLIYLP	
tryb2	SV...KGYPN	QTRLIYLP	
leish	KV...KGYAN	QTRILLVE	
ratL	PG...SGYTN	IMRVLSVS	
ratR	PG...SGYTN	IMRVLSVS	
humanL	PG...SGYTN	IMRVLSIS	
humanR	PG...SGYTN	IMRVLSIS	
humanM1	PG...SGFTN	TMRVVPVP	
humanM2	PG...SGFTN	TMRVVPVP	
catM1	PG...SGFTN	TMRVVPVP	(530)
ratM1	PG...SGFTN	TMRVVPVP	
ratM2	PG...SGFTN	TMRVVPVP	
chickM1	PG...SGYTN	TMRVVPVP	
ecolIII	MS..TVGSTN	TTRILTVE	

bacste DGGILVTVST DADMPAIEK AAAIITEEGG LTSHAAVVGL SLGIPVIVGV

bacste ENATTLFKDG QEITVDGGFG AVYRGHASVL

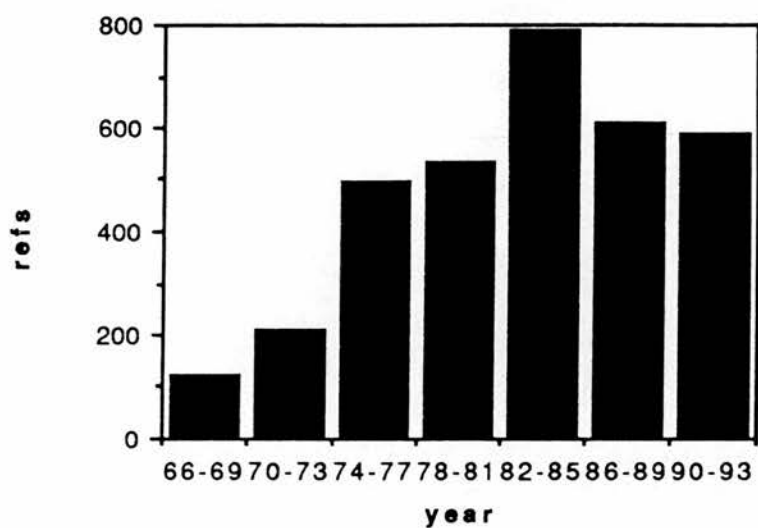


Fig. 1      Number of references in which pyruvate kinase is mentioned against the year of publication.  
Number of references generated by Medline CD-ROM database search using the key words "pyruvate kinase".

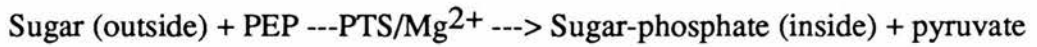
## 1.2 THE IMPORTANCE OF PYRUVATE AND PHOSPHOENOLPYRUVATE

Pyruvate and phosphoenolpyruvate (PEP) play essential roles in the metabolism of virtually all organisms from bacteria to higher eukaryotes. The three carbon  $\alpha$ -keto structure of pyruvate serves as a major metabolic intermediate in a number of important cellular pathways. In eukaryotes, pyruvate is derived from glucose-6-phosphate, alanine and lactate. The reduction of pyruvate catalysed by lactate dehydrogenase serves to regenerate  $\text{NAD}^+$ , enabling glycolysis to proceed transiently under anaerobic conditions. Lactate formed in active tissues is subsequently oxidised back to pyruvate, primarily in the liver. Another readily reversible reaction in the cytosol is the transamination of pyruvate, an  $\alpha$  - keto acid, to alanine, the corresponding amino acid. Several amino acids can be synthesised from carbohydrate precursors by this route. A third fate of pyruvate is its carboxylation to oxaloacetate inside mitochondria. This reaction, and the subsequent conversion of oxaloacetate into PEP, bypass an irreversible step of glycolysis and hence enable glucose to be synthesised from pyruvate. The carboxylation of pyruvate is also important for replenishing intermediates of the citric acid cycle. A fourth fate of pyruvate is its oxidative decarboxylation to acetyl CoA. This irreversible reaction inside mitochondria is a decisive reaction in metabolism: it commits the carbon atoms of carbohydrates and amino acids to oxidation by the citric acid cycle or to the synthesis of lipids. The pyruvate dehydrogenase complex, which catalyses this irreversible funnelling, is stringently regulated by multiple allosteric interactions and covalent modifications. Pyruvate is rapidly converted into acetyl CoA only if ATP is required or if two-carbon fragments are needed for the synthesis of lipids.

Phosphoenolpyruvate also serves as an important intermediate in aromatic amino acid biosynthesis in bacteria and also in the transport of sugar molecules into the cell via the phosphotransferase system (PTS). An unusual feature of the bacterial phosphotransferase system is that PEP, rather than ATP or another nucleoside triphosphate, is the phospho donor.



The overall reaction carried out by the phosphotransferase system is:



In tropical plants, PEP is formed from pyruvate via the C4 pathway. The reaction is catalysed by pyruvate orthophosphate dikinase:



As can be seen from the brief outline described above, pyruvate and PEP occupy often pivotal roles in the metabolism of many organisms and it is essential that cells can respond rapidly to varying intracellular concentrations of these compounds. As a result it is often the case that enzymes utilising either of these compounds as substrates are under stringent control.

### 1.3 A COMPARISON OF YEAST AND VERTEBRATE PYRUVATE KINASES

Yeast pyruvate kinase is between 49-51% identical at the amino acid level with the vertebrate pyruvate kinases so far sequenced (Tables 1 and 16). The enzyme from cat skeletal muscle has been sequenced and a high resolution crystal structure has been elucidated (Muirhead et al., 1986). The X-ray crystallographic studies on pyruvate kinase have tended to use the M1 isoenzyme as it can easily be prepared in large quantities in a relatively stable form. It is sometimes possible to crystallise alternative forms of an enzyme, corresponding to different conformational states. The T (tense) state is the less active form and is usually characterised by having a low affinity for substrate. The R (relaxed) form is often the more active form of an enzyme, and has a higher affinity for substrates. The three-dimensional image produced from X-ray crystallographic studies of the cat muscle enzyme, in the presence of  $\text{NH}_4$  ions (which would bind at the potassium site), is almost certainly that of the R quaternary structure. This is supported by the fact that the binding of substrates to the crystalline form gives rise to only small conformational changes (Stammers & Muirhead, 1975).

The enzyme from the majority of sources is a tetramer of identical subunits (Fig.2). Each subunit is composed of four domains; a small N-terminal domain and domains A, B and C (Fig. 3). Domain A is composed of an eight-stranded alpha/beta barrel, a structural motif found in a number of other, seemingly unrelated, proteins e.g. triosephosphate isomerase. The domain structure found is assumed to be a general feature of the other vertebrate enzymes and is probably very similar to the other, non-vertebrate, enzymes. This is demonstrated by the ability of the yeast sequence to be modelled into a structure that can be readily superimposed on to the cat structure (Clayden, 1987; Murcott, 1990).

The main difference between the yeast and the vertebrate enzymes is the larger size of the N-terminal domain in the latter. In the non-allosterically regulated enzymes so far sequenced (human, cat, rat and chicken skeletal muscle

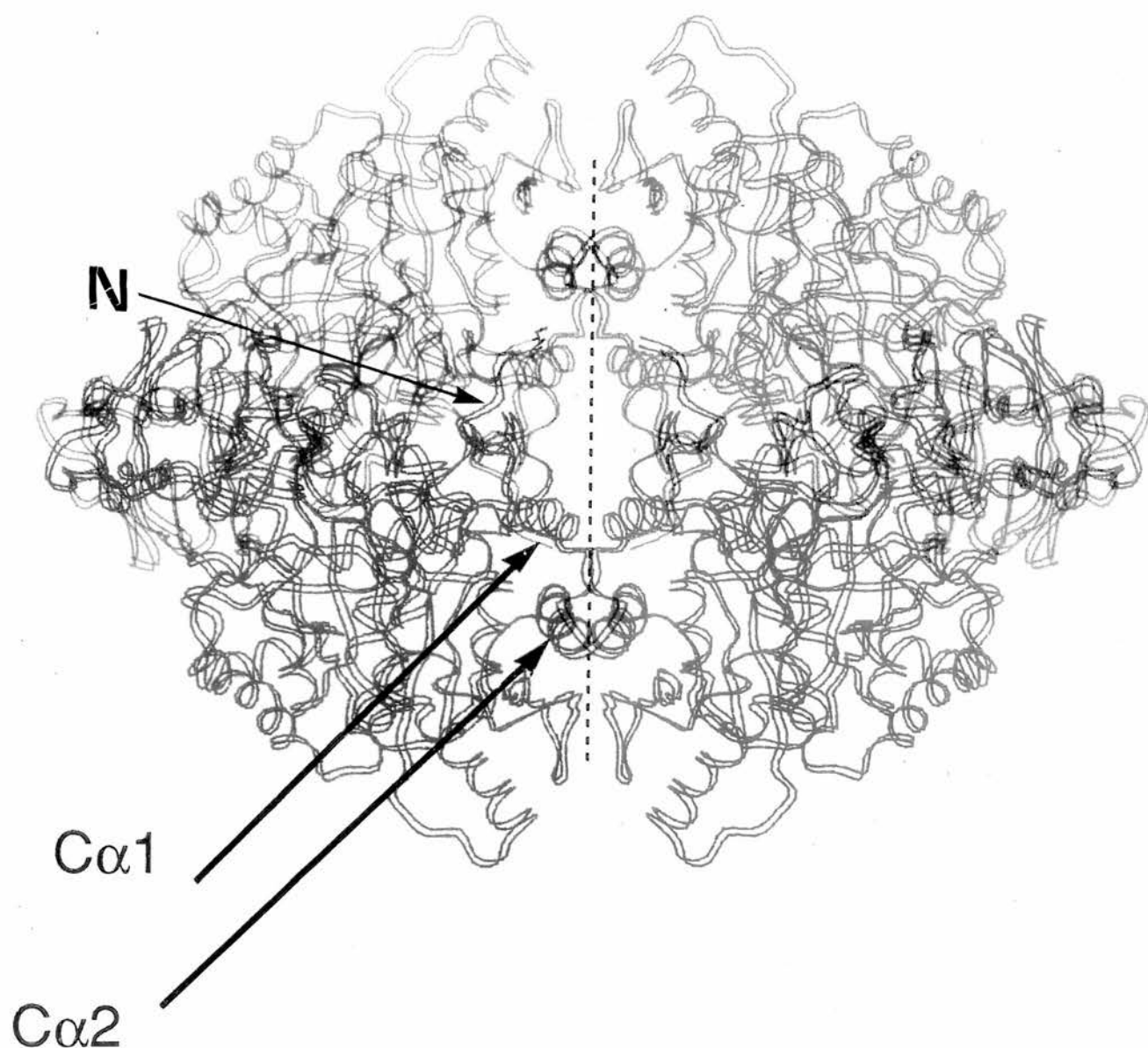


Fig. 2 Yeast pyruvate kinase tetramer.  
 Each subunit is coloured separately.  
 The C $\alpha$ 1 and C $\alpha$ 2 helices are labelled.  
 N = N-terminal domain.  
 The structure shown is the yeast sequence that has been modelled to fit the coordinates of the cat muscle enzyme determined by X-ray crystallographic studies (Muirhead et al., 1987).  
 Note how the C $\alpha$ 2 helices and (to a lesser extent) the C $\alpha$ 1 helices of adjacent subunits lie close to one another.

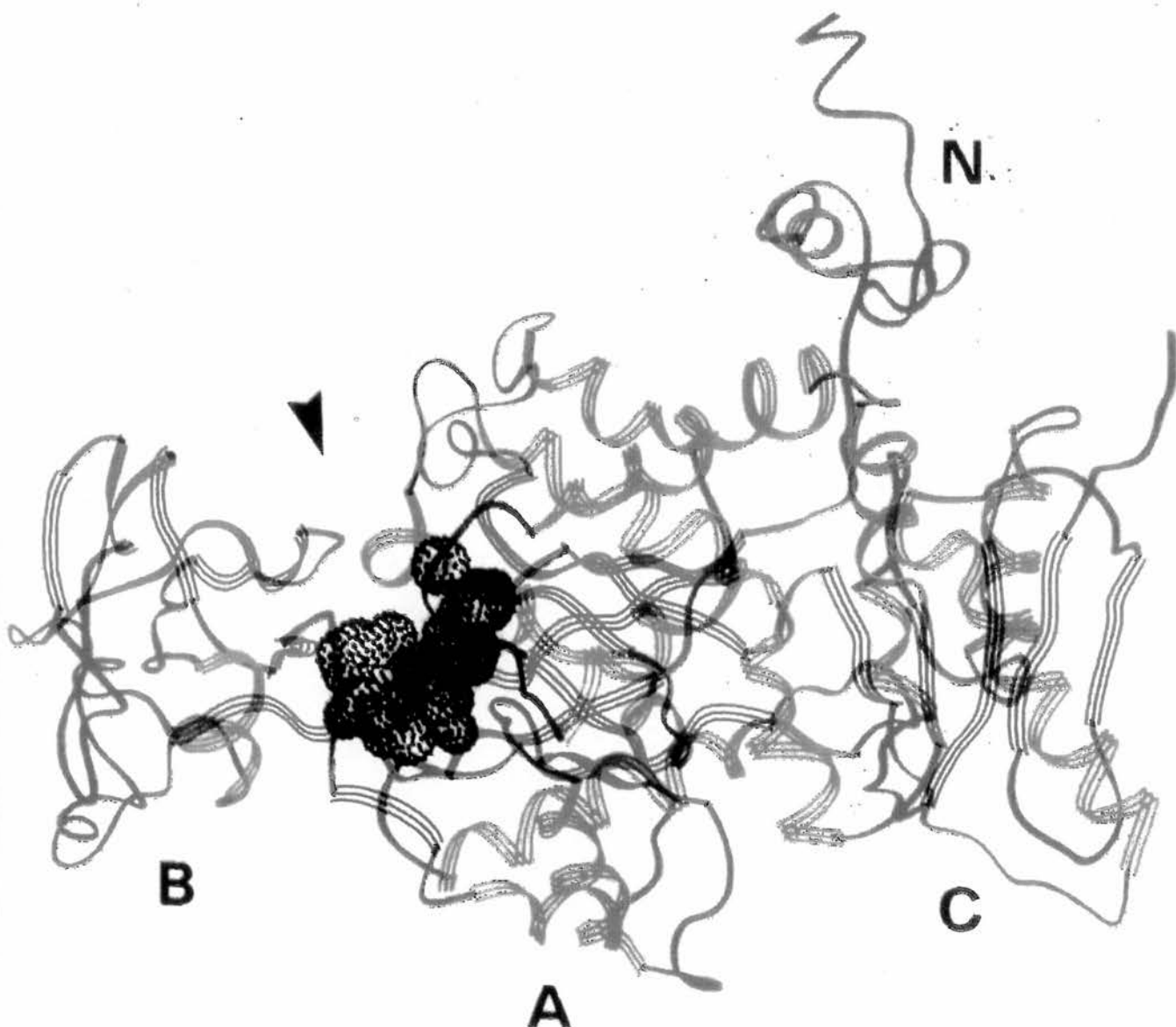


Fig. 3 Yeast pyruvate kinase monomer.  
 Ribbon diagram showing the domain structure of the enzyme.  
 Domains are labelled A, B, C and N.  
 Green - alpha helix, Red - beta strand, Blue - random coil  
 The arrow indicates the cleft between domains A and B leading to the  
 active site. Black spheres represent space filling models of the  
 substrates PEP and ADP.

M1 isoenzymes), the N-terminus is 23 residues longer than the yeast enzyme in each case. The allosterically regulated enzymes (human and rat muscle M2 isoenzymes), and those regulated by phosphorylation (human and rat liver, human and rat red blood cell isoenzymes), show an even larger difference in the size of the N-terminal domain. These enzymes are between 23 and 67 residues longer than the yeast enzyme at the N-terminus. It is thought that the N-terminal domain interacts with the other domains in the enzyme, particularly the C-domain, and hence may subtly influence enzyme activity and intersubunit communication.

A region considered to be essential in the transmission of the allosteric effect upon effector binding is the C-domain, especially two alpha helices ( $C\alpha 1$  and  $C\alpha 2$ ) which form close contacts with the other subunits. Both helices contain 13 amino acid residues (Table 2). On comparing the known vertebrate sequences with each other, the two alpha helices appear to be very similar in terms of identical or conserved residues. This suggests that only slight changes in sequence are required to significantly alter the enzyme's response to the presence of another molecule such as an allosteric effector. Such a change could arise simply by random mutation of certain key residues over the course of evolution. A comparison of the  $C\alpha 1$  and  $C\alpha 2$  helices between yeast and vertebrate enzymes shows that the yeast  $C\alpha 1$  sequence is most similar to the allosterically regulated isoenzymes and the yeast  $C\alpha 2$  sequence is most similar to the non-regulated isoenzymes. The pronounced differences in the  $C\alpha 2$  sequences may indicate that this region may be more important than  $C\alpha 1$  in contributing to the allosteric effect. Three of the 13 residues of  $C\alpha 2$  are identical between the yeast and the regulated isoenzymes, with a further six residues being conserved. By comparison, there are no identical residues between the yeast  $C\alpha 2$  sequence and the non-regulated isoenzymes and only four residues are conservative changes.

		Cα1		Cα2
<b>A</b>	YEAST	LPNYDDMRNCTPK	PTST	TETVAASAVAAVF
	CATM1	RKLFEELVRGSSH	STD	MEAMAMGSVEASY
	HUMM1	LQLFEELRRLAPI	TSDP	TEATAVGAVEASF
	RATM1	RLIFEELARASSQ	STDP	LEAMAMGSVEASY
	CHKM1	RQFEEILRHSVH	HREP	ADAMAAGAVEASF
		.....	..	*...*
		Cα1		Cα2
	YEAST	LPNYDDMRNCTPK	PTST	TETVAASAVAAVF
	HUMM2	LQLFEELRRLAPI	TSDP	TEATAVGAVEASF
	RATM2	LQLFEELAAARPL	PATP	QKLPPWVPWRPPS
	HUML	RQLFEELRRAAPL	SRDP	TEVTAIGAVEAAF
	RATL	RQLFEELRRAAPL	SRDP	TEVTAIGAVEASF
	HUMR	RQLFEELRRAAPL	SRDP	TEVTAIGAVEAAF
	RATR	RQLFEELRRAAPL	SRDP	TEVTAIGAVEASF
		.....*	...	.....

<b>B</b>	YEAST	KAKAIVLSTSGTTPR
	CATM1	LAAALIVLTESGRSAH
	HUMM1	CSGAIIVLTKSGRSAH
	RATM1	LAAALIVLTESGRSAH
	CHKM1	LAAALIVMTESGRSAH
		..*...*

YEAST	KAKAIVLSTSGTTPR
HUMM2	CSGAIIVLTKSGRSAH
RATM2	AVGPLSCSPSLARSAH
HUML	CAAAIIVLTTTGRSAQ
RATL	CAAAIIVLTKTGRSAQ
HUMR	CAAAIIVLTTTGRSAQ
RATR	CAAAIIVLTKTGRSAQ
	.. ..

Table 2: Comparison of yeast and vertebrate Cα1 and Cα2 regions and putative effector binding regions.

\* indicates identical residues, . indicates conserved residues

- A) upper box- yeast Cα1/Cα2 region compared to the equivalent region from vertebrate non-allosterically regulated enzymes.  
lower box- yeast Cα1/Cα2 region compared with the equivalent region from vertebrate allosterically regulated enzymes.
- B) upper box- yeast putative effector binding site compared with the equivalent region from vertebrate non-allosterically regulated enzymes.  
lower box- yeast putative effector binding site compared with the equivalent region from vertebrate allosterically regulated enzymes.

The site proposed to be involved in effector binding in the regulated forms of the enzyme is also located in the C-domain and lies adjacent to the important alpha helices in the amino acid sequence. Contacts with the N-domain may also be important in defining the effector binding site. This sequence contains 16 residues and forms a small beta strand (C $\beta$ 1) and part of another alpha helix (C $\alpha$ 3). A comparison of the yeast enzyme (which is regulated by the effector fructose-1,6-bisphosphate) and the non-regulated vertebrate enzymes show that they are very similar. Five of the 16 residues are identical and a further eight are conservative changes with only three residues being completely different. The regulated vertebrate enzymes share no identical residues with the yeast enzyme in this region. Eight residues are conservative changes and eight residues are completely different. This region was identified in X-ray crystallographic studies using the non-regulated cat muscle enzyme (Muirhead et al., 1986) and by inhibition-protection studies using the regulated *E.coli* enzyme (Speranza et al., 1990).

The active site lies in a cleft between domains A and B and the residues involved in binding and catalytic activity are conserved in all known sequences (Table 1). A more detailed comparison of the 31 sequences in Table 1 is given in the Discussion (Section 4.13).

## 1.4 THE REACTION MECHANISM

The pyruvate kinase reaction mechanism has been elucidated by studying almost exclusively the enzymes derived from rabbit and cat skeletal muscle and the yeast *Saccharomyces cerevisiae*. Fortunately, studies have shown that the sequence identity between these enzymes and those derived from other eukaryotic sources are sufficiently similar for meaningful parallels to be drawn regarding both the interaction of substrate(s) with the enzyme and the actual mechanism of catalysis.

Early work concentrated on determining the nature of the phospho transfer reaction. Indeed, as early as 1955 (Harrison et al.) it had been shown by isotope studies that various kinases could transfer phospho groups without exchange of the phospho oxygens with water or substrates. These studies also showed that phospho transfer occurred directly from donor to acceptor molecules without the formation of a covalent phospho-enzyme intermediate. This was confirmed for pyruvate kinase in particular in later studies using  $^{32}\text{P}$  labelling experiments (Hass et al., 1961).

In a direct transfer mechanism, ADP and ATP would be expected to share one binding site, whilst pyruvate and PEP would be expected to share another binding site on the enzyme, with a further provision that the binding occur so that the transferable phospho group of ATP and PEP occupied a common position on the enzyme. These properties were confirmed for the rabbit muscle enzyme by direct binding studies of the substrates PEP and ADP (Reynard et al., 1961). A simple schematic illustrating the relations between substrates and a transition state for the enzyme are shown in Fig 4.

### 1.4.1 NMR SPECTROSCOPY AND THE REACTION MECHANISM

Nuclear magnetic resonance spectroscopy (NMR) has been used to determine the location and disposition of substrates and effectors during catalysis.

Molecular contact between the partially positive phosphorus atom of the  $\gamma$ -phospho group of ATP with the carbonyl oxygen of pyruvate (Fig 5) would facilitate carbonyl



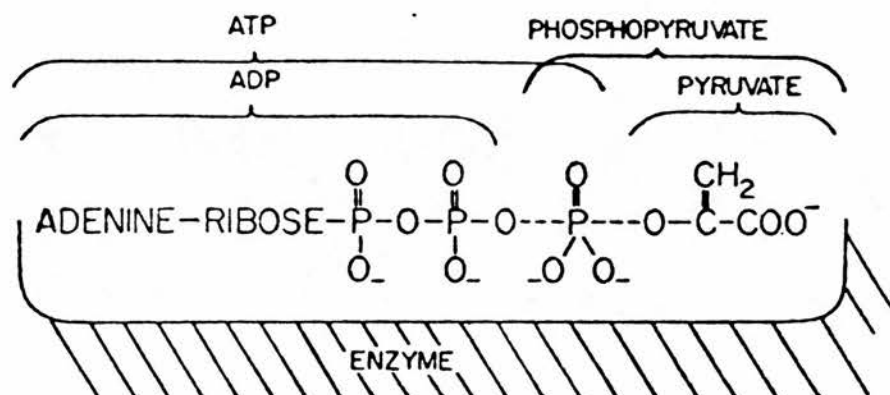


Fig. 4 Schematic illustration of relations among substrates and a transition state for pyruvate kinase (from Reynard et al, 1961).

polarization and enolization of pyruvate. This is consistent with direct phospho transfer from PEP to ADP (Mildvan et al., 1976).

A tentative reaction mechanism for the rabbit muscle enzyme was proposed (Mildvan & Cohn, 1966). This is illustrated in Figs. 6, 7 and 8. In the first step, Fig. 6, the divalent activator ( $Mn^{2+}$ ) is shown to combine with an imidazole group and another ligand Y, which may either be an  $\epsilon$ -amino group or an atypical sulphydryl group. The ligands for the divalent cation have since been identified as Glu 271, Ala 292 and Arg 293 (Muirhead et al., 1987). The combination of cation and ligand results in a conformational change of the protein and yields a binary complex in which the rotational motion of water molecules remaining in the coordination sphere is considerably hindered. The substrate ADP combines with the  $Mn^{2+}$ -enzyme complex (Fig. 7) and donates one ligand to the bound  $Mn^{2+}$ . The substrate PEP donates a ligand to the  $Mn^{2+}$  and also causes a further conformational change which may "open up" the site. The group designated X-H in Fig. 7 is in a position to protonate the vinyl carbon atom of PEP. The structure of the quaternary E- $Mn^{2+}$ -ADP-PEP complex (Fig. 8) is merely the superposition of the structures of the two ternary complexes of Fig. 7. Preceding or during the phospho transfer from PEP to ADP, the group X-H protonates the vinyl carbon atom of PEP, converts it to a methyl group, and thus effects the keto-enol tautomerization (Rose, 1960). The product complex in Fig. 8 indicates that ATP donates two ligands to the bound  $Mn^{2+}$ . The ligand X-H may be the residue Lys 269 as determined by X-ray crystallographic studies (Muirhead et al., 1987).

These mechanistic speculations were designed as a working hypothesis to guide future experimentation. The role of the required monovalent activator was omitted in the formulation although it was shown that the monovalent ion controls the conformation of the ternary complexes. The chemical basis for this control was then not clear.

The use of NMR spectroscopy has also been applied to the study of the function of  $K^+$  in the pyruvate kinase reaction mechanism. The binding of PEP and PEP- analogues to  $Mn^{2+}$ -complexes of muscle pyruvate kinase was investigated (Nowak & Mildvan, 1972). Their results suggested that coordination of the carboxyl

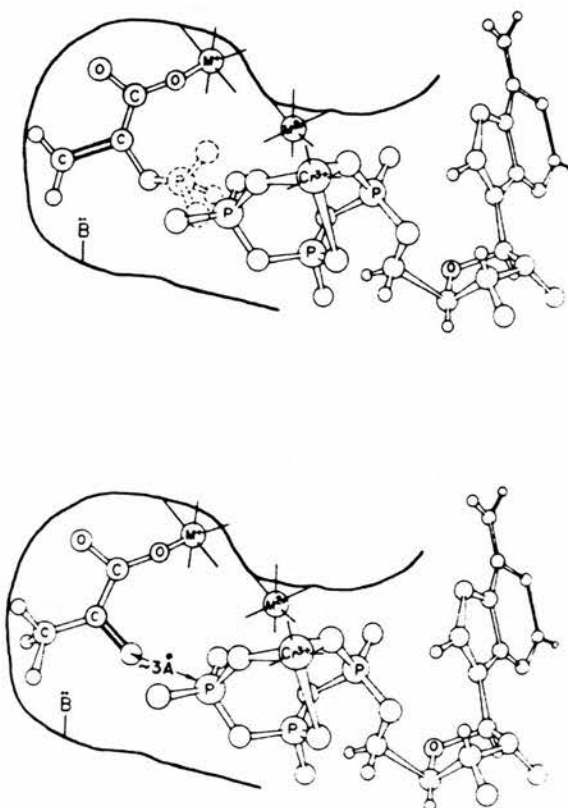


Fig. 5

A) Hypothetical complex of rabbit muscle pyruvate kinase, monovalent ( $K^+$ ) and divalent ( $Mn^{2+}$  or  $Co^{2+}$ ) cations, CrATP and PEP consistent with NMR data and the observed competition between ATP and PEP.

B) Active complex of rabbit muscle pyruvate kinase, monovalent ( $K^+$ ) and divalent ( $Mn^{2+}$  or  $Co^{2+}$ ) cations, CrATP and pyruvate consistent with NMR data and the model above.

The group labelled B is is probably involved in deprotonation of pyruvate.

$Cr^{3+}$ ,  $Mn^{2+}$  and  $Co^{2+}$  are used for their paramagnetic properties.

(from Mildvan et al, 1976).

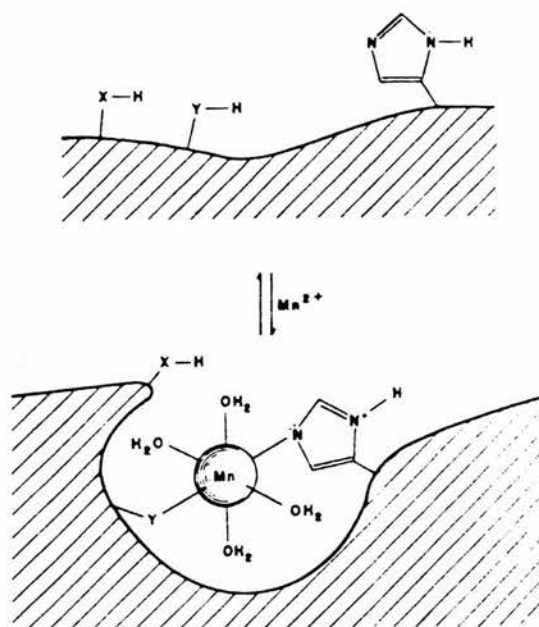


Fig.6

The formation of the binary (E-Mn<sup>2+</sup>) complex in the pyruvate kinase reaction.

Y represents an  $\epsilon$ -amino group or an atypical sulphydryl group.

X-H represents an unidentified proton donor.

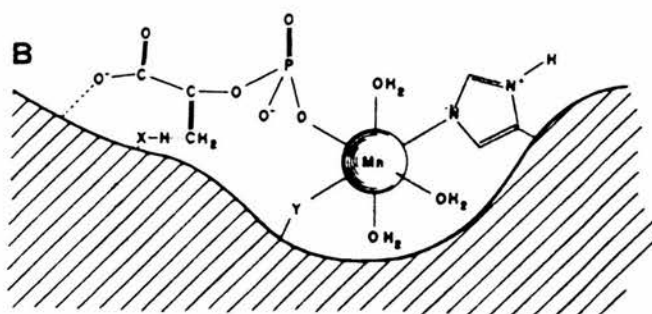
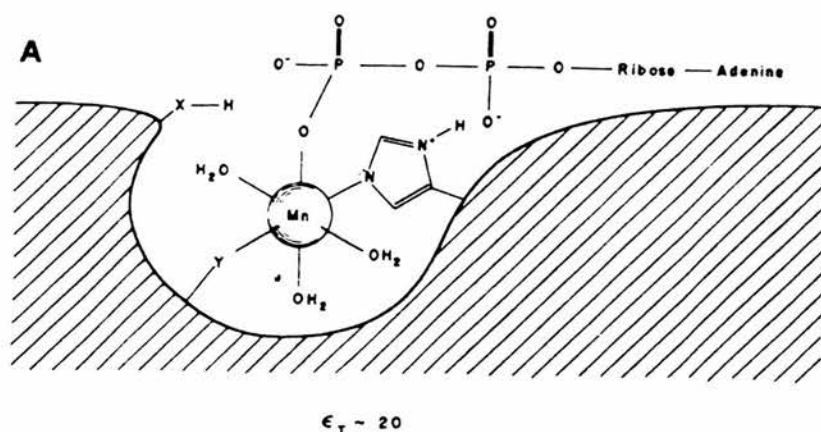


Fig. 7

Postulated ternary complexes in the pyruvate kinase reaction.

A = ADP, B = PEP.

(from Mildvan & Cohn, 1966).

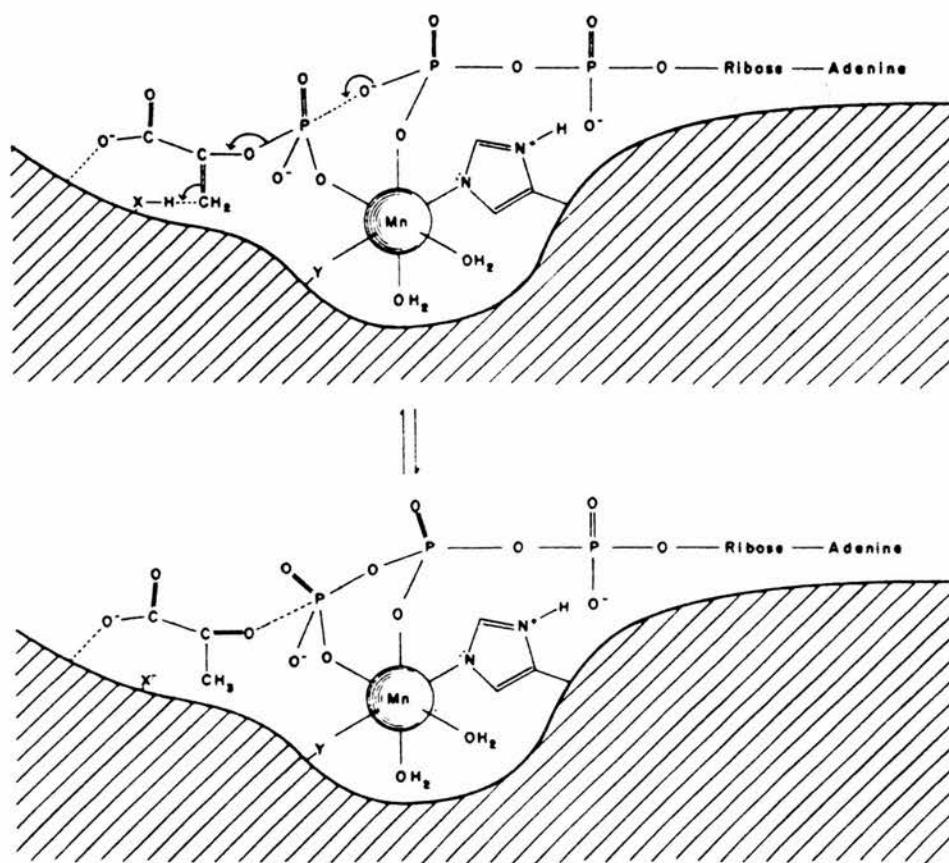


Fig. 8 Mechanism of the conversion of the substrate complex ( $E\text{-Mn}^{2+}\text{-ADP-PEP}$ ) to the product complex ( $E\text{-Mn}^{2+}\text{-ATP-pyruvate}$ ) in the pyruvate kinase reaction. Note the deprotonation of the group  $X\text{-H}$  during the reaction. (from Mildvan & Cohn, 1966).

group of PEP and its analogues by enzyme-bound  $K^+$  changed the conformation of the enzyme- $Mn^{2+}$ -PEP complex to its catalytically active form.

The nature of the phospho group transfer can be probed more deeply by using substrates labelled with various isotopes that can be resolved by NMR spectroscopy. This procedure helped elucidate the phospho transfer mechanism as more likely to occur by an associative mechanism than by a dissociative mechanism (Hassett et al., 1982). In the associative mechanism, bond-making precedes bond-breaking, and the attack of the acceptor group on phosphorus occurs in a transition state in which the central phosphorus is pentacovalent and has trigonal bipyramidal geometry. In the dissociative reaction, bond-breaking leads, and monomeric metaphosphate is formed as a discrete intermediate before it collapses on to the acceptor nucleophile.

If the reaction catalysed by pyruvate kinase were dissociative, one should expect that each of the phospho group donors (PEP in one direction and ATP in the other) would, on binding to the enzyme, dissociate partly or wholly to produce enolpyruvate and metaphosphate or ADP and metaphosphate. In the absence of the cosubstrate acceptor, these enzyme-bound species would simply collapse back to the intact donor molecules. There is no evidence, from positional isotope exchange nor racemization at the  $\gamma$ -phosphorus of ATP, to suggest that the phospho transfer reaction of pyruvate kinase proceeds by a dissociative mechanism (Hassett et al., 1982). Phospho transfer has indeed been found to proceed with inversion of configuration at phosphorus- indicating that the reaction proceeds by an associative mechanism in which the metal ion might be imagined to stabilise the pentacovalent phosphorus transition state via electrostatic interactions (Blattler & Knowles, 1979). These stereochemical approaches provide an access to the otherwise cryptic events that are involved in phospho group transfer within the ternary complexes of pyruvate kinase and its substrates. A study of a number of enzyme-catalysed phosphorus reactions other than that of pyruvate kinase suggest that a mechanism involving simple, direct in-line transfer of the phospho group between the two participating substrates is mechanistically more economic than reactions involving putative phospho-enzyme intermediates (Blattler & Knowles, 1979).

### 1.4.2 PEP ANALOGUES AND THE REACTION MECHANISM

Evidence from the use of PEP analogues, such as phosphoglycolate and phosphoenolketobutyrate, indicated that the enzyme preferentially binds the trianionic form of the compound over the dianionic form. This is consistent with the idea that the phospho group must be fully ionized so it can enter the coordination sphere of the metal during turnover (Dougherty & Cleland, 1985).

The reaction mechanism of yeast pyruvate kinase, particularly the proton transfer reactions, were studied and compared with those of the rabbit muscle enzyme (Ford & Robinson, 1976). They found no difference between the two reactions catalysed i.e. the transfer of a phospho group from PEP to ADP preceded the transfer of a proton from water to enolpyruvate. Two lines of experimental evidence supported this conclusion. First, as no proton transfer from PEP to water occurred in the absence of a functional phospho acceptor (ADP) this suggested that phospho transfer was required for proton transfer from PEP. This did not prove that phospho transfer preceded proton transfer, but was a necessary consequence of such a mechanism. Second, the rate of enolization of pyruvate was 1-2 orders of magnitude faster than the rate of phospho transfer from ATP to form PEP in the reverse reaction. The faster rate would be observed if proton transfer occurred before phospho transfer in the reverse reaction. Therefore, in the forward reaction, proton transfer must follow phospho transfer.

The binding site for PEP must consist of at least two subsites (Mildvan et al., 1971); a phospho binding site and a carboxyl binding site. The bound monovalent cation was thought to bind at the carboxyl binding site as  $K^+$  was found to decrease the affinity of the E- $Mn^{2+}$  for PEP analogues lacking a free carboxyl group (Nowak & Mildvan, 1972).

In other studies (Cottam et al., 1972) where water proton relaxation rate measurements and kinetic studies of ternary complexes were used, it was concluded that the reaction mechanism of pyruvate kinase from *S.cerevisiae* suggested that an ordered addition of substrates to the enzyme was likely. This was confirmed when it was found that in the fructose-1,6-bisphosphate and  $K^+$ -activated pyruvate kinase from *S.cerevisiae*, the reaction mechanism was an ordered type with PEP binding



first, followed by ADP and  $Mg^{2+}$  (MacFarlane & Ainsworth, 1972). Pyruvate release also took place before  $MgATP$ . It was suggested that  $Mg^{2+}$ , by binding separately, bridged the two substrates. Pyruvate kinase is unusual in that it requires two distinct divalent cations. One binds at a site on the protein and the other interacts primarily with the nucleotide phospho acceptor (Fig. 10).

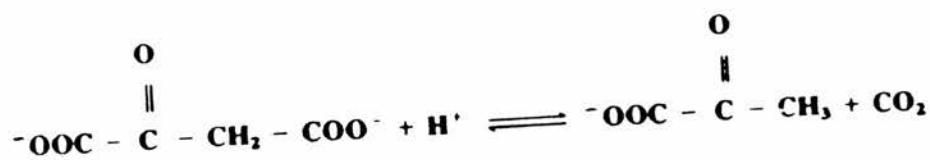
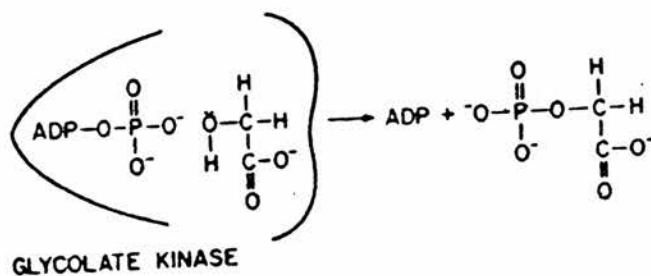
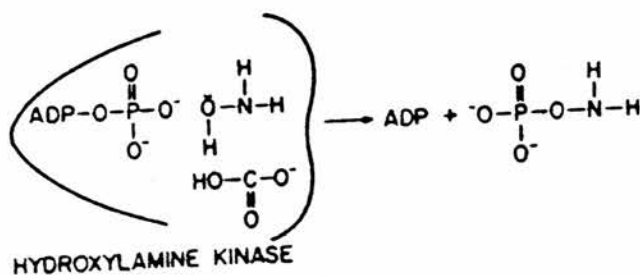
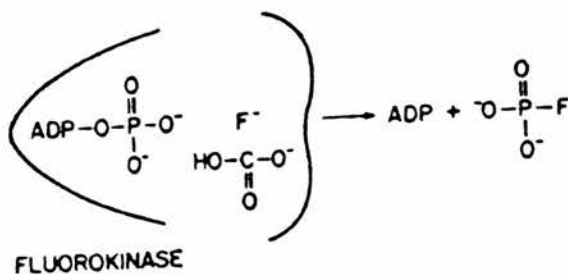
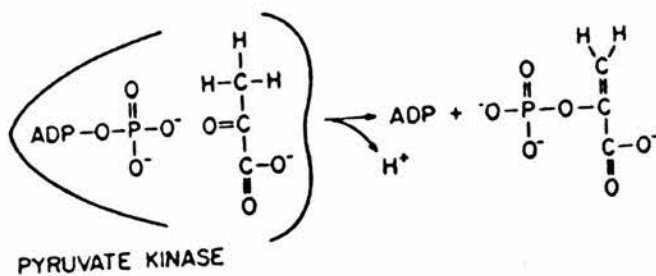
The theory that the essential divalent metal ion did not bind at the active site until after both PEP and ADP were bound was supported by the work of independent groups (MacFarlane & Ainsworth, 1972; Fell et al., 1974). In this respect the yeast enzyme differed from the rabbit muscle enzyme as the latter displayed random order binding of PEP, ADP and  $Mg^{2+}$ .

Tritium exchange and trapping experiments (Robinson & Rose, 1972) suggested that product release was rate-limiting with regard to both the forward reaction as well as the enolization (back) reaction, and that phospho transfer preceded protonation. These authors also suggested that the catalytic mechanisms of the muscle and yeast enzyme were highly similar.

### **1.4.3 SECONDARY REACTIONS CATALYSED BY PYRUVATE KINASE**

It has long been known that pyruvate kinase also catalyses a number of secondary reactions (Boyer 1962). These reactions were studied in some detail (Leblond & Robinson, 1976). The secondary reactions identified were the ATP-dependent phosphorylations of fluoride, hydroxylamine and glycolate. All of these secondary reactions occur at the same site on the enzyme as the phospho transfer. The study of these reactions allowed some inferences to be made regarding the active site of the enzyme and the mechanism of the reaction. Each of the three secondary reactions can be considered to be a nucleophilic attack on the terminal phosphorus of ATP.

Bicarbonate, an essential cofactor for the fluoride and hydroxylamine reactions, may act by occupying a carboxylic subsite normally occupied by PEP or pyruvate, and inducing conformational changes essential for catalysis. The disposition of subsites in the active site of the enzyme for each of the secondary



Oxaloacetate decarboxylase

Fig. 9

Comparison of the primary and secondary reactions of pyruvate kinase.  
(from Leblond & Robinson, 1976).

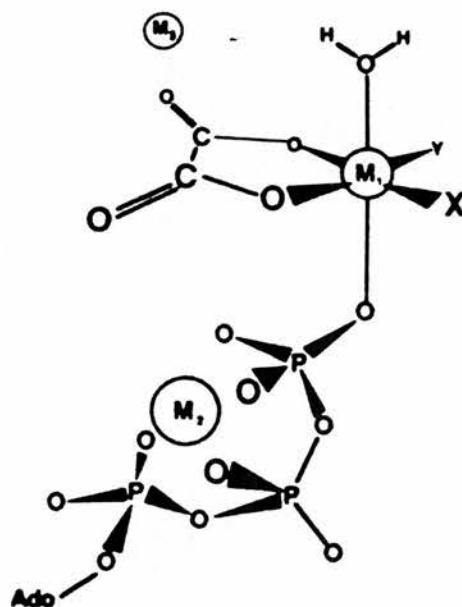


Fig. 10

Schematic drawing of the active site of rabbit muscle pyruvate kinase with oxalate, ATP and the three inorganic cofactors present.

X and Y are likely to be two of the three originally proposed ligands i.e. the carboxyl group of Glu 271 or the carbonyl groups of Ala 292 or Arg 293.

M1 and M2 are divalent cations (usually  $Mg^{2+}$ )

M3 is a monovalent cation (usually  $K^+$ ).

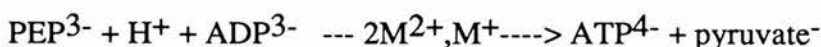
(from Lodato & Reed, 1987).

reactions is illustrated schematically in Fig. 9. Subsequently, a further secondary reaction catalysed by pyruvate kinase has been discovered, the decarboxylation of oxaloacetate (Creighton & Rose, 1976).

#### 1.4.4 OTHER STUDIES

A mechanism for the *reverse* reaction of pyruvate kinase was postulated (Lodato & Reed, 1987). They suggested, from analysis of electron paramagnetic resonance (EPR) data, that a divalent cation at a protein-based site (distinct from the ADP-bound cation) activated the keto-acid substrate through chelation and promoted phospho transfer by simultaneous coordination to the enolate oxygen and to the remaining non-coordinated oxygen from the  $\gamma$ -phospho group of ATP (Fig 10). Electron spin echo envelope modulation (ESEEM) studies suggested a function for the protein-based divalent cation, namely that it coordinated to the phospho group that was transferred from PEP to MgADP during catalytic turnover (Tipton et al., 1989). The ESEEM technique of pulsed EPR spectroscopy resolves superhyperfine interactions that are obscured by the intrinsic line width of the continuous wave EPR signal. As a result, paramagnetic metal cation probes such as  $Mn^{2+}$  can provide information on the nuclei of atoms not directly bound to the probe.

In the normal reaction, the inorganic cations together with the proton that adds to the enolate of pyruvate, balance the net negative charges carried by the substrates at neutral pH.



Extensive isotope trapping studies by a number of workers over many years have now revealed details of the pyruvate kinase reaction (Rose, 1960; Rose & Kuo, 1989; Kuo & Rose, 1978). The catalytic reaction occurs in separate phosphate and proton transfer stages:-

$K^+$ ,  $Mg^{2+}$  and  $MgADP$  are required for the phospho transfer steps, and  $K^+$  and  $Mg^{2+}$  with allosteric stimulation by  $MgATP$  are important for proton transfer.

The use of isotope methods with  $^3H$ -labelled water have been used to identify the proton donor and determine when in the sequence of the catalytic cycle it was generated (Rose & Kuo, 1989).

#### 1.4.5 DISSECTING THE REACTION

The pyruvate kinase reaction is best described by the succession of two reactions:

$H^+ + ADP + PEP \longrightarrow ATP + \text{enolpyruvate}$

$\text{enolpyruvate} \longrightarrow \text{pyruvate}$

The evidence for this was as follows:

- 1)  $^3H$  exchange between pyruvate and water occurred in the absence of nucleotides (Rose, 1960).
- 2) The enzyme catalysed the stereospecific ketonization of added enolpyruvate and phosphorylated a variety of acceptors (Kuo & Rose, 1978).
- 3) Significant amounts of enolpyruvate bound to the enzyme have been detected (Seeholzer et al., 1991).
- 4) The equilibrium constants for both proposed half reactions have been determined (Seeholzer et al., 1991).

Previous studies (Rose & Kuo, 1989) showed that:

- 1) The enzyme, not the medium, was the immediate source of protons for the ketonization step.
- 2) The proton donating group was fully formulated prior to the kinase step.
- 3) The donor group was an  $\epsilon$ -amino group of a lysine residue, probably the lysine 269 suggested by Muirhead (1987).
- 4) Glutamate 271 was appropriately placed to conduct protons between the medium and the donor.

### 1.4.6 ISOTOPE INHIBITION

When D<sub>2</sub>O was used as the solvent for the enzyme it had a profound effect on the kinetics of the reaction. The effect of D<sub>2</sub>O on  $k_{cat}$  in the steady state suggested that the forward rate was determined by hydrogen transfer to the enzyme (Rose et al., 1991). Further evidence indicated that the kinetically important proton in question was the proton used for ketonization of enolpyruvate i.e. the substrate proton.

The ketonization half-reaction was believed to occur within the domain of the eight alternating helix and strand sequences, the alpha/beta barrel, that constitutes about half the mass of each of the four identical subunits of the enzyme.

The pyruvate kinase reaction, as measured by pyruvate production, has long been known to show a large D<sub>2</sub>O inhibition (Kayne & Suelter, 1968). The broad pH range over which this effect is seen would seem to rule out some general medium effect acting to alter the distribution of conformational states (Rose & Kuo, 1989). Its magnitude, greater than five-fold, would imply a primary kinetic effect.

This isotope effect was shown to derive from the reprotonation of the product form of the enzyme:



In fact, this step may be *the* rate-limiting step in the steady state.

The assignment of lysine 269 as the donor was made from a crystal of cat muscle pyruvate kinase infused with PEP since no other prototropic amino acid residue seemed suitably located in the region designated as the active site (Muirhead et al., 1986). Note that the molecule on which the donor will act is not PEP but enolpyruvate and that the process of getting to enolpyruvate from PEP might produce significant changes in the PEP binding site. A lysine residue with a pKa of 9.1 in the free enzyme was assigned as being the catalytic base responsible for enolization (Dougherty & Cleland, 1985). From other studies (Seeholzer et al., 1991) it can be shown that the pKa of this lysine remains unchanged by pyruvate binding.

Despite many studies suggesting the role of enolpyruvate as a bound intermediate in the pyruvate kinase reaction, direct evidence for its occurrence was lacking until its isolation as a bromine derivative (Seeholzer et al., 1991). The

technique used exploited the high reactivity of enolpyruvate with bromine compared with the slow rate of ketonization to pyruvate or spontaneous generation of enolpyruvate from pyruvate. Bromine in acid was therefore used to trap enolpyruvate which could be liberated and measured upon denaturation of the enzyme.

#### 1.4.7 SUMMARY

A summary of the findings to date allow a catalytic mechanism for pyruvate kinase to be proposed (Muirhead, 1986). Pyruvate kinase catalyses the transfer of the phospho group of PEP to MgADP via an enolate intermediate that is then protonated to form pyruvate. The enzyme is unique among kinases for its absolute requirement for enzyme-bound cations,  $Mg^{2+}$  and  $K^+$ . The divalent cation coordinates substrates in the large active site pocket. PEP possibly only binds correctly in the presence of the divalent cation. The binding of  $Mg^{2+}$  also enhances the binding of the phospho group. Thus  $Mg^{2+}$  assists in orientating the phospho groups of ATP and ADP to allow phospho transfer between ATP and pyruvate and between ADP and PEP, respectively. The nucleotide-bound  $Mg^{2+}$  serves to reduce the electrostatic repulsion between the phospho donor ( $\gamma$ -phospho, or PEP) and the nucleophile ( $\beta$ -phospho or enolate), as well as to position the  $\alpha$  and  $\beta$  phospho groups at the active site. The phospho donor and acceptor bind at sites such that phospho transfer can occur directly from donor to acceptor without a conformational change in the enzyme being necessary to bring the two sites closer together. The phospho transfer reaction probably occurs by an in-line associative mechanism, with inversion of configuration. The monovalent cation may also be involved in phospho transfer by polarizing the phospho group to be transferred. The enolization reaction is brought about by the interaction of a base, possibly lysine 269, with the methyl group.

A sequence of events for the overall reaction can be postulated (Fig 11).

**Step 1:** PEP and ADP bind (not shown in Fig. 11).

- a) A phospho group is essential for the correct binding of pyruvate.
- b)  $K^+$  binds to glutamate 363, glutamine 328 and to a carboxyl group on PEP.
- c) A phospho group binds near serine 242, arginine 72 and arginine 293.



d) PEP displaces a molecule of water from the inner coordination sphere of  $\text{Mg}^{2+}$ .

e) The phospho group is transferred to ADP.

**Step 2:** An ATP-enolate intermediate is formed

a) Enolate is stabilised by  $\text{Mg}^{2+}$ .

b) Enolate of pyruvate and ATP are formed.

**Step 3:**

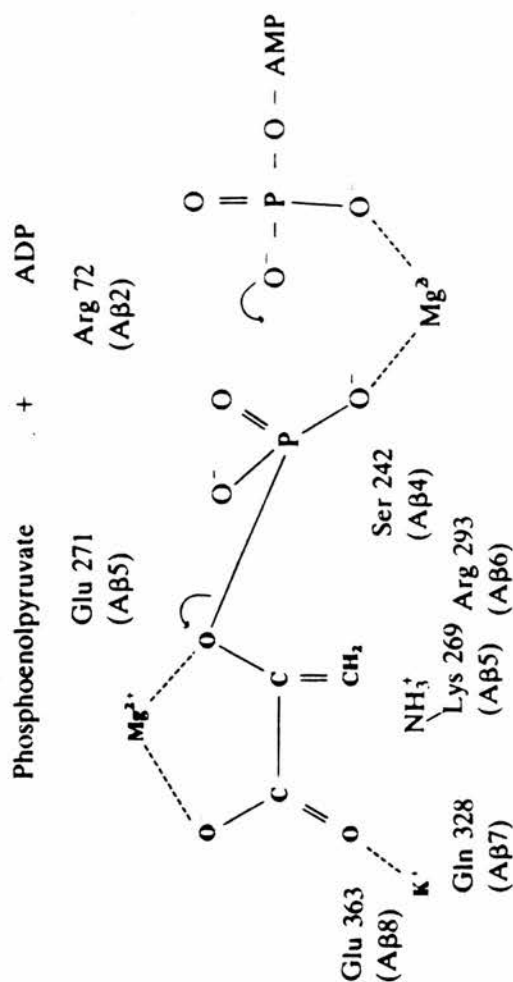
Lysine supplies a proton leading to the formation of pyruvate and ATP.

**Step 4:**

Water enters and outer sphere complexes are formed.

**Step 5:**

Pyruvate leaves, giving an ATP complex.

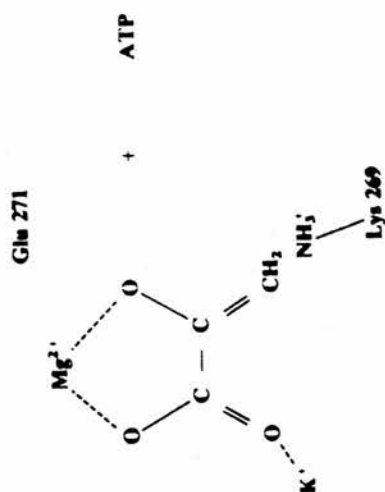


**Step 2** ATP-enolate intermediate is formed.

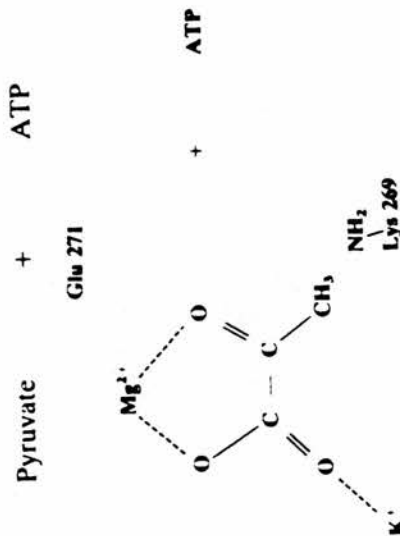
(a) Enolate is stabilized by  $Mg^{2+}$ .

(b) Enolate of pyruvate and ATP formed.

Fig. 11 Pyruvate kinase reaction mechanism as determined from X-ray crystallographic studies (from Muirhead, 1987).



**Step 3** Lysine supplies a proton leading to the formation of pyruvate and ATP.



**Step 4** Water enters and outer sphere complexes are formed.  
**Step 5** Pyruvate leaves, giving an ATP complex.

## 1.5 THE ACTIVE SITE

The residues important in catalysis, and substrate binding and orientation, in many forms of pyruvate kinase, have been determined by a variety of techniques. Chemical modification with substrate analogues or compounds that react specifically with a certain type of amino acid residue were once the only way of determining residues essential for activity. These techniques have now largely been superseded by spectroscopic studies which have the advantage of not altering the enzyme during measurement and so can relay information about the actual events that are occurring at the active site. More detailed information has been obtained by the use of X-ray crystallography of the cat skeletal muscle enzyme (Muirhead et al., 1987). From these studies it was found that the active site was located in a cleft between domains A and B. The active site was found in electron density maps by soaking crystals of pyruvate kinase in solutions containing divalent metal ions and PEP at pH8. This section is followed by chapters on substrate specificity (1.6), the divalent cation (1.7) and the monovalent cation (1.8).

### 1.5.1 EARLY STUDIES

The first attempt to describe an active site for pyruvate kinase was by Reynard et al. (1961) in which they diagrammatically represented the active site as two adjacent overlapping sites; one for pyruvate/phosphoenolpyruvate and another for ADP/ATP, with the overlap being most pronounced at the site of phospho transfer (Fig 2). A tentative role for the metal ions,  $Mg^{2+}$  and  $K^{+}$ , was also suggested although they indicated that  $K^{+}$  may not be needed in the catalytic reaction at all but may simply be required for the protein to adopt its proper conformation. Indeed,  $K^{+}$  or other monovalent cations have been found not to be a necessary requirement for full catalytic activity in many pyruvate kinase enzymes, particularly those from bacterial sources. This may reflect differences in the three dimensional conformations adopted by eukaryotic and prokaryotic forms of the enzyme (Benzimen, 1969; Ozaki & Shiio, 1969; Chuang & Utter, 1979). The susceptibility of the terminal phospho group to nucleophilic attack may be enhanced by the presence of  $Mg^{2+}$  (Reynard et al., 1961).

### 1.5.2 INHIBITION-PROTECTION STUDIES

One of the earliest ways in which information about the active site was obtained, prior to the widespread use of X-ray crystallography and site-directed mutagenesis, was inhibition/protection studies. This technique relies on incubating the enzyme of interest with a compound known to react only with certain specific amino acid sidechains to produce a covalently bound, usually inactive, inhibitor-enzyme complex. By including substrates, individually or in various combinations, prior to the addition of inhibitor and determining how much protection from inhibition these treatments afforded, residues essential for binding substrates and products or essential for catalytic activity could be identified. This approach has been used with pyruvate kinase from various sources with varying degrees of success.

Tanaka et al. (1967) used the sulphydryl inhibitor p-chloromercuribenzoate (p-CMB) and found that the allosteric isoenzyme from rat liver was thirty times more sensitive to inhibition by this reagent than the non-allosteric rat muscle enzyme. However, Jacobsen and Black (1971) found no significant difference in the reactivity of the allosteric human red blood cell enzyme and non-allosteric rabbit muscle enzyme to iodoacetamide. If the kinetic similarity of the rat liver and human erythrocyte enzymes is a reflection of structural similarity, this suggested that differences exist in the environment of the reactive group of the isoenzymes in the absence of substrates or cations. These differences can be detected with the relatively large p-CMB molecule, but are insufficient to have any effect on reaction with the much smaller iodoacetamide molecule. The rabbit muscle enzyme can be protected against p-CMB inhibition by PEP, ADP and  $Mn^{2+}$  (Mildvan & Cohn, 1965; 1966). Jacobsen and Black however, found that PEP, ADP and  $Mg^{2+}$  alone offered no protection against iodoacetamide inhibition of the rabbit muscle enzyme but that  $K^{+}$  and  $MgADP$  did protect. These experiments demonstrate the difficulty of interpreting what is actually occurring within the enzyme. Conflicting data are often produced in chemical modification experiments. However, it appears to be the case in these experiments that certain substrates and effectors can protect the enzyme from chemical modification and hence a flexible environment at the active site can be inferred. That

identical data are not produced from all the isoenzymes studied means that differences in the isoenzyme active site do occur upon substrate/effector binding.

2,4,6-trinitrobenzene-1-sulphonic acid (TNBS, picrylsulphonic acid) has been used to inactivate lysine sidechains in the active site of rabbit muscle pyruvate kinase (Hollenberg et al., 1971). They observed protection against inactivation by ADP,  $Mg^{2+}$  and  $K^{+}$  separately. TNBS has also been used to inactivate four lysine residues essential for the activity and cooperativity of the enzyme from *S.carlsbergensis* (Roschlau & Hess, 1972). Protection against inactivation was given by PEP, ADP and  $Mg^{2+}$ . Fructose-1,6-bisphosphate did not protect against inactivation.

Lysine sidechains have also been inactivated in the rabbit muscle enzyme with pyridoxal 5'-phosphate, due to Schiff base formation (Johnson & Deal, 1970). Protection against inactivation was afforded by PEP, ADP and ATP. Two ionisable groups susceptible to inhibition and deduced to be involved in  $Mn^{2+}$  binding were identified (Mildvan & Cohn, 1966). Jacobsen and Black (1971) argued that if these groups are also those found to be susceptible to inhibition by iodoacetamide in their study then they can justifiably be included within the active site as these sidechains are protected from inhibition by substrates and cations. Subsequent X-ray crystallographic studies suggest that the ligands for the divalent cation are Glu 271, Ala 292 and Arg 293 (Muirhead et al., 1987).

Data from TNBS inhibition of rabbit muscle pyruvate kinase (Hollenberg et al., 1971) suggested that the four lysyl- $\epsilon$ -amino groups inhibited by this compound were essential for catalytic activity and that these groups were involved in the binding of ADP by the enzyme. Of the ligands identified by X-ray crystallographic studies as being involved in ADP binding, only residue 114 is a lysine. Lysine 269 however, is implicated as the proton-donating catalytic residue (Muirhead et al., 1987). It should also be noted that three arginine residues (Arg 72, 119 and 293) were also implicated as being important for ADP binding, and these could have been labelled by TNBS and mistaken for the other lysine residues.

Thallium and manganese NMR binding studies indicated that the  $Mg^{2+}$  and  $K^{+}$  binding sites are close together in the rabbit muscle enzyme (Kayne & Reuben,

1970). The possibility that  $K^+$  and MgADP protect against inactivation is more likely due to a shielding effect or a minor conformational change in the vicinity of the active site.

Flashner et al.(1972) confirmed the findings of other workers when they stated that pyruvate kinase has four active centres and that modification of the enzyme with 5,5'-dithiobis (2-nitrobenzoic acid)(DTNB) did not appreciably alter the active site despite it becoming otherwise catalytically inactive. The reagent used appeared only to react with eight sulphhydryl groups per tetramer, four not being required for activity and four being essential for activity.

Inhibition studies with DTNB and iodoacetamide on the pyruvate kinase from *Saccharomyces carlsbergensis* allowed the identification of thiol groups that, when chemically altered, affected the catalytic and allosteric properties of the enzyme (Wieker & Hess, 1972). They produced a model in which they identified three cysteine residues per subunit (labelled X1-3 in Fig 12) as essential for activity. The model presents the enzyme after substitution at the most reactive of the three cysteine residues studied, X1. The group X1 is localised outside the active and allosteric site, but is close enough to the active site such that substitution by a group R can influence the binding of the substrate depending upon the size and/or charge of R. The group X2 is part of the active site, together with one other amino acid residue or a group of several amino acid residues, A. The pH dependence of the pyruvate kinase reaction revealed that a group with  $pK_a=9.0$  is involved in substrate binding and that this group becomes more acidic in the enzyme-substrate complex,  $pK_a=8.4$  i.e. this group is ionised both in the free enzyme and the enzyme-substrate complex. Since these  $pK_a$  values are consistent with those of cysteine residues, it can be assumed that the binding of substrates occurs at the group A and that the binding properties of group A are determined by the state of protonation of X2, probably via a hydrogen bond between A and X2.

The group X3 is part of the allosteric site together with another amino acid residue or group of several amino acid residues, B. The substitution at X3 may cause an inhibition by allosteric interactions changing the properties of the active site. This inhibition can be overcome by fructose-1,6-bisphosphate, and therefore, the direct binding of the activator has to occur at an additional group other than X3. This group,

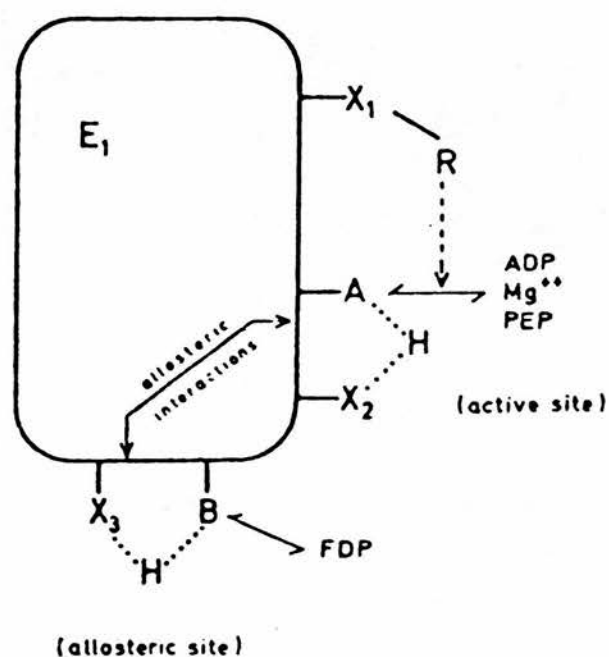


Fig. 12 Schematic presentation of the functional thiol groups of one subunit of pyruvate kinase (for explanations see text)  
(from Wieker & Hess, 1972)



B, may be attached to X3 by a hydrogen bond. As the sequence of the *S.carlsbergensis* enzyme is not known, it is impossible to know precisely the location of the cysteine residues referred to. It is probable that chemical modification of any residue will result in a decrease in activity due simply to steric hindrance. From what is known of the seven cysteine residues per subunit in the *S.cerevisiae* enzyme, as revealed by computer modelling based on a knowledge of the X-ray crystal structure, none of these residues are well placed for an essential catalytic role.

In separate experiments, using inhibition-protection of *S.carlsbergensis* pyruvate kinase with TNBS, (Bornman et al., 1972; Roschlau & Hess, 1972) lysine and histidine residues and the carboxyl groups of either glutamic acid and/or aspartic acid were found to be essential for enzymatic activity. Thus, the groups A and B may be composed of these amino acid residues.

### 1.5.3 NMR AS A PROBE OF THE ACTIVE SITE

The powerful technique of NMR spectroscopy has been applied to the study of the muscle pyruvate kinase active site since the early 1970s (Nowak & Mildvan, 1972). These authors used competitive analogues of PEP and measured the longitudinal and transverse relaxation rates of their protons and phosphorus atoms to analyze reactions at the enzyme active centre. They concluded that substrates become more tightly bound as the reaction centre phosphorus is approached (i.e. the phosphorus atom destined to take part in the phospho transfer reaction). Such immobilization would allow orientational or entropic effects to operate in enzyme catalysis. They also described diagrammatically a composite model of the ternary analogue and normal substrate complexes of pyruvate kinase, indicating likely conformations around the active site (Fig 13). A role for  $K^+$  is also noted. The geometry of the composite model is based on kinetic and binding data and on distances calculated from nuclear relaxation data on the  $Mn^{2+}$ -activated enzyme. Motion of the analogues (and by implication, the natural substrate PEP) is hindered at the reaction centres where protonation and phospho transfer are taking place.

An early consensus as to the likely structure of the active site suggested a relatively rigid conformational arrangement of the two substrates and two activating

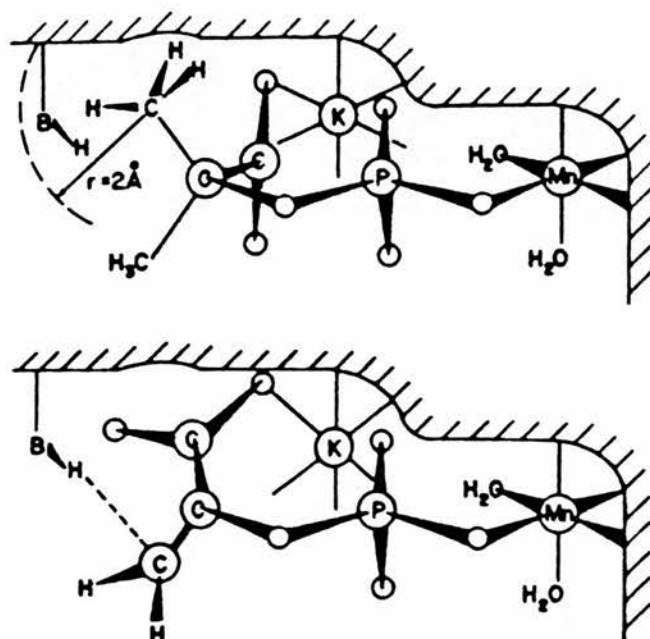


Fig. 13 Upper figure- a composite model of the ternary analogue complex of rabbit muscle pyruvate kinase ( $E\text{-Mn}^{2+}\text{-phospholactate-K}^{+}$ ) based on NMR data. The van der Waals radius of the methyl group of phospholactate is shown to interact with the group BH which protonates PEP. Lower figure- ternary complex as above except that the substrate PEP replaces the substrate analogue. (from Nowak & Mildvan, 1972).

cations (Kayne, 1973). Accessibility to the solvent was assumed to be good due to the high turnover number ( $250\text{s}^{-1}$ ), the report of the stereospecific reduction of pyruvate and the results of tritium exchange experiments discussed elsewhere. In contrast however, an exclusion of solvent ( $\text{H}_2\text{O}$ ) is implied by the limited amount of  $\text{H}_2\text{O}$  in the  $\text{Mn}^{2+}$  coordination sphere measured by proton relaxation rate enhancements of the binary complex, and by the fact that  $\text{H}_2\text{O}$  would make an excellent phospho acceptor if available to the group undergoing transfer. Further NMR studies indicated that the metal- $\gamma$  phosphate distance of 5Å (Sloan & Mildvan, 1976) for pyruvate kinase-bound ATP was equal to that found for the phosphorus atom of PEP and  $\text{Co}^{2+}$  on pyruvate kinase (Melamud & Mildvan, 1975) which was consistent with the overlap in space of the PEP phosphorus and the  $\gamma$ -phospho group of ATP at the active site.

#### 1.5.4 ADP ANALOGUES AS PROBES OF THE ACTIVE SITE

The ADP analogue 5'-p-fluorosulphonylbenzoyl-adenosine (FSBA) reacts with the active centre of the *S.carlsbergensis* pyruvate kinase and also at a secondary site (probably the other nucleotide binding site on the enzyme) to produce an inactive complex (Likos et al., 1980). The reagent reacted with both lysine and tyrosine residues and these have therefore been considered to be important residues in the nucleotide binding site.

Other ADP and ATP analogues have also been used in an attempt to further characterise the nucleotide binding site in pyruvate kinase. Rabbit muscle pyruvate kinase was inhibited by 8-thiocyano-ATP (Scheiner-Bobis et al., 1992). Use of the ADP analogue 2',3'-dialdehyde-ADP has also been demonstrated (Bezares et al., 1987). Studies using the ATP analogue 8-(4-bromo-2,3-dioxobutyl)thiol-adenosine 5'-triphosphate resulted in the inactivation of the rabbit muscle enzyme due to covalent modification of cysteines 48, 62 and 151. Protection against inactivation was given by PEP,  $\text{K}^+$  and  $\text{Mn}^{2+}$  to cysteines 48 and 151 only, indicating that these two residues are involved in the maintenance of enzyme activity, possibly through

substrate binding (Vollmer & Colman, 1990). According to Muirhead et al. (1987), the primary residues involved in binding the phosphate groups of ADP in the cat muscle enzyme are Cys 455, Lys 114, Arg 119 and possibly Arg 72 and Arg 293. Residues involved in binding the adenine ring of ADP are Ile 118, Val 215, Val 220 and Phe 243. All of these residues are conserved in the yeast enzyme except Val 220 which is changed to leucine. The fact that three cysteine residues have reacted with the ADP analogue does not mean that they are necessarily involved in ADP binding. The sulphhydryl groups are the most reactive sidegroups in proteins (Scopes, 1987) and would be expected to react with any reactive ADP-analogue under the conditions of the assay.

### 1.5.5 OTHER SPECTROSCOPIC STUDIES OF THE ACTIVE SITE

Studies by Lodato and Reed (1987) exploited the intrinsic selectivity of the protein-based site for  $Mn^{2+}$  and of the nucleotide-based site for  $Mg^{2+}$  for analysis by electron paramagnetic resonance spectroscopy (EPR) of the ligands for  $Mn^{2+}$  at the protein-based site. They used oxalate, a structural analogue of the enolate form of pyruvate, as a surrogate for the reactive form of pyruvate in complexes with enzyme,  $Mn^{2+}$ ,  $Mg^{2+}$  and ATP. The results showed that oxalate is bound at the active site as a bidentate chelate with  $Mn^{2+}$ . Further experiments revealed that ATP bridges  $Mn^{2+}$  and  $Mg^{2+}$  at the active site. The authors were able to postulate a mechanism for the reverse reaction of pyruvate kinase by analysis of the structure of the enzyme- $Mn^{2+}$ -oxalate- $Mg^{2+}$ -ATP complex. They also described a model of the conformation of substrates at the active site (Fig 10).

The essential lysine residue present in the active site of the cat skeletal muscle pyruvate kinase (Muirhead et al., 1986) has also been identified in bovine and rabbit sources (Johnson et al., 1969; Bezares et al., 1987) and in *S.cerevisiae* (Imarai et al., 1988) by modification with TNBS. Protection experiments suggested that these residues were related to the nucleotide-binding site of the enzyme. The lysine residue in question was identified by peptide analysis as lysine 337 in *S.cerevisiae* (see Table 1).

Electron spin echo envelope modulation (ESEEM) spectroscopy studies of

rabbit muscle pyruvate kinase in the presence of substrates, products and cofactors indicated that ATP was directly coordinated to  $Mn^{2+}$  at the protein based site (Tipton et al., 1989). Furthermore, the close proximity of the monovalent cation and the protein based divalent cation was also demonstrated. From the ESEEM studies a picture of the active site emerged in which it appeared to be a flexible and dynamic environment. In addition to observing coordination of ligands to the protein based metal ion, the authors determined that the position of the catalytic lysine in the active site was sensitive to the nature of the monovalent cation and to the presence of other species in the active site. Furthermore, the monovalent cation appeared to play a role in determining active site geometries.

The high density of negative charge carried into the active site by the anionic substrates is balanced by the triad of inorganic cations that specifically activate the enzyme.

Recent data on the pyruvate kinase catalysed decarboxylation of oxaloacetate indicated that metal coordinated water was displaced during the binding of substrates and effectors (Kiick & Cleland, 1989).

Knowledge of the conformations and arrangement of substrates bound at the active sites of enzymes can yield valuable information as to the mechanism of enzyme action. Although the active site and mechanism of action of pyruvate kinase have been a subject of study for many years, geometric information on the active site has thus far been incomplete. X-ray crystallographic studies have been able to unambiguously locate the binding sites of the two substrates. The thermodynamic and kinetic properties of complexes detected in the crystallographic state are difficult to determine, leaving open the possibility that they are not functional in catalysis. Information from NMR studies (Mildvan et al., 1976) using information from two paramagnetic probes, allowed the construction of the total substrate geometry at the active site of the rabbit muscle pyruvate kinase enzyme (Figs 8 and 10).

### 1.5.6 SUMMARY

A variety of studies have identified many residues important in catalysis and substrate binding. Early studies utilised residue-specific modifying agents to identify

ligands important in catalysis. These studies were limited largely to the identification of highly reactive residues such as lysine, arginine, histidine and cysteine. Later studies exploited more sensitive spectroscopic techniques. This allowed highly sensitive measurements to be made and resulted in the determination of the total geometry of the active site. X-ray crystallographic studies have identified the specific ligands involved in substrate binding and catalysis.

Analogues of the substrates ADP and PEP, and the metal cations  $Mg^{2+}$  and  $K^{+}$ , allowed theories of the structure and disposition of ligands at the active site to be postulated and tested.

In summary, ADP appears to be coordinated to an enzyme-bound divalent cation and to another divalent cation not linked to the enzyme. The PEP molecule is coordinated to the monovalent cation by its carboxyl group. As a result, the phospho group of PEP is sufficiently close to undergo transfer to ADP to form ATP and pyruvate. A proton is donated to the enol-form of the product, which is postulated to exist in a transition state complex with the enzyme, via lysine 269. The proton is ultimately derived from the solvent and is transferred to the active site by a proton relay mechanism probably involving Glu 271. This results in the formation of the keto-form of the product, which is subsequently released.

## 1.6 SUBSTRATE SPECIFICITY

Early studies on the enzyme revealed that pyruvate kinase has a broad specificity towards the nucleotide substrate of the reaction (Boyer, 1962). Specific activities and Michaelis constants for several diphosphates have been determined (Plowman & Krall, 1965). The maximum velocities at pH 7.5 were in the order: ADP = GDP > IDP > dADP > UDP > CDP > dCDP with CDP having 30% and dCDP having 0.3% the activity of ADP. However, the  $K_M$  ADP was a factor of four lower than for GDP or any of the others. This suggests that the nucleotide binding portion of the active site does not have very stringent steric (or catalytic) requirements. Studies on ADP analogues shows that the phosphate ester portion of the molecule does have some structural restrictions (Setondji et al., 1971). Reversible inhibitors of PEP-utilising enzymes have been used to characterise the substrate binding properties of these enzymes. Useful compounds include 1-hydroxy-1-cyclopropane carboxylic acid phosphate (O'Leary et al., 1981), phosphoglycolate, phospholactate and phosphoenol-a-ketobutyrate (Rose, 1970).

Work using PEP analogues indicated quite a high degree of specificity towards the phosphate donor component of the reaction. There is no carbon asymmetry in the enolpyruvate or pyruvate, but the introduction of deuterium and tritium into the molecule allowed a determination of any stereospecificity in the reaction. By using phosphoenol-a-ketobutyrate as the substrate, and studying the stereochemistry of the product, it was discovered that proton addition to PEP occurs from a specific direction i.e. the 2-si face of the molecule (Rose, 1970).

Dead-end inhibition of the pyruvate kinase catalysed decarboxylation of oxaloacetate by the physiological substrate PEP indicated that PEP binds only to the enzyme-metal ion complex and not to the free enzyme (Kiick & Cleland, 1989).



## 1.7 THE DIVALENT CATION

The necessity for a divalent cation in the pyruvate kinase reaction has long been known (Boyer et al., 1954). It is now known that two divalent cations are required for catalysis of the enolization of pyruvate in the presence of ADP. One divalent cation is bound directly to the enzyme and interacts with the bound ATP through an intervening water ligand (site 1). The second divalent cation is directly coordinated to the phospho groups of ATP and does not interact with the enzyme (site 2) (Gupta et al., 1976). A requirement for two divalent cations per active site has previously been suggested for PEP carboxylase (Foster et al., 1967). A dual divalent cation requirement for pyruvate kinase is consistent with all of the early and more recent structural and binding data on this enzyme (Mildvan, 1974). The interaction of the metal ions and the substrates are shown in detail in Fig 10, derived from NMR studies and model building.

In *vivo*,  $Mg^{2+}$  serves as the divalent metal ion. In *vitro* however,  $Mn^{2+}$ ,  $Co^{2+}$  and  $Ni^{2+}$  can all serve (Robinson & Rose, 1972; Melamud & Mildvan, 1975; Kwan et al., 1975).

The role of the enzyme-bound metal is probably to adjust the protein conformation and to orientate water ligands near the phospho groups of the substrate (Suelter & Melander, 1963). More specifically, the enzyme-bound  $M^{2+}$  serves to position the substrates and influences the electronic distribution at the C2-O bond of pyruvate and the acidity of the C3-H. The nucleophilic C2-O of the enolpyruvate carries out the in-line displacement of the  $\beta$  bridge oxygen of ATP to form PEP and ADP, in the reverse reaction (Hasset et al., 1982). The enzyme-bound divalent cation has also been implicated in the cooperative binding of PEP to the enzyme- $Mn^{2+}$  complex (Nowak & Lee, 1977).

The role of the nucleotide-bound metal is probably to adjust the polyphosphate conformation and to polarise, and thereby increase the electrophilicity of, the  $\gamma$ -phospho group of ATP which is in molecular contact with the carbonyl oxygen of pyruvate, as determined by NMR spectroscopy (Mildvan et al., 1976). The nucleotide-bound metal has no direct role in adjusting the protein conformation,

since its role can be filled by  $\text{Cr}^{3+}$  which is substitution inert and therefore cannot acquire ligands from the enzyme. Another role of the nucleotide-bound metal is to activate the base which deprotonates pyruvate in the reverse reaction (Robinson & Rose, 1972).

It was found that  $\text{Ca}^{2+}$  is an activator of the enzyme at low  $\text{Mg}^{2+}$  and  $\text{Ca}^{2+}$  concentrations; otherwise it is an inhibitor at the protein-based site (Boiteux et al., 1983). These effects can be explained by assuming that  $\text{Ca}^{2+}$  has the same binding properties as  $\text{Mg}^{2+}$  but does not allow a catalytic turnover.

Crystallographic studies have identified the  $\text{M}^{2+}$  binding sites as oxygen atoms of the protein and substrates (Muirhead et al., 1986). These are contained in an alpha/beta barrel domain of the enzyme. The residues involved were found to be the carboxyl group of Glu 271, and the carbonyl oxygens of Ala 292 and Arg 293. A charged lysine 269 is believed to be well-placed for transfer of a proton to the 2-si face of enolpyruvate (Rose, 1970).

A variation in the rate of the enolization reaction was seen when different divalent cations were used to activate the enzyme. The rates decreased in the order  $\text{Co}^{2+} > \text{Ni}^{2+} = \text{Mn}^{2+} > \text{Mg}^{2+}$  which correlated with the increasing pKa of the water ligands of these divalent cations indicating that the electronegativity of the nucleotide-bound, rather than that of the enzyme-bound metal, determined the rate of enolization.

$^{25}\text{Mg}^{2+}$ -NMR has recently been adapted as a useful spectroscopic tool in the study of  $\text{Mg}^{2+}$  interactions with macromolecules. Such studies of magnesium-binding proteins can provide valuable information, such as pKa values for binding-site ligands, binding constants and exchange rates for the  $\text{Mg}^{2+}$ -protein complexes, and  $\text{Mg}^{2+}$  binding to genetically altered enzymes. Such studies have also been applied to rabbit muscle pyruvate kinase, although the results in this instance were inconclusive due to experimental difficulties which resulted in the precipitation of the enzyme (Lee & Nowak, 1992).

## 1.8 THE MONOVALENT CATION

Pyruvate kinase was the first enzyme which was shown to require a monovalent cation for activity (Boyer et al., 1942). A monovalent cation requirement has since been found for many different classes of enzyme e.g. acetate kinase (EC 2.7.2.1), oxaloacetate decarboxylase (EC 4.1.1.3) and threonine dehydratase (EC 4.2.1.16) (Suelter, 1970). The mode of action of the monovalent cation has yet to be fully elucidated for any of the systems studied. The general role proposed for monovalent cations has been to induce a conformational change in the enzyme yielding the active form (Kachmer & Boyer, 1953; Evans & Sorger, 1966; Happold & Beechey, 1958). The primary bases for this suggestion were the correlation of enzymatic activity with the ionic radii of the ions, and the high concentrations of monovalent cations required for maximal effect (5-100mM). These findings were confirmed by others who also found that activating cations could change the spectroscopic (Suelter et al., 1966) and immunoelectrophoretic (Sorger et al., 1965) properties of an enzyme or the NMR spectral properties of an enzyme-Mn<sup>2+</sup>-substrate complex (Mildvan & Cohn, 1966).

From a survey of enzymes requiring monovalent cations a direct role for K<sup>+</sup> in stabilizing an enolate intermediate formed during catalysis was proposed (Suelter, 1970). Further, a direct role for K<sup>+</sup> in the pyruvate kinase reaction was obtained by Tl<sup>+</sup> NMR studies indicating that the monovalent activator binds within 8Å of the Mn<sup>2+</sup> binding site (Kayne & Reuben, 1970). This was confirmed in ESEEM spectroscopic studies of the rabbit muscle enzyme (Tipton et al., 1989).

The observation that K<sup>+</sup> decreased the affinity of enzyme-Mn<sup>2+</sup> for PEP analogues which lacked a free carboxyl group, and the evidence that Mn<sup>2+</sup> binds the phospho group being transferred (Mildvan et al., 1976) suggested that the carboxyl group of PEP and its analogues were coordinated by the enzyme-bound K<sup>+</sup>. This would allow the proper alignment of its phospho group for nucleophilic attack. Indeed, it has been proposed that this single event may be sufficient to activate the enzyme.

NMR relaxation techniques provided evidence that the monovalent cation has a specific binding site on the enzyme near the PEP/pyruvate binding site (Rauschel &

Villafrancha, 1980).

Studies have revealed that  $\text{NH}_4^+$  also activates pyruvate kinase in the absence of  $\text{K}^+$ . It also appears that activating  $\text{NH}_4^+$  and  $\text{K}^+$  facilitate one another's binding, but do not appear to compete for binding at a single site (Rhodes et al., 1986).

Studies on the pyruvate kinase catalysed decarboxylation of oxaloacetate indicated that there is no change in the initial velocity patterns or the kinetic parameters in the presence or absence of  $\text{K}^+$ , indicating that this cation is not required for this reaction. It has been noted that monovalent cations are often not required for the normal pyruvate kinase reaction in several bacterial forms of the enzyme and that the ligands implicated in cation binding are not necessarily conserved between species.



## 1.9 BINDING OF FRUCTOSE-1,6-BISPHOSPHATE

Very little is known about the details of Fru-1,6-P<sub>2</sub> binding to pyruvate kinase. A second nucleotide binding site was identified in X-ray crystallographic studies (Muirhead et al., 1987). It was postulated that this site could also function as an effector binding site in the allosterically regulated enzymes. As the muscle enzyme is not regulated by allosteric effectors, any indication of a binding site must remain tentative until a crystal structure of an allosterically regulated form of the enzyme in the presence of effector is determined. Three peptides purporting to define the effector binding site in *E.coli* were isolated and sequenced (Speranza et al., 1989) and supported this earlier work. Differences between these regions and those of various plant pyruvate kinases have been indicated as the explanation for the non-binding of Fru-1,6-P<sub>2</sub> to these enzymes. (Blakeley et al., 1990). A direct relationship between the Fru-1,6-P<sub>2</sub> binding region and hydrophobic regions on the enzyme surface emerged from studies of the binding of the fluorescent probe 8-anilino-1-naphthalene sulphate to the enzyme. The effector was observed to displace the bound probe from approximately half the sites, indicating the apolar character of the Fru-1,6-P<sub>2</sub> specific region (Kapoor, 1976).

Studies on Fru-1,6-P<sub>2</sub> binding to the pyruvate kinase from *E.coli* demonstrated that this effector binds to the enzyme via its phospho groups. This was deduced by examining the effect of increased ionic strength of the assay media on the extent of Fru-1,6-P<sub>2</sub> activation (Speranza et al., 1989). Hydrogen bonds between enzyme and effector are also implicated. Potential ligands for the sugar moiety of Fru-1,6-P<sub>2</sub> have been identified in computer modelling studies of the yeast enzyme (Clayden, 1987). The effect of Fru-1,6-P<sub>2</sub> on the *E.coli* enzyme can be modified by the hydrogen bond-disrupting agent formamide (Speranza et al., 1989).

The importance of phospho groups in the binding of Fru-1,6-P<sub>2</sub> had also been suggested for the yeast enzyme some time earlier (Haeckel et al., 1968). Other workers (Fell et al., 1974) observed that Fru-1,6-P<sub>2</sub> affected the thiol group

reactivity and cold lability of the yeast enzyme suggesting a significant conformational change occurs on the binding of this molecule.

## 1.10 CONFORMATIONAL CHANGES IN PYRUVATE KINASE

The major conformational change that occurs in allosteric proteins, that is of interest to kineticists, is the R to T transition. Allosteric proteins are assumed to adopt two extreme conformations. The inactive T state is characterised by a low affinity for substrate, whilst the active R state is characterised by a higher substrate affinity. The change from T to R is assumed to occur upon binding an allosteric activator. Conversely, allosteric inhibitors favour the adoption of the T state over the R state, and decrease the activity of the enzyme. The allosteric pyruvate kinase enzymes appear broadly to follow this pattern of two extremes of possible conformation. The non-allosteric muscle enzyme can be made to adopt a less active conformation in the presence of non-physiological amounts of the allosteric inhibitor phenylalanine, otherwise it appears to be permanently locked in the active R state. The finding that two conformations can be induced in the rabbit muscle enzyme has made this protein a model for studying allosteric transitions. This may be more to do with the availability and stability of muscle enzyme preparations than the physiological relevance of the results. The kinetic properties of the various pyruvate kinase isoenzymes can be explained by the existence of several different conformational states for the tetrameric enzyme ranging from a T-state with a low affinity to an R-state with high affinity for the substrate. The high affinity state is stabilized by PEP, Fru-1,6-P<sub>2</sub> and low pH. The low affinity T-conformation is stabilized by ATP, alkaline pH, gluconeogenic amino acids such as alanine and the phosphorylation of a serine residue near the N-terminus (present only in the R and L isozymes from vertebrates)

Sequence variability in the intersubunit contact areas may affect the equilibrium between the R and T quaternary structures and give rise to the different kinetic properties observed.

A variety of techniques can be used to study conformational changes occurring in proteins upon the binding or release of substrates, products and effectors. Experimental techniques such as fluorescence quenching and relaxation, phosphorescence and NMR spectroscopy point to a rather fluid, dynamic structure



for globular proteins involving rapid conformational fluctuations which allow relatively easy, if somewhat transient, accessibility of interior groups to solvent and molecular probes.

On the other hand, data from X-ray crystallographic studies indicated that the packing densities of groups within globular proteins are as high as those found for solid, crystalline amino acids and small organic compounds suggesting a rather rigid and static view of these proteins.

Although it is difficult to conceive macroscopic systems having both fluid and solid-like behaviour at one and the same time, these properties are perfectly compatible with the microscopic nature of individual protein molecules.

### 1.10.1 FLUORESCENCE MEASUREMENTS

One of the earliest techniques to be used in this way on pyruvate kinase was analysis of fluorescence quenching of tryptophan residues in the enzyme from *S.cerevisiae* (Kuczenski & Suelter, 1971). This technique had been used successfully to show that binding of cations to the rabbit muscle pyruvate kinase resulted in relatively low tryptophan fluorescence quenching and thus minor changes in conformation (Suelter, 1970). More extensive changes in conformation in the yeast enzyme were recorded after the addition of  $Mg^{2+}$ ,  $K^+$ , PEP, ADP and also after raising the temperature of the enzyme solution from  $0^{\circ}C$  to  $30^{\circ}C$ . The results suggested that the conformation adopted in the presence of  $Mg^{2+}$ ,  $K^+$  and PEP is an intermediate on the path to the kinetically active conformer. The nucleotide, ADP, is required to complete the transition. However, an alternative explanation, arising if ADP does not provide the driving force to complete the conformational transition, argues for the existence of two different active conformers controlled by fructose-1,6-bis-phosphate or  $K^+$ . This alternative was supported by the antagonistic effect of  $K^+$  on the binding of Fru-1,6- $P_2$  and further suggested a dual role for  $K^+$ :

- 1) as a required cation for catalysis in the presence and absence of Fru-1,6- $P_2$
- 2) in producing a unique active conformer in the absence of Fru-1,6- $P_2$

Such a dual role is consistent with the observation that  $Na^+$  can substitute for  $K^+$

only in the presence of Fru-1,6-P<sub>2</sub> (Hunsley & Suelter, 1969). The similar fluorescence changes seen in the rabbit muscle enzyme and the yeast enzyme as the temperature is lowered indicated a common conformational transition in both proteins. The similarity of the responses in the Fru-1,6-P<sub>2</sub>- activated enzyme to those of the muscle enzyme further suggested a similar active conformer for each, especially when one considers that the rabbit muscle enzyme is considered not to be allosterically activated whereas the yeast enzyme is typical of the allosteric isoenzymes activated by Fru-1,6-P<sub>2</sub>

Many allosteric enzymes contain metal ions or require the addition of metal ions for activity. Hence, an approach to the understanding of the mechanism of allosteric interactions is to compare the binding of metal ions and substrates to allosteric and non-allosteric enzymes which catalyse the same reaction. Such a comparative study has been undertaken for pyruvate kinase (Cottam et al., 1972). They used water proton relaxation rate measurements and kinetic studies of ternary complexes in the analysis of rabbit muscle and yeast pyruvate kinase. Their results indicated that similar structures exist for the ternary complexes enzyme-Mn<sup>2+</sup>-substrate of the yeast and muscle enzymes. They suggested that, as with the muscle enzyme, the yeast enzyme may bind the phospho group of PEP through a Mn<sup>2+</sup> bridge. Fructose-1,6-bisphosphate appeared to increase the affinity of the yeast enzyme for PEP, perhaps by adjusting the structure of its proposed carboxyl binding site. Fructose-1,6-bisphosphate appeared to have no effect on the binding of ADP but abolished the homotropic effect of PEP.

A variety of different techniques have been developed over the years to detect and measure the extent of conformational changes in pyruvate kinase derived from many different sources, such as ultraviolet difference spectroscopy (Suelter & Melander, 1963), tryptophan fluorescence (Suelter, 1967), ultraviolet circular dichroism spectra (Wildes et al., 1971), sedimentation velocity and optical rotatory dispersion studies (Kayne & Suelter, 1968). Thermodynamic data obtained from equilibrium studies of the conformational changes could apparently be described adequately by a model in which the yeast enzyme existed in two conformations, the equilibrium between which were strongly temperature dependent (Kayne & Suelter,

1968).

Electron paramagnetic resonance (EPR) studies of enzyme-Mn<sup>2+</sup> binary complexes have given direct evidence for the muscle enzyme existing in more than one conformational state (Reed & Cohn, 1972).

Study of *E.coli* pyruvate kinase (Markus et al., 1980) allowed an extension of the concerted model of allosteric interaction between enzymes and effector molecules (Monod et al., 1965). The extension proposed consisted of three conformational states and four protomers. Only one conformational state forms the catalytically active complex with PEP, ADP and Mg<sup>2+</sup>. A second conformational state binds ADP and Mg<sup>2+</sup>. In the absence of ligands, most of the enzyme is in a third state that can bind ADP at the active site and ATP at an allosteric site. Fructose-1,6-bisphosphate is assumed to exert its effect by binding exclusively to the allosteric site of the conformational state that forms the active complex (Fig. 14A).

Binding of substrates to the enzyme in solution causes a reduction in the radius of gyration of the tetramer such as might occur as a result of a substrate-induced closure of the cleft of the active site (Consler et al., 1988).

Some studies on the nature and conformation of pyruvate kinase have produced unusual results. Rabbit muscle pyruvate kinase was correctly identified as a tetramer with a monomeric subunit size of 57.2kD (Steinmetz & Deal, 1966). However, it was suggested that the enzyme existed as two identical catalytic particles (or protomers) each 115kD in size, with each protomer consisting of two polypeptide chains. It was erroneously thought that the two polypeptides within each protomer were not identical due to the incorrect finding that only one Mn<sup>2+</sup> and one PEP molecule bound to each protomer. This study did however, confirm the lack of any covalent linkages between subunits as it was found that complete dissociation of the enzyme occurred in 4M urea.

Protein difference spectroscopy has been used to measure the dissociation constants for the interaction of monovalent cations, divalent cations and substrates with the yeast enzyme (Suelter et al., 1966). The difference spectrum was found to be due to a change in the environment of the tryptophanyl residue brought about by a change in the conformation of the protein molecules (Kayne & Suelter, 1968). A difference spectrum was observed when PEP or pyruvate interacted with the activated

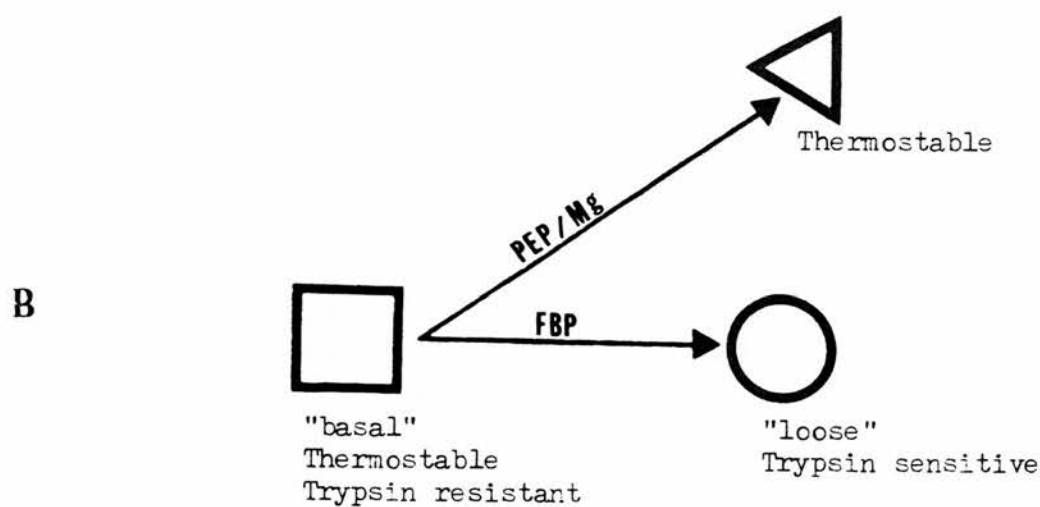
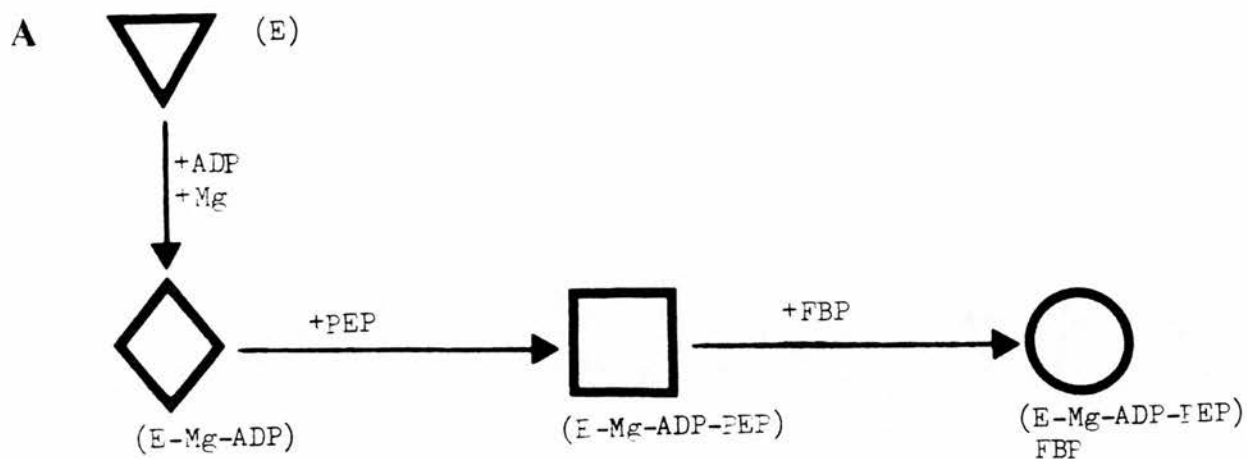


Fig. 14 Different conformations of *E.coli* pyruvate kinase induced by various ligands.  
 A) Data from Markus et al., 1980  
 B) Data from Speranza et al., 1989  
 See text for details.

or non-activated enzyme although no significant difference spectrum was observed when ADP or ATP was titrated with either enzyme form.

Studies on *Neurospora* pyruvate kinase revealed several ligand-induced conformational changes by measuring the intrinsic protein fluorescence of the native enzyme and variously ligated complexes. Ultraviolet difference spectroscopy, chemical modification of exposed residues, interaction with fluorescent probes, differential proteolysis and inactivation by protein denaturants showed similar results (Kapoor, 1976). As a result it was concluded that the two state model based on the symmetry model of Monod et al. (1965) was clearly inadequate to describe the conformational changes induced in the protein upon ligand binding.

Thermodynamic analyses tell us little of the nature of the fluctuations or their kinetics that occur within proteins. Presumably the majority of the fluctuations involve small, rapid changes in the bond lengths and angles of individual groups in the polypeptide chain, but these may readily combine to give gross changes in conformation. It was apparent from studies involving relaxation processes (Grinvald & Steinberg, 1974) that sizeable conformational fluctuations are possible and cover a time range from nanoseconds, or less, up to minutes or hours (Cooper, 1976).

Studies of the interactions of monovalent and divalent cations with rabbit muscle pyruvate kinase by a variety of techniques indicated that the metal-enzyme complex had a conformation that was different from that of the free enzyme. As a result of this conformational transition, a blue shift in the protein spectrum was observed, which could be interpreted as meaning that one or more tryptophanyl residues were brought into an aqueous environment. A similar spectral shift was observed when the temperature of an aqueous solution of pyruvate kinase was lowered from 30°C to 0°C. The fluorescence emission difference spectrum has a broad maximum between 330-350nm. Such emission is characteristic of tryptophanyl fluorescence, confirming the perturbation of such residues during a conformational transition, suggesting a transfer from a non-aqueous to an aqueous environment. The correspondence between the spectrophotometric and fluorimetric observations confirmed the existence of at least two different enzyme forms.

Pyruvate kinase is a model regulatory enzyme as demonstrated by its extreme flexibility, witnessed by the array of conformational transitions detectable in

interaction with a range of ligands- e.g. metal ions (Nowak, 1976), substrates (Reubens & Kayne, 1971) and allosteric effectors (O'Brien & Kapoor, 1975). The effects of ligands on the quaternary structure of *Neurospora* pyruvate kinase was evaluated by means of intersubunit cross-linking utilizing diimidoesters, dimethylsuberimide (DMS) and dimethyladipimide (DMA) (Kapoor, 1976). The results of these cross-linking experiments indicated that the binding of Fru-1,6-P<sub>2</sub> leads to an alteration of the interprotomeric distance between crucial lysine residues, involved in the cross-linking reaction. This conclusion was based on the following evidence: DMS reacts with the unligated enzyme to form primarily monomers and cross-linked dimers whereas DMA treatment resulted in the formation of cross-linked dimers, trimers and tetramers. On repeating these experiments using pyruvate kinase preincubated with Fru-1,6-P<sub>2</sub>, the cross-linking pattern was dramatically altered: DMS treatment now led to the formation of cross-linked trimers and tetramers which could be prevented by addition of the allosteric inhibitor valine. This suggested that in the enzyme-(Fru-1,6-P<sub>2</sub>) complex the ε-amino groups of the lysyl residues participating in the interprotomeric cross-linking are situated further apart allowing the longer DMS molecule to "fit" between them. The conformational change promoted by Fru-1,6-P<sub>2</sub> results in a significant alteration of the geometrical arrangement of the subunits in the pyruvate kinase tetramer.

### 1.10.2 TEMPERATURE-INDUCED CONFORMATIONAL CHANGES

Low temperature instability in proteins (such as that observed in certain forms of pyruvate kinase) indicate that associations between apolar groups, significantly weakened at low temperature, are important in such proteins (Kauzmann, 1959). An examination of the kinetics of dissociation of *S.cerevisiae* pyruvate kinase, produced by low temperature incubation of the enzyme in the absence of activating metal cations, suggested the existence of two types of subunit interaction (Kuczenski & Suelter, 1970). Hydrophobic forces are assumed to predominate between the dimers whilst electrostatic forces predominate between subunits of the dimer. The



dissociation at low temperature was promoted by Fru-1,6-P<sub>2</sub>. This is taken as direct evidence that this ligand produced an alteration in the quaternary structure of yeast pyruvate kinase and supports the contention that allosteric ligands affect conformational transitions from one enzyme form to another. These authors concluded their report by postulating the existence in solution of an equilibrium between two or more tetrameric forms of the enzyme, and that both forms exist in the absence of Fru-1,6-P<sub>2</sub>. Inactivation in the absence of Fru-1,6-P<sub>2</sub> would depend on the equilibrium distribution, and addition of Fru-1,6-P<sub>2</sub> would merely produce a shift in equilibrium concentration of the two forms.

### 1.10.3 SUBSTRATE-INDUCED CONFORMATIONAL CHANGES

A mechanism of protection by a shielding effect or a minor conformational change in the vicinity of the active site is an interesting theory. It could be brought about by the binding of substrates, with the result that a group susceptible to inactivation is no longer exposed (Jacobsen & Black, 1971).

A significant role for ADP in the determination of enzyme conformation in *S.cerevisiae* pyruvate kinase was suggested from analysis of the fluorescence quenching data (Kuczenski & Suelter, 1971), although this was contrary to the kinetic data reported earlier (Hunsley & Suelter, 1969).

After an investigation into the mechanism of reaction of kidney (M2) and muscle (M1) pyruvate kinases by kinetic, equilibrium and structural measurements (Consler et al., 1989), the simplest model which seemed to rationalize the experimental data was a concerted, allosteric model analogous to the two-state model of Monod, Wyman & Changeux (1965). It was found that at pH 7.5 and 23°C, the kidney enzyme existed mostly in an inactive form whilst the muscle enzyme was present almost exclusively in the active conformation.

The conformational transition underlying the regulation of pyruvate kinase activity involves a contraction and expansion of the global structure of the enzyme regulated by the presence of metabolites. The change in the hydrodynamic properties was characterised by a rotation of one domain (domain B) relative to the remainder of



the subunit. PEP,  $Mg^{2+}$  and  $K^{+}$  are the ligands that facilitate the domains to move closer to each other, "priming" the enzyme for catalytic activity. However, these domain movements only affect the local region around the active site of each subunit.

From X-ray crystallographic data (Stammers & Muirhead, 1977) it was shown that the inter-domain region which was involved in cleft closure did not participate directly in intersubunit contacts: thus it was highly unlikely that this structural region was responsible for the intersubunit contact that led to the cooperative nature of the structural change. Hence, additional conformational changes must accompany the domain movement, and these must involve intersubunit contact sites so that conformational communication exists among the four subunits.

The fluorescence excited state lifetimes of tryptophan residues has been used as a probe for conformation in the M1 and M2 isozymes from rabbit muscle. Studies on the rabbit muscle M1 and M2 isozymes imply that in the absence of allosteric effectors these two isozymes may normally exist in different distributions between conformational states and that interconversion between alternate conformers occurs.

The abolition of the sigmoidicity by Fru-1,6-P<sub>2</sub> observed in the *E.coli* enzyme, suggested that this ligand binds to the allosteric site of the catalytically active state (R1) more strongly than it does to the other conformational states of the enzyme. The addition of Fru-1,6-P<sub>2</sub> thus displaces the various conformations towards the state R1.

#### **1.10.4 THEORETICAL CONSIDERATIONS ON CONFORMATIONAL CHANGE**

Abrupt transitions in spectroscopic properties of proteins are conventionally ascribed to conformational change. This may be misleading, because spectral properties can be affected by other processes not necessarily associated with discernable changes in polypeptide geometry (Cooper, 1981).

A general model whereby ligand induced changes in protein dynamics could produce allosteric communication between distinct binding sites, even in the absence of a macromolecular conformational change, has been produced (Cooper & Dryden,

1984). The effect arises out of the possible changes in frequencies and amplitudes of macromolecular thermal fluctuations in response to ligand attachment. Long range influence of kinetic processes at different sites might also be mediated by a similar mechanism.

Allosteric effects, involving communication between distant ligand binding sites on biological macromolecules, are central to many physiological control and receptor processes. Conventionally, these effects are ascribed to ligand-induced conformational changes transmitted through the macromolecule and across subunit boundaries.

It was shown that it was possible to explain cooperative ligand binding in terms of the frequency and amplitude of atomic motions about fixed mean positions i.e. without a conformational change in any sense that could be determined structurally.

It would appear that high concentrations of Fru-1,6-P<sub>2</sub> (greater than 1mM) loosen the structure of pyruvate kinase, simultaneously destroying the basis for inter-site interaction and releasing the constraints that limit substrate affinity in the unmodified enzyme (Morris et al., 1986).

As the observed enzymic activity is the sum of a series of different reactions e.g. substrate and effector binding, protein isomerization, etc, any change in the primary sequence might affect a specific equilibrium e.g. isomerization, which would ultimately lead to a change in the regulatory behaviour of the enzyme. Also, sequence changes might exert a global effect on the enzyme, leading to changes in most if not all of the equilibria characterising the enzyme reaction (Consler et al., 1989).

A non-physiological T to R state conformational change can be induced in rabbit muscle pyruvate kinase by high concentrations (12mM) of phenylalanine. This system has acted as a model for the allosteric transition in some studies. Through intensive kinetic and structural analysis, rabbit muscle pyruvate kinase was shown to be well described by a simple two state model (Consler et al., 1989). All kinetic behaviour of the enzyme could be explained by changes in distribution between the T and R states caused by ligand and substrate binding. The T to R transition was shown to involve global conformational change. A general equation

was derived to express the kinetic data in terms of equilibrium constants for the binding of substrates and ligands, rate constants for catalysis, and the isomerization constant for the R to T equilibrium. In this way it was possible to predict the distribution between R and T states. For example, the distribution of pyruvate kinase from 91% R to almost 100% T could be achieved by the addition of 12mM phenylalanine. It was also possible to predict the distribution of the T state as a function of phenylalanine concentration in the presence or absence of the substrate PEP.

The pyruvate kinase-phenylalanine complex exhibited a larger Stokes radius i.e. it was more asymmetric or expanded, which is an observation that is in total agreement with that from a study using neutron scattering (Heyduk et al., 1992).

Crystallographic data showed that for a number of protein systems, transition between the allosteric states involved a significant rotation of the subunits with respect to each other (Evans, 1992). Furthermore, in all the crystalline structures, all subunits assumed the same structure i.e. structural symmetry was always preserved, regardless of the specific conformational state that the protein was in. Hence, it seems that systems exhibiting a positive cooperative mechanism undergo a concerted global structural change as is the case with pyruvate kinase (Heyduk et al., 1992).

#### **1.10.5 FRUCTOSE-1,6-BISPHOSPHATE-INDUCED CONFORMATIONAL CHANGES**

Studies on the Fru-1,6-P<sub>2</sub> activated pyruvate kinase from *E.coli* indicated that Fru-1,6-P<sub>2</sub> formed ionic bonds with the enzyme through its two phosphate groups and also that hydrogen bonding played a critical role in stabilizing both the inactive and active enzyme conformers (Speranza et al., 1990).

By using NaCl and formamide to disrupt ionic and hydrogen bonding respectively it was found that formamide weakened hydrogen bonds peculiar to the inactive enzyme conformation, which predominated at low substrate concentrations, thus facilitating the transition to the active conformation. Also, formamide hampered the formation of new alternative hydrogen bonds which stabilized the active

conformation. Thus, the transition from the inactive to the active conformation of the enzyme mainly depends on the breaking and formation of sets of hydrogen bonds peculiar to each of the conformers (Speranza et al., 1990).

By comparing the crystallographic structures of the different conformational states, it is possible to glean better insights into the molecular mechanisms of allostery. At present only six protein systems have crystallographic data on their respective different conformational states. These include haemoglobin, *E.coli* aspartate transcarbamylase, porcine kidney fructose-1,6-bisphosphatase, glycogen phosphorylase, bacterial phosphofructokinase and *Bacillus stearothermophilus* glyceraldehyde-3-phosphate dehydrogenase. A common feature among the conformational states exhibited by these protein systems is the rearrangement of subunit-subunit contacts, resulting in a change in the global structure of the proteins (Evans, 1992).

Studies on the Fru-1,6-P<sub>2</sub> activated form of pyruvate kinase from *E.coli* demonstrated the existence of different conformational states of the enzyme produced by the addition of the substrates and effectors. By analysing the thermostability and resistance to tryptic digestion in the presence and absence of effectors, three distinct conformations were detected. The first "basal" conformational state, generated in the absence of both PEP and Fru-1,6-P<sub>2</sub>, is highly resistant to trypsin digestion and is also moderately thermostable. Binding of Fru-1,6-P<sub>2</sub> induced a "loosening" of the enzyme structure observed in the second conformational state, resulting in a more easily digested form of the enzyme. In the presence of PEP and Mg<sup>2+</sup> the third conformation is produced and is characterised by a remarkable thermal stability (Fig. 14B).

Thus, the mechanism of the allosteric activation by Fru-1,6-P<sub>2</sub> may be due to the fact that it switches the enzyme from its "basal" to its "loose", more accessible, conformation. The third "highly stable" conformation may conceivably reflect the "closing-up" of the enzyme on the substrates, to ensure the exclusion of water from the active site during phospho transfer (Fothergill-Gilmore, 1986).

### 1.10.6 OTHER CONFORMATIONAL STATES OF PYRUVATE KINASE

It has been shown that Fru-1,6-P<sub>2</sub> caused the association of monomeric pyruvate kinase M<sub>2</sub> subunits into the active tetrameric form of the enzyme. This association was demonstrated *in vivo*. At physiological levels of glucose (4-6mM) 30-35% of the pyruvate kinase existed as monomer. When cells were deprived of glucose tetrameric pyruvate kinase M<sub>2</sub> was rapidly converted to monomer. On the subsequent addition of glucose tetramer formation increased. The levels of Fru-1,6-P<sub>2</sub> decreased concomitantly with that of glucose. These results indicated that monomer-tetramer interconversion is a major *in vivo* cellular regulatory mechanism in response to changes in the extracellular concentration via Fru-1,6-P<sub>2</sub> (Ashizawa et al., 1991). This mechanism was demonstrated on the M<sub>2</sub> isozyme and may also occur with the L and R isozymes.

## 1.11 ALLOSTERY

Allostery can be defined as a change from one conformation of a protein, possessing two or more different receptor sites, to another conformation when one of the receptor sites is occupied by a compound other than the substrate or product. This definition does not require the two receptor sites to interact with each other in any way, nor does it imply that the protein must be composed of more than one polypeptide chain.

Allosteric interactions and their effects are now widely accepted as being of fundamental importance in metabolic regulation. In a period of a few years, in the early and mid-1960s, papers by Monod, Changeux and Jacob (1963), Monod, Wyman and Changeux (1965) and Koshland, Nemethy and Filmer (1966) attempted to explain a host of previously inexplicable results (from the studies of numerous enzyme reactions by many different authors) by developing new theories on how enzymes interact with small molecules, both substrates and other compounds, that appeared to modulate enzyme activity. By defining new terms they interpreted established findings in a new and challenging fashion which emphasised the subtlety of the enzyme's interactions with itself and other molecules. The "symmetry" or "concerted" model of Monod, Wyman and Changeux and the "sequential" model of Koshland, Nemethy and Filmer have become yardsticks by which to interpret enzyme kinetic data in an attempt to define the precise nature of the intersubunit communication and the effect on this of the binding of various molecules.

The biological activity of many proteins is controlled by specific metabolites which do not interact directly with the substrates or products of the reactions. The effect of these regulatory agents appeared to result exclusively from a conformational alteration (allosteric transition) induced in the protein when it bound the agent. It was suggested that this mechanism played an essential role in the regulation of metabolic activity. In other words, certain proteins, acting at critical metabolic steps, were endowed with specific functions of regulation and coordination. Thus, a biochemical reaction could be controlled by a metabolite acting as a physiological signal rather than as a chemically necessary component of the reaction itself.

Briefly then, the properties of such systems can be described as follows. The



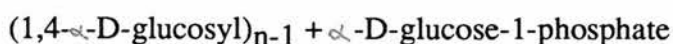
functional structures of controlling proteins are assumed to possess two, or at least two, stereospecifically different, non-overlapping receptor sites. One of these, the active site, binds the substrate and is responsible for the biological activity of the protein. The other, or allosteric site, is complementary to the structure of another metabolite, the allosteric effector, which it binds specifically and reversibly. The formation of the enzyme-allosteric effector complex does not activate a reaction involving the effector itself: it is assumed only to bring about a discrete reversible alteration of the molecular structure of the protein or *allosteric transition*, which modifies the properties of the active site, changing one or several of the kinetic parameters which characterise the biological activity of the protein.

An essential feature of this model is that the allosteric effector, since it binds at a site altogether distinct from the active site and since it does not participate in any stage of the reaction activated by the protein, need not bear any particular chemical or metabolic relation of any sort with the substrate itself. The specificity of any allosteric effect and its actual manifestation is therefore considered to result exclusively from the specific construction of the protein molecule itself, allowing it to undergo a particular, discrete, reversible, conformational change, triggered by the binding of the allosteric effector.

Direct evidence of reversible conformational alterations provoked by the binding of a "regulatory" metabolite have been obtained with several proteins of higher organisms. I shall consider a few of them briefly here.

### **MUSCLE GLYCOGEN PHOSPHORYLASE (EC 2.4.1.1)**

Reaction catalysed:  $(1,4\text{-}\alpha\text{-D-glucosyl})_n + \text{orthophosphate} \text{ ---->}$

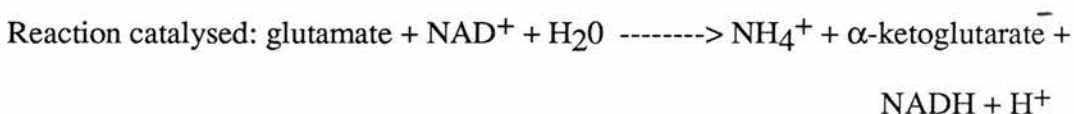


This was probably the first allosteric enzyme mechanism to have been discovered and analysed in detail (Helmreich & Cori, 1964). The enzyme was isolated in two forms; phosphorylase a and phosphorylase b. Muscle phosphorylase b is a dimer ( $M_r$  2 x 97.3k) and is active only in the presence of high concentrations of AMP or IMP, which act allosterically- they bind to a nucleotide binding site and alter the conformation of phosphorylase b. ATP and ADP act as a negative allosteric



effectors by competing with AMP. Glucose-6-phosphate also inhibits phosphorylase b, primarily by binding to the AMP site. Under most physiological conditions, phosphorylase b is inactive because of the inhibitory effects of ATP and glucose-6-phosphate. In contrast, phosphorylase a is fully active, irrespective of the levels of AMP, ATP and glucose-6-phosphate. However, at low levels of  $P_i$ , its activity is stimulated by AMP. Glucose is an allosteric inhibitor. Phosphorylase b can be converted to phosphorylase a by a MgATP-requiring enzyme termed phosphorylase kinase (Krebs & Fischer, 1956) which catalyses transfer of the  $\gamma$ -phospho group of ATP to a unique serine hydroxyl located close to the N-terminus of the protein (Titani et al., 1975). This is accompanied by a further dimerization to give a tetramer ( $M_r$  4 x 97.4k). The proportion of active enzyme is determined primarily by the rate of phosphorylation and dephosphorylation. In resting muscle, nearly all the enzyme is in the inactive b form. Thus, this system shows that a reversible non-covalent interaction between an allosteric effector and a protein may mimic the effects of an irreversible stable modification of protein structure involving a covalent reaction. Indeed, differences between the a and b forms of this enzyme have been directly determined from comparison of the X-ray crystallographic patterns of the isolated enzyme (Sprang & Fletterick, 1979).

### GLUTAMATE DEHYDROGENASE (EC 1.4.1.2)



The activity of this enzyme is allosterically regulated. The vertebrate enzyme consists of six identical subunits, which can polymerise further. GTP and ATP are allosteric inhibitors, whereas GDP and ADP are allosteric activators. Numerous other metabolites have been found to act on this enzyme causing either activation or inhibition. Activation by leucine and diethylstilbestrol both show evidence of cooperative effects. The complex allosteric reactivity of glutamate dehydrogenase reflects its multivalent role in cellular metabolism. The effectors which activate or inhibit the activity of this enzyme act by inducing a conformational alteration as does

the binding and release of the cofactor  $\text{NAD}^+/\text{NADH}$  (Engel & Dalziel, 1969).

## HAEMOGLOBIN

Haemoglobin is an example of a non-enzymic protein whose specific regulatory competence has long been recognised. As is well known, the dissociation curve of oxyhaemoglobin as a function of oxygen tension is sigmoid, demonstrating cooperativity in the binding of oxygen. By contrast, the dissociation of oxygen from myoglobin is a simple adsorption isotherm. An empirical equation designed by Hill (1910),  $y = kp^n / (1+kp^n)$ , gave a reasonable approximation to the haemoglobin data with  $n=2.6$ . Adair (1925) obtained a closer fit using a four constant equation in which the constants related the successive affinity constants of oxygen to the haem groups of haemoglobin. Adair's equation did not provide any theoretical explanation for the changing affinity constants, but it was capable of fitting the data quite accurately. Pauling (1935) made the first attempt to relate the change in these constants to the geometry of the protein by assuming a single affinity constant and an interaction term which depended on the geometry of the four subunits. This functional difference between haemoglobin and myoglobin is now known to depend upon the tetrameric structure of the former and the monomeric state of the latter.

Adult haemoglobin consists of two types of subunit ( $\alpha$  and  $\beta$ ) arranged in an  $\alpha_2\beta_2$  tetrameric array. Haemoglobin can be dissociated into its constituent chains.

The properties of the  $\alpha$  chain are very much like those of myoglobin. The  $\alpha$  chain by itself has a high oxygen affinity, a hyperbolic oxygen dissociation curve and oxygen binding characteristics that are insensitive to pH, carbon dioxide concentration and 2,3-bisphosphoglycerate levels. The isolated  $\beta$  chain readily forms a tetramer ( $\beta_4$ , also called haemoglobin H). Like the  $\alpha$  chain and myoglobin,  $\beta_4$  entirely lacks the allosteric properties of haemoglobin and has a high oxygen affinity. In short, the allosteric properties of haemoglobin arise from interactions between the two types of subunit.

It was demonstrated by X-ray crystallography (Perutz, 1960) that in

haemoglobin the four haem groups are actually quite far apart, excluding the possibility of direct interaction and implying that any interaction is indirect, presumably due to a conformational alteration.

Haemoglobin exhibits three kinds of allosteric effects. First, the oxygen binding curve of haemoglobin is sigmoidal, which means that the binding of oxygen is cooperative. Second,  $H^+$  and carbon dioxide promote the release of oxygen from haemoglobin, an effect that is physiologically important in enhancing the release of oxygen in metabolically active tissues. Conversely, oxygen promotes the release of  $H^+$  and carbon dioxide in the alveolar capillaries of the lungs. These allosteric linkages between the binding of  $H^+$ , carbon dioxide and oxygen are known as the Bohr effect. Third, the affinity of haemoglobin for oxygen is further regulated by 2,3-bisphosphoglycerate, a small molecule with a high density of negative charge. This molecule can bind to deoxyhaemoglobin but not to oxyhaemoglobin and as a result lowers the affinity of haemoglobin for oxygen.

The allosteric properties of haemoglobin arise from interactions between its  $\alpha$  and  $\beta$  subunits. The T (tense) quaternary structure is constrained by salt links (electrostatic interactions) between different subunits, giving it a low affinity for oxygen. These intersubunit salt links are absent from the R (relaxed) form, which has a higher affinity for oxygen. On oxygenation, an iron atom moves into the plane of the haem group, pulling a proximal histidine with it. This motion cleaves some of the salt links, and the equilibrium is shifted from T to R. The deoxy (T) state is stabilised by 2,3-bisphosphoglycerate binding to positively charged groups surrounding the central cavity of haemoglobin.

# THE CONCERTED AND SEQUENTIAL MODELS OF ALLOSTERIC INTERACTION

## A) THE CONCERTED MODEL

The ligand binding properties of various proteins led Monod, Wyman and Changeux to propose a model for allosteric interactions. Their scheme imagines the binding of ligand at one site to have no direct effect on the affinity of the other sites, but to alter the conformational equilibrium between the two alternative quaternary conformations of the protein: one having low intrinsic affinity for the ligand at all its sites, was designated T (for "tense", since it was imagined to be constrained in some manner); the other, having high affinity for the ligand, was designated R (for "relaxed"). These two forms with  $i$  ligand molecules bound are often referred to as  $T_i$  and  $R_i$ . According to the model, these two conformations coexist even in the absence of ligand, with an equilibrium constant  $L$  between  $T_0$  and  $R_0$ . The  $T_0$  form is favoured, and the protein has relatively low affinity for the first ligand molecule. Since the R conformation has the higher affinity by a factor  $c$ , ligand molecules will be bound to it preferentially. This will pull the conformational equilibrium toward the R state, since the conformational change and ligand binding are linked functions, and the conformational equilibrium between the two conformations with one ligand molecule bound will be  $cL$ . The other vacant sites on the  $R_1$  molecule will then be in the high affinity form; therefore the average affinity of the vacant sites of the entire population will be increased, giving positive cooperative homotropic interactions.

In this model, called the concerted model, heterotropic interactions arise by the preferential binding of other ligands to either of the two states. Affinity is decreased by molecules that bind preferentially to the T state, since they pull the conformational equilibrium back toward T. Affinity is increased by any molecule that binds preferentially to the R state. Different ligands control the apparent affinity simply by shifting the equilibrium between the two states.

## **B) THE SEQUENTIAL MODEL**

Allosteric interactions can also be accounted for by a sequential model (Koshland, Nemethy & Filmer, 1965). The simplest form of the model makes three assumptions:

- 1) There are only two conformational states (R and T) accessible to any one subunit.
- 2) The binding of ligand changes the shape of the subunit to which it is bound. However, the conformation of the other subunits in the protein molecule is not appreciably altered.
- 3) The conformational change elicited by the binding of ligand in one subunit can increase or decrease the ligand-binding affinity of the other subunits in the same protein molecule.

Ligand binding is cooperative if the affinity of the RT conformational state for ligand is greater than that of the TT states.

## **DIFFERENCES BETWEEN THE TWO MODELS**

The two models differ in terms of protein conformation primarily with respect to the conformations of the partially ligated states. Both models imply that ligand binding has effects on the protein conformation; in the sequential model, such effects extend directly to the other binding sites; affecting their ligand affinity. In the concerted model they need extend only to the interface between subunits to alter the conformational equilibrium between the R and T quaternary states. The concerted model envisages the two conformations to be present even in the absence of ligand, R<sub>0</sub> and T<sub>0</sub>, whereas in the sequential model the R conformation is induced only upon ligand binding. The sequential model predicts that the conformational change upon ligand binding should parallel the extent of ligand binding, whereas the two need not coincide with the concerted model, since conformational change should tend to occur at one stage of ligand binding at each molecule. Thus, hybrid RT intermediates are allowed in the sequential model but excluded in the concerted model. The concerted model proposes that symmetry is essential for the interaction of subunits in

oligomeric proteins and therefore requires it to be conserved in allosteric transitions. In contrast, the sequential model assumes that subunits can interact even if they are in different conformational states.

The concerted model is much more restrictive than the sequential model. The only parameters that may be varied are  $L$ , the conformational equilibrium constant in the absence of any ligand, and the affinities of the two states for each ligand; the relative affinities of the two states specify the allosteric parameter  $c$ . Also, the parameters  $L$  and  $c$  are not independent. Alteration of one also changes the other. This interdependence probably reflects the linkage between the conformational change and the change in affinity for the ligand in state  $T$ .

The greatest restriction of the concerted model is that it does not predict negative cooperativity, since the ligand can pull the conformational equilibrium only toward the high affinity form (Creighton, 1984).

## **OTHER MODELS ARE COMPATIBLE WITH THE OBSERVED DATA**

Contrary to the model proposed by Monod et al. (1965), it is not necessary for a tetramer of identical subunits to maintain a symmetrical arrangement on undergoing a conformational change to adequately describe the ligand binding data observed. Atkinson et al. (1966) proposed an important model for ligand binding that differed significantly from the model of Monod et al. (1965). This model explained complex data obtained from substrate and modifier interactions with phosphofructokinase and isocitrate dehydrogenase by assuming progressive changes in ligand site interactions. In this model, binding of ligand at one site could either increase or decrease the affinity of ligand at a second site, which could in turn affect the binding at a third site, etc.

Several kinds of cooperative models have been used to explain sigmoidal relationships between velocities and substrate concentrations observed with regulatory enzymes e.g. allosteric interactions between subunits and multiple binding site models. Even though cooperative models can explain sigmoid data, cooperativity is not essential. Models requiring single, independent active sites with multiple reaction pathways by which the binding sites are occupied can also explain sigmoid



data. It appears that sigmoid data can only eliminate ordered sequence models (i.e. those with a single reaction pathway) which involve the binding of only one molecule of each substrate to one molecule of enzyme (Sweeny & Fisher, 1968). These authors presented a series of models that did not require cooperativity or binding of more than one molecule of substrate to each catalytic site at a given time in order to exhibit sigmoidicity.

The classical oxygen binding curves of haemoglobin have served most usefully in bringing out the importance of cooperative effects in the binding of ligands to proteins. These results have led to the association of sigmoidicity with cooperativity which has been applied to enzymes as well as to proteins that only bind ligands. The models developed by Sweeny and Fisher (1968) took into account all the low molecular weight components in the system, did not require the presence of subunits (although their presence was not excluded), and were readily amenable to further kinetic approaches. It should have been possible to test these models using isotope exchange techniques and other related experimental approaches. To the knowledge of the author these possible experiments have not been performed.

Changes in the allosteric properties of an enzyme by heating or other techniques involving changes in the conformation of the enzyme have been used as evidence for cooperativity in the enzyme system. If it can be assumed that changes in the conformation of the enzyme could result in changes in the magnitude of the rate constants involved in the mechanism, then these non-cooperative models can explain the data equally well. In many of the models described by Sweeny and Fisher (1968), a change in one of the rate constants induced or eliminated sigmoidicity. It seems reasonable to expect that changing the conformation of an enzyme could indeed change the relative magnitude of rate constants and thereby change its kinetic characteristics. In a similar way an added inhibitor or other effector could modify the relative magnitude of terms in the rate expression in such a way as to change the observed relationships between velocity and substrate concentration.

The crystal structures of the six allosteric enzymes that have so far been crystallised in both their R and T states suggests that the symmetry model of Monod et al. (1965) is the most consistent in terms of explaining the data produced. In all of the crystal structures a symmetrical arrangement of subunits is found. This symmetry



is preserved in both the R and T forms. It should be noted that the R0 and T0 structures are the two extremes of a range of possible structures available to the enzymes. Some intermediate structures would be compatible with either the symmetry or sequential model, and so the absence of certain structures does not rule out the sequential model on these grounds.

## 1.12 COOPERATIVITY IN PYRUVATE KINASE

It was observed in many enzyme systems that at substrate concentrations below half maximal saturation, the reaction velocity increased faster than the substrate concentration, while at low inhibitor concentrations the rate decreased faster than the inhibitor concentration. This implies that the enzyme molecule is able to bind more than one substrate or inhibitor molecule at a time and that in the native enzyme there is some sort of *cooperative* interaction between the homologous binding sites. Further, interaction could enhance or diminish the binding of further substrate or effector molecules i.e. that cooperativity could be *positive* or *negative*. Also, binding of one type of molecule could affect either the binding of the same type of molecule or the binding of a different molecular species entirely i.e. cooperativity could be *homotropic* or *heterotropic*. A plot of reaction velocity against substrate concentration typically shows a sigmoidal relationship when cooperativity between ligands occurs (Fig 15A).

How is cooperativity measured? If the interaction of ligand A to an enzyme is measured by some function  $f_A$ , and this interaction is also measured in the presence of ligand B, giving  $f_{A/B}$ , we have a quantitative measure of the extent of interaction of A. If A interacts with the protein independent of ligand B,  $f_A = f_{A/B}$

If the presence of B affects the interaction of A to the protein, then  $f_{A/B} - f_A$  is a measure of the extent of interdependence or *cooperativity*, which can either be in a positive or negative sense. The apparent free energy of binding ( $\Delta G^0$ ) was used (Nowak and Lee, 1977) as a parameter to measure the extent of interaction of the substrates and cations with the enzyme. More usually however, the data obtained when initial reaction velocity is determined as a function of substrate concentration are used. A Hill plot is constructed (Hill, 1925) where  $\log_{10} (v/V_m - v)$  is plotted against  $\log_{10} [S]$ . A typical plot is shown in Fig 15B. The slope is taken as  $n_H$ , the Hill coefficient, which is usually interpreted as a measure of the cooperativity of a given ligand. When  $n_H = 1$ , no cooperativity is observed and a Michaelis-Menten type

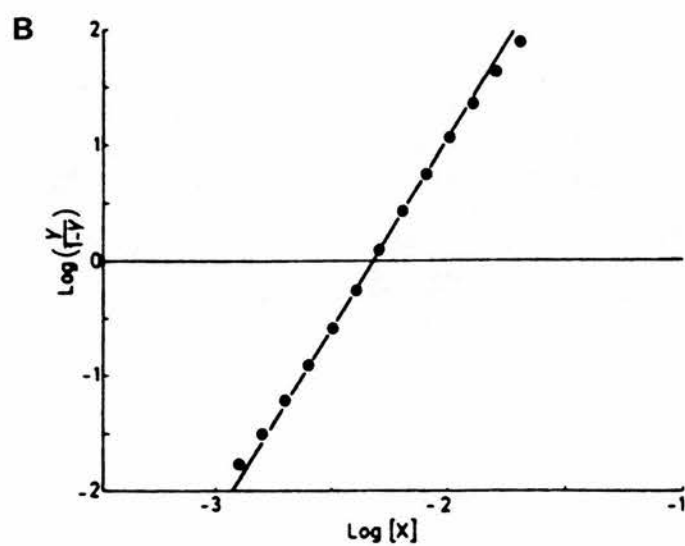
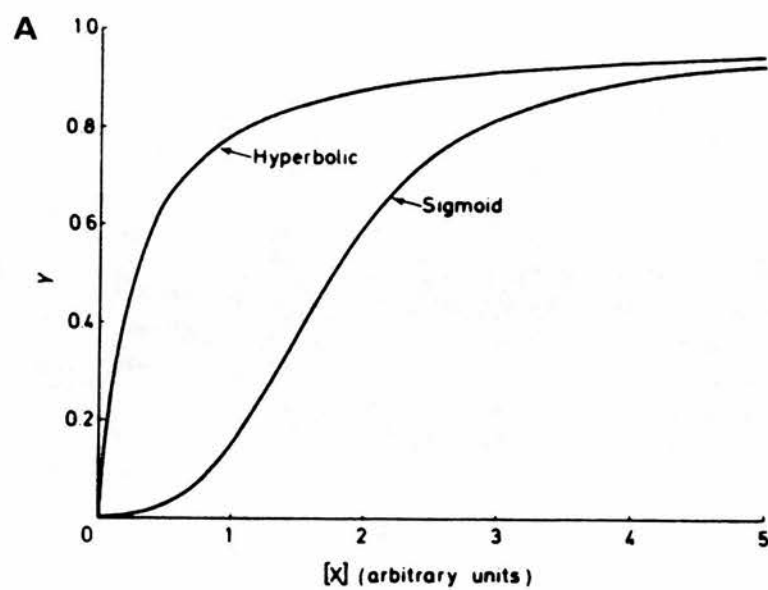


Fig. 15 A) Comparison of a hyperbolic binding curve with a sigmoid curve.  
B) A Hill plot.

hyperbola is usually found. A value greater than 1 indicates positive cooperativity and a value less than 1 indicates a negative cooperative interaction between ligands.

A brief review of the types of cooperative interactions found in pyruvate kinase follows. The consequence that each ligand has on the binding of other ligands is summarised in Table 3.

## 1) COOPERATIVE EFFECTS INVOLVING PHOSPHOENOLPYRUVATE

In pyruvate kinase from *S.cerevisiae* positive homotropic effects were observed in the binding behaviour of PEP (Morris et al., 1984). Sigmoidal kinetics were transformed to hyperbolic in the presence of fructose-1,6-bis phosphate.

Using the calculated apparent free energy of binding as a parameter to measure the extent of interaction of substrates and cations with pyruvate kinase it was shown that PEP had four binding sites per mole of enzyme (Nowak & Lee, 1977). This value was in contrast to the 2.4 reported by Renard et al. (1961) but in accord with a value of  $3.8 \pm 0.3$  reported by Kayne (1973) and now known to be correct from more detailed analysis.

The direct heterotropic interaction between PEP and ADP was reported to be small and negative (Morris et al., 1984), but the overall interaction between these substrates became positive when their positive interactions with  $Mg^{2+}$  were taken into account. The affinity of the enzyme for  $Mg^{2+}$  increases by over 70-fold in the presence of PEP. The coupling free energies were rather large in a negative direction, indicating a strongly positive cooperative interaction (Nowak and Lee, 1977). The heterotropic interactions of the substrates are comparable with those revealed by the rabbit muscle enzyme and it was suggested that they have a common origin in charge interactions within the active site (Morris et al., 1984). Different conformations of the enzyme affect substrate binding in a significant manner. On studying differences between the rabbit M1 and M2 isoenzymes it was found that in each case PEP binds to the active R state by at least one order of magnitude more tightly over the inactive T state (Consler et al., 1989).

## 2) COOPERATIVE EFFECTS INVOLVING ADP

Positive homotropic effects in the binding of ADP to pyruvate kinase from *S.cerevisiae* were reported by Morris et al. (1984). This is in contrast to other workers (Hunsley & Suelter, 1969) who reported that ADP did not display any cooperativity in binding and also appeared not to be strongly affected by Fru-1,6-P<sub>2</sub>. The lack of cooperativity in ADP binding was confirmed in further experiments which also implicated possible conformational changes in the enzyme-M<sup>2+</sup>-substrate complex as being important in mediating the altered binding properties.

## 3) COOPERATIVE EFFECTS INVOLVING M<sup>2+</sup> AND M<sup>+</sup>

Cooperative binding of Mg<sup>2+</sup>, Mn<sup>2+</sup>, K<sup>+</sup> and NH<sub>4</sub><sup>+</sup> to pyruvate kinase was observed in *S.cerevisiae* (Hunsley & Suelter, 1969).

From an analysis of the kinetic data it was shown that Mn<sup>2+</sup> increased the binding affinity of the enzyme for PEP by more than two orders of magnitude (Nowak & Lee, 1977). The coupling free energies were rather large in a negative direction, indicating a strongly positive cooperative interaction.

In the formation of the ternary enzyme-M<sup>2+</sup>-ADP complex, there was little, if any cooperativity involved.

Magnesium displayed positive homotropic interactions in its binding behaviour (Morris et al., 1984). The binding of univalent and bivalent cations was mutually cooperative (Rhodes et al., 1986) but appeared not to involve competition at a single site in the case of the univalent ions. The cooperative effects calculated for the bivalent-monovalent cation interactions with pyruvate kinase suggested that no ligand-ligand interaction takes place.

Cooperativity was also observed in the binding of Mn<sup>2+</sup> and pyruvate. The extent of cooperativity was significantly less than that observed with PEP and substantial evidence exists to suggest that no direct coordination of these substrates occurs (Fig. 10 and 13). The binding of Mn<sup>2+</sup> to the enzyme-PEP-ADP complex was also observed to be cooperative.

#### 4) COOPERATIVE EFFECTS INVOLVING Fru-1,6-P<sub>2</sub>

Fructose-1,6-bisphosphate binding, which yielded positive homotropic cooperative kinetics, transformed the sigmoidal kinetics of K<sup>+</sup>, Mg<sup>2+</sup>, NH<sub>4</sub><sup>+</sup> and PEP to hyperbolic and lowered the apparent K<sub>M</sub> for each variable. ADP was reported not to be strongly affected by Fru-1,6-P<sub>2</sub> (Hunsley & Suelter, 1969). On changing from sigmoidal to hyperbolic kinetics in the presence of 1.2mM Fru-1,6-P<sub>2</sub>, the affinity of the enzyme for ADP increased 1.2-fold, the affinity for PEP increased 12-fold and the affinity for Mg<sup>2+</sup> increased 7-fold (Morris et al., 1986).

Data clearly indicated that in pyruvate kinase from *S.cerevisiae*, Fru-1,6-P<sub>2</sub> acted solely by changing the affinity of the enzyme for its substrates. Low concentrations of Fru-1,6-P<sub>2</sub> appeared to mediate enzyme activity while leaving the substrate interactions of both kinds (heterotropic and homotropic) largely the same. By contrast, high effector concentrations seemed to exert their major effect on the homotropic interactions of PEP and Mg<sup>2+</sup> both decreasing their magnitude and causing a compensatory increase in the affinity of the enzyme for these substrates. The heterotropic interactions remained relatively unaffected. It appeared therefore, that high effector concentrations loosen the structure of pyruvate kinase, destroying the basis for inter-site interaction and releasing the constraints that limit substrate affinity in the unmodified enzyme. This conclusion is supported by the observation that the reactivity of the enzyme towards pyridoxal-5'-phosphate is increased in the presence of Fru-1,6-P<sub>2</sub> (Valentini et al., 1991). Fell et al. (1974) reported that the reactivity of the thiol groups and cold inactivation of the yeast enzyme was increased in the presence of Fru-1,6-P<sub>2</sub>, indicating a different conformation for the enzyme could be adopted.

The cooperative binding of the allosteric activator Fru-1,6-P<sub>2</sub> to yeast pyruvate kinase was investigated by equilibrium dialysis and fluorescence quench titration. The results showed that yeast pyruvate kinase binds four molecules of Fru-1,6-P<sub>2</sub> per tetramer (Murcott et al., 1992). When Fru-1,6-P<sub>2</sub> is titrated into yeast pyruvate kinase the resulting binding behaviour is compatible with a model whereby

the enzyme molecule acts as a dimer of dimers with two steps in the heterotropic cooperative transition of the enzyme from the low affinity T state to the high affinity R state. A two-step model for the cooperative binding of Fru-1,6-P<sub>2</sub> to yeast pyruvate kinase was proposed. The first ligand binds to the quaternary T state and induces a conformational change to an intermediate state, R', which has increased affinity for ligand. Binding of the second ligand is to this R' state. Binding of the third ligand induces a further conformational change to the full R state, which has the greatest affinity for the ligand. These data suggested to the authors that the cooperative binding of Fru-1,6-P<sub>2</sub> to yeast pyruvate kinase could be best described by the model of Eigen (1967) in which a concerted and a sequential element in the transition are proposed.

## **5) COOPERATIVE EFFECTS INVOLVING H<sup>+</sup>**

Binding of H<sup>+</sup> to *S.cerevisiae* pyruvate kinase shows positive homotropic cooperativity and the protonated enzyme is catalytically inactive. It was also found that H<sup>+</sup> interacts positively with PEP but negatively with both ADP and Mg<sup>2+</sup>. This suggested that H<sup>+</sup> was bound in a position that enhanced the binding of PEP through its negatively charged carboxylate group while repelling the positively charged magnesium ion. The negative interaction between H<sup>+</sup> and ADP may also be caused by the repulsion of Mg<sup>2+</sup>, for it has been suggested that the nucleotide depends on Mg<sup>2+</sup> for one of its links to the enzyme (Kinderlerer, 1986).

## **SUMMARY**

From data gathered from a variety of sources there is substantial evidence to suggest that there is no requirement for direct ligand-ligand interaction to be necessary for cooperative effects to occur. Cooperative effects can occur by the first ligand inducing a conformational change in the enzyme, affecting the binding site for the second ligand to increase (or decrease) the binding affinity for the second ligand. The heterotropic interactions of pyruvate kinase may originate in charge interactions at the active site and homotropic interactions may reflect intersite events (Ainsworth & MacFarlane, 1973). Table 3 summarises the data presented in this chapter.



TABLE 3

COOPERATIVITY BETWEEN SUBSTRATES AND EFFECTORS IN  
*S.CEREVISIAE* PYRUVATE KINASE

	PEP	ADP	M <sup>2+</sup>	K <sup>+</sup>	H <sup>+</sup>	FBP	NH <sub>4</sub> <sup>+</sup>
PEP	+	-	+			+	
	(1)	(1)	(1,2)			(6)	
ADP		+	+				
		(1)	(1)				
		o					
		(3)					
M <sup>2+</sup>	+	-	+	+			+
	(2)	(6)	(1,3)	(4)			(4)
K <sup>+</sup>	+		+	+			+
	(7)		(4)	(3)			(4)
H <sup>+</sup>	+	-	-		+		
	(5)	(5)	(5)		(5)		
FBP	-	-	-			+	-
	(1,3)	(3)	(3)			(3)	(3)
NH <sub>4</sub> <sup>+</sup>			+	+			+
			(4)	(4)			(3)
+	increase in cooperativity						
-	decrease in cooperativity						
o	no change in cooperativity						

References:

- 1) Morris et al, 1984
- 2) Nowak & Lee, 1977
- 3) Hunsley & Suelter, 1969
- 4) Rhodes et al, 1986
- 5) Kinderlerer, 1986
- 6) Cottam et al, 1972
- 7) Nowak & Mildvan, 1972

## CAVEAT: SIGMOIDICITY WITHOUT COOPERATIVITY

Cooperative effects can arise in a simple way without the need for special assumptions about the quaternary structure of the protein. Apparent cooperative effects can arise in reactions involving a pair of substrates if a random non-equilibrium addition of the substrate to the enzyme occurs (Ferdinand, 1966). Conformational relaxation might give rise to cooperative protein-ligand interactions although it is not clear if this model is thermodynamically possible (Atkinson, 1966).

The model of Rabin (1967) requires neither an allosteric site nor a second substrate. It postulates instead two conformational states of the enzyme, E and F, E being preferred in the absence of substrate (Fig 15). Both forms can bind the substrate, but only F catalyses the reaction. Product release yields the free enzyme in the F form. At high substrate concentrations, this is immediately reconverted to FS-the enzyme-substrate complex. At lower substrate concentrations, however, F has a lower chance of isomerising to E. A significant portion of the flow then proceeds via ES, the rate of product formation being limited by the isomerisation of ES to FS.

Another possible non-cooperative explanation for kinetic, or binding curve, data that departs from the simple classical pattern is the presence of non-identical sites for the substrate or ligand. A mixture of two isoenzymes, for instance, will not give "linear" kinetics unless the two forms have the same  $K_M$ .

Non-identity may also arise in more subtle ways: proteins may have identical subunits arranged in non-equivalent positions. There might be, for instance, distinguishable "top" and "bottom" sets of subunits; the behaviour of one set might be altered by the mere presence of the other set, if, for example, one set of binding sites were near the interface between the two sets of subunits. However, the sites with greatest affinity would bind the ligand preferentially, and thus non-identical sites can only be invoked in cases of apparent "negative cooperativity"- i.e where initial binding appears to impede subsequent binding (Engel, 1981).

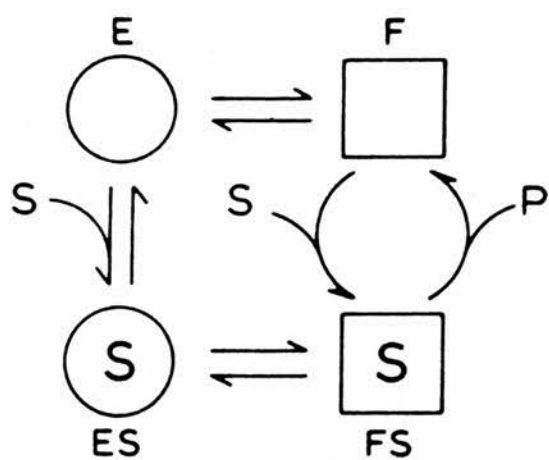


**Fig.16** Rabin's model to explain substrate cooperativity without postulating allosteric sites.

## 1.13 ALLOSTERY AND CONFORMATIONAL CHANGE IN THE GLYCOLYTIC PATHWAY

The enzymes usually described as the key regulatory steps in glycolysis - hexokinase, phosphofructokinase (PFK) and pyruvate kinase- are all known to be regulated *in vivo* by a number of molecules. Yeast hexokinase is an excellent example of an enzyme that exhibits conformational changes upon ligand binding (Dela Feunte, 1970). Phosphofructokinase has been found to be regulated by as many as 28 different compounds *in vitro*. Pyruvate kinase from a number of sources is also known to be regulated allosterically. The number and type of effectors and their efficacy depends upon the source of the enzyme as it is a direct reflection of the importance to the organism in being able to switch rapidly from glycolysis to gluconeogenesis and back again.

I shall briefly describe how allosteric interactions affect the activity of hexokinase and PFK as it is interesting to note that three kinase reactions are important regulatory steps in the glycolytic pathway and all three enzymes appear to undergo significant changes in protein conformation upon substrate and effector binding. The topic of allostery and conformational changes in pyruvate kinase has been extensively covered in the previous sections of Chapter 1 and is, of course, the subject matter for the rest of this thesis. It is important to note that conformational changes probably occur in all enzymes to some extent upon ligand binding and that these changes will also be present in the other enzymes of the glycolytic pathway but that not all of these enzymes are endowed with the specific regulatory features that have made hexokinase, PFK and pyruvate kinase the subject of such intense study.

### HEXOKINASE (EC 2.7.1.1)

Reaction catalysed:  $\text{glucose} + \text{MgATP} \rightarrow \text{glucose-6-P} + \text{MgADP}$

Of the kinase structures known to date many have very similar structural features i.e. many appear to have bilobed structures of two domains, with a marked cleft between them containing the active site. This common structural feature probably reflects the need for conformational changes upon substrate binding and catalysis, as has been shown quite dramatically for hexokinase (Bennett et al., 1980). Upon

binding its substrate, glucose, the two lobes of hexokinase rotate, essentially as rigid bodies, by  $120^\circ$  relative to each other, resulting in relative movements of as much as  $8\text{\AA}$ . Ligands that bind but do not produce this conformational change are not substrates; such movement therefore is probably essential for catalysis. Following rotation of the lobes, the glucose molecule is almost engulfed by the enzyme, so that it cannot enter or leave the active site; dissociation of product from the enzyme is quite slow and rate-limiting, probably being limited by the opening of the cleft. X-ray diffraction studies show that the binding of both the sugar and the nucleotide cause extensive changes in tertiary structure (Fig 17).

As a consequence of glucose binding and the conformational change, the apparent affinity for ATP increases 50-fold. It also binds within the cleft, interacting with both domains, in a way that is favoured by the conformational change. That the conformational change involves rotation of otherwise unchanged domains, rather than rearrangements within them, is suggestive of a relatively rigid architecture for each. Another function of this conformational change may be to permit the enzyme to embrace totally the substrate in the transition state, placing functional groups in the proper orientation all around the substrate and providing them with the appropriate environment e.g a hydrophobic environment would be expected to facilitate the electrostatic interactions between enzyme and substrate believed to be of prime importance for catalysis. A conformational change would be necessary simply to permit products to dissociate and substrates to bind. Further conformational changes probably take place in hexokinase after binding the second substrate ATP, since the glucose-6-hydroxyl and ATP  $\gamma$ -phospho groups are observed to be  $6\text{\AA}$  apart, too far for the reaction to occur in one step. The detailed nature of these changes is not yet known.

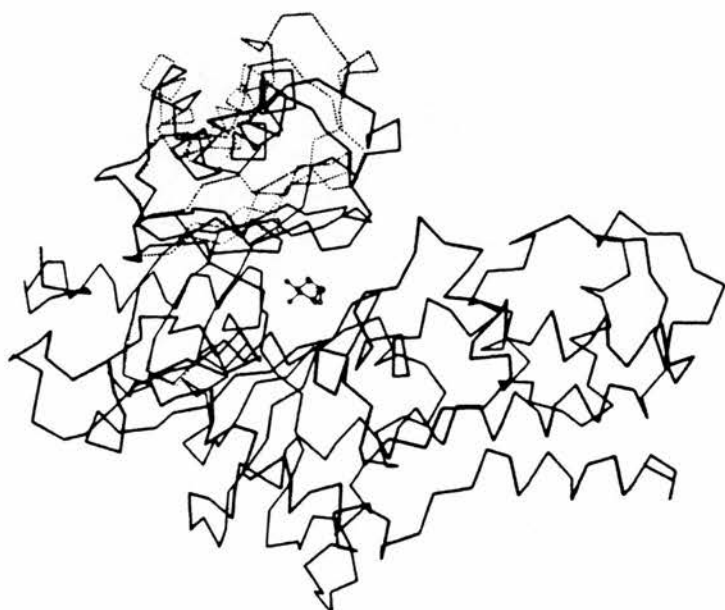


Fig. 17      The conformational changes induced in hexokinase by glucose binding. The solid line shows the  $\alpha$ -carbon backbone in the presence of glucose. The dotted line shows the backbone of the part of the enzyme that is different in the absence of glucose. (From Fersht, 1984).

## PHOSPHOFRUCTOKINASE (EC 2.7.1.11)

Reaction catalysed: fructose-6-P + MgATP -----> fructose-1,6-bisphosphate  
+ MgADP

The reaction catalysed by PFK is essentially irreversible under physiological conditions (principally because of the high  $K_M$  for F-1,6-P<sub>2</sub>), and the reverse reaction is catalysed by a different enzyme, fructose-1,6- bis phosphatase. The PFK reaction is considered the principal regulatory step in glycolysis. The enzyme is regulated in most species and tissues, but its regulators vary, depending on physiological requirements. The enzymes from the bacteria *E.coli* and *Bacillus stearothermophilus* have been best characterised to date (Evans,1992). Four different crystal structures have been deduced, representing both the active R-state and the inhibited T-state conformations. This has greatly increased knowledge about the catalysis and regulation of this enzyme. *E.coli* PFK shows strongly sigmoidal kinetics with respect to fructose-6-P, but not to ATP. It is activated by the reaction product MgADP, and inhibited by PEP. Recent studies of *E.coli* PFK have shown that the allosteric behaviour is rather more complicated than was at first thought. In particular, although the kinetics with respect to ATP are hyperbolic, ATP does nevertheless behave as an allosteric inhibitor at low fructose-6-P concentrations, and binding of fructose-6-P in the absence of ATP is non-cooperative.

The bacterial PFKs are tetramers, each subunit containing about 320 residues. As was observed in hexokinase, and is common with most other kinases, each subunit consists of two domains. The large domain binds ATP and the smaller binds fructose-6-P. Each subunit makes contact with two other subunits, a close contact within the dimer and a smaller contact between dimers. The tetramer is a dimer of dimers.

Of particular importance in understanding the allosteric behaviour of PFK is the location of the substrate and effector binding sites in the tetramer. Each monomer contains three binding sites, two forming the active site and binding the substrates fructose-6-P and MgATP, and one allosteric effector site, which binds both the activator MgADP and the inhibitor PEP. It is typical of enzymes catalysing a



bimolecular reaction that each substrate should bind to a different domain of the enzyme, with the catalytic site between the domains. This allows some adjustment of the relative orientation of the two substrates by movement of the domains. In PFK such domain flexibility appears to be important, and three of the important catalytic residues lie on a polypeptide loop (residues 125-129) linking the two domains. The position of the binding site for the cooperative substrate fructose-6-P lies in the interface between dimers. Thus the dimers are linked by the fructose-6-P sites. The two subunits within the dimer are linked by the allosteric effector site, which is buried in the interface.

Conformational changes occurring during catalysis have been deduced by comparison of crystals of PFK in the active R-state grown from a mixture of reaction products (F-1,6-P<sub>2</sub> and MgADP) and the same crystals soaked in a substrate mixture (fructose-6-P and MgATP analogue and the activator MgGDP). The effect of the observed conformational change is to bring the two substrates together. In the "open" subunit, the distance between the  $\gamma$ -phospho of ATP and the phospho acceptor of fructose-6-P, is just over 4Å, too far for a direct nucleophilic attack. In the "closed" subunit, this distance is reduced to just under 3Å, positioning the two substrates perfectly for the reaction to take place. All other structures of PFK resemble the "open" subunit conformation and this therefore appears to be the normal conformational state.

Analysis of mutant forms of PFK produced by site-directed mutagenesis have identified residues important in regulating the allosteric transition. As a result it was observed that it is interactions with the  $\gamma$ -phosphate of ATP which are important for ATP acting in effect as an allosteric inhibitor, leading to the cooperative kinetics observed with respect to fructose-6-P. From kinetic studies on bacterial PFKs, it appears that the regulation of activity is achieved primarily through the modulation of activity for the substrate fructose-6-P. The most important physiological effect in bacteria is likely to be inhibition by PEP causing inhibition of fructose-6-P binding.

Fluorescence data suggest that the enzyme exists in two major conformational states, differing in their affinities for fructose-6-P, consistent with allosteric models and with the structures observed in crystals. The major conformational states, the

active high affinity R state and the inactive low affinity T state are best considered as families of conformations. All protein structures are altered to a greater or lesser extent by the binding of ligands, and comparison of the structures of R-state PFK crystals with different ligands bound show conformational changes around the binding sites, in some cases remote from the binding sites, but it is the large shift of conformation between the R-state and T-state families which causes the allosteric behaviour (Fig 18).

The structural characterisation of the allosteric transition comes from a comparison of two structures of *B.stearothermophilus* PFK; an R-state structure and a T-state structure. Comparison of these two structures shows a major change in the quaternary structure which can be most simply described as a rotation by about 70° around the molecular p-axis (Fig 18). This conformational change removes the sidechain of arginine 162 from the active site, where it binds the phospho group of fructose-6-P, and replaces it in space by glutamate 161. The removal of a positive charge and its replacement by a negatively charged or neutral residue is probably sufficient to account for the low affinity of the T-state for fructose-6-P, although there may be additional steric hindrance to binding, since the active site is somewhat more constricted in the T-state. The two subunits make approximately the same number of contacts in both the R and T-states, but they are different. The change in conformation of a loop formed from residues 156-162 is intimately linked to the quaternary structure change, such that change in the loop will tend to trigger the quaternary structure change, and conversely the quaternary change will force the loop change on all four subunits in the tetramer, thus favouring concerted change. The four active sites are effectively linked by their position in the interface between rigid dimers.

The effector site binds both allosteric activators such as MgADP, MgATP and P<sub>i</sub>, and the allosteric inhibitors PEP and 2-phosphoglycolate. These ligands bind in a deep cleft, with the phosphate or  $\beta$ -phosphate in a common position. When the cleft is fully closed the enzyme takes up its T-state conformation. Mutations affecting this cleft closure e.g. serine 159 to asparagine, lock the enzyme in the T-state with a concomitant decrease in affinity for fructose-6-P.

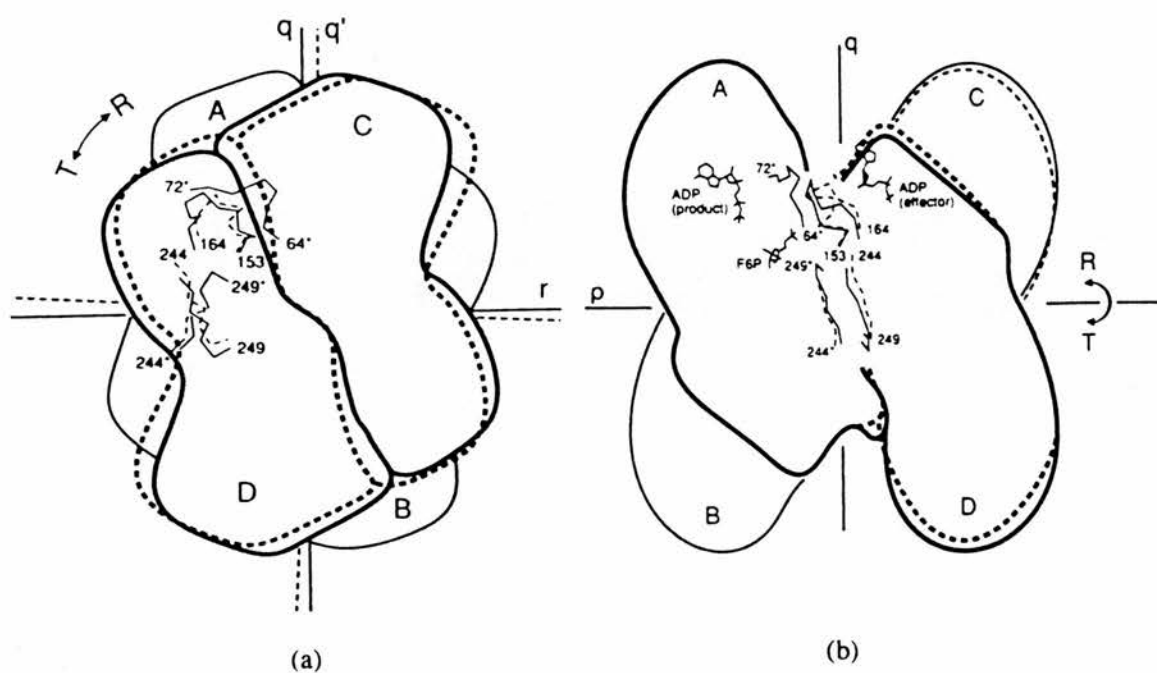


Fig. 18 General view of the allosteric transition between inactive T state (solid outline) and active R state (dashed outline) of phosphofructokinase from *E.coli*.  
(From Evans, 1992).

## **1.14 ISOENZYMES OF PYRUVATE KINASE**

According to the recommendations of the Commission on Biological Nomenclature of IUPAC-IUB (1977), isoenzymes are defined as, "multiple molecular forms of an enzyme occurring within a single species, as a result of the presence of more than one structural gene."

Isoenzymes of pyruvate kinase have been best described from various vertebrate species but they are also found in fish, plants, bacteria, fungi, protozoa and algae. A brief description of the properties of pyruvate kinase isoenzymes from some of these different sources is given in the following pages.

### **VERTEBRATE PYRUVATE KINASE ISOENZYMES**

In vertebrate tissues four different isoenzymes of pyruvate kinase are found. These isoenzymes are tissue specific, have kinetic properties reflecting the different metabolic requirements of the tissues and differ in the regulation of gene expression.

The M1 type is the major form of adult skeletal muscle, heart and brain and shows predominantly hyperbolic Michaelis-Menten kinetics. The M2 type is the only form detected in early foetal tissues and is present in most adult tissues. The R type is expressed only in erythrocytes and the L type is the major form in adult liver. In contrast to M1, the M2, R and L types are all allosterically regulated and show sigmoidal kinetics with respect to the substrate phosphoenolpyruvate. In addition, R and L are regulated by reversible protein-kinase mediated phosphorylation of a specific serine near the N-terminus (reviewed by Muirhead, 1990).

The crystal structure of an M1 isoenzyme is known (Muirhead et al., 1986) and amino acid sequences are available for M1, M2, R and L isoenzymes. Alignment of these sequences shows them to be highly conserved and implies that the tertiary and quaternary structures of all isoenzymes are very similar.

Genetic studies have suggested the presence of only two structural genes in mammals: one coding for both the M1 and M2 and another coding for both R and L. The R and L type enzymes are produced from a single L gene by the use of differential promoters (Noguchi et al., 1987). The mRNAs are identical except in the 5'-terminal region. The L gene is composed of twelve exons and eleven introns. The

first and second exons encode the 5'-terminal sequence specific for the R and L types respectively. The remaining downstream exons encode common sequences (Fig 19). In contrast, M1 and M2 are produced from the same gene transcript by alternative RNA splicing (Noguchi et al., 1986). The M gene contains two adjacent exons, one which codes for residues 380-435 in M1 and the other for the corresponding residues in M2. Apart from this region coded by alternative exons, the sequences in M1 and M2 are identical (Fig. 20).

Pyruvate kinase isoenzymes are different only due to small perturbations at key structural locations, which in turn lead to changes in not one specific equilibrium constant but in a majority of the equilibrium constants governing the basic behaviour of the enzymes. As a consequence of these changes, the isoenzymes exhibit quantitatively different kinetic behaviours under the same experimental conditions.

The structural elements which are responsible for the change in chemical equilibrium and which are most likely involved in subunit contacts were identified by X-ray crystallographic studies as the N-terminal domain (residues 10-40, cat muscle numbering) and helices 1 and 2 of domain C (residues 385-425). It can be shown that these elements of structure do differ among the isoenzymic forms of pyruvate kinase (Table 1). It can be imagined that these structural units play an important role in intersubunit communication and thus are responsible for the transmission of information between the subunits. They probably participate in the switching between the alternative conformations of pyruvate kinase. If this structural region plays an important role in conferring specific allosteric behaviour in pyruvate kinase, then one might expect that this region will be sensitive to mutation (i.e. mutation of individual residues within this region would significantly affect the allosteric behaviour of the enzyme- as has been shown to be the case in bacterial phosphofructokinase). Indeed, a change in the allosteric properties of the human R isoenzyme has been found as a result of a naturally occurring threonine to methionine point mutation at position 384 within the first alpha helix of domain C (Kanno et al., 1991). Other natural mutations detected in the human L type isoenzyme have also been studied. For example, an arginine 132 to cysteine mutation resulted in altered allosteric properties whereas a threonine 353 to methionine mutation did not severely affect allosteric interactions. Both enzymes however showed an increased thermolability and reduced specific

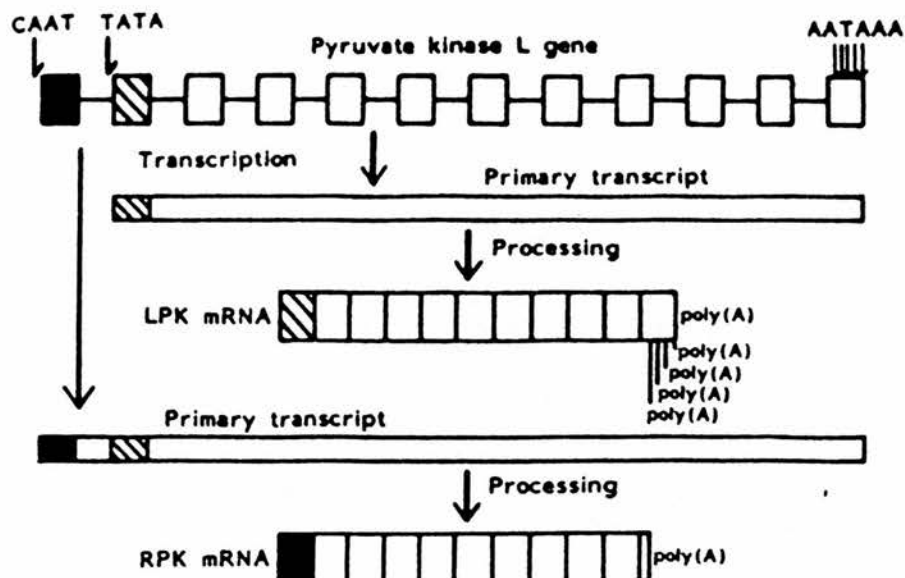


**FIG.19 Schematic representation of expression of the pyruvate kinase L gene.** Exons R and L are indicated by *closed* and *hatched* boxes, respectively. The exons common to both mRNAs are shown by *open* boxes. CAAT, CAT box; TATA, TATA box; AATAAA, polyadenylation signal; LPK, L-type pyruvate kinase; RPK, R-type pyruvate kinase.  
(from Inoue et al., 1986)

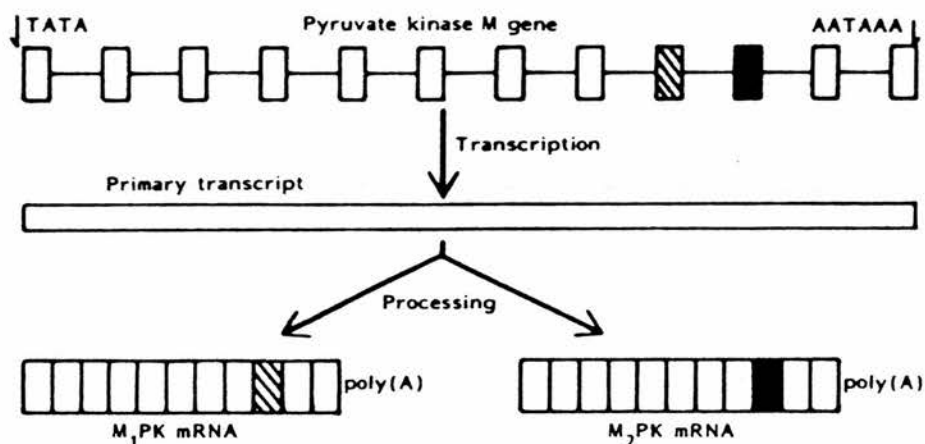


**FIG.20 Schematic representation of expression of the pyruvate kinase M gene.** The  $M_1$  exon is indicated by the *hatched* box and the  $M_2$  exon by the *closed* box. The exons common to both mRNAs are shown by *open* boxes. TATA, TATA box; AATAAA, polyadenylation signal;  $M_1$ PK,  $M_1$ -type pyruvate kinase;  $M_2$ PK,  $M_2$ -type pyruvate kinase.  
(from Noguchi et al., 1986)



activity (Neubauer et al., 1991).

The differences between rat M1 and M2 isoenzymes are located solely in the C $\alpha$ 1 and C $\alpha$ 2 regions mentioned earlier. The different properties of rat L and R isoenzymes may also be due to a limited difference in amino acid sequence in a localised region. In this case the region of structure that is affected is the N-terminal domain. This structural element is in close contact with the C $\alpha$ 1 and C $\alpha$ 2 helices and helps to form the network of subunit interactions between the four identical subunits of the tetramer (Table 1, Fig. 2). In addition, the catalytic activity of the L isoenzyme is known to be allosterically regulated by phosphorylation. The site of this covalent modification is serine 12, which is precisely in the N-terminal domain of the enzyme. The fact that M1 and M2 lack that sequence extension in the N-terminus explains why these two isoenzymes are not phosphorylated and are not regulated by this post-translational modification.

It is becoming clear that differences in a localised region in the sequence and structure of pyruvate kinase, the intersubunit contact region, confer characteristic properties on each of the four vertebrate isoenzymes. The perturbation of this subunit interface by amino acid substitution, by covalent modification, or by alteration of solution conditions leads to an allosteric transition between conformers of the enzyme. These states each have characteristic catalytic properties and thus allow for precise regulation of pyruvate kinase activity in a tissue specific manner. A unifying working hypothesis is therefore proposed for the regulation of pyruvate kinase, based upon the existence of a characteristic allosteric transition between alternate states of the enzyme. Changes in primary sequence affect the various equilibrium reactions in spite of the fact that there is also a great deal of sequence identity among these isoenzymes.

## **PLANT PYRUVATE KINASE ISOENZYMES**

Different pyruvate kinase isoenzymes are found in the cytosolic and plastidic compartments of several plant tissues (Plaxton, 1989). Their occurrence within these compartments may be a reflection of the proposed origin of certain plant organelles i.e. chloroplasts are thought to have arisen by an invasion of a primitive eukaryotic



cell by a cyanobacterial progenitor (Alberts et al., 1983). As a result, these isoenzymic forms of pyruvate kinase can differ markedly in their structure and function.

Sequence information on plant pyruvate kinase isoenzymes is not well reported in the literature and I am indebted to Prof.W.C.Plaxton and Dr.S.Blakeley for their permission to use sequences determined in their laboratories in advance of publication.

There appear to be at least three distinct plastidic forms of pyruvate kinase in plants. These have been termed PKpA, PKpB and PKpG. The genes for these plastidic variants have been cloned and sequenced from several different plants (S.Blakeley, pers.comm). Import data into chloroplasts suggests that the G isoenzyme is stromal and the A isoenzyme may be located in the plastid envelope. It was originally thought that PKpA and PKpB were different subunits in a heterotetrameric isoenzyme but they are now considered to form distinct homotetramers themselves. The plastid isoform of plant pyruvate kinase is as distinct from the cytosolic enzyme as it is from other eukaryote pyruvate kinases. In contrast, the cytosolic plant enzyme is closely related to eukaryote pyruvate kinases and quite dissimilar to the plastid form (Blakeley et al., 1991). This can be more clearly seen by reference to the matrix of differences presented in Table 16 (Section 3.11).

Five complete plastidic isoenzyme DNA and deduced amino acid sequences are known. Castor bean isoenzymes PKpA and PKpB appear to be produced from the same gene by the use of alternative mRNA splicing in a manner analogous to the M1 and M2 mammalian isoenzymes. Tobacco plastidic forms PKpA and PKpG have also been sequenced. The A form is the largest pyruvate kinase yet found (593 residues). The G isoenzyme is shorter at 562 residues. Most of the difference appears to be located in the N-terminus. The G isoenzyme gene from *Brassica napus* has also been sequenced. It encodes a protein of 567 residues. The plastidic forms are all much larger than their cytosolic counterparts (with the exception of PKpB from castor bean) and more variable in size. The reasons and implications of these differences have yet to be explained. However, the increased size of the plastidic forms may be related to their importation into intracellular organelles.

Four cytosolic pyruvate kinase genes have been cloned from three different

plant species. All the cytosolic enzymes are approximately the same length, 508- 510 residues. This is much shorter than the reported lengths of the plastidic isoenzymes and may reflect a real difference in properties, the precise nature of which remains elusive. The difference in length between the cytosolic and chloroplastic enzymes appears to be mainly localised to the N-terminus, and may therefore be related to the mechanism of import into the chloroplast. Some of the plant enzymes are affected by allosteric effectors. The differences between the plant enzymes in the crucial C $\alpha$ 1 and C $\alpha$ 2 helices and in the N-terminus may be sufficient to explain these different properties (Table 1).

Expression of pyruvate kinase and the organisation of genes for this enzyme in plants is complex. Castor bean PKc is apparently expressed both as a homo- and a hetero- tetramer while PKp from the same species is apparently expressed as a heterohexamer (Blakeley et al., 1991). From an analysis of the genomic DNA, potato tuber PKc is encoded by at least three genes. Much work remains to be done on plant pyruvate kinases. Information on enzyme structure and regulation of enzyme activity remains poor but is progressing rapidly.

## **FISH PYRUVATE KINASE ISOENZYMES**

Isoenzymic forms of pyruvate kinase have been detected in fish tissues but information about their different physical and kinetic properties is very scant. Two isoenzymes from the white muscle and liver of the rainbow trout have been identified (Somero & Hochachka, 1968). The muscle isoenzyme appears to be activated by fructose-1,6-P<sub>2</sub> whereas the liver isoenzyme is not affected. This is the opposite situation to mammalian tissues and may reflect the different metabolic stresses undergone by these tissues in these different organisms. Studies of pyruvate kinase from the skipjack tuna (*Euthynnus pelamis*) resulted in the isolation of heart muscle and skeletal muscle forms of the enzyme (Guppy & Hochachka, 1979). The Michaelis constant for the substrate PEP appeared to exhibit temperature dependence in the skeletal muscle but not in the heart muscle isoenzyme. The Michaelis constant for the other substrate ADP displayed temperature independence in both forms of the

enzyme. Both enzymes were inhibited by alanine and ATP. This inhibitory effect was abolished in the presence of Fru-1,6-P<sub>2</sub>.

Fish pyruvate kinase isoenzymes are notable in having quite acidic pH optima and this may be of physiological advantage allowing the enzyme to work maximally under conditions of severe muscular exertion (as in catching prey/ avoiding predators) or in conditions of anoxia (oxygen depletion due to depth of habitat or due to ice cover in winter) (Zamora et al., 1992).

## **BACTERIAL PYRUVATE KINASE ISOENZYMES**

Several different bacterial species have been identified as possessing isoenzymic forms of pyruvate kinase, although none have been well characterised to date.

*E.coli* has been reported to contain two distinct pyruvate kinase isoenzymes (Malcovati & Kornberg, 1969). Genes encoding both have been cloned and sequenced (Bledig et al., 1991; Dorit et al., 1989). One isoenzyme (PKI) is activated by Fru-1,6-P<sub>2</sub> resulting in a thirty-fold increase in the affinity for the substrate phosphoenolpyruvate. This form is also inhibited by ATP. The other isoenzyme detected in this species, PKII, is not affected by Fru-1,6-P<sub>2</sub> but is activated by AMP. PKII is not inhibited by increases in ATP.

*Streptococcus faecalis* has also been reported to possess two isoenzymes of pyruvate kinase (PKI and PKII). Information about these forms is poor. PKI is not affected by allosteric activators, whereas PKII appears to be activated by Fru-1,6-P<sub>2</sub>. The PKII form has been reported as having a molecular mass of 100kD and so the possibility of PKII being a degradation product of PKI cannot be excluded (Wittenberger et al., 1973).

## FUNGAL PYRUVATE KINASE ISOENZYMES

Study of the filamentous dimorphic fungus *Mucor rouxii* has identified three distinct isoenzymes of pyruvate kinase (Passerson & Roselino, 1971). The expression of the different isoenzymes depends on the life-cycle of the organism and the carbon source of the growth media. Ungerminated sporangiospores contain only PKI. This form has a molecular mass of 180-190kD, a  $K_M$ PEP of 2.5mM and is allosterically activated by Fru-1,6-P<sub>2</sub>. Extracts of fungal mycelia grown with amino acids as the carbon source contain PKIII. This form also has a molecular mass of 180-190kD. The  $K_M$ PEP is reduced to 1mM but is still activated by Fru-1,6-P<sub>2</sub>. During the aerobic germination of spores and the conversion of yeast-like cells to mycelium, PKII appears. This form appears to be a hybrid of types I and III. Similar in size to both PKI and PKIII it has a  $K_M$ PEP of 2.5mM and is activated by Fru-1,6-P<sub>2</sub>.

## PROTOZOAN PYRUVATE KINASE ISOENZYMES

Of the three isoenzymic forms of pyruvate kinase detected in *Entodinium* species only one has been characterised (Wakita & Hoshino, 1989). This form is activated by AMP and Fru-1,6-P<sub>2</sub> and inhibited by ATP and so appears to be analogous to the PKI isolated from *E.coli*.

Two pyruvate kinase isoenzymes have been isolated from the parasitic protozoan *Leishmania mexicana amazonensis* (Ponte-Sucre et al., 1993). One enzyme (PYK1) displayed hyperbolic kinetics and was inhibited by fructose-2,6-bis-phosphate (Fru-2,6-P<sub>2</sub>), whereas the other enzyme (PYK2) showed sigmoidal kinetics for the substrate PEP and was activated by Fru-2,6-P<sub>2</sub>. The apparent molecular size of PYK1 from gel filtration chromatography was 200kDa whilst that of PYK2 was 55kDa. The observation that the monomeric PYK2 displays sigmoidal kinetics with respect to its substrates gives support to the theory of Rabin, that cooperativity between active sites is not necessary to explain sigmoidicity. An alternative explanation is that the conditions of purification have caused the dissociation of PYK2 into its constituent monomers, and that under physiological

conditions it too exists primarily as a tetramer.

Genes encoding two isoenzymes of pyruvate kinase have been cloned and sequenced from the protozoan *Trypanosoma brucei* (stock 427). Each isoenzyme was found to consist of 498 amino acid residues and have molecular masses of 54,378 and 54,363 Daltons respectively. These isoenzymes are 41-51% identical at the amino acid level to pyruvate kinases from other sources. The two isoenzymes differed from each other in only five positions. The sequence differences were clustered in domain C, supposedly involved in the regulation of enzyme activity (Allert et al., 1991).

### **ALGAL PYRUVATE KINASE ISOENZYMES**

Isoenzymes of pyruvate kinase from these organisms have been best described from the green alga *Selenastrum minutum*. Two isoenzymes were isolated corresponding to chloroplastic (PKI, PKp) and cytosolic (PKII, PKc) forms respectively (Lin et al., 1989). Both isoenzymes showed hyperbolic substrate saturation kinetics and both were activated by DHAP and inhibited by ATP, citrate, oxalate,  $P_i$  and Fru-1,6- $P_2$ . However, they differed in other respects. PKp appeared to be heat labile and very sensitive to inhibition by the thiol reagent N-ethylmaleimide (NEM), whereas PKc was heat stable and only slightly sensitive to NEM inhibition. Furthermore, PKp appeared to be a homotetramer of  $M_r$  240k whilst PKc appeared to be a homodecamer of  $M_r$  590k. The great size of the PKc isoenzyme is unusual and may be due to the formation of high molecular weight precipitates during purification. Also, PKp was uniquely inhibited by ribose-5-phosphate, malate, ribulose-1,5-bisphosphate and 2-phosphoglycerate and PKc was inhibited specifically by glutamate. The Michaelis constants for the substrates PEP and ADP were 0.18mM and 0.2mM for PKp and 0.09mM and 0.05mM for PKc respectively. The two isoenzymes also displayed different pH optima with PKp showing greatest activity at pH 6.5 and PKc most active at pH 7.0.



## OTHER PYRUVATE KINASE ISOENZYMES

Monomeric pyruvate kinase has been isolated as a thyroid hormone binding protein from human epidermoid carcinoma A431 cells (Kato et al., 1989). This protein (p58) shows 91% sequence identity to the rat M2 isoenzyme at the nucleotide level and 97% identity at the amino acid level. The monomer is in equilibrium with the tetrameric enzyme *in vivo* and in the absence of Fru-1,6-P<sub>2</sub> the formation of the tetramer is inhibited and the monomer stabilised. The tetramer does not bind thyroid hormone whereas the monomer does. As far as is known, this form of regulation has only been found in mammalian cell cultures and, as a result, may not be physiologically relevant.

*In vivo* hybridisation of the M2 and L subunits has been confirmed in mammals by the generation of additional isoenzymes from a presumed (M2)<sub>2</sub>L<sub>2</sub> band isolated from bovine kidney. The hybrid had first been denatured with urea and then allowed to renature following removal of the urea by dialysis (Cardenas et al., 1977). Hybridisation of subunits has been confirmed in human tissue by the observation of M2-L hybrids in hepatomata and their host livers (Hammond and Balinsky, 1978) and the discovery of a five-membered hybrid set in foetal brain resulting from the hybridisation of M1 and M2 subunits.

The possibility of many more hybrid varieties of pyruvate kinase being discovered in different tissues or cell cultures in the future is highly likely and can only shed more light on to the fascinating subject of enzyme regulation, particularly as it occurs *in vivo*.

## 1.15 GENE STRUCTURE OF YEAST PYRUVATE KINASE

Pyruvate kinase is encoded by a single gene (*PYK1*) in *S.cerevisiae*. The gene is located on chromosome 1 (Fig. 21). This locus has also been identified as being important in cell division and has been designated *cell division cycle 19* (*cdc19*).

Like many other glycolytic enzymes, pyruvate kinase is regulated at the transcriptional level in response to carbon source, increasing 10-20 fold when glucose is added to yeast cultures growing on non-fermentable carbon sources. Pyruvate kinase is one of the first glycolytic enzymes to be induced during the switch from non-fermentative to fermentative growth (Maitra & Lobo, 1971). The pyruvate kinase gene contains two Upstream Activating Sequences (UAS) located between -811 and -634 relative to the initiation codon, one Upstream Repressible Sequence (URS) between -468 and -344 (Nishizawa et al., 1989), and a putative Downstream Activation Site (DAS) located within the coding region (Purvis et al., 1987), all of which contribute to transcriptional activity. The UAS1 (which contains a RAP1/GRF1 binding site, Nishizawa et al., 1989), UAS2 and DAS are all required for high level transcription on glucose, but the role of these sequences in carbon source regulation is not clear. The URS partially represses *PYK1* transcription in glucose-grown and glycerol-ethanol grown cultures (Nishizawa et al., 1989). A second URS, located between -868 and -854, has been proposed (Luche et al., 1992). Conventional eukaryotic transcription and translation regulatory signals are also found eg TATA boxes, ATG translation initiation codon, TAA translation termination codon, and polyadenylation signals, as well as yeast-specific signals eg CT rich regions, CAAG high expression box and an adenine at -3. A comprehensive list of such regulatory signals is given in Fig.22.

The *PYK1* gene encodes a protein of 499 amino acids (excluding the N-terminal methionine) in a single open reading frame with a monomer molecular weight of 54,544. The N-terminus is blocked, probably with an acetyl group as is the case in the similar enzyme from *S.carlsbergensis*. The amino acid sequence of yeast pyruvate kinase is specified by a highly restricted set of codons. Only 39 of the possible 61 codons are utilised and 97% of these amino acids are specified by a



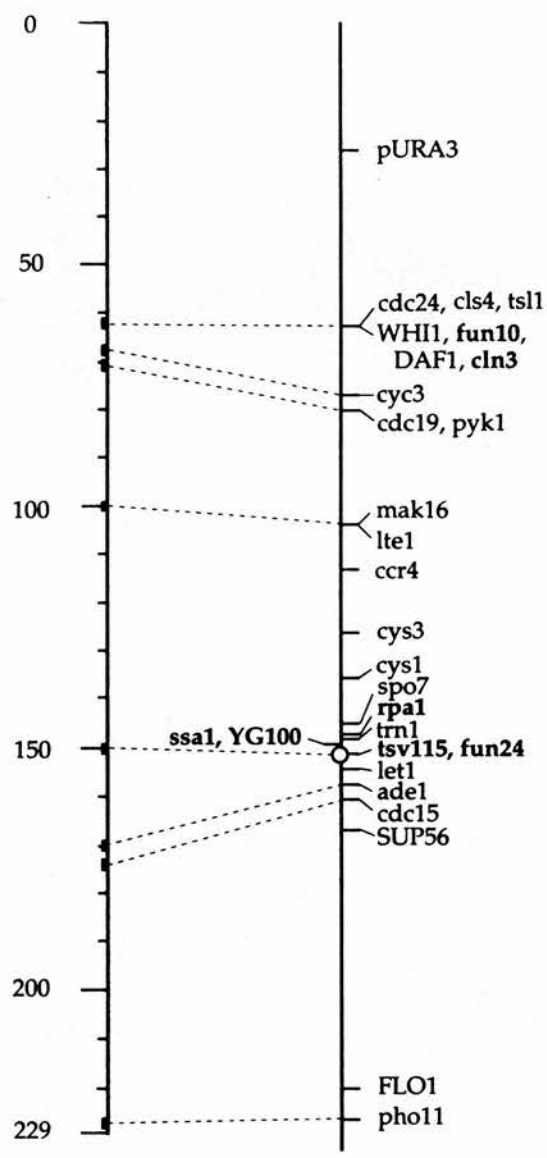


Figure 1.

tRNA (Ser) IGA  
FLO5

Fig.21 Map of chromosome 1 from *S.cerevisiae*.



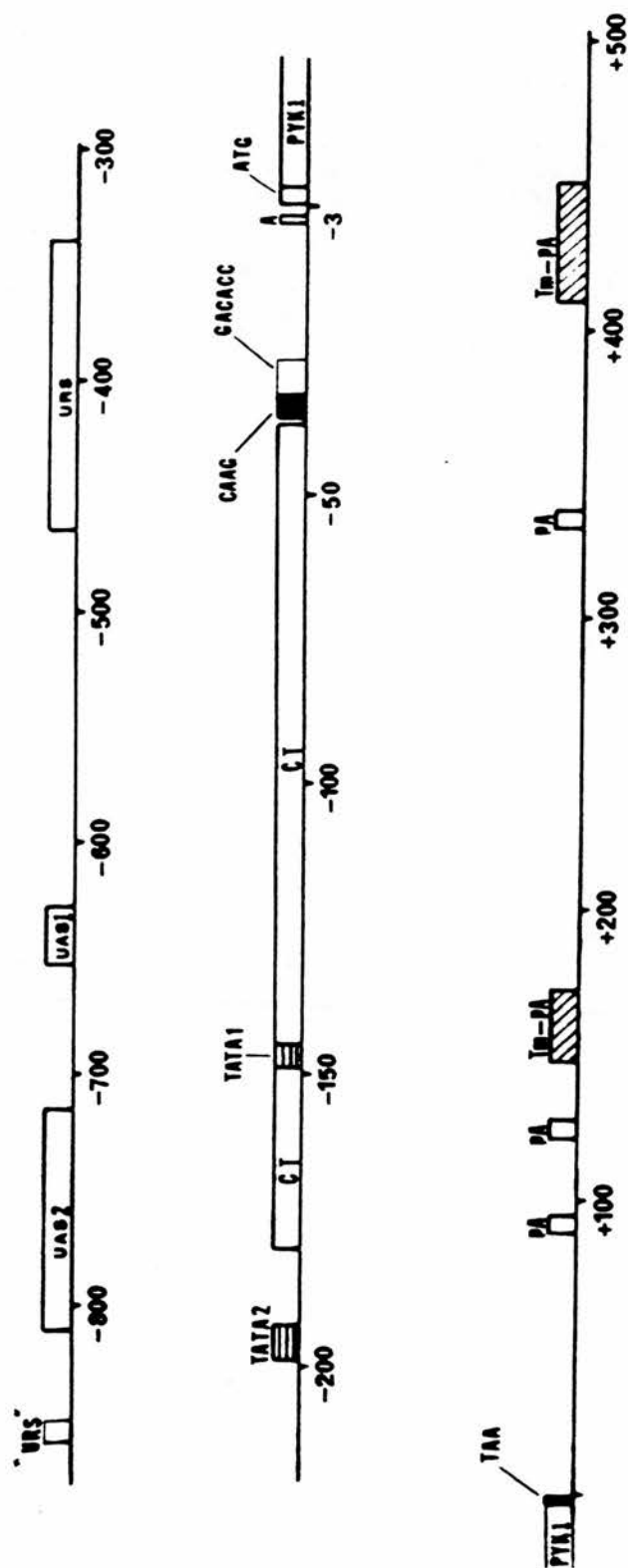


Fig. 22 Upstream and downstream regulatory regions of *PYK1* from *S. cerevisiae*.  
For details see facing page.

subset of only 26 codons. The amino acid composition is very similar to the average for a cross section of unrelated proteins (Fig. 23; Klapper, 1977).

The non-coding strand of *PYK1* also contains a large open reading frame with the potential to encode a 326 residue protein. This sequence begins and ends with conventional initiation and termination codons and also contains some sequences typical of eukaryotic upstream sequences, particularly TATA boxes and the adenine at -3. No strong candidates for 3' transcription termination sequences are found. The putative protein is distinctly atypical by the criteria of Klapper (1977) and does not contain any similarities to existing proteins as determined by a database search of current primary sequences. The large open reading frame probably originated through the introduction of silent mutations in *PYK1* destroying stop codons in the non-coding sequence that usually prevent the formation of alternate reading frames. The alternate explanation, that *PYK1* encodes two distinct proteins on separate strands of the same gene is difficult to reconcile with traditional concepts of gene expression and evolution. However it is important to note that similar open reading frames may exist in other genes and may represent a considerable source of error as future genome sequencing projects generate large amounts of data which may lead to the identification of non-existent proteins.

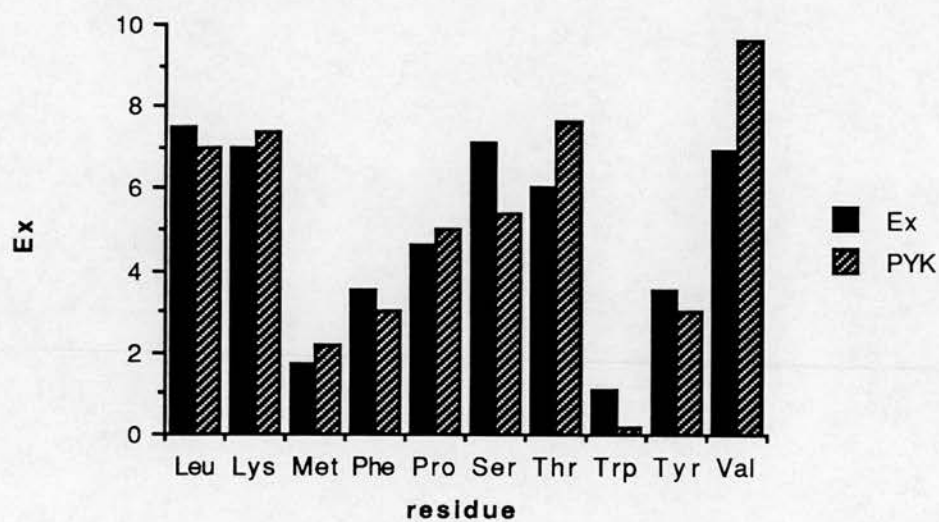
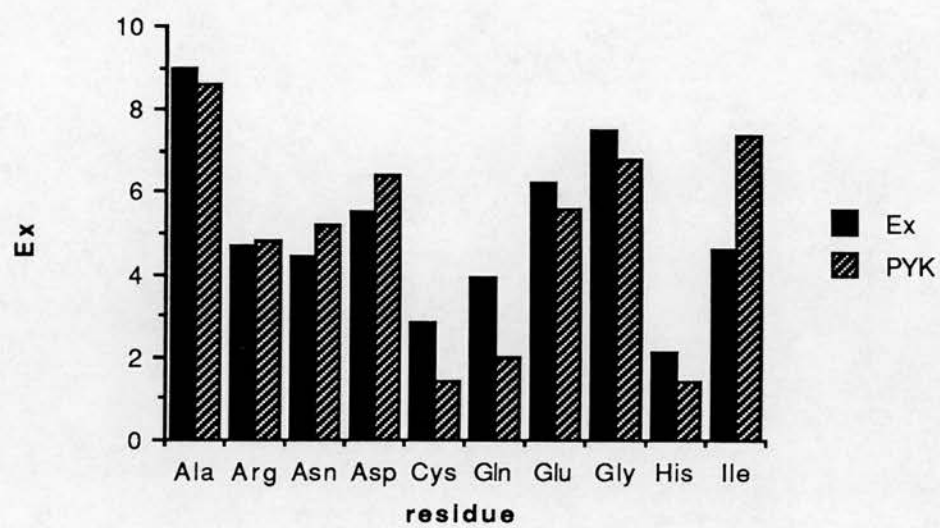


Fig. 23 Occurrence of amino acid residues in yeast pyruvate kinase compared with other proteins.  
 PYK = % frequency of each amino acid residue occurring in the yeast pyruvate kinase coding sequence.  
 Ex = % frequency of each amino acid residue occurring in a cross-section of 207 unrelated proteins of known sequence (data from Klapper, 1977).

## 1.16 CLONING AND OVEREXPRESSION STRATEGY

The plasmid used for overexpressing the various forms of pyruvate kinase was pMA91-pyk. This was designed and constructed by Mellor et al. (1985) and is used in this project with their permission.

The size of the *PYK1* gene necessitated a complex mutagenesis and subcloning strategy to be devised. This was done entirely by the author's predecessor, T.McNally, as part of her PhD thesis, with assistance from Dr.I.Purvis at the University of Glasgow.

The mutagenesis protocol is outlined below. The entire wild-type pyruvate kinase gene from *S.cerevisiae* was cloned into the plasmid pAYE434 as a 5kbp Hind III fragment (Fig. 24A). A 2kbp EcoRI fragment, containing most of the pyruvate kinase coding region and a large non-coding upstream region, was excised and 'force-cloned' into the vector pSP65. This vector had been cut with EcoRI and SalI. The forcible ligation of EcoRI and SalI termini in this way caused in the resulting site to be resistant to either EcoRI or SalI cleavage, due to the loss of the requisite recognition sequences. The *PYK1* encoding region could then be simply cloned into the vector pK19 via the EcoRI and Hind III sites (Fig. 24B).

A 0.9kbp BglII-Hind III fragment containing the regions of *PYK1* that were to be mutated was excised from pSP65-pyk and cloned into M13ab1 for the site-directed mutagenesis reactions. The method of Kunkel et al. (1985) was the mutagenesis protocol of choice. Due to the instability of large insertions into M13, the entire *PYK1* sequence could not be incorporated into this vector, thus complicating the mutagenesis strategy. After the various mutagenesis reactions had occurred successfully, the modified BglII-Hind III fragments were excised and cloned back into pK19-pyk vectors that had themselves been cut with the same two enzymes. This allowed the construction of a series of pK19-pyk plasmids containing the majority of the *PYK1* coding sequence each with a single engineered point mutation at a specific known site.

In a separate experiment, a 7.5kbp Hind III fragment containing the entire wild-type pyruvate kinase coding region obtained from a digest of

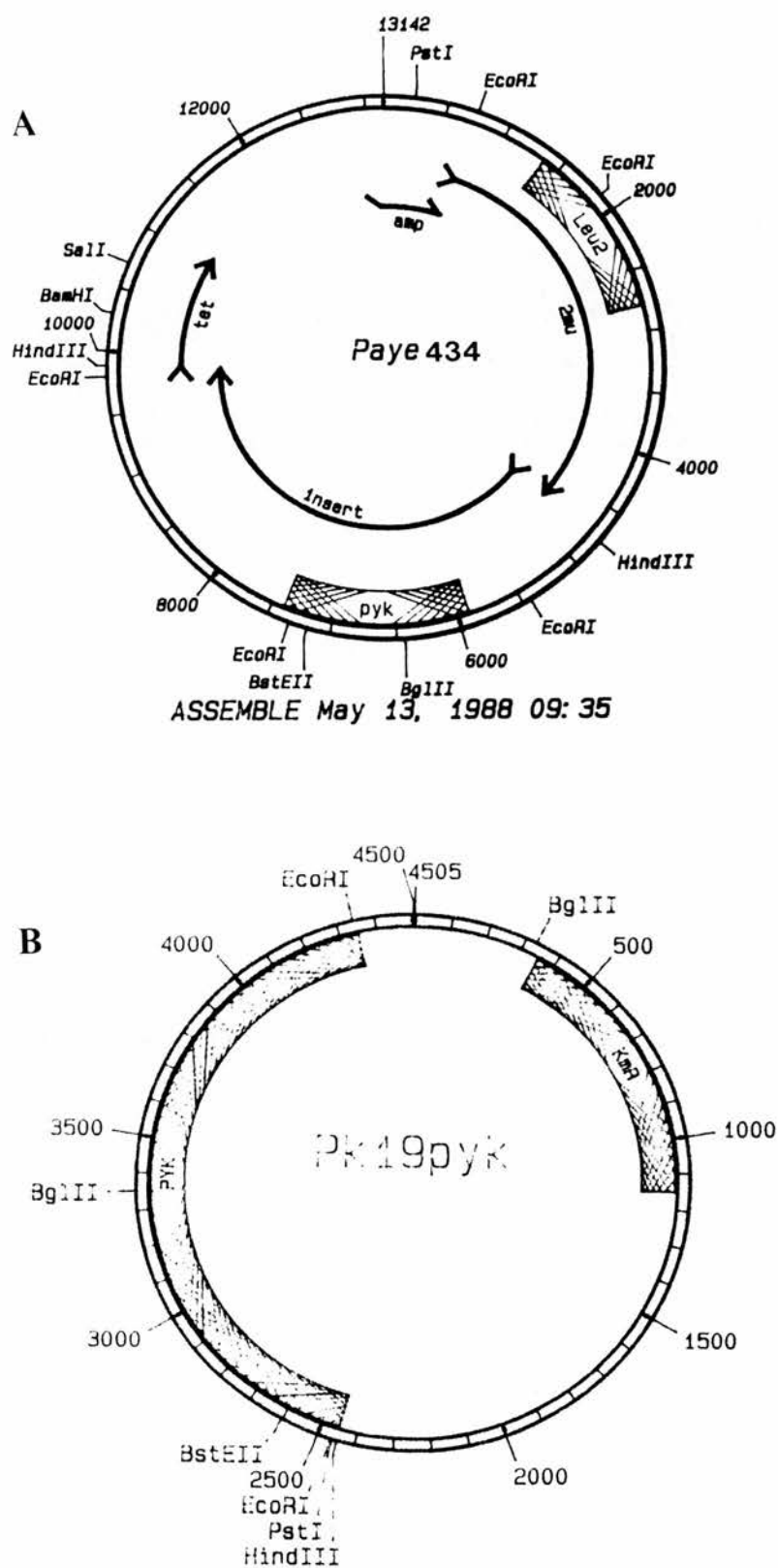


Fig. 24 Plasmid maps  
 A) pAYE 434  
 B) pK19pyk



genomic *S.cerevisiae* DNA, was cloned into the vector pUC18 to generate the plasmid pPYK20 (Fig.25A).

The various pK19-pyk plasmids were digested with the restriction enzymes BglII and BstEII and the resultant 0.75kbp fragments containing the modified *PYK1* sequences were purified and cloned into similarly digested pPYK20 plasmids. This allowed the generation of a series of pPYK20 vectors each containing the complete *PYK1* coding sequence and each containing a single point mutation of interest.

After propagation of these pPYK20 plasmids in *E.coli*, a BglIII-SstI fragment was excised and cloned into the vector pMA91-pyk that had been similarly digested. This final stage resulted in the entire *PYK1* coding sequence being reconstituted in an *E.coli/S.cerevisiae* shuttle vector, in either its wild-type or mutated form, linked to the highly active phosphoglycerate kinase promoter (Fig. 25B). This routinely allowed overexpression of protein up to 5-10% of the total cellular contents.

Obviously, this complex scheme is very time-consuming and prone to losses of product and contamination at every subcloning stage and it would be very much more beneficial for an easier mutagenesis protocol to be devised. A system based on the phagemid pVT-U/L (Vernet et al., 1987) may be a suitable alternative. A preliminary investigation into the feasibility of this method was undertaken, and samples of pVT vectors were kindly provided by Dr. Vernet. It was felt that this particular avenue of investigation, although very promising in its scope for rapid mutagenesis and overexpression of recombinant protein, would be too time-consuming to initiate at such a late stage of these investigations. Such studies would, however, make an ideal component of any further investigations in this area.

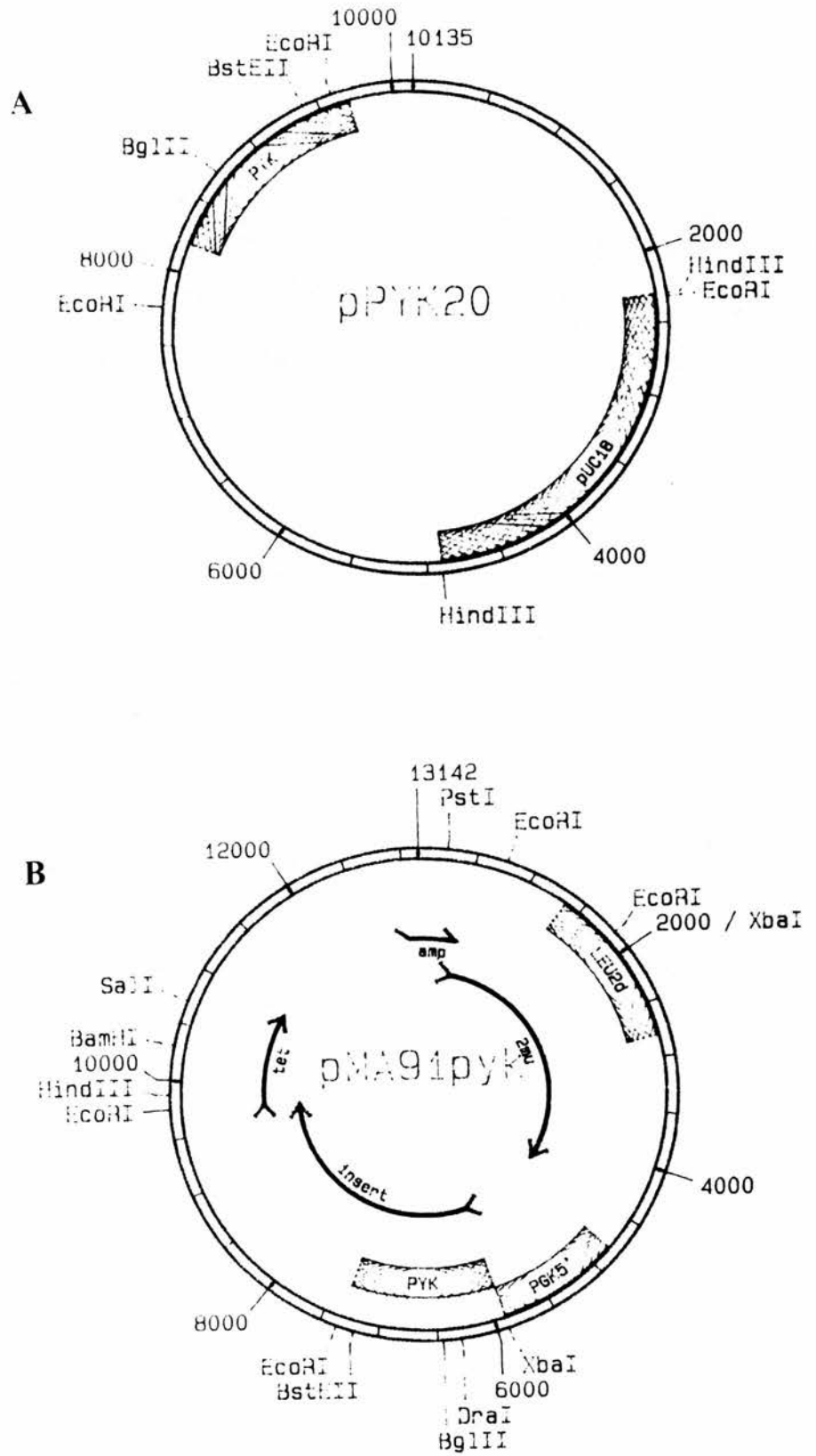


Fig. 25 Plasmid maps  
 A) pPYK20  
 B) pMA91pyk

## 1.17 AIMS OF THE PROJECT

This project involves the overexpression, purification and characterisation of a mutant form of the glycolytic enzyme pyruvate kinase from the yeast *Saccharomyces cerevisiae*.

The enzyme is a tetramer of identical subunits, each about 55kDa in size (Fig. 3). From an analysis of a computer model of the yeast enzyme, it was observed that the residue serine 384, present in the middle of an alpha helix, lay in an important intersubunit contact zone. As a result, it was thought that this residue may have a role in contributing to the communication of conformational changes, induced by ligand binding, to the other subunits. The quaternary structure of the enzyme can be likened to a dimer of dimers (Fig.3), where serine 384 of one subunit lies in close proximity to the equivalent residue in its neighbouring subunit. The effect of any mutation involving serine 384 is, therefore, likely to be enhanced by the close proximity of these residues to each other.

Serine 384 was replaced by a proline residue by site-directed mutagenesis (McNally, 1989). This substitution would have a significant effect on the alpha helix into which it was introduced. It was hoped that this would have measurable effects on the interaction of the enzyme with substrates and effectors, and also on the physical properties of the enzyme such as its stability. The various different properties of the mutant enzyme can be characterised by a number of techniques. Traditional enzyme assay methods provides information on catalytic activity, substrate and effector binding affinities, and cooperativity between binding sites. The mutation was also expected to change the conformation of the enzyme. This aspect can be addressed by a number of techniques such as spectroscopy (uv absorption, CD, and fluorimetry), chemical modification, protease susceptibility, and physical methods such as thermal stability.

As the effects of the point mutation could not be predicted in advance, antibodies against wild type pyruvate kinase will be raised and purified from rabbit serum. These will be useful for purifying any catalytically inactive forms

of the enzyme that may be produced. It is also considered necessary to modify the purification protocol to allow rapid reproducible production of large amounts of enzyme suitable for kinetic and physical characterisation.

As many complete pyruvate kinase amino acid sequences as possible will be collected and compared in an attempt to further characterise the enzyme in terms of residues essential for catalysis, substrate and effector binding, conformational stability and intersubunit communication. It is hoped that future targets for mutagenesis can be identified in this way. A phylogenetic analysis might provide information about the origin and evolution of the various pyruvate kinase enzymes.

## **2. MATERIALS AND METHODS**

### **2.1 MATERIALS**

All chemicals were of the highest grade available and were purchased mainly from Sigma Chemical Co Ltd, Poole, Dorset; Aldrich Chemical Co Ltd, Gillingham, Dorset; BDH Laboratory Supplies, Lutterworth, Leicestershire and Boehringer Mannheim UK, Lewes, East Sussex. Major exceptions were solvents and reagents for molecular biological applications which came from IBI Ltd, Cambridge, UK; DNA purification and sequencing kits from Promega, Madison, USA; and enzyme chemiluminescent kits, radiochemicals and autoradiography film from Amersham International plc, Amersham, UK. Restriction enzymes and lambda Hind III DNA molecular size markers were from a variety of sources mainly Boehringer Mannheim UK; Amersham International plc; Pharmacia Biosystems Ltd, Milton Keynes, UK and Northumbria Biologicals Ltd, Cramlington, UK. Growth media were from Unipath Ltd, Basingstoke, UK and Difco Laboratories, East Molesey, Surrey. Equipment and other important reagents not reported here are mentioned throughout the text where appropriate.

### **2.2 STRAINS AND PLASMIDS USED**

#### **2.2.1 STRAINS**

*Escherichia coli* TG1 K12  $\Delta$ (lac-pro, supE, thi-1, hsdD5/F' traD36, proA<sup>+</sup>B<sup>+</sup>, lacIq, lacZ $\Delta$ M15).

*Saccharomyces cerevisiae* SF747  $\Delta$ pyk9 mat $\alpha$ , leu2, ura3, trp1, gal10, pyk1::ura3 (constructed by McNally, 1989).

#### **2.2.2 VECTORS**

pK19 (Pridmore, 1987)

pMA91pyk (Mellor et al, 1985)

pJDB207 (Beggs, 1981)

pPYK20 (McNally, 1989)

pAYE434 (McNally, 1989)

pK19pyk(117) K239R

pK19pyk(118) S384H

pK19pyk(119) S384R

pK19pyk(213) S384P

pK19pyk(979) K239H

pMA91pyk (K239H)

pMA91pyk (S384P)

The pK19pyk and pMA91pyk derivatives were also created by McNally (1989).

The nomenclature S384X, used above, indicates that serine 384 of the yeast pyruvate kinase protein has been mutated to the residue X by site-directed mutagenesis.

## 2.3 PYRUVATE KINASE ASSAY

Many different methods are available for analysing the catalytic activity of pyruvate kinase. These include monitoring the loss of pyruvate from the reaction media spectrophotometrically (Pon & Bondar, 1967), determining the amount of  $^{14}\text{C}$ -pyruvate as it is formed from  $^{14}\text{C}$ -phosphoenolpyruvate (Kaslow & Garrison, 1983) and recording the loss of NADH as it is converted to  $\text{NAD}^+$  in a coupled enzyme assay with lactate dehydrogenase (Bucher and Pfeleiderer, 1955). By far the most commonly used technique is the latter, i.e coupling the reaction:



to the simultaneous reaction:



Conditions are chosen such that the pyruvate is converted to lactate as soon as it is produced via the first reaction. The stoichiometry is such that the rate of the second reaction, determined by the rate of decrease of absorbance at 340nm, is equivalent to the rate of the first reaction (assuming that the coupled reaction is never limiting).

Throughout the work described in this thesis, pyruvate kinase was assayed by the method of Bucher and Pfeleiderer (1955) with some slight modifications.

The reaction mixture contained: 5.61  $\mu\text{moles}$  phosphoenolpyruvate monocylohexylammonium salt, 2.4  $\mu\text{moles}$  ADP di(monocylohexylammonium) salt, 0.4  $\mu\text{moles}$  nicotinamide adenine dinucleotide (reduced form) as the trisodium

salt (NADH), 1.1 Units rabbit muscle lactate dehydrogenase, 100  $\mu$ moles KCl, 15  $\mu$ moles  $\text{MgCl}_2$ , 0.5  $\mu$ moles EDTA, 100  $\mu$ moles MES-TPA, pH 6.5. The reaction was started by the addition of phosphoenolpyruvate. The MES-TPA, KCl,  $\text{MgCl}_2$  and EDTA were mixed together and termed the "assay buffer". The EDTA was present to chelate traces of divalent cations present in the solutions in experiments where different divalent cations were being tested. TPA was chosen as the counter-ion to MES as KOH and NaOH would interfere with the concentration of monovalent cations present in the assay mixture.

The constituents were dissolved in assay buffer and stored on ice until required. The assay mixture was allowed to warm to 25°C before the addition of enzyme. The temperature was maintained with a thermostatically controlled water bath accurate to  $\pm 0.1^\circ\text{C}$ . The total reaction volume was 1ml.

In other assays, e.g. in which allosteric effectors were added, or in which the concentrations of substrates were altered over a certain specified range, the reaction volume was kept constant at 1ml by adjustments in the volume of assay buffer used.

The rate of decrease in absorbance at 340nm of NADH was followed electronically on a Philips PU8400 uv/visible spectrophotometer. This device greatly increased the number of samples that could be analysed in a given time and allowed statistically meaningful interpretation of data.

Results could be plotted on a graph automatically and rates could be calculated to  $\pm 0.001\text{AU/min}$ .

### **2.3.1 CALCULATION OF SPECIFIC ACTIVITY**

The spectrophotometer calculated reaction rates in absorbance units per minute ( $\text{AU min}^{-1}$ ). The Beer-Lambert law  $A = E \cdot c \cdot l$ , where A is the absorbance at 340nm, E is the molar extinction coefficient of NADH ( $6220 \text{ M}^{-1}\text{cm}^{-1}$ ), l is the pathlength of the incident light beam (1cm) and c is the concentration of the species of interest in the cuvette (M), can be used to calculate the specific activity of any pyruvate kinase sample.

If  $A = E \cdot c \cdot l$ , then  $c = A/E \cdot l$



as  $l = 1\text{cm}$ , this simplifies to  $c = A/E$  (units of  $\text{mol L}^{-1} \text{min}^{-1}$ )

The amount of NADH consumed in the cuvette is determined by multiplying by the volume of the reaction mixture in the cuvette (0.001L) and dividing by the amount of enzyme present (mg). This gives the specific activity of the preparation in terms of  $\text{mol min}^{-1}\text{mg}^{-1}$ . This will usually be an extremely small value and so correction to  $\mu\text{mol min}^{-1}\text{mg}^{-1}$  is made by multiplying by  $10^6$ . For the purposes of this thesis, a unit of pyruvate kinase activity is defined as the amount of enzyme that converts one mmol of phosphoenolpyruvate to pyruvate per minute under the standard conditions used in the assay (described in section 2.2).

## **2.4 MEASURING INTRACELLULAR METABOLITES**

The measurement of the intracellular concentrations of various glycolytic intermediates requires the rapid lysis of cells. Various methods for disrupting yeast cells have been devised. However, the purpose of these protocols was usually the recovery of genomic or plasmid DNA and so employed compounds such as phenol or SDS that would severely compromise any attempt to assay intracellular metabolites enzymatically. The following method avoids these problems.

### **2.4.1 YEAST CELL LYSIS**

At specific time points after inoculation, 1.5ml culture medium was aseptically removed from the culture flask into eppendorf tubes and centrifuged ( $6500\text{rpm} \times 5 \text{ min}$ ,  $5000g$ ) to pellet the yeast cells. The pellet was washed twice with distilled water and drained thoroughly. The pellet was resuspended in 0.1ml assay buffer and glass beads (100 mesh) were added to the level of the meniscus. The tubes were vortexed vigorously for one minute followed by incubation on ice for one minute. This process was repeated three times. The base of the tubes were pierced with a needle and seated in a glass test tube inside a bench top centrifuge. The cell contents were separated from the glass beads by centrifugation ( $2000\text{rpm} \times 30 \text{ secs}$ ). The contents of the glass tubes were transferred to clean eppendorf tubes and assayed immediately or stored at  $-20^\circ\text{C}$ .

## 2.4.2 PHOSPHOENOLPYRUVATE ASSAY

In a 1ml cuvette were added the following:

NADH	0.4μmol
ADP	2.4 μmol
Fructose-1,6-bisphosphate	1.1μmol
Lactate dehydrogenase	1.1 units
Pyruvate kinase assay buffer	0.905ml
Yeast cell lysate	0.05ml
Pyruvate kinase	0.5 units

The reaction was followed by monitoring the decrease in absorbance at 340nm due to oxidation of NADH. The reaction was followed until the loss of NADH reached a plateau.

## 2.4.3 FRUCTOSE-1,6-BISPHOSPHATE ASSAY

(from Murcott et al. 1992)

In a 1ml cuvette were added the following:

NAD <sup>+</sup>	0.5mM
Triosephosphate isomerase (TIM)	2 units
Glyceraldehyde-3-phosphate dehydrogenase (GAPDH)	2 units
Aldolase (ALD)	1.0 unit
Buffer (0.1M Tris-HCl, pH7.5)	0.93ml
Yeast cell lysate	0.05ml
Potassium arsenate	1mM

The constituents were mixed and allowed to react for 24hrs at room temperature.

The potassium arsenate reacts with glyceraldehyde-3-phosphate and prevents equilibration of the reaction.

The reactions occurring are:

Fructose-1,6-bisphosphate ----ALD----> Dihydroxyacetone phosphate +  
Glyceraldehyde-3-phosphate

Dihydroxyacetone phosphate ----TIM----> Glyceraldehyde-3-phosphate

Glyceraldehyde-3-phosphate + NAD<sup>+</sup> + P<sub>i</sub> ---GAPDH----> 1,3-bisphosphoglycerate  
+ NADH

The net reaction therefore is:

Fructose-1,6-bisphosphate + 2 NAD<sup>+</sup>----> 2 1,3-bisphosphoglycerate + 2NADH

## 2.5 PROTEIN DETERMINATION

The amount of protein in a sample was determined using a modification of the method of Bradford (1976). This involved incubating the sample in an acidic solution of a dye (Bradford solution) whose spectral properties vary when it has protein bound to it.

## **BRADFORD SOLUTION**

Phosphoric acid (85%w/v)	100ml
Ethanol	50ml
Coomassie Brilliant Blue G250	0.1g
Distilled water	to 1 litre

The dye was dissolved in the ethanol. To this solution was added the phosphoric acid. The resulting solution was diluted to 1 litre with distilled water and filtered to remove undissolved particles of dye. The final solution was copper brown in colour. The solution was stored at room temperature in a dark bottle.

The samples to be analysed were pipetted into clean glass test tubes. The volume of the sample was less than 0.1ml and the protein content was between 0-50mg. The samples were made up to 0.1ml with distilled water. To this was added 0.9ml Bradford reagent. The tubes were vortexed and allowed to stand at room temperature for ten minutes. The absorbance of the samples was measured at 595nm and read against a suitable reference blank. A calibration curve was constructed using known amounts of bovine serum albumin in the range 0-50µg. The amount of protein in the test samples was calculated by interpolation from the calibration curve.

## **2.6 PURIFICATION OF PYRUVATE KINASE**

The basic protocol for the large scale purification of pyruvate kinase was as follows:

### **2.6.1 HARVESTING YEAST CELLS**

One litre of overnight culture of the appropriate strain of *S.cerevisiae* was harvested by centrifuging, in 250ml pots, for ten minutes at 5000rpm in a JA14 rotor in a Beckman J2/21 centrifuge. The supernatant was discarded, the pellets resuspended in extraction buffer and pooled into one of the pots and recentrifuged as above.

### **EXTRACTION BUFFER**

50mM Tris-HCl, pH 7.6  
20% glycerol  
3mM MgCl<sub>2</sub>  
1mM DTT

The supernatant was again discarded. The pellet was resuspended in the

minimum of extraction buffer (5ml).

### **2.6.2 INHIBITING ENDOGENOUS PROTEASES**

To this mixture, a cocktail of protease inhibitors was added.

#### **PROTEASE INHIBITORS**

1,10-phenanthroline (100mM in DMSO; inhibits metalloenzymes)  
Dichloroisocoumarin (DCIC, 50mM in DMSO; inhibits serine proteases)  
E64 (50mM in methanol; inhibits thiol proteases)  
Benzamidine hydrochloride (100mM in methanol)  
PMSF (100mM in methanol)

The volume of each stock solution used in each preparation was dependent upon the volume of the cell/buffer mixture. A final concentration of 0.1mM 1,10-phenanthroline, 1mM DCIC, E64 and PMSF, and 50mM benzamidine hydrochloride were required prior to cell lysis.

### **2.6.3 CELL LYSIS**

A sufficient quantity of 100 mesh acid-washed glass beads was added to the cell suspension to form a thick slurry. The mixture was then homogenised using a Teflon pestle mounted on a power drill, firmly attached to a retort stand, for six minutes. During lysis the slurry was cooled by an ice bath. The mixture was then cooled on ice for five minutes and the process repeated. The resultant lysed cell-glass bead mixture was washed with 200ml extraction buffer in 25ml aliquots. The washings were transferred to a clean beaker whilst the glass beads were cleaned to enable reuse.

### **2.6.4 CLEANING GLASS BEADS**

The glass beads were extensively washed in dH<sub>2</sub>O to remove cell debris and buffer. In a large beaker, the glass beads were stirred vigorously for an hour in a large volume of dH<sub>2</sub>O to which had been added 1-2ml concentrated nitric acid. The beads were then rinsed extensively in dH<sub>2</sub>O and dried in an oven.

### **2.6.5 CONFIRMING CELL LYSIS**

The bead washings were centrifuged for 20 minutes at 5000rpm to remove cell debris and extraneous glass beads. The supernatant was transferred to a fresh beaker. A sample of the pellet was examined under high power (400x magnification) on a light microscope to assess the extent of cell lysis. If a large proportion of intact

yeast cells were observed, the pellet was resuspended in buffer and protease inhibitors and relysed with fresh glass beads as described above. Usually, only one lysis step was required.

#### **2.6.6 AMMONIUM SULPHATE PRECIPITATIONS**

Finely powdered solid ammonium sulphate was added to the supernatant from the centrifuged bead washings (after a small sample was removed for Bradford and enzyme activity assays) to bring it to 40% (w/v) saturation. The amount of solid to add to the solution can easily be calculated from readily available saturation tables. This solution was stirred continuously, at room temperature, for two hours, avoiding frothing. The solution was then centrifuged in thick-walled tubes (13,000rpm x 30 min). This step removed a large proportion of the relatively insoluble proteins found in cells. The supernatant was decanted and saved whilst the pellet was discarded.

To the supernatant, more solid ammonium sulphate was added to bring the solution to 70% (w/v) saturation (again after saving a sample for protein and activity assays). The solution was stirred for two hours and centrifuged exactly as described above. The resulting pellet was saved for gel filtration whilst the supernatant was discarded.

#### **2.6.7 GEL FILTRATION**

The pellet from the previous step was resuspended in a minimum volume of extraction buffer (typically 5-6ml) and applied to a Sephacryl S200 HR column (90 x 1.6 cm) equilibrated in identical buffer. The flow rate was kept constant by the use of a Gilson Minipuls 2 peristaltic pump and 5ml fractions were collected automatically via a fraction collector (ISCO model 1850). The pyruvate kinase was barely retained by the matrix and eluted soon after the void volume. The fractions were assayed for activity and those found to contain pyruvate kinase were pooled. The addition of solid ammonium sulphate to 75% (w/v) saturation, followed by centrifugation in a benchtop microcentrifuge (13,000rpm x 10 min) resulted in the precipitation of the protein.

#### **2.6.8 ION EXCHANGE CHROMATOGRAPHY**

The surface of the pellets from the previous step were gently rinsed several times with extraction buffer to remove as much ammonium sulphate as possible. This process reduced the ionic strength sufficiently to enable maximal binding of

impurities to the ion-exchange matrix. The pellets were pooled and resuspended in 2ml of extraction buffer and then applied to a Whatman DE52 (DEAE-cellulose) anion exchange column (10 x 2.6cm). The remaining impurities bound to this column and the pyruvate kinase eluted in the void volume. Fractions (2.5ml) were collected automatically as before. The fractions were assayed for activity as described in section 2.3. Active fractions were pooled.

#### **2.6.9 STORAGE OF ACTIVE FRACTIONS**

Enzyme was precipitated with ammonium sulphate as described above and stored at 4°C as a slurry in a sterile glass test tube sealed with Nesco film. Enzyme stored in this way remained active for at least one month.

### **2.7 CONFIRMATION OF HOMOGENEITY**

To confirm that the enzyme preparation was homogeneous polyacrylamide gel electrophoresis in the presence of the detergent sodium dodecyl sulphate (SDS-PAGE) was carried out, followed by staining of the gel with Coomassie blue dye. The resultant gel was scanned with a densitometer.

#### **2.7.1 SDS-PAGE**

The apparatus for pouring and running the gel (Tall Mighty Small, Hoeffer Scientific Instruments, San Francisco, USA) was wiped with methanol to remove traces of grease and other dirt and assembled according to the manufacturer's instructions. The base of the assembly that was to hold the gel-forming solution whilst it was polymerising was sealed with 0.5% (w/v) molten agar solution. Whilst the agar was setting the gel-forming solution was prepared. The resolving capability of the gel depends approximately on the concentration of polyacrylamide that it contains. The % polyacrylamide of the gel can be calculated from the following formula:

$$(a + b)/m$$

where a= acrylamide (g), b= N', N-bismethyleneacrylamide ("bis"), m= total volume of the solution.

Thus a 9% polyacrylamide gel would contain:

2.75ml 30%(w/v) acrylamide stock solution  
(containing 28:2 acrylamide:"bis")



2.95ml dH<sub>2</sub>O  
3.40ml buffer (1.0M Tris-HCl, pH 8.8; 1.0% SDS)  
0.055ml 10% (w/v) ammonium persulphate  
0.015ml TEMED

The solutions were mixed together in a clean beaker. The ammonium persulphate and TEMED were added last as they cause the initiation and polymerisation reactions which lead to the formation of the gel. The mixture was rapidly pipetted into the space between the glass plates of the assembled apparatus. The apparatus was set aside for about 15 minutes for the gel to set. The meniscus of the solution was flattened by the addition of about 0.1ml butanol.

Whilst the separating gel was setting, the stacking gel mixture was prepared in another clean beaker. The stacking gel mixture consisted of:

0.4ml acrylamide stock solution  
1.05ml dH<sub>2</sub>O  
1.50ml buffer (0.5M Tris-HCl, pH 6.8; 1.0% SDS)  
0.04ml 10% (w/v) ammonium persulphate  
0.01ml TEMED

This mixture produced a 4% stacking gel after polymerisation was complete. When the separating gel had set, the butanol was poured off and the top of the gel rinsed with dH<sub>2</sub>O. The stacking gel mixture was quickly pipetted in and the appropriate well-forming comb inserted. The gel was left to set for a further 15 minutes.

When the gel had set the comb was removed and the whole apparatus assembled ready to run. Electrode buffer (diluted from a 10x stock solution) was prepared and poured into the chambers of the apparatus.

#### **ELECTRODE BUFFER (10x stock)**

30.2g Tris  
10g SDS  
186g Glycine  
The pH was adjusted to 8.3 with concentrated HCl.  
The volume was then adjusted to 1L.

250ml 1x electrode buffer was sufficient for each gel. The samples were loaded into the wells, one sample per well. Each well (for a 10-well comb) could accept a maximum of 20 µl of sample. Along with the samples to be analysed, molecular size standards were also applied in order to determine the size of bands of interest and to compare gels run on different days. The gel assembly was connected



to a transformer and run at constant current to minimise heating effects. A current of 20-25mA (variable voltage 75-400V) was used. Electrophoresis was considered to be complete when the dye front reached the bottom of the separating gel. This usually took about 1.5 hours. The current was then switched off and the gel apparatus disassembled. The gel was either stained or used directly for electrophoretic blotting onto a nylon membrane (Western blotting).

### **2.7.2 SAMPLE PREPARATION**

The sample to be analysed was mixed with an equal volume of SDS boiling mix in an eppendorf tube and heated for 15 minutes in a bath of boiling water. The tube was sealed to prevent evaporation of the sample but the top was pierced with a needle to allow the expanding air to escape.

#### **SDS BOILING MIX**

50mM Tris-HCl, pH 6.8  
0.05% (w/v) Bromophenol blue  
10% (v/v) Glycerol  
100mM DTT  
2% (w/v) SDS

### **2.7.3 GEL STAINING**

After electrophoresis, the gel had to be stained in order to detect any proteins that were present. The stain solution contained:

70% (v/v) dH<sub>2</sub>O  
8% (v/v) glacial acetic acid  
22% (v/v) methanol  
0.25% (w/v) Coomassie Brilliant Blue G250

The gel was incubated with about 50ml stain for as long as possible (more than two hours and preferably overnight) in a sealed plastic box at room temperature on a shaking platform. After staining was complete the gel had to be destained. This process removed excess stain from the gel, leaving the proteins visible as blue bands against a colourless background.

### **2.7.4 GEL DESTAINING**

The destaining solution was identical to the stain solution except that it lacked Coomassie blue dye. The staining solution was poured from the gel and saved for reuse. After rinsing the gel with distilled water to remove excess stain, 100ml

destaining solution was added. The gel was incubated, as for staining above. Two pieces of sponge were added to the destaining gel to absorb particles of stain as they were released during the destaining process to prevent redeposition onto the gel. The destain solution was replaced with fresh solution at frequent intervals to ensure a clear background. Destaining was usually complete within two hours. For a permanent record, the gel was mounted onto a damp piece of blotting paper and dried under vacuum using a commercial gel-drying apparatus (Atto AE-3700 gel dryer and processor, Atto Corp, Tokyo, Japan).

### **2.7.5 DENSITOMETER SCANNING**

The homogeneity of protein preparations could be further confirmed by the use of a densitometer. This device scans the gel and records how much of the scanning beam of light is absorbed by the densely-stained protein bands.

The gel was removed from the destain solution and rinsed in dH<sub>2</sub>O. It was essential that the background was as clear as possible. The wet gel was placed onto a clean glass platform mounted in the machine and smoothed out to remove any trapped air bubbles. The width of the beam was controlled by choice of aperture and the path to be followed by the beam was carefully adjusted by controls mounted on the platform. The device (Joyce Loebel Chromascan 3) then scanned the gel automatically and provided a linear plot of peaks, the size of which corresponded to the density of staining. The number, and area, of all peaks able to be resolved were presented graphically or as a table. The molecular size of unknown proteins could be calculated by first scanning a lane of the gel in which a series of molecular size standards was run. The R<sub>f</sub> values of these standards could then be plotted against the log<sub>10</sub> of their molecular size to obtain a calibration curve from which the size of unknown proteins could be interpolated.

## **2.8 WESTERN BLOTTING**

### **2.8.1 TRANSFER OF PROTEIN TO MEMBRANE**

The usual procedure for the transfer of proteins to a membrane used in our laboratory was semi-dry electrophoretic transfer. The polyacrylamide gel, fresh from SDS-PAGE, was soaked in buffer A to remove excess salts which would interfere in

protein transfer and subsequent steps.

#### **BUFFER A**

0.4M 6-amino-n-caproic acid  
0.025M Tris-HCl, pH 9.4  
20% (v/v) methanol

A nylon membrane (Hybond N<sup>+</sup>, Amersham International plc, Amersham, UK) was cut to the same size as the gel, rinsed in 100% methanol and stored in buffer B until required.

#### **BUFFER B**

0.025M Tris-HCl, pH 10.4  
20% (v/v) methanol

The blotting apparatus was assembled as follows:

Two layers of filter paper cut to the same size as the gel and soaked in buffer C were placed onto the surface of the lower half of the blotting apparatus (BioRad). This lower half was composed of a slab of graphite and formed the anode of the apparatus.

#### **BUFFER C**

0.3M Tris-HCl, pH 10.4  
20% (v/v) methanol

On top of these layers were placed two layers of filter paper soaked in buffer B. The nylon membrane was placed on top of these layers followed by the gel, care being taken to exclude any trapped air bubbles. On top of the gel were placed four layers of filter paper soaked in buffer A. The upper half of the transfer unit, forming the cathode, was placed on top of the assembled filter paper/gel/membrane stack and connected to the power supply. A constant current (0.8mA/cm<sup>2</sup>) was applied for one hour. After this time, the power was switched off and the transfer unit carefully disassembled. The gel was stained with Coomassie Blue as described earlier to assess the extent of transfer to the membrane. The membrane was rinsed in water and stored wrapped in clingfilm until required.

#### **2.8.2 DETECTION OF IMMOBILISED PROTEIN**

After transfer, the membrane was placed in a clean plastic tray containing about 100 ml of blocking buffer and incubated (all incubations described in this section occurred at room temperature on a gently shaking platform) for two hours to

block any remaining protein binding sites.

### **BLOCKING BUFFER**

10mM Tris-HCl, pH 8.0  
150mM NaCl  
0.05% Tween 20  
1% (w/v)BSA

The mixture of 150mM NaCl and 10mM Tris-HCl is known as Tris- buffered saline (TBS). When Tween 20 was also added it was known as TBST.

After blocking, the membrane was rinsed in a little TBST and incubated in 50ml primary antibody solution for one hour.

### **PRIMARY ANTIBODY SOLUTION**

50ml TBST  
0.25g BSA  
0.3ml purified rabbit anti-PK IgG (1:1500 dilution of antisera)

After incubation with primary antibody, excess IgG was removed by washing the membrane three times, for ten minutes each time, in 100ml aliquots of washing buffer. The buffer was discarded between washes.

### **WASHING BUFFER**

TBS  
0.05% (v/v) Tween 20

After washing, the membrane was incubated with 50ml secondary antibody solution for two hours.

### **SECONDARY ANTIBODY SOLUTION**

50ml TBST  
0.25 BSA  
0.03ml goat anti-rabbit IgG conjugated to horseradish peroxidase

After this secondary antibody incubation, the membrane was rinsed in three changes of washing buffer (100ml per wash, each for ten minutes) before incubation with the colour development solution.

### **2.8.4 COLOUR DEVELOPMENT REACTION**

The horseradish peroxidase activity conjugated to the secondary antibody was utilised in order to locate specific protein bands. The specificity of the conjugated enzyme for substrate is quite broad and a number of dye precursors have been used for localisation reactions. The reaction described here used 4-chloro-1-naphthol

which could be oxidised to give a purple precipitate that was deposited onto the membrane. The composition of the development mixture was as follows:

0.1ml 4-chloro-1-naphthol (100mg/ml in methanol)  
0.07ml H<sub>2</sub>O<sub>2</sub> (30% v/v)  
8ml TBS

The development mixture was poured onto the membrane and agitated constantly to ensure even wetting of the surface. Colour development began immediately and lasted up to 30 minutes. When the colour had developed to the required level the reaction was stopped by rinsing the membrane in an excess of distilled water. The membrane could be photographed or stored damp in a sealed plastic bag. Once the reaction had ended the membrane had to be kept in the dark to prevent fading of the purple colour. On prolonged incubation with the reaction mixture the dye became olive green in colour.

### **2.8.5 IMMUNODIFFUSION**

Combination of antibody (Ab) and antigen (Ag) in a restricting gel environment causes Ab-Ag precipitates to become visible as pale precipitin lines.

A number of clean glass microscope slides were coated with a film of molten agarose-buffer solution which was allowed to cool and solidify.

#### **AGAROSE-BUFFER SOLUTION**

50mM Tris-HCl, pH 7.6  
100mM KCl  
15mM MgCl<sub>2</sub>  
1% (w/v) agarose

Wells were cut into the gel with a scalpel in identical positions on all the slides. The wells were cut so that six wells surrounded a single central well, all an equal distance apart. In the central well was placed 3.5µl undiluted pre-immune, or anti-pyruvate kinase, serum. The other wells contained 3.5µl of solutions of the following: BSA (0.1mg/ml), rabbit muscle pyruvate kinase (1mg/ml), yeast wild type pyruvate kinase (1mg/ml), *E.coli* cell extract, *Bacillus subtilis* cell extract, *Staphylococcus aureus* cell extract and *Thermophilus acidophilum* cell extract (all approximately 1mg/ml). The slides were laid on tissue paper moistened in buffer and incubated in a closed container at 4°C for 24 hours. The slides were stained for protein as described

in Section 2.7.3. The agar strips could be preserved by mounting them on mats of filter paper and compressing them with a heavy weight. The filter paper was changed at regular intervals until the agar strip was completely dry.

## **2.8.6 IMMUNOTITRATION**

Immunoremoval of pyruvate kinase activity was tested by mixing 2.5µg wild type pyruvate kinase with 25mM Hepes-NaOH, pH 7.5, containing 10% (v/v) glycerol, 1mM dithioerythritol, and varying amounts of rabbit anti-yeast wild type pyruvate kinase antiserum, or pre-immune serum, diluted in the same buffer. Dilutions of antiserum or pre-immune serum were in the range 1:50 to 1:1000. The reactions occurred in a total volume of 0.1ml. The mixtures were incubated at room temperature for one hour, followed by two hours incubation on ice. Precipitates were removed by centrifugation (13,000rpm x five mins). The residual pyruvate kinase activity in a 5µl aliquot of supernatant was assayed as described earlier (Section 2.3).

## **2.9 IMMUNISATION**

### **2.9.1 ADVANTAGES OF USING RABBITS FOR IMMUNISATION**

Polyclonal antisera can be raised in a large variety of laboratory animals. The rabbit is generally considered to be one of the most useful as it can be made to produce considerable quantities of antisera (up to 20ml per fortnight) of high affinity and titre. These antisera are predominantly of the IgG type. Other advantages of using rabbits are their docility, the ease with which they can be housed and handled and the relatively low cost of their upkeep.

The introduction of yeast-derived protein presented no difficulties with respect to toxicity or reduced antigenicity due to species relatedness. The best yield and titre of polyclonal antisera is obtained via a series of injections of the antigen. Two female, 3kg (4-5 months old), New Zealand White rabbits were purchased (City Farms, West Lothian) and housed in the Faculty Animal Area. All antigen injections and subsequent bleedings were performed by trained staff and not by the author himself.

### **2.9.2 IMMUNISATION PROTOCOL**

Yeast pyruvate kinase (2mg/ml) in 70% (w/v) saturated ammonium sulphate was kindly provided by Dr. Toby Murcott, University of Bristol. The ammonium



sulphate was reduced by overnight dialysis against assay buffer at room temperature.

Before inoculation, a 5-10 ml sample of blood was taken from each rabbit and a serum fraction prepared from it to act as a control blank in subsequent experiments.

The primary injection consisted of 0.5ml antigen solution and 0.5ml Freund's complete adjuvant (FCA) thoroughly mixed to form a stable emulsion. FCA consists of a mineral oil mixed with heat-killed bacillus and an emulsifier and acts to increase the immune response to injected antigens. Equal volumes (0.5ml) were injected into each rabbit sub-cutaneously at multiple sites.

After two weeks a further injection was made. This consisted of 0.1mg antigen in 0.2ml FCA:antigen emulsion. The mode of injection was as before.

After a further seven weeks a third injection was made. This consisted of 0.15ml antigen solution mixed with an equal volume of Freund's incomplete adjuvant (FIA). FIA is identical to FCA except that it does not contain a heat-killed bacillus fraction and so reduces the possibility of granuloma formation at the site of injection.

Four weeks after the final antigen injection 5-10ml whole blood was removed from each animal and the antisera prepared as described in the next section. A simplified version of the immunisation schedule is shown in table 15 (Section 3.9).

### **2.9.3 PREPARATION OF ANTISERA**

A sample of blood (5-10ml) was removed from each animal by a qualified technician and stored in sterile, plastic, screw-capped containers. The blood was allowed to clot at 37°C for one hour. The clot was then detached from the walls of the tube, until it was moving freely, by a sterile wooden cocktail stick. The clot was allowed to retract at 4°C for 24 hours. After this process, a layer of straw-coloured clear fluid could be seen above a dense mass of cells that lay at the bottom of the tube. The clotted blood was centrifuged (4000rpm x 10 min) to fully separate the serum from the blood cells. The upper serum layer was pipetted into a length of freshly prepared dialysis tubing sealed at one end by a watertight plastic clamp. As much air as possible was gently squeezed out of the tubing before the other end was sealed with another plastic clamp. The sealed tubing was immersed in a beaker containing 200ml phosphate buffer (20mM  $\text{KH}_2\text{PO}_4$  - NaOH, pH 7.2). Dialysis continued at 4°C for 24 hours with frequent replacement of the buffer.



## **PREPARATION OF DIALYSIS TUBING**

A 10cm length of Visking dialysis tubing (Medicell International Ltd, London, UK) was boiled in 500ml 2% (w/v) sodium bicarbonate, 1mM EDTA solution for 10min. The tubing was rinsed in a large volume of distilled water and boiled for a further ten minutes. After further rinsing, the tubing was ready for use. It was handled with gloves at all times and was kept submerged to prevent drying.

After dialysis, the serum was removed to a sterile tube and an equal volume of anion exchange resin (Whatman DE52, DEAE-cellulose) equilibrated in dialysis buffer was added. The mixture was allowed to stand for one hour at room temperature with occasional mixing. The antisera/resin slurry was then poured into the barrel of a 5ml sterile syringe and the antisera expressed through a sterile 0.2mm filter unit (Millipore S.A, Molsheim, France)) into sterile eppendorf tubes. Aliquots of 1ml were stored at -20°C until required.

## **2.10 DNA PURIFICATION**

Plasmid DNA purification can be done on many scales depending on the quantity and quality of the required material. Smaller quantities (1-5µg) are sufficient for most uses eg restriction enzyme digests but higher quality preparations may be needed for transformation or mutagenesis experiments. Small scale preparations (minipreps) have the advantage of being rapid but care must be taken to prevent contamination with endogenous RNases. Large scale preparations (maxipreps) do not suffer from RNase contamination but as a result are much more time consuming to perform.

### **2.10.1 PLASMID MINIPREPS**

The protocol outlined below is basically the same as that described by Sambrook et al. in "Techniques in Molecular Biology" vol.1,4.15-4.19, Cold Spring Harbor,1989.

Sterile apparatus and solutions were used and gloves were worn throughout the procedure.

A 10ml overnight culture of the bacteria containing the plasmid of interest was aliquoted into eppendorf tubes and the cells pelleted by spinning them in a benchtop

centrifuge (MSE Microfuge, Fisons,UK) for four minutes at 13,000rpm. The supernatants were removed and the pellets resuspended in 0.2ml solution 1.

### **SOLUTION 1**

50mM glucose  
25mM Tris-HCl, pH8  
10mM EDTA

To the resuspended cells, 0.4ml solution 2 was added. This resulted in cell lysis and protein denaturation.

### **SOLUTION 2**

0.2M NaOH  
1% (w/v) SDS

To this mixture 0.3ml solution 3 was added. This deproteinated the nucleic acid, facilitating its solubilisation.

### **SOLUTION 3**

17.4ml glacial acetic acid  
10.8g KOH

The KOH was dissolved in 30ml dH<sub>2</sub>O to which the acetic acid was then added. A large amount of heat was liberated and care was taken during the mixing process. The volume was adjusted to 60ml with dH<sub>2</sub>O.

On addition of solution 3 a large amount of protein was precipitated. The resulting mixture was centrifuged at 13,000rpm for ten minutes in a benchtop microcentrifuge. The supernatant was transferred to a fresh tube whilst the pellet was discarded. To the supernatant, 1/10 of the volume of 3M sodium acetate and two volumes of absolute ethanol were added. The solution was incubated at -20°C for two hours. After incubation, the plasmid DNA was precipitated by centrifugation at 13,000rpm for ten minutes. The supernatant was discarded, the pellet dried in a vacuum desiccator and resuspended in 50ml 1xTE.

### **1x TE**

10mM Tris-HCl, pH 8.0  
1mM EDTA

To each fraction of plasmid DNA, 2ml ribonuclease A solution was added and

the tubes incubated at 37°C for 30 minutes. This resulted in the degradation of any RNA contaminants copurifying with the plasmid DNA.

### **RIBONUCLEASE A PREPARATION**

10mg bovine pancreatic ribonuclease A (Boehringer Mannheim GmbH, Germany) was dissolved in 1ml 0.01M sodium acetate (pH 5.2). The mixture was heated to 100°C for 15 minutes and then allowed to cool slowly to room temperature. The mixture was dispensed in 50µl aliquots into sterile eppendorf tubes and stored at -20°C until required.

After ribonuclease treatment, an equal volume of phenol:chloroform was added to each tube. The mixture was shaken until an emulsion formed. After brief centrifugation (13,000rpm for 15 secs) the aqueous and organic layers separated. The DNA partitioned to the upper aqueous layer whilst the ribonuclease remained in the organic layer. The aqueous phases from separate tubes were pooled into one tube to which an equal volume of chloroform was added. This removed traces of phenol. The mixture was briefly centrifuged as before. The upper aqueous layer was removed to a fresh eppendorf tube. The plasmid could be precipitated from this fraction by the addition of 1/10 volume of 3M sodium acetate and two volumes of absolute ethanol followed by a two hour incubation at -20°C and a high speed centrifugation step (13,000rpm for 10 mins). The supernatant was discarded, the pellet dried under vacuum and either stored at -20°C until required or resuspended in 1xTE and used immediately.

### **PHENOL PREPARATION**

Phenol was stored in a dark glass bottle at -20°C. It was melted by immersing the bottle in a water bath heated to 60°C for several minutes. A fraction was poured into a 50ml Falcon tube and 8-hydroxyquinoline (0.1% w/v) was added. This compound acts as a weak inhibitor of RNAase and its pale yellow colour serves to easily identify the phenolic phase in mixtures of immiscible liquids. An equal volume of 1M Tris-HCl, pH 8.0 was added and the two liquids mixed vigorously for a few minutes. After the two phases separated, the upper buffer layer was removed and the procedure repeated. The pH of the phenol layer was tested using pH indicator paper. An organic phase pH of between 7.5 and 8.5 units was required. The phenol was

stored under 0.1M Tris-HCl, pH 8 in a 50ml Falcon tube wrapped in aluminium foil to prevent light- induced degradation. The tube was stored at 4°C. Under these conditions the phenol remained stable for about one month. A pronounced darkening of the phenol phase, from pale yellow to deep orange, was observed upon prolonged storage and indicated that the phenol was no longer fit for use.

### **2.10.2 PLASMID MAXIPREPS**

This follows basically the same procedure as for the miniprep method but on a larger scale. All equipment was sterile and gloves were worn throughout the preparation.

A bacterial culture was grown with vigorous shaking in a 37°C incubator to the desired cell density. The cells were pelleted by a brief centrifugation step (5000rpm for 10 mins in 250ml capacity plastic pots in a Beckman J2-21 centrifuge fitted with a JA14 rotor). The supernatant was decanted and the pellet resuspended in solution 1 (4ml per 100ml starting culture, Section 2.10.1). A sample of the resuspended cells was removed and plated onto selective agar plates to confirm that the culture contained only the transformed cells of interest. The plates were incubated at 37°C and examined after 16-20 hours. To the resuspended cells solution 2 was added (8ml per 100ml starting culture). After ensuring the complete lysis of the cells by gentle mixing, solution 3 was added (6ml per 100ml starting culture). The mixture was centrifuged in thick-walled tubes at 13,000rpm for 15 minutes in a Beckman JA20 rotor. The supernatant was decanted into 50ml Falcon tubes. Sodium acetate and absolute ethanol were added just as described for the miniprep. An incubation at -20°C for two hours, followed by a further centrifugation at 13,000rpm for 15 minutes, resulted in the precipitation of the plasmid DNA. The supernatant was decanted and the pellets washed in 80% (v/v) ethanol. The plasmid was repelleted by centrifuging at 13,000rpm for ten minutes. The ethanol was poured off and the pellets dried under vacuum for a few minutes. At this stage the pellet was a pale yellow in colour due to RNA contamination. The pellets were resuspended in 4ml sterile 1xTE. Caesium chloride (1g/ml) was added and the tubes incubated at 50°C for a few minutes to ensure the complete dissolution of the salt. To every 5ml of CsCl-DNA solution, 0.4ml ethidium bromide (10mg/ml) was added. The mixture was centrifuged at 8,000rpm for ten minutes. This caused RNA to precipitate as a deep

red pellet and also allowed the removal of extraneous protein as this formed a floating scum layer. The clear red-coloured liquid was transferred to special ultracentrifugation tubes (Beckman). The tubes were topped up with mineral oil and sealed by melting the tops in a sealing device provided by the manufacturer of the tubes. Before sealing, the mass of the plasmid-containing tubes were corrected to within 0.5% of each other by the addition or subtraction of oil. The tubes were then placed in a Beckman Ti70.1 rotor and centrifuged at 45,000rpm for 48 hours at 22°C in a Beckman L60 ultracentrifuge. After this period the plasmid was visible as a pale red band about halfway down the tube.

### **2.10.3 RECOVERING PLASMID FROM CsCl GRADIENT**

The process is described diagrammatically in Fig.25. The tubes were carefully removed from the rotor to prevent disturbing the CsCl gradient. The plasmid DNA was visible as the lower of two pale red bands located about halfway down the tube. The tube was carefully held in a clamp attached to a retort stand. A needle (21 gauge) was used to pierce the top of the tube such that it penetrated the mineral oil layer. Another needle was used to pierce the tube just above the plasmid band of interest. A third large bore (18 gauge) needle was used to pierce the tube directly at the level of the plasmid band. This needle was attached to a sterile 1ml syringe and the plasmid band was carefully extracted. The large bore of the needle prevented shearing of the DNA, especially high molecular weight species of plasmid. The needle was removed from the syringe and the contents expressed into a sterile eppendorf tube.

### **2.10.4 REMOVAL OF ETHIDIUM BROMIDE FROM CsCl PURIFIED PLASMID**

To the solution of DNA an equal volume of 1-butanol saturated with water was added. The two phases were mixed by gently shaking the tube. The phases were separated by briefly centrifuging (6500rpm for 15 seconds). The upper butanol layer was removed and discarded. Further water-saturated butanol was added and the process repeated several times until all the pink colour disappeared from both the aqueous and organic phase. The CsCl was removed by diluting the DNA solution with three volumes of water and precipitating the DNA with two volumes of absolute ethanol at 4°C for 15 minutes followed by centrifugation at 13,000rpm for ten minutes at 4°C. The supernatant was removed and the plasmid pellets dried under

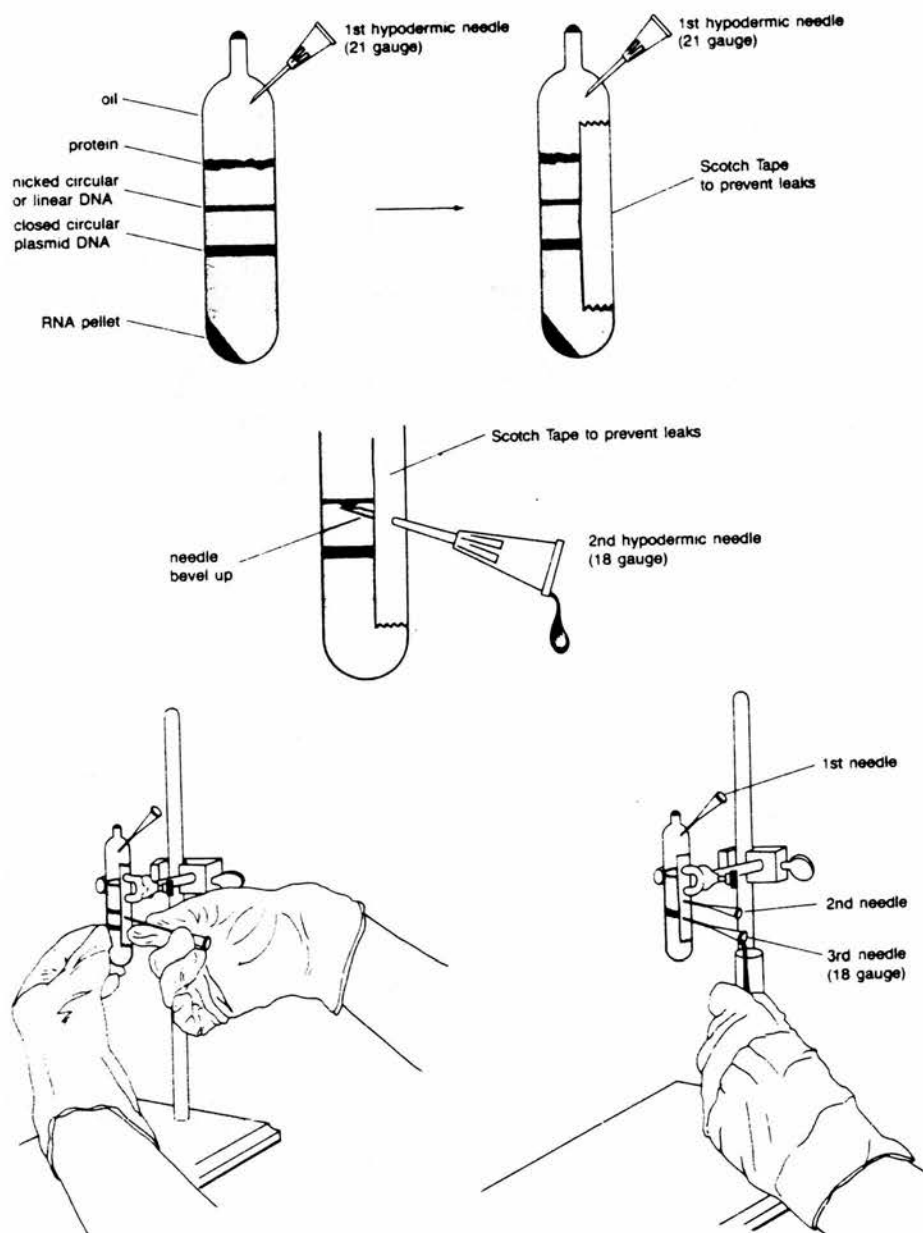


Fig. 26 Collection of plasmid DNA from CsCl gradients containing ethidium bromide.  
(from Sambrook et al., 1989)

vacuum for a few minutes. The plasmids were stored at -20°C until required.

## **2.11 BACTERIAL TRANSFORMATION**

### **2.11.1 PREPARATION OF COMPETENT CELLS**

Before transformation of bacterial cells can occur they must be made able to take up foreign DNA i.e. made competent. This can be done in a variety of ways but by far the quickest and easiest method is to incubate the cells in a solution of alkali-metal salt, usually calcium chloride.

The following procedure is a modification of the method developed by Cohen (1972) as described in "Molecular Cloning: A Laboratory Manual", 2nd edition, (1989, Cold Spring Harbor Laboratory Press, NY, USA,) by Sambrook, Fritsch and Maniatis, Volume 1, pp 1.82-1.84.

All equipment coming into contact with the bacterial cultures was sterile and gloves were worn throughout.

A single colony of *E.coli* TG1, from a plate freshly grown for 16-20 hours at 37°C, was transferred to 10ml LB media and incubated at 37°C with vigorous shaking for 16 hours. A portion of this culture (1ml) was used to seed 100ml SOB media in a 1 litre flask. This culture was incubated at 37°C with shaking until the OD<sub>600</sub> reached 0.3-0.4 (this usually took 3-4 hours).

#### **SOB MEDIA (100 ml)**

2.0g tryptone  
0.5g yeast extract  
0.05g NaCl  
1ml 250mM KCl  
0.5ml 2M MgCl<sub>2</sub>  
dH<sub>2</sub>O to 100ml  
Sterilised by autoclaving

The cells were then transferred to 50ml Falcon tubes and cooled on ice for ten minutes. The cells were pelleted by centrifuging at 4000rpm for ten minutes. The media was decanted and discarded. The tubes were inverted to allow as much fluid as possible to drain away. The pellets were resuspended in 10ml 0.1M CaCl<sub>2</sub> and stored on ice for a further ten minutes. The cells were then pelleted as before. The supernatant was decanted and the pellets resuspended in 2ml ice-cold 0.1M CaCl<sub>2</sub>.



The cells were then ready for transformation.

### **2.11.2 TRANSFORMATION**

Competent cells (0.2ml) were pipetted into sterile eppendorf tubes. The DNA was added to each tube (no more than 50ng in 10ml 1xTE). A control experiment in which no DNA was added was included in each transformation experiment. The tubes were incubated on ice for 30 minutes. The cells were then heat-shocked at 42°C for 90 seconds to encourage them to take up the added DNA. The tubes were then chilled on ice for two minutes. Growth media (0.8ml LB, Section 2.11.3) was added to each tube and the cells incubated, without shaking, at 37°C for 60 minutes. This allowed the cells to recover from the transformation and to begin to express the antibiotic resistance encoded by the newly incorporated plasmid. The transformed cells were pelleted by a brief centrifugation (6500rpm for 15 secs) and the excess fluid removed. The pellets were resuspended in the residual media (100-150µl). Equal volumes of transformed cells (50µl) were pipetted into the centre of selective agar plates and the fluid spread evenly over the surface by a sterile bent glass rod. The plates were incubated at 37°C for 16-20 hours, after which time single colonies were visible.

The agar plates incorporated an antibiotic such that only successfully transformed cells were able to grow. A negative control plate was also used. This contained an antibiotic that transformed cells cannot grow in the presence of and demonstrated that no unusual plasmid had been introduced. A positive control consisting simply of rich media with no added antibiotics of any kind was also used. Untransformed cells can grow on this and so colonies visible on these plates after appropriate incubation demonstrated that the cells had survived the transformation procedure.

### **2.11.3 GROWTH MEDIA**

#### **AGAR PLATES**

##### **2xTY**

16g/l tryptone  
10g/l yeast extract  
5g/l NaCl  
15g/l agar

1 pellet NaOH  
Sterilised by autoclaving

Kanamycin monosulphate (20mg/ml in dH<sub>2</sub>O) to a concentration of 0.07mg/ml was added, after the media had cooled to below 50°C.

**LB**  
10g/l tryptone  
5g/l yeast extract  
5g/l NaCl  
15g/l agar  
1 pellet NaOH  
Sterilised by autoclaving

Ampicillin (sodium salt, 20mg/ml in dH<sub>2</sub>O) was added to a concentration of 0.1mg/ml, after the media has cooled to below 50°C.

For non-selective rich media 2xTY plates were used without antibiotic addition. To prepare one batch of twenty 90 x 12mm plates, 500ml of media was required. For liquid growth media, the above recipes were prepared except that the agar was omitted.

#### **2.11.4 STORAGE OF BACTERIAL STRAINS**

To enable a constant supply of viable cells of the correct genotype to be available, frozen stocks of each strain were kept. These stocks consisted of the relevant bacterial strain grown in a liquid medium, containing the appropriate selective antibiotic, and supplemented with sterile glycerol (0.67ml culture grown to a density of OD<sub>600</sub> 0.8-1.0 + 0.33ml sterile glycerol in a sterile 1ml eppendorf tube). After vortexing, to ensure even mixing of the culture with the glycerol, the tubes were labelled and stored in a freezer at -20°C where they remained viable for up to 24 months. The cells could be revived by taking a sterile loop and scraping the frozen surface of the stock culture and spreading the cells onto the appropriate selective agar plate and incubating for 16-20 hours at 37°C. The agar plates themselves could be wrapped in clingfilm to keep them airtight and stored at 4°C for up to four months before replating of the cells became necessary.

#### **2.12 YEAST TRANSFORMATION**

Like bacterial cells, yeast can be made competent to take up foreign DNA by pretreatment with alkali metal salts. The method described here is a variation of the lithium acetate pretreatment protocol of Ito et al. (1983). As with the transformation

of bacteria, all solutions and glassware coming into contact with the yeast cells were sterile. The yeast strain to be transformed had its native *PYK1* gene disrupted by an insertion of the *URA3* gene (McNally, 1989).

A single colony of the recipient strain was picked from a freshly grown selective plate and used to inoculate 10ml of selective media. The cells were grown at 30°C with shaking for 48 hours. The 10ml culture was used to seed 300ml of identical media in a one litre flask, which was also grown at 30°C with shaking for 48 hours. A sample of the cells (2 x 50ml) were harvested by centrifuging in Falcon tubes in a benchtop centrifuge for ten minutes at 2500rpm. The supernatant was discarded and the cells resuspended in 10ml 1xTE. The cells were pelleted exactly as before. The supernatant was again discarded and the pellets resuspended in 10ml lithium acetate solution.

#### **LITHIUM ACETATE SOLUTION**

0.1M lithium acetate  
10mM Tris-HCl, pH 8.8  
1mM EDTA  
Sterilised by filtration

The cells were pelleted exactly as before. The pellets were finally resuspended in 1ml lithium acetate solution and incubated at 30°C with gentle shaking (100rpm) for one hour. The yeast cells were now ready to be transformed.

Aliquots of competent cells (100µl) were pipetted into 1.5ml eppendorf tubes. The DNA (1-10µg) was dissolved in 1xTE and added to the cells in a volume of 50µl. A control, in which no DNA was added to the cells was included in every transformation experiment. The cells were incubated, without shaking, at 30°C for 30 minutes. To each tube 0.7ml PEG solution was then added and the cells thoroughly mixed by pipetting up and down using a 200µl pipette.

#### **PEG SOLUTION**

40% (w/v) polyethylene glycol 3350  
dissolved in lithium acetate solution.  
Sterilised by filtration.

Following the addition of the PEG solution, the cells were incubated (without

shaking) for 45 minutes at 30°C. The tubes were then placed in a water bath at 42°C for five minutes. The cells were pelleted by briefly centrifuging at 6500rpm for 15 seconds. The supernatant was discarded and the cells resuspended in 1ml YEPD. The cells were incubated at 30°C for one hour and then repelleted exactly as before. The majority of the supernatant was poured off and the cells resuspended in about 100-200µl of the remaining fluid. The cells (50µl per plate) were spread onto selective plates using a sterile bent glass rod and incubated for upto 14 days at 25°C.

## 2.13 GROWTH AND MAINTENANCE OF YEAST STRAINS

One strain of yeast was routinely used throughout this project:

*Saccharomyces cerevisiae* SF747 (*mata $\alpha$  leu2, ura3, trp1, gal10* )

This strain was further modified by disrupting the *PYK1* gene by the insertion of the *ura3* gene. This prevented the expression of native pyruvate kinase protein. As a result, this strain could be used as the recipient for expression vectors containing native or modified versions of the *PYK1* gene enabling the production and subsequent purification of a variety of different forms of the enzyme. The disruption of *PYK1* also means that this strain cannot utilise glucose as a carbon source and so must be grown on pyruvate-containing media which enables the pyruvate kinase step in glycolysis to be bypassed.

The disrupted strain, designated  $\Delta pyk9$ , was grown on the synthetic medium Yo leu<sup>+</sup>ura<sup>-</sup>pyruvate.

### **Yo leu<sup>+</sup>ura<sup>-</sup>pyruvate**

6.7g/litre yeast nitrogen base (without amino acids)  
5.0g/litre ammonium sulphate  
20g/litre pyruvate  
10ml/litre 100x amino acid stock  
Sterilised by autoclaving

N.B. The pyruvate was added as a solution after the media has cooled. It was sterilised by filtration through a 0.22mm pore diameter filter.

## 100x AMINO ACID STOCK

Compound	100x concentration (g/litre)	1x concentration (mM)
adenine	5.0	0.37
L-arginine	2.4	0.14
L-aspartate	12.0	0.90
L-glutamate	12.0	0.65
L-histidine	2.4	0.15
L-leucine	6.0	0.45
L-lysine	3.6	0.25
L-methionine	2.4	0.16
L-phenylalanine	6.0	0.36
L-serine	45.0	4.30
L-threonine	24.0	2.00
L-tryptophan	2.0	0.10
L-tyrosine	3.6	0.20
L-valine	18.0	1.54

Tryptophan was prepared separately as a 100x stock solution at 2g/litre. It was stored at 4°C in the dark. Leucine was also prepared as a 100x stock solution at 6g/litre. It was stored at -20°C as were the other amino acid stocks.

For growth of transformed strains pyruvate was replaced with glucose (which could be added before autoclaving) and leucine was omitted. Solid media could be prepared from these solutions by the addition of 15g/litre agar prior to autoclaving.

### 2.14 PLOTTING A GROWTH CURVE

Growth rate experiments were performed on all strains. All strains were grown on the appropriate synthetic media as described in the last section. The strain *pyk1::ura3* was grown on Yo leu<sup>+</sup>ura<sup>-</sup>pyruvate. Transformed strains were grown on Yo leu<sup>-</sup>ura<sup>-</sup>glucose. A 10ml starter culture was inoculated with a single colony aseptically transferred from a freshly grown plate of selective media. This was incubated at 30°C with vigorous shaking for 16-20 hours. This starter culture was used to seed 100ml selective media which was also incubated at 30°C with shaking. At recorded times, 1ml samples were aseptically removed from the culture and the cell density measured spectrophotometrically at 600nm. The measure of light scattering of the culture is proportional to the cell density. At absorbances above 1.0, the culture was diluted by a known amount and the optical density remeasured. The actual

OD<sub>600</sub> was then derived by back-calculation. This method obviated any deviation from non-linearity observed at high cell densities. The results were plotted as OD<sub>600</sub> against time after inoculation (in hours) to give a growth curve for that particular strain. A plot of log OD<sub>600</sub> enabled the growth rate to be determined from the linear portion of the resultant curve.

## **2.15 PLASMID RESCUE**

To confirm that transformation had been successful, the plasmid was purified from transformed yeast cells and compared with an original plasmid preparation. Factors such as size, restriction digest patterns and selectable markers were compared between the two plasmids.

A sample of yeast culture (1.5ml) was pelleted by brief centrifugation (6500rpm for 15 seconds). The supernatant was discarded and the pellet resuspended in the residual fluid (100- 150μl). To each pellet 0.2ml yeast lysis buffer, 0.2ml phenol- chloroform (1:1) and 0.3g acid-washed glass beads were added.

### **YEAST LYSIS BUFFER**

2% (v/v) Triton X-100  
1% (w/v) SDS  
100mM NaCl  
10mM Tris-HCl, pH8.0  
1mM EDTA

The mixture was vortexed for two minutes and then centrifuged (13,000rpm x 10 minutes) to pellet cell debris. The supernatant was transferred to a clean eppendorf tube and 1/10 volume of 3M sodium acetate and two volumes absolute ethanol were added, followed by incubation at -20°C for 20 minutes. Centrifugation (13,000rpm x 10 minutes) after the incubation pelleted the DNA. The supernatant was removed and the pellet dried under vacuum. The pellet was dissolved in 10ml 1xTE and used to transform competent bacteria. After transformation, the bacteria were plated onto selective agar plates and incubated at 37°C for 16-20 hours. Any colonies that grew indicated that they were successfully transformed with the yeast-derived plasmid. More plasmid could be obtained by maxi- or minipreps and the two compared by restriction digest patterns.

## **2.16 RESTRICTION ENZYME DIGEST**

All restriction enzyme digests were performed in 1x KGB buffer (McClelland, 1987) as described in the paper. All incubations were carried out at 37°C for at least one hour except when BstE11 was used. This is a heat stable enzyme and the optimal temperature for use was 60-65°C. Digests were carried out in a volume of 20µl and 0.5-2.0µg DNA was digested at a time. When the digests were performed for analysis by agarose gel electrophoresis the digestion was stopped by the addition of 6µl gel-loading buffer.

### **GEL LOADING BUFFER**

0.225ml dH<sub>2</sub>O  
0.1ml 500mM EDTA, pH8.0  
0.5ml 2.5% (w/v) Bromophenol Blue  
0.625ml Glycerol

## **2.17 AGAROSE GEL ELECTROPHORESIS**

After restriction enzyme cleavage had taken place, the fragments were separated by agarose gel electrophoresis.

A gel caster (85mm x 105mm) was washed and dried and the ends sealed with autoclave tape to prevent the molten agarose from escaping. A 0.75% (w/v) agarose solution was prepared.

### **AGAROSE SOLUTION**

0.75g pure agarose (molecular biology grade)  
100ml 1x TBE

The agarose was melted by heating in a microwave oven (650W) on full power for 30 seconds and was allowed to cool for a few minutes prior to the addition of 5µl 10mg/ml ethidium bromide to make a final concentration 0.5µg/ml. The ethidium bromide was added after a period of cooling to prevent the formation of toxic vapour as it is relatively volatile. When the agarose was still molten it was poured into the gel caster and a well-forming comb inserted. The gel was allowed to cool thoroughly. This took 10-20 minutes. The gel appeared opaque when fully set. When the gel was set the comb and the autoclave tape sealing were removed. The gel,



still in its caster, was placed in a buffer tank (Gel Electrophoresis Apparatus GNA100, Pharmacia, Sweden) which was filled with about 350ml electrode buffer (1x TBE containing 0.5µg/ml ethidium bromide)

#### **ELECTRODE BUFFER STOCK (10x TBE)**

54.0g Tris base  
27.5g Boric acid  
20.0ml 0.5M EDTA, pH 8.0  
dH<sub>2</sub>O to 1 litre

The pH was adjusted to 8.3 by the addition of concentrated HCl.

This stock was diluted for use, with dH<sub>2</sub>O, to a 0.5x working concentration.

The samples were carefully pipetted into the wells in the gel. Each well could hold about 20µl sample. The coloured loading buffer enabled the sample to be seen, making loading easier. The glycerol kept the sample from dispersing on loading. The bromophenol blue migrated down the gel during electrophoresis and enabled the approximate position of the bands to be monitored so that excessive electrophoresis can be avoided. The lid of the buffer chamber was attached. The lid contained the connections to the terminals. The leads from the terminals were attached to a transformer (Shandon Southern Products Ltd,UK) and a constant voltage of about 50-80V was applied across the gel. The current was switched off when the bromophenol blue had migrated about 80% of the way down the gel. Under these conditions, electrophoresis was complete in about 1.5-2 hours.

The gel was removed from the caster and examined under ultraviolet light on a transilluminator. The ethidium bromide intercalates between the bases of the DNA and causes fluorescence under uv illumination. In this way the position of the fragments can be visualised. A permanent record of what the gel looked like could be obtained by photographing the gel using uv-sensitive film (Polaroid 665).

## **2.18 SOUTHERN BLOTTING**

Southern blotting is a method by which DNA present in an agarose gel can be transferred and permanently bound to a solid matrix, usually a nylon membrane, and then specific sequences detected using an oligonucleotide probe complementary to a

sequence of interest.

### **2.18.1 TRANSFER OF DNA FROM GEL TO MEMBRANE**

After electrophoresis, the gel was transferred to a small plastic tray. The bottom left hand corner of the gel was trimmed off to orientate the gel in subsequent steps. The double stranded DNA present in the gel was denatured by soaking in several changes of 1.5M NaCl, 0.5M NaOH with constant agitation for 1-2 hours. The gel was rinsed briefly in dH<sub>2</sub>O and neutralised by washing in several changes of 1.5M NaCl, 1M Tris-HCl (pH 7.5) for one hour. The gel was then transferred to the blotting apparatus designed for the capillary transfer of DNA to membranes. The apparatus consisted of a mat of filter paper, 10cm square and 6cm deep, placed into a large plastic box and saturated with 10xSSC. Excess 10xSSC was poured into the box to a level halfway up the side of the filter paper stack. The top layer of filter paper was covered in an impermeable layer of clingfilm into which a hole, the same dimensions as an agarose gel, had been cut. This ensured that buffer only passed through the gel to reach the membrane above.

#### **20X SSC**

175.3g NaCl  
88.2g Sodium citrate

Dissolved in dH<sub>2</sub>O, pH adjusted to 7.0 with concentrated HCl and the volume made up to 1litre with dH<sub>2</sub>O.

A nylon membrane (Hybond -N<sup>+</sup>, Amersham International plc, Amersham, UK) was cut to exactly the same dimensions as the gel. It was wetted briefly with dH<sub>2</sub>O and then soaked in 10xSSC for five minutes.

The gel was removed from the neutralising solution and inverted so that its underside was uppermost and carefully placed onto a filter paper support. The gel and filter paper was placed on top of the stack of saturated filter papers in the plastic box. The membrane was laid on top of the gel. It also had a corner trimmed off and this was aligned with that of the gel, again for orientation purposes. Two sheets of filter paper, cut to just smaller than the membrane, were moistened in 10xSSC and placed on top of the membrane. Paper towels, cut to just smaller than the size of the membrane, were stacked 5-6cm high on top of the gel-membrane - filter paper

assembly. Care was taken to ensure that buffer could only pass through the gel and membrane into the paper towels. The transfer was allowed to proceed for up to 24 hours. During this period the denatured ssDNA was eluted from the gel and deposited onto the nylon membrane. The paper towels above the gel became saturated with buffer and were replaced when necessary to maintain the flow of buffer.

After transfer was complete the apparatus was disassembled. The positions of the wells were marked on the membrane with a soft pencil.

### **2.18.2 BINDING DNA TO THE MEMBRANE**

To prevent elution of the DNA from the membrane during subsequent washing steps the DNA must be covalently linked to the support. This was achieved by wrapping the membrane in clingfilm and exposing it to uv light from a transilluminator for three minutes.

### **2.18.3 CONFIRMING TRANSFER OF DNA TO MEMBRANE**

After the transfer, the gel was removed from the filter paper stack and soaked in dH<sub>2</sub>O containing 0.5µg/ml ethidium bromide for one hour on a rotating platform. The gel was then examined under uv illumination. Any DNA that had not transferred to the membrane would fluoresce. Usually no extraneous fluorescence was observed after the transfer process.

### **2.18.4 DETECTION OF IMMOBILISED DNA**

The immobilised DNA was detected using a commercially available enzyme-linked chemiluminescent (ECL) kit (Amersham International plc, Amersham, UK). The procedure involved labelling the specific oligonucleotide at its 3' end with fluorescein-11-dUTP. This labelled oligonucleotide hybridised to target sequences on membrane-immobilised ssDNA and was detected using anti-fluorescein antibodies conjugated to horseradish peroxidase (HRP). The HRP catalysed the oxidation of luminol present in the detection reagent to give an oxidised product. As the luminol breaks down it passes through an excited intermediate stage and as this falls to the ground state, light is emitted ( $\lambda_{\text{max}}$  428nm). This light output was detected on blue-light sensitive film, providing a permanent hard copy result.

#### **2.18.4.1 LABELLING OF OLIGONUCLEOTIDE PROBE**

A suitable oligonucleotide probe was chosen (five different probes were available, corresponding to the five oligonucleotides used for the initial mutagenesis reactions). To a sterile eppendorf tube, on ice, the following labelling reaction components were mixed:

oligonucleotide	10 $\mu$ l
fluorescein-11-dUTP	10 $\mu$ l
cacodylate buffer	16 $\mu$ l
sterile water	102 $\mu$ l
terminal transferase	16 $\mu$ l
total	160 $\mu$ l

The components were mixed by gently tapping the tube. The reaction mixture was incubated at 37°C for 90 minutes. After incubation the reaction mixture was either used immediately or stored at -20°C until required. A 10cm x 10cm membrane required only 16 $\mu$ l labelled oligo for most detection purposes.

#### **2.18.4.2 PREHYBRIDISATION**

Prior to the addition of labelled oligonucleotide, the nylon membrane was prehybridised for 2-3 hours in a shaking water bath set at the temperature at which hybridisation was to occur. The membrane was sealed into a plastic bag containing 25ml hybridisation buffer. Care was taken to exclude as much air as possible before sealing the bag.

#### **HYBRIDISATION BUFFER**

5xSSC  
0.1% (w/v) hybridisation buffer component  
0.02% (w/v) SDS  
0.5% (w/v) blocking agent

The hybridisation temperature was 37°C.

#### **2.18.4.3 HYBRIDISATION**

After prehybridisation, 16 $\mu$ l labelled oligo was added to the buffer in the plastic bag. The bag was resealed and incubated at 37°C for 16 hours in a shaking water bath.

#### **2.18.4.4 STRINGENCY WASHING**

The blot was removed from the hybridisation solution and placed in a clean container. It was covered with 100ml 5xSSC, 0.1% (w/v) SDS and incubated at room temperature for five minutes. The buffer was discarded and the process repeated. This buffer was also discarded and replaced with 100ml stringency wash buffer prewarmed to the required temperature (42°C).

#### **STRINGENCY WASH BUFFER**

1xSSC  
0.1% (w/v) SDS

Prewarmed to 42°C.

The membrane was incubated at 42°C, in a shaking water bath, for 15 minutes. The buffer was discarded and the process repeated.

#### **2.18.4.5 MEMBRANE BLOCKING**

The following procedures were all performed at room temperature and all required constant agitation of the blots.

The membrane was placed in a clean container and rinsed for one minute with buffer 1.

#### **BUFFER 1**

0.15M NaCl  
0.10M Tris-HCl, pH 7.5

The wash solution was discarded and replaced with 25ml block solution and incubated for 30 minutes.

#### **BLOCK SOLUTION**

0.5% (w/v) blocking agent in buffer 1.

After incubation in block solution the membrane was rinsed for one minute in buffer 1.

#### **2.18.4.6 ANTIBODY INCUBATION**

The anti-fluorescein HRP conjugate stock was diluted by a factor of 1250x (20µl conjugate in 50µl buffer 2 containing 0.5% (w/v) BSA) and incubated for 30 minutes.

## **BUFFER 2**

0.4M NaCl  
0.1M Tris-HCl, pH 7.5

The blots were then placed in a clean container and washed for five minutes in buffer 2. This was repeated a further three times to ensure complete removal of any non-specifically bound antibody.

### **2.18.5 SIGNAL GENERATION AND DETECTION**

Equal volumes of detection solutions 1 and 2 (provided in the Amersham ECL kit) were mixed immediately prior to use to give a final volume of 12ml. Once made up, the detection solution could be reused 4-5 times if stored in the dark at 4°C. The blot was incubated in this solution for exactly one minute. The blot was then removed from the solution, briefly dried on filter paper and wrapped in clingfilm, care being taken to smooth out the wrinkles as much as possible. In a dark room the blot was placed into a light-tight film exposure cassette and covered with a piece of blue-light sensitive film (Hyperfilm-MP, Amersham international plc, Amersham, UK) cut to approximately the same dimensions as the membrane. The cassette was firmly sealed and the film exposed to the blot for exactly one hour at room temperature. Exposure for longer than one hour greatly increased the background signal. The cassette was opened in a dark room and the film developed in an automatic developer (X-ograph X2, Fuji). The film provided a permanent record of the blotting experiment and allowed judgements about washing stringency and exposure times to be made in order to optimise conditions for future experiments. The membrane could be stored damp, wrapped in clingfilm, at 4°C.

## **2.19 SEQUENCING OF DNA**

In order to support the contention that the altered physical properties of any enzyme produced was actually due to the single point mutation introduced it was necessary to sequence the plasmid DNA extracted from cells producing the mutant enzyme.

### **2.19.1 AMPLIFICATION OF DNA**

In order to produce sufficient template for sequencing it was decided to amplify a short stretch of DNA by the polymerase chain reaction (PCR) and subject it

to PCR sequencing via the chain-termination method using a mixture of deoxy- and dideoxynucleoside triphosphates. Two oligonucleotide primers were designed to be exactly complementary to regions either side of the serine 384 that had been mutated. The primers (a 19mer and a 22mer) were synthesised by the Oswel DNA Synthesis Facility (Department of Chemistry, University of Edinburgh). The primers were analysed for internal secondary structure using the UWGCG programs SQUIGGLES and CIRCLES (Devereux, 1984). The mass of the primers and PCR product were confirmed independently by the use of laser desorption mass spectroscopy at the WELMET Protein Characterisation Facility (Department of Biochemistry, University of Edinburgh). The PCR product was desalted by HPLC prior to analysis. The oligonucleotide primers were analysed without prior purification. The analyses were carried out by Ms. Shona Cunningham.

The target DNA sequence was a 253bp region encoding residues 334-419 of the yeast pyruvate kinase subunit. The target was amplified from several sources, either the 0.75kbp subcloned *PYK* fragments present in plasmid pK19 or the entire *PYK* sequence present in the vectors pPYK20, pAYE434 and pMA91.

The PCR amplification reaction was prepared using the "fmol DNA Sequencing System" (Promega, Madison, WI, USA) and consisted of the following components:

template DNA (ds plasmid DNA, CsCl purified)	2µl
oligonucleotide primer	1µl
10x PCR buffer	10µl
dNTP mix (2mM)	8µl
Taq polymerase (5000U/ml)	0.4µl
MgCl <sub>2</sub> (25mM)	6µl
dH <sub>2</sub> O	72µl
mineral oil	20µl

The reaction mixtures were prepared in 0.5ml eppendorf tubes. The mineral oil was added last and formed a covering layer to prevent evaporation during the various incubations. The PCR incubations were performed using a thermocycler (Techne PCH2, USA) which allowed rapid alteration and stable maintenance of the programmed incubation temperatures. The thermocycler was allowed to heat to 95°C



before the tubes were placed in the heating block. The tubes were packed tightly into the spaces provided to prevent their expulsion by trapped air expanding during the rapid heating steps. An initial incubation at 95°C for two minutes ensured that the ds target DNA was sufficiently denatured to allow the annealing of the primer oligos later. This initial heating was followed by 30 cycles of denaturation/annealing/extension.

Denaturation	95°C, 1 min
Annealing	56°C, 1 min
Extension	72°C, 1 min

The annealing temperature was chosen to be 4-5°C lower than the melting temperature of the oligonucleotides. The melting temperature was calculated from the formula:

$$69.5 + (0.41 \times \%GC) - 650/\text{length of oligonucleotide (bp)}$$

After the 30 cycles were completed the thermocycler cooled the tubes to 15°C where the activity of the Taq polymerase is effectively halted. The reaction mixtures were stored at 4°C until required.

The size and amount of PCR product was determined by analysing a sample of the reaction mixture by agarose gel electrophoresis (section 2.2.2.2). An agarose concentration of 1.5% was necessary to detect the smaller DNA products generated using the primers chosen for this reaction.

A theoretical maximum amplification of target DNA of  $2^{30}$  ( $1.07 \times 10^9$ ) is possible, although this is almost never practically achievable and a yield of  $2^{20}$  ( $1.05 \times 10^6$ ) is more usual.

## 2.19.2 DNA SEQUENCING METHODOLOGY

Several different DNA sequencing methodologies exist. The chain-terminating reaction using dideoxynucleoside triphosphates (ddNTPs)(Sanger et al., 1977) is generally considered the easiest and most convenient method and was the method utilised in the present work.

2',3'-ddNTPs differ from conventional dNTPs in that they lack a hydroxyl residue at the 3' position of deoxyribose. They can be incorporated by DNA polymerases into a growing DNA chain through their 5'-triphosphate groups.

However, the absence of a 3'-hydroxyl residue prevents the formation of a phosphodiester bond with the succeeding dNTP. Further extension of the growing DNA chain is therefore impossible. Thus, when a small amount of one ddNTP is included with the four conventional dNTPs in a reaction mixture for DNA synthesis, there is competition between extension of the chain and infrequent, but specific, termination. The products of the reaction are a series of oligonucleotide chains whose lengths are determined by the distance between the terminus of the primer used to initiate DNA synthesis and the sites of premature termination. By using the four different ddNTPs in four separate enzymatic reactions, populations of oligonucleotides are generated that terminate at positions occupied by every A, C, G, or T in the template strand.

### 2.19.3 THE SEQUENCING REACTION

The materials required for PCR sequencing were obtained from a commercial kit, "fmol DNA Sequencing System" (Promega, Madison, WI, USA). The reaction mixtures were prepared in 0.5ml eppendorf tubes. Four tubes were labelled A, C, G and T and into each was pipetted 2µl of the appropriate dNTP/ddNTP mixture. In a separate tube were mixed the following components:

ds template DNA (derived from PCR)	5µl
primer	4µl
$\gamma$ - <sup>35</sup> S-dATP (1000Ci/mmol)	0.5µl
Taq polymerase (5000U/ml)	1µl
5x sequencing buffer (0.25M Tris-HCl, pH9.0, 10mM MgCl <sub>2</sub> )	5µl
dH <sub>2</sub> O	1.5µl

Aliquots (4µl) of this mixture were then added to the dNTP/ddNTP solutions in the four labelled tubes prepared earlier. After the reaction mixtures had been prepared they were subjected to exactly the same PCR conditions as had been used to generate the DNA template. The PCR was stopped by the addition of 3µl Stop Solution and stored at -20°C until ready for loading onto the sequencing gel.

## **STOP SOLUTION**

10mM NaOH  
95% formamide  
0.05% bromophenol blue  
0.05% xylene cyanole

The chain-termination reaction products were separated according to chain length on a polyacrylamide gel and visualised by exposure to photographic film.

In other experiments, DNA sequencing was performed using the Sequenase commercial kit (USB) exactly following the manufacturer's instructions.

### **2.19.4 PREPARATION OF THE SEQUENCING GEL**

The sequencing gel was prepared from 100ml gel-forming solution.

#### **GEL-FORMING SOLUTION**

40% acrylamide solution	75ml
10x TTE	50ml
urea	230g

The urea took several hours to dissolve completely. The volume was adjusted to 500ml with distilled water.

#### **ACRYLAMIDE SOLUTION**

Acrylamide	140g
N, N'-methylene-bis-acrylamide	10g

The components were dissolved in distilled water and the volume adjusted to 500ml to produce a 40% (w/v) solution.

#### **TTE**

Tris	108g
Taurine	36g
EDTA	0.5g

The components were dissolved in distilled water and the volume adjusted to 1000ml to produce a 10x stock solution. The stock solution was diluted to a 1x working solution with distilled water. To 100ml of the gel-forming solution in a 250ml flask, 0.14ml TEMED and 0.34ml 10% (w/v) ammonium persulphate solution were added and swiftly poured between pre-assembled sequencing plates.

When DNA was sequenced via the Sequenase methodology, 1xTTE was replaced with 1xTBE in both the gel-forming solution and the running buffer.

### **2.19.5 ASSEMBLY OF SEQUENCING APPARATUS**

A sequencing gel is typically 30 x 30 x 0.2 cm in dimension. Two glass plates of slightly differing sizes (42 x 34 x 0.4 cm and 39 x 34 x 0.4 cm) were thoroughly washed with hot water and detergent and dried. Both plates were then wiped with ethanol and allowed to air dry. The smaller plate was coated on one side with Sigmacote (a special silicone solution in heptane, Sigma Chemical Co Ltd, Poole, Dorset, UK) and allowed to air dry under a fume hood. This coating acts to ease separation of the glass plate from the gel at a later stage.

The larger plate was laid with the side to be in contact with the gel uppermost. Two plastic spacers (42 x 1 x 0.2 cm) were laid lengthways along the sides of the plate. The smaller plate was laid on top of the larger plate, its treated side innermost, forming a sandwich. The plates were secured along the sides and base with electrical tape (Scotch tape, 3M, St.Paul, MN, USA). Special care was taken to exclude air bubbles beneath the tape to reduce the possibility of leakage of the polyacrylamide solution.

### **2.19.6 POURING THE SEQUENCING GEL**

The gel-forming solution was prepared as described in section 2.19.4. After the addition of TEMED and ammonium persulphate the solution was rapidly poured into the gap between the two plates. Any air bubbles that formed were removed by alternately rocking and tapping the plate assembly, or scooping them out using a sharks tooth comb. Sometimes it was impossible to remove all the air bubbles. If this happened the gel solution could be quickly poured out and repoured or the bubbles were left in position and lanes chosen so that they caused no interference in the running of the samples. In extreme cases the apparatus had to be completely disassembled and reprepared from the beginning. After successfully pouring the gel, the plate assembly was laid on the bench with the open end slightly raised, to prevent seepage of the gel solution, and allowed to set overnight. The well-forming comb was inserted into the top of the gel with its flat edge in contact with the gel solution. This ensured the formation of a perfectly flat surface to the top of the gel facilitating sample loading. The upper part of the plate assembly was wrapped in clingfilm to prevent the top of the gel drying out. When polymerisation was complete, the comb and tape were removed and the assembly rinsed with water to remove deposits of

urea and polyacrylamide that may have accumulated. The plate assembly was connected to the electrophoresis equipment, ensuring that the smaller plate was towards the back, and checked to ensure that no leakage of buffer was possible. Any small gaps were plugged with silicone grease. The gel was pre-run without samples for one hour, at a constant power output of 50W, in order to warm the gel.

### **2.19.7 LOADING THE SEQUENCING GEL**

After the pre-run, the power was switched off and a sharks tooth comb inserted into the top of the gel so that the teeth just penetrated the surface. The samples to be loaded were heated for two minutes at 80°C in a heating block. The samples (3.0µl) were loaded into adjacent wells. The order of loading was always A, C, G, T (i.e. alphabetically). Two sets of four samples were loaded, corresponding to the two different primers used in the chain-termination reactions. The leads were reconnected and the samples run at 50W constant power. To obtain maximal sequence information the first samples were allowed to run for two hours before a second loading of samples was applied to the gel, in different lanes from the first. Electrophoresis was continued for a further 2-3 hours. This procedure allowed sequence very close to, and quite distant from, the primer to be read.

### **2.19.8 AUTORADIOGRAPHY**

When electrophoresis was complete the power was switched off and the leads disconnected. The glass plates were prised apart with a spatula. The gel remained attached to the non-silicone treated plate. The plate with attached gel was submerged in a tray of fixing solution for five minutes.

#### **FIXING SOLUTION**

10% (v/v) methanol  
10% (v/v) glacial acetic acid  
80% (v/v) distilled water

This served to fix the gel and remove urea which would prevent the gel from drying properly and cause it to stick to the autoradiography film. The plate was removed from the fix solution and excess solution allowed to drain from the gel. A piece of filter paper (3MM Chr, Whatman) slightly larger than the dimensions of the gel was cut and carefully smoothed over the gel excluding any air bubbles. In a continuous movement, the paper was peeled away from the glass plate. The gel

adhered to the paper. A piece of clingfilm was laid over the gel, again care being taken to exclude air bubbles. The gel was then transferred to a gel dryer and dried under a vacuum at 80°C for several hours. When the gel was thoroughly dry the clingfilm was removed and excess filter paper trimmed off. The gel was loaded into a large film cassette and, in a dark room, a sheet of autoradiography film (Hyperfilm-HP, Amersham International plc, Amersham, UK) laid in contact with the gel. The film was exposed at room temperature for 48-72 hours. After exposure the film was removed from the cassette and developed using an automatic film developer (X-ograph Compact X2). The sequence was read from the bottom of the gel up as the shortest terminated chains, corresponding to DNA sequence nearest the 3' end of the primer, migrated farther down the gel.

## **2.20 FLUORESCENCE MEASUREMENTS**

All fluorescence measurements were produced on a Perkin-Elmer LS3B, or LS50, fluorescence spectrometers with attached recorders (Perkin- Elmer Corp, Norwalk, Connecticut, USA).

The sample, containing 30-50µg protein, was loaded into a 0.5ml quartz fluorimetry cuvette and placed in the appropriate cell holder inside the machine. The excitation and emission wavelengths, monochromator slit widths and wavelength scan speed were adjusted using controls on the fluorimeter panel. The chart speed and sensitivity (mV gain) were set with controls located on the chart recorder.

Fluorescence was measured at right angles to the incident beam in a pathlength of 1cm. The cuvette was kept at  $25 \pm 0.1^{\circ}\text{C}$  with a thermostatted water bath. The upper and lower limits of the chart recorder trace, corresponding to maximum and minimum detectable fluorescence emission respectively, were set using a reference cuvette containing buffer and unligated wild type pyruvate kinase. The emission wavelength was set on the sample emission maximum. A sample of buffer, without added protein, allowed calibration of the fluorescence minimum.

To take a measurement, the shutter was first closed to prevent excessive illumination of the sample. The pyruvate kinase sample was loaded into the cuvette and mixed thoroughly with the cuvette contents. The shutter was opened and the



sample illuminated for 20 seconds prior to measurement (it was noted that severe fluctuation occurred in the fluorimeter read-out in the initial few seconds following illumination). After this pre-illumination period had elapsed, the average fluorescence was calculated by a 15 seconds integration performed by the fluorimeter.

When ligands were added they were allowed to mix with the sample for one minute in the unilluminated fluorimeter chamber before the pre-measurement illumination. Volume changes on addition of ligands were kept to a minimum. For consecutive additions of ligand to a sample, the shutter was closed, the ligand added and incubated for one minute and then pre-illuminated for 20 seconds prior to measurement.

Results were plotted as change in fluorescence between unligated and ligated sample versus concentration of ligand. These data could also be transformed into Hill-type plots.

## **2.21 PROTEIN SEQUENCING**

In order to confirm that the protein being studied was indeed a mutated form of yeast pyruvate kinase, the purified protein was chemically fragmented, the individual peptides purified by HPLC and sequenced via automated Edman degradation.

### **2.21.1 CYANOGEN BROMIDE CLEAVAGE**

Cyanogen bromide (CNBr) is capable of cleaving thioethers, and thus provides a method to cleave proteins specifically on the carboxy-side of methionine residues.

The protein pellet from the ion-exchange chromatography step was washed several times in distilled water and repelleted by centrifugation (13,000rpm x 15 mins). The excess fluid was removed by aspiration and the pellet dissolved in 0.5ml 90% formic acid. Aliquots (0.175ml) were transferred to sterile eppendorf tubes and a small crystal of CNBr was added. The tubes were covered in aluminium foil and incubated at room temperature in a fume cupboard for 24 hours. After this time, 0.2ml distilled water was added and the mixtures reduced to dryness in a vacuum desiccator. A blank containing no added protein was also prepared.



### 2.21.2 PURIFICATION OF PEPTIDES

The peptides generated by CNBr digest were separated by reverse phase chromatography using a microbore HPLC system (model 130A, Applied Biosystems). The column (2.1mm id x 30mm) contained a matrix of 7µm particles coated in octadecylsilane (C18) with an effective pore size of 300Å. Peptides were eluted with a buffer gradient from 100:0 to 0:100 (buffer A : buffer B). Buffer A contained distilled water and 0.1% trifluoroacetic acid (TFA). Buffer B contained 70% acetonitrile and 0.1% TFA. The flow rate was 0.2ml per minute. The peptide mixture was resuspended in 0.18ml 4M guanidine hydrochloride and centrifuged to remove any insoluble precipitate. The sample (0.17ml) was loaded onto the column via a 0.2ml displacement loop. Each run took 65 minutes to perform. The eluant was monitored at 220nm and the absorbance against time was displayed on a chart recorder connected to the HPLC apparatus. Fractions were collected by hand.

### 2.21.3 SEQUENCING PEPTIDES

The peptides were sequenced in the Welmet Protein Characterisation Facility (Department of Biochemistry, University of Edinburgh) by Mr.D.Lamont using an Applied Biosystems 477A protein microsequencer. The method utilised automated Edman degradation of the peptide followed by HPLC separation of the derivatised amino acids and their identification by comparison of their retention time with calibrated standards. The results were analysed by comparing the deduced order of residues removed from the peptides with the known sequence of peptides likely to be produced with CNBr.

## 2.22 ELECTRON MICROSCOPY

Yeast cells were grown in the appropriate selective media to late log phase and samples (1.5ml) pelleted by centrifugation (13,000 rpm x three mins). The pellet was resuspended in 1ml fixative solution.

### FIXATIVE SOLUTION

Sodium cacodylate, pH7.4	0.1M
Paraformaldehyde	2% (w/v)
Glutaraldehyde	2.5% (v/v)
Calcium chloride	2mM

The cells were then washed for two hours with three changes of buffer solution.

**BUFFER SOLUTION**

Sodium cacodylate, pH7.4	0.1M
Calcium chloride	2mM

The cells were then fixed for one hour in a second fixative solution.

**SECOND FIXATIVE SOLUTION**

Sodium cacodylate, pH 7.4	0.1M
Osmium tetroxide	1% (w/v)
Calcium chloride	2mM

After the second fixing step, the cells were pelleted and resuspended in 0.05ml 2% (w/v) molten low melting point agarose. Care was taken to ensure that the molten agarose had cooled sufficiently to avoid damaging the cells. The agarose blocks were then trimmed into 1-2mm square cubes and dehydrated by washing in increasing concentrations of ethanol and water.

% ETHANOL (v/v)	TIME (min)
50	10
70	10
80	10
90	10
95	10
100	15
100	15
100	15

After the final ethanol wash, the cells were washed twice for 15 minutes each in propylene oxide. The cells could now be embedded in araldite resin. A 50ml Falcon tube containing 20ml araldite CY212 and 20ml dodecyl succinic anhydride was incubated in a water bath until both were thoroughly mixed. When mixing was complete, 0.8ml benzyldimethylamine was added and mixed in thoroughly. The dehydrated agarose cubes were transferred to glass vials and infiltrated with a 1:1 mixture of propylene oxide and araldite mix for 30 minutes. The cells were then transferred to 100% araldite mix and infiltrated overnight. The cubes were transferred to fresh araldite mix and infiltrated for a further six hours. The cubes were placed into embedding moulds. A slip of paper identifying each sample was added and the moulds filled with fresh araldite mix. The resin was polymerised in an oven set to 60°C for 48 hours. The cells, now sealed in an araldite block, were removed from the moulds and taken to the Department of Pathology where they were sectioned by microtome, stained with uranyl acetate, and mounted onto copper microscopy grids. These procedures were all performed by a qualified technician. The grids were examined under an electron microscope housed in the Department of Biochemistry

with the assistance of Mrs. S.Bury. The cells were examined under low magnification (4000-8000x) and photographs taken via a built-in mounted camera.

## **2.23 ALIGNMENT AND PHYLOGENETIC ANALYSIS OF PYRUVATE KINASE SEQUENCES**

The multiple alignment of amino acid sequences was performed using the program PILEUP of the GCG package (University of Wisconsin, USA). The alignment was manually adjusted using the program SEQUENCES APPLICATION. The percentage of identity between pairwise aligned sequences was calculated after the exclusion of areas containing deletions and insertions.

The multiple alignments of amino acid sequences were converted to the appropriate input format for the PHYLIP package (version 3.5; Felsenstein, 1993) using the program READSEQ (Gilbert, 1993). The number of substitutions between sequences was measured using the program PRODIST (PHYLIP package) correcting for multiple substitutions according to Kimura (1993). Based on the distance matrix, a phylogenetic tree was constructed using the least-squares method of the program FITCH (PHYLIP package; Fitch & Maroliash, 1967). To test the reliability of the tree, the bootstrap method was applied (Efron, 1982; Felsenstein, 1985). From the original data set 100 bootstrap replicates were obtained allowing the construction of the corresponding distance matrices and phylogenetic trees using the program SEQBOUT (PHYLIP package). The program CONSENSE (PHYLIP package) was used to obtain a consensus tree as confidence levels for monophyletic groups.

All phylogenetic analyses were carried out on a R4000 Silicon Graphics Iris Indigo computer by I. Ernest (International Institute of Cellular and Molecular Pathology, Research Unit for Tropical Diseases, Brussels, Belgium).

### **3.0 RESULTS**

- 3.1 Morphological and biochemical studies on parent and transformed cells.
- 3.2 Peptide sequencing.
- 3.3 DNA sequencing.
- 3.4 Purification of the wild type and mutant enzymes.
- 3.5 Fluorescence and circular dichroism spectroscopy studies.
- 3.6 Trypsin digestion of wild type and mutant pyruvate kinase.
- 3.7 NEM inhibition of wild type and mutant pyruvate kinase.
- 3.8 Thermal stability studies.
- 3.9 Antibody studies.
- 3.10 Computer predictions of secondary structure.
- 3.11 Alignment and phylogenetic analysis of pyruvate kinase sequences.

### 3.1 MORPHOLOGICAL AND BIOCHEMICAL STUDIES ON THE PARENT AND TRANSFORMED CELLS

One of the fundamental characteristics of transformed yeast cells that can be measured is the growth rate and its comparison with the parent untransformed strain. The  $\log_{10}$  of the optical density at 600nm against time of sampling is shown for the parent strain and the strains transformed with wild type and mutant enzyme-overexpressing plasmids (Fig. 27). The slope of the linear part of the plots can be used to determine the doubling time of the cells. All the cells are grown on the selective media appropriate for that strain.

The parent strain contains a disrupted genomic copy of the *PYK1* gene making it incapable of growth on glucose. The efficiency of utilisation of various carbon sources by the parent strain was examined and the results displayed in Fig. 28.

The external and internal morphology of the parent and transformed strains was examined under the electron microscope. The results are shown in Fig. 29. The author would like to thank Mrs.S.Bury for assistance with using the electron microscope.

The possibility of cells containing a disrupted gene for pyruvate kinase or a deficient copy of the enzyme being able to utilise glucose as a carbon source is rationalised by examining alternate pathways for glucose catabolism in yeast (Scheme 1).

The effect of 10mM potassium cyanide on the growth of the parent and transformed strains is shown in Fig. 30.

The intracellular amounts of the allosteric effector Fru-1,6-P<sub>2</sub> in the parent and transformed cells is shown in Fig. 31.

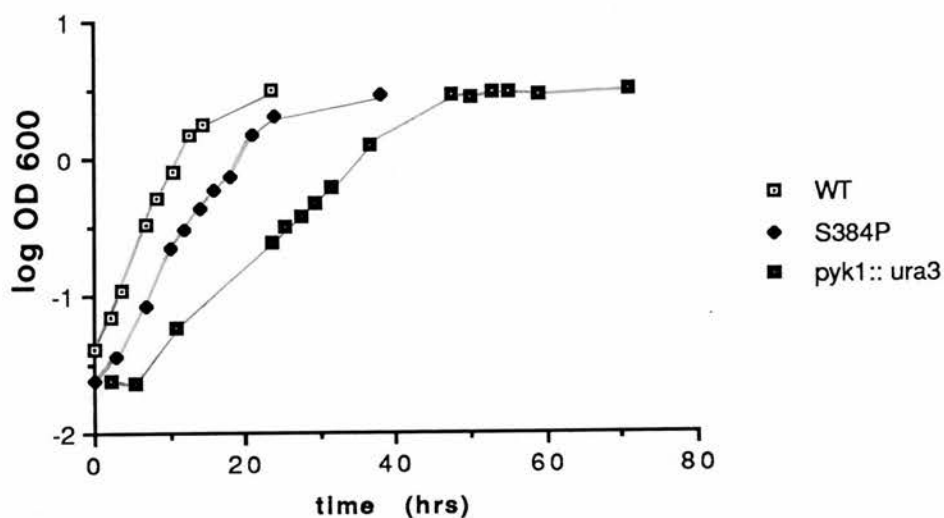


Figure 27: Growth curves of parental and transformed yeast cells.

pyk:: ura3

Parent *S.cerevisiae* strain in which *PYK1* gene has been disrupted by an insertion of *URA 3*.

Grown on leu<sup>+</sup> ura<sup>-</sup> glycerol-ethanol.

WT

Parent strain transformed with plasmid pMA91pyk(WT) overexpressing wild type pyruvate kinase.

Grown on leu<sup>-</sup> ura<sup>-</sup> glucose.

S384P

Parent strain transformed with plasmid pMA91pyk(S384P) overexpressing mutant pyruvate kinase.

Grown on leu<sup>-</sup> ura<sup>-</sup> glucose.

Log OD600 plotted against time of sampling.

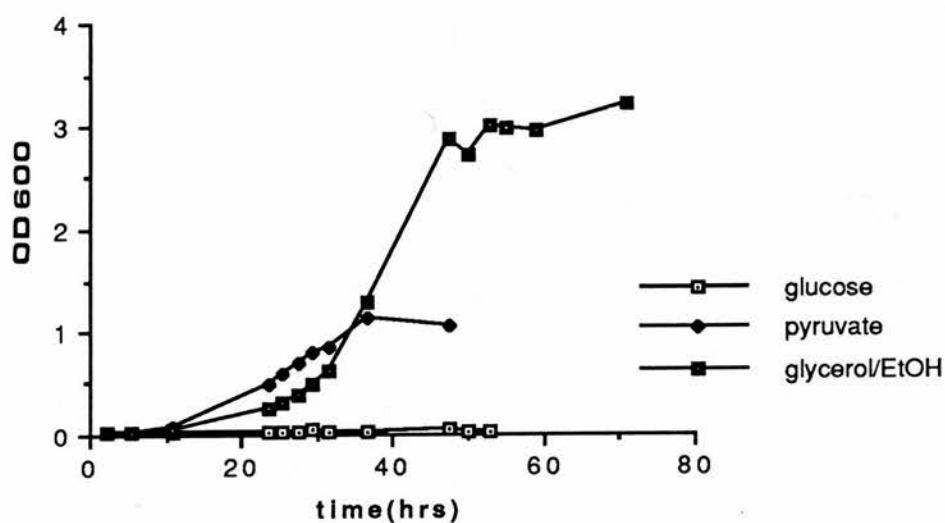


Figure 28: Growth of *pyk::ura3* on different carbon sources. Minimal media as defined in section 2.13 was used and supplemented with 2% (w/w) indicated carbon source. Ethanol (EtOH), where present, added as 2% (v/v). OD600 plotted against time of sampling.



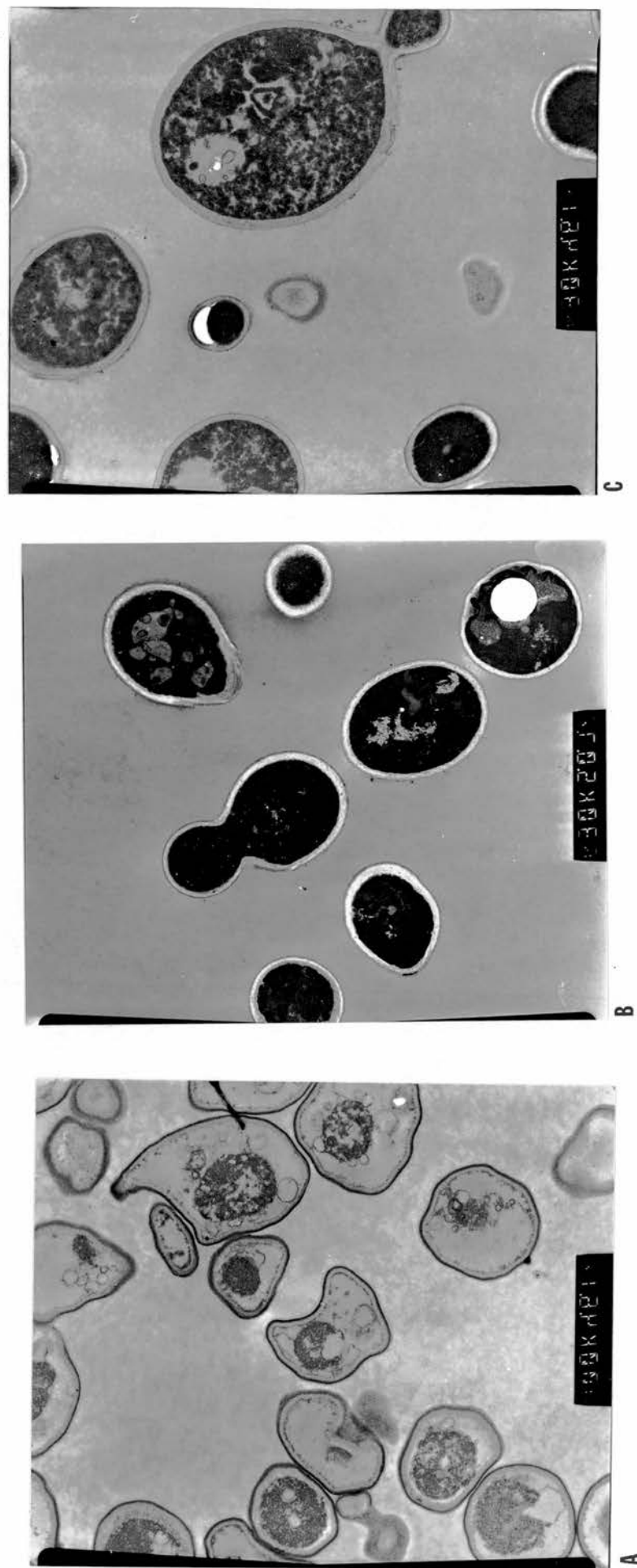
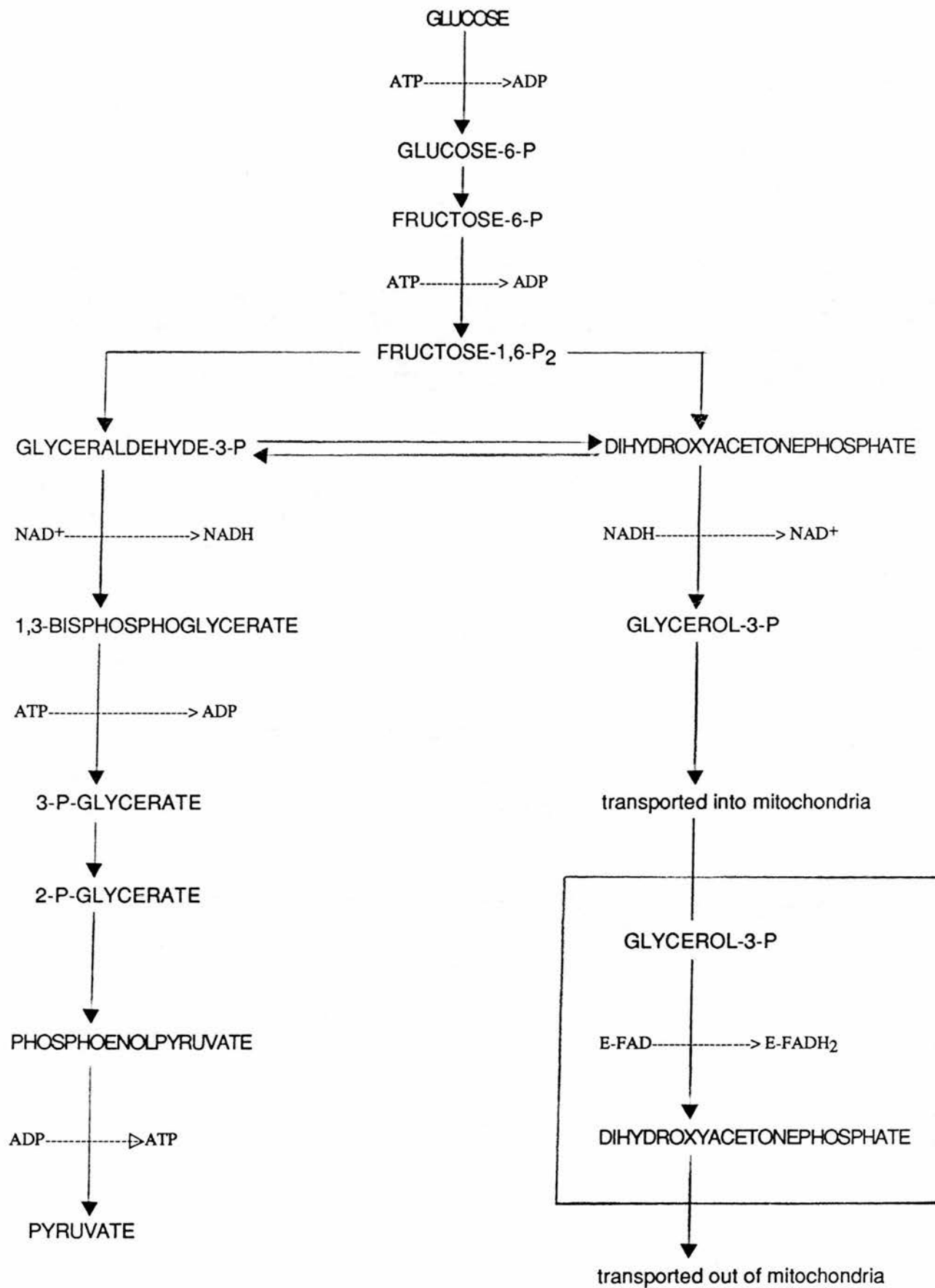


Figure 29: Electron micrographs of parental and transformed yeast cells  
 A) *pyk::ura3*-untransformed parental strain [mag. 8000x]  
 B) *pyk::ura3*-transformed with pMA91pyk (WT) [mag. 6300x]  
 C) *pyk::ura3*-transformed with pMA91pyk (S384P) [mag. 6300x]

Sample preparation as described in section 2.22



Scheme 1: Possible alternate pathways for glucose metabolism in yeast

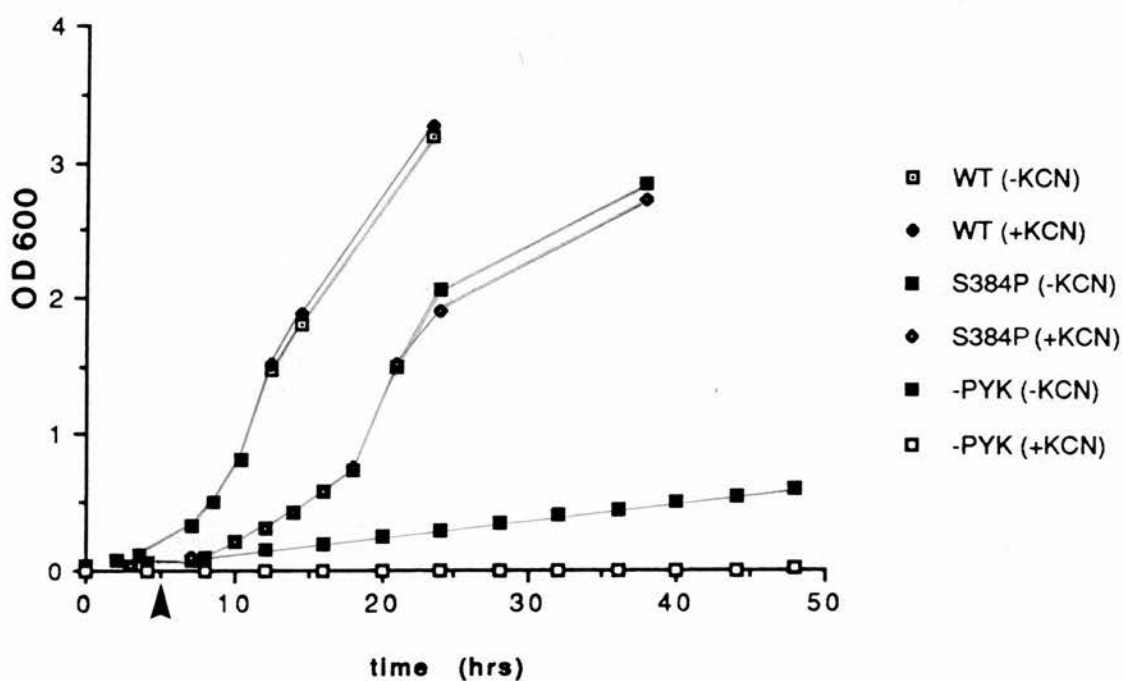


Figure 30: Effect of KCN on growth of parental and transformed yeast cells. Arrow indicates point of addition of KCN solution to each culture. KCN, where present, was 10 $\mu$ M.

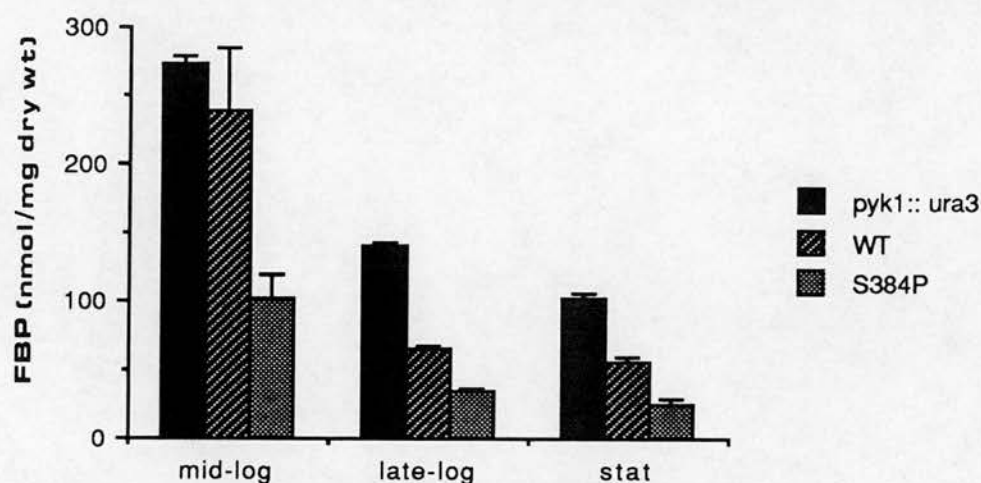


Figure 31: Intracellular fructose-1,6-bisphosphate levels in parent and transformed cells at different stages of growth. Metabolite levels determined as described in Section 2.3.1

**mid-log** = stage of cellular growth midway through exponential phase as determined from a plot of log OD600 against sampling time.

**late-log** = stage of cellular growth still in exponential phase but immediately prior to cells entering stationary phase.

**stat** = stationary phase.

### 3.2 PEPTIDE SEQUENCING

In order to confirm the presence of the serine 384 to proline point mutation in the mutant enzyme an attempt was made to determine the sequence of a peptide containing the region of interest.

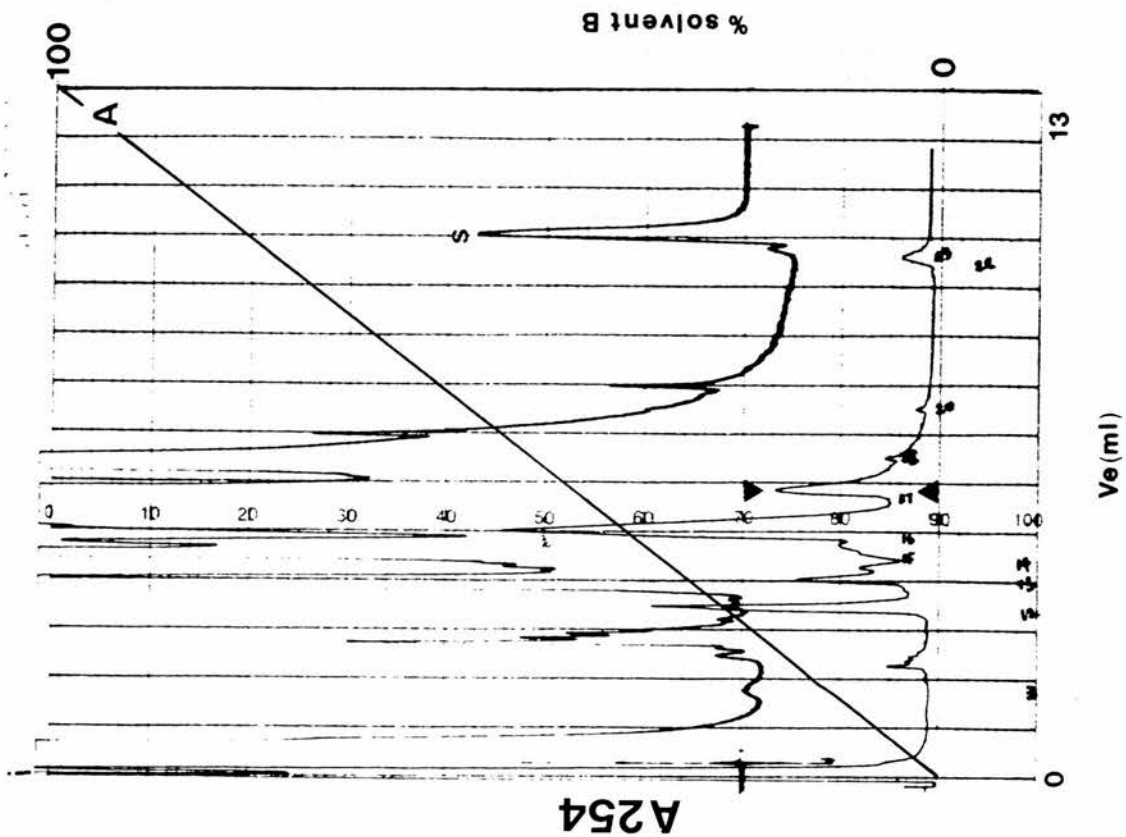
A sample of the purified enzyme was cleaved into peptides by overnight incubation in the presence of cyanogen bromide. The peptides were separated by HPLC on a microbore reverse phase column. The chromatogram obtained is shown in Fig. 32A. A control sample, containing all the reaction components but lacking enzyme, was also run. The chromatogram of this control sample is shown in Fig. 32B.

The expected number of peptides, and the sequence of their first 15 N-terminal residues, is shown in Table 4.

The peptides were sequenced by automated Edman degradation. The peak isolated by HPLC chromatography, and subsequently sequenced, contained a mixture of peptides, making detailed analysis difficult. The PTH-derivatised amino acid residues were separated by HPLC. A standard chromatogram, showing the retention times of the PTH-derivatised residues and Edman reaction by-products, is shown in Fig. 33. An example of a typical chromatogram produced during automated Edman degradation is shown in Fig. 34. The yield of each PTH-derivatised amino acid (pmol) is given in Table 5. From this the peptide sequence can be deduced. The sequence of the peptides detected is shown in Table 6.

A comparison of the peptide having the most prominent signal against the Swisprot database of protein sequences is shown in Fig. 35.







Theoretical CNBR fragments from Pyruvate Kinase

---

1..S R L E R L T S L N V V A G S  
2..N F S H G S Y E Y H K S V I D  
3..I F T T D D K Y A K A C D D K  
4..Y V D Y K N I T K V I S A G R  
5..V F A S F I R T A N D V L T I  
6..V A R G D L G I E I P A P E V  
7..L E S  
8..T Y N P R P T R A E V S D V G  
9..L S G E T A K G N Y P I N A V  
10..A E T A V I A E Q A I A Y L P  
11..R N C T P K P T S T T E T V A

Table 4      Fragments expected from complete CNBr digest of pyruvate kinase.  
Fragments are listed according to their position in the protein, from N-terminal to C-terminal. Only the first 15 residues of each peptide are listed.

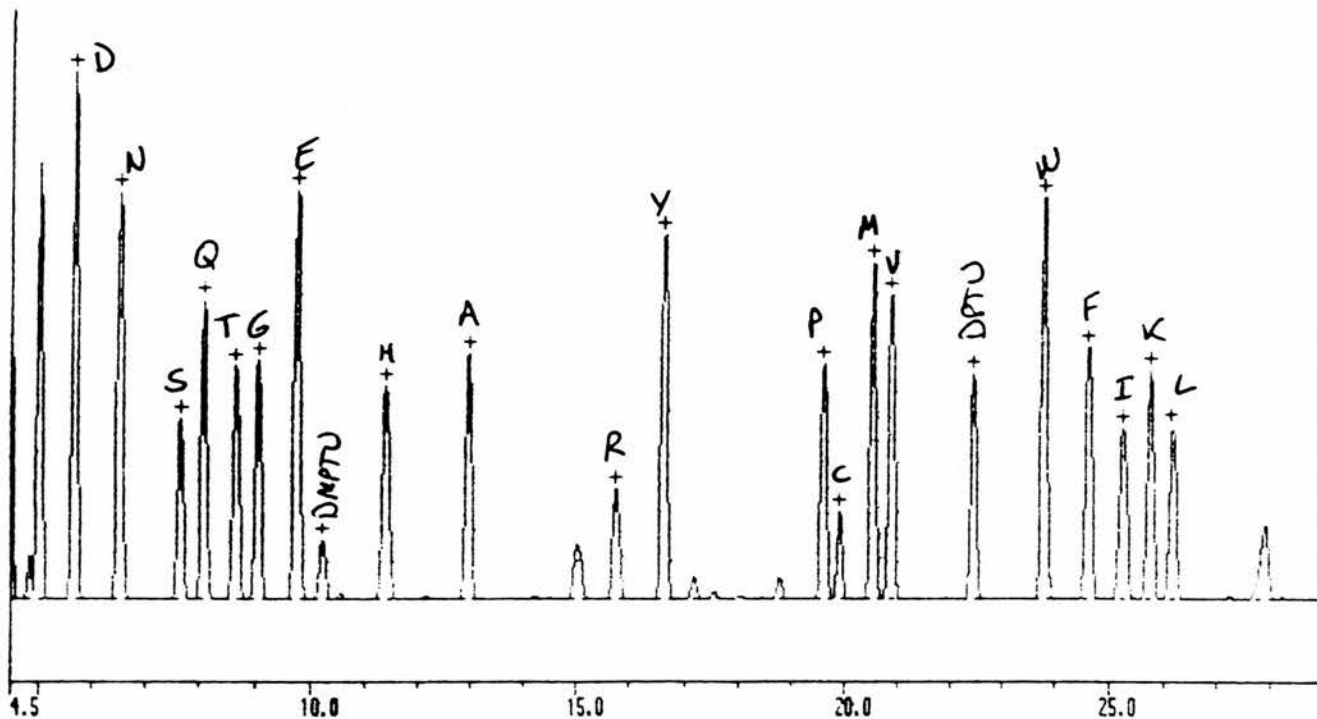
# - Applied Biosystems 477A Protein Sequencer Chromatogram Report -

SAMPLE : RC FR17 CNBR  
[ Initiated 21 Apr 1993 11:51am ]

## CYCLE SUMMARY :

Reaction cycle	: BEGIN-1	Data collect time	: 0.0 to 29.0 min
Conversion cycle	: BEGIN-1	Data interval	: 1.0 sec
Gradient	: NORMAL-1	Inject volume	: 50 of 150 uL

CALIBRATION # 1 [ 21 Apr 1993 12:58pm ] 0.0100 FU  
Filtered Data



Retention Time: Minutes

PEAK TABULATION : ( 100% injection )

Calibration : D-6

Peak ID	R.Time (min)	C.Time (min)	Height (uAU)	Pmol	Peak ID	R.Time (min)	C.Time (min)	Height (uAU)	Pmol
	4.83		1944			17.18		1047	
	5.02		19455			18.78		954	
ASP	5.68	5.68	23556	75.00	PRO	19.62	19.62	10488	75.00
ASN	6.52	6.52	18231	75.00	CYS	19.92	19.92	3903	75.00
SER	7.65	7.65	8058	75.00	MET	20.52	20.52	14988	75.00
GLN	8.08	8.08	13371	75.00	VAL	20.87	20.87	13623	75.00
THR	8.67	8.67	10380	75.00	DPT	22.43	22.43	10026	75.00
GLY	9.07	9.07	10692	75.00	TRP	23.78	23.78	17901	75.00
GLU	9.77	9.77	18306	75.00	PHE	24.63	24.63	11274	75.00
DMP	10.23	10.23	2646	75.00	ILE	25.27	25.27	7596	75.00
HIS	11.42	11.42	9477	75.00	LYS	25.75	25.75	10209	75.00
ALA	12.97	12.97	10986	75.00	LEU	26.17	26.17	7734	75.00
	15.02		2487			27.92		3291	
ARG	15.75	15.75	4950	75.00					
TYR	16.63	16.63	16335	75.00					

Fig.33 Calibration chromatogram of PTH-derivatised amino acid residues and reaction by-products.

# - Applied Biosystems 477A Protein Sequencer Chromatogram Report -

SAMPLE : RC FR17 CNBR

[ Initiated 21 Apr 1993 11:51am ]

## CYCLE SUMMARY :

Reaction cycle : NORMAL-1  
Conversion cycle : NORMAL-1  
Gradient : NORMAL-1

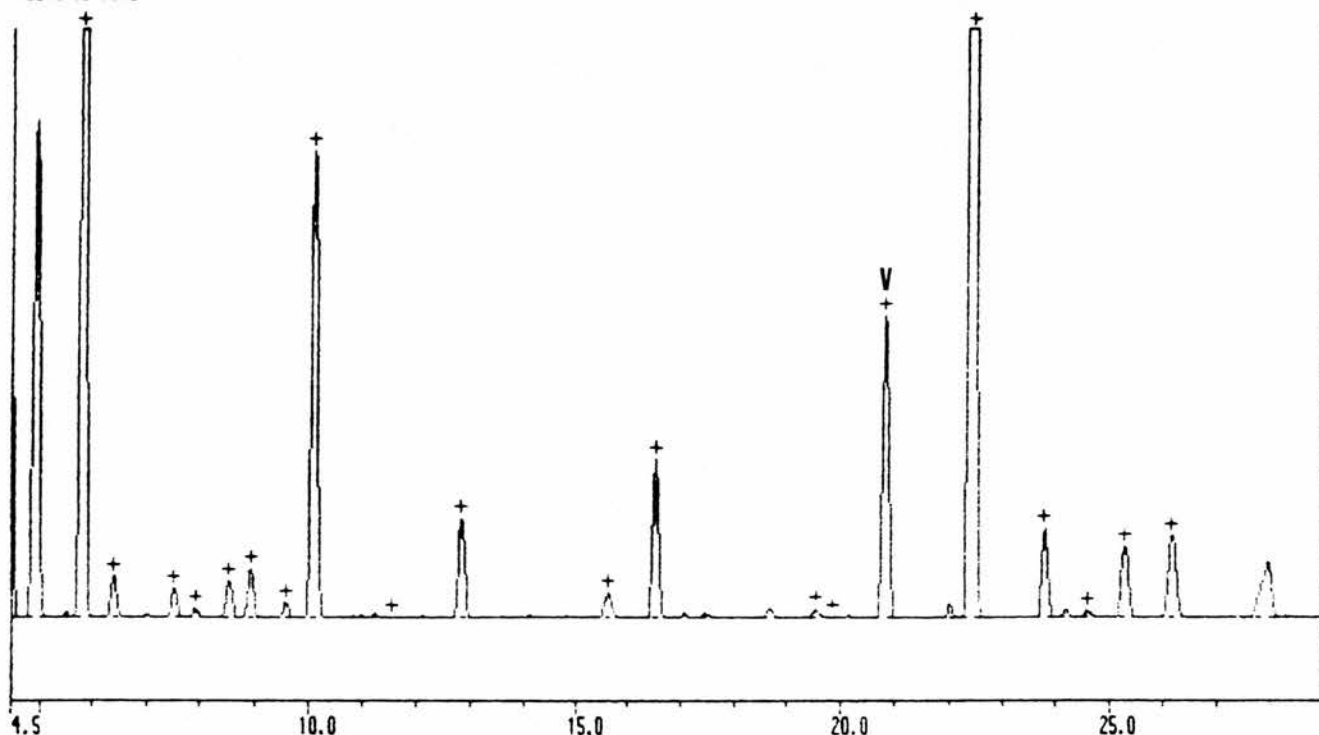
Data collect time : 0.0 to 29.0 min  
Data interval : 1.0 sec  
Inject volume : 50 of 150 uL

AMINO ACID # 1

[ 21 Apr 1993 1:42pm ]

0.0100 FU

Filtered Data



Retention Time: Minutes

PEAK TABULATION : ( 100% injection )

Calibration : D-6

Peak ID	R.Time (min)	C.Time (min)	Height (uAU)	Pmol	Peak ID	R.Time (min)	C.Time (min)	Height (uAU)	Pmol
	4.93		22128		VAL	20.83	20.87	13473	74.17
ASP	5.82	5.68	45963	146.34		22.00		729	
ASN	6.40	6.52	1860	7.65	OPT	22.42	22.43	116064	868.22
SER	7.52	7.65	1272	11.84	TRP	23.78	23.78	4002	16.77
GLN	7.92	8.08	369	2.07	PHE	24.60	24.63	279	1.86
THR	8.55	8.67	1644	11.88	ILE	25.30	25.27	3168	31.28
GLY	8.95	9.07	2193	15.38	LEU	26.20	26.17	3636	35.26
GLU	9.60	9.77	684	2.80		27.95		2463	
DMP	10.12	10.23	20766	588.61					
HIS	11.57	11.42	60	0.47					
ALA	12.83	12.97	4413	30.13					
ARG	15.62	15.75	1068	16.18					
TYR	16.53	16.63	7089	32.55					
PRO	19.55	19.62	354	2.53					
CYS	19.87	19.92	42	0.81					

Fig.34

Chromatogram from first round of automated Edman degradation of peak 17 (as identified in Fig.32).

The residue identified as the first amino acid in the sequence is indicated V, for valine.

- Applied Biosystems Tabulation Report -

SAMPLE : RC FR17 CNBR  
Sample Amount : 1000 pmol  
Date/Time of Run : 21 April 1993 11:51am  
Cycles Run : 1 STD, 15 AA

Raw Data Tabulation ... (in pmols)

	A	R	N	D	C	E	Q	G	H	I	L	K	M	F	P	S	T	W	Y	U
Cycle	ALA	ARG	ASN	ASP	CYS	GLU	GLN	GLY	HIS	ILE	LEU	LYS	MET	PHE	PRO	SER	THR	TRP	TYR	VAL
1	30.1	16.2	7.7	146.3	0.8	2.8	2.1	15.4	0.5	31.3	35.3	0.0	0.0	1.9	2.5	11.8	11.9	16.8	32.5	74.2
2	23.3	3.0	30.6	3.8	0.2	20.9	1.7	7.3	0.9	4.3	9.0	0.0	0.3	54.3	2.1	5.1	4.5	5.8	14.6	36.4
3	35.1	9.4	17.1	23.6	0.9	5.4	1.3	8.4	0.7	3.3	6.1	0.0	0.4	7.7	2.3	12.0	21.4	4.3	3.3	8.9
4	16.1	2.5	4.3	6.6	0.3	4.0	1.6	22.0	1.4	2.9	5.3	0.5	0.9	1.3	15.4	12.4	35.3	3.1	23.8	5.1
5	5.2	6.4	2.3	19.8	0.0	3.7	0.8	11.8	0.5	3.3	6.9	12.7	0.5	16.9	27.9	4.1	11.0	3.7	4.7	12.4
6	5.9	5.0	19.8	17.2	1.6	3.0	1.7	7.1	1.4	29.8	30.4	3.9	0.2	4.8	17.9	4.4	5.8	13.8	4.6	8.2
7	13.0	13.4	11.5	10.6	1.7	3.4	2.1	19.2	0.5	30.1	10.1	8.8	0.6	1.6	28.0	4.6	9.0	4.2	4.1	6.0
8	8.5	10.6	4.8	6.5	0.8	10.9	1.9	12.8	0.8	25.4	8.3	3.9	0.3	1.7	23.9	3.5	38.6	2.3	9.4	7.0
9	30.0	9.9	4.4	4.9	0.6	14.7	8.9	9.4	0.7	9.6	5.8	12.8	0.4	2.2	13.0	7.2	14.8	2.1	6.6	6.8
10	24.1	6.7	14.3	6.3	0.2	12.8	4.2	8.9	1.9	18.4	6.5	8.6	0.2	2.9	11.3	6.7	13.7	3.7	5.2	24.1
11	17.4	4.7	6.3	11.9	0.0	6.8	3.1	9.5	1.5	30.5	6.6	5.2	0.2	2.0	22.2	6.1	14.1	1.8	3.0	16.3
12	30.1	14.2	5.0	7.0	0.3	8.1	2.2	9.8	1.3	13.9	6.3	3.0	0.6	2.1	13.2	13.5	10.3	1.5	2.5	19.5
13	23.6	6.7	4.4	10.4	0.0	5.5	2.5	8.7	1.1	6.1	12.1	0.6	0.1	2.8	15.6	7.5	7.5	8.2	6.3	11.3
14	13.8	5.5	3.9	11.5	0.2	9.4	2.5	15.3	0.7	6.6	12.1	0.0	0.4	2.2	10.8	6.9	3.5	10.2	3.7	14.4
15	12.5	14.4	4.0	3.7	0.2	7.3	2.4	13.7	1.1	9.3	6.1	0.6	0.4	2.2	13.5	5.2	5.0	11.1	2.4	18.9

Table 5      Yield of PTH-derivatised amino acids from each round of Edman degradation (pmol).

Sequence's detected from - RC FR17 CNBR

---

nb : In decending order of positive assignment

a) V F A S F I R T A N D V L T I

b) Y - D Y K N I T K V I S - G R

c) V - R G D L G - E I P A P E V

d) A E T - V I A E Q - I A Y L P

e) I F T T D - K Y A - - + D D K

f) R N + T P - P T S - T E - V -

g) N F S H - S - E - H - S - I -

+ : No signal, possible unmodified cysteine residue.

- : No positive assignment for this residue, possibly  
due to multiple signals.

Table 6      Sequence of peptides detected in peak 17 in order of positive assignment. Interpretation of data performed by D.Lamont (Welmet).

```

10
VFASFIRTAN
|||||
kpyk_y NLPGTDVDPALSEKDEDLRFVGKNGVHMVFASFIRTANDVLTIREVLGEQGKDVKIIV
180 190 200 210 220 230

```

**Fig.3.5** Comparison of the peptide giving the most prominent signal with Swissprot database of protein sequences.

### 3.3 DNA SEQUENCING

To confirm that the overexpressed pyruvate kinase under study contained the desired serine to proline mutation a portion of the plasmid DNA containing the region around the mutation was sequenced. The method used was PCR sequencing using a commercially available kit (Promega, Madison, USA).

Two oligonucleotide primers were designed to be exactly complementary to a short region 80-100bp either side of the site of the mutation. The relation of the primers to the *PYK1* insert are shown in Fig. 36. The sequence and other properties of the primers are shown in Table 7.

The potential secondary structure of the oligonucleotides was checked using the UWGCG programs SQUIGGLES and CIRCLES (Devereux et al., 1984) and the results are displayed in Fig. 37. There appears, from these figures, to be the potential for a significant amount of secondary structure to form. Under the conditions in which the primers are used however, these structures probably do not exist.

The size of the oligonucleotides was checked by laser desorption mass spectrometry (LDMS) (Fig. 38)

The region of interest (residues 333 to 418 inclusive) was amplified from a variety of different plasmid sources by the polymerase chain reaction (Fig. 39). The resultant product was analysed by agarose gel electrophoresis and its size deduced by comparing the distance it migrated against a calibration curve derived from the distance migrated by DNA fragments of known sizes run under identical conditions (Fig. 40). An attempt was also made to determine the size of the PCR product by laser desorption mass spectrometry (Fig. 42). Prior to LDMS the PCR product was purified by reverse phase chromatography (Fig. 41).

The PCR product was used directly, without further purification, as the template for double-stranded PCR sequencing using Taq polymerase. The sequence around the site of the engineered point mutation is shown in Fig. 43. The wild-type sequence is shown alongside for comparison.



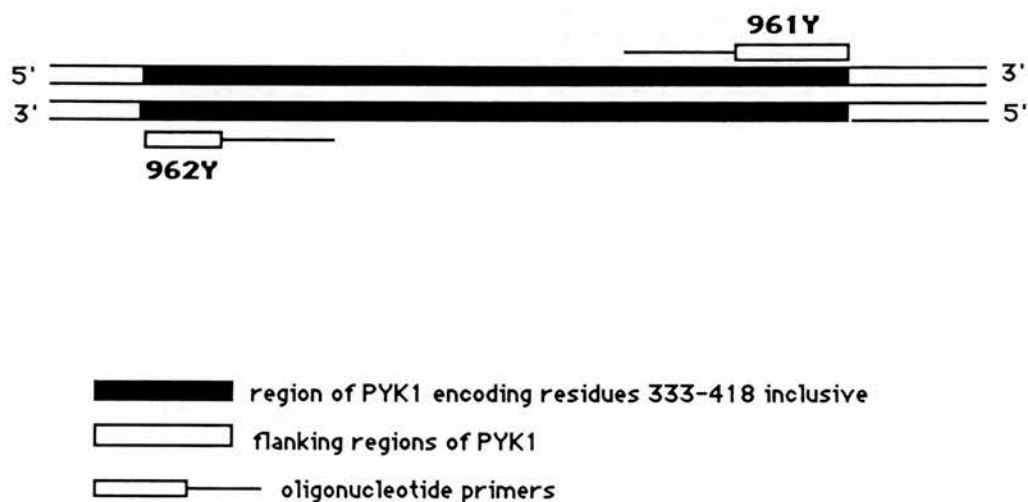


Figure 36: DNA amplification strategy  
 A portion of *PYK1* present on the plasmid pMA91pyk was amplified using the polymerase chain reaction (PCR) and two oligonucleotide primers (961Y and 962Y).  
 The reaction details are described in Section 2.19

PRIMER	MASS (Da)		MASS Da	DIFFERENCE %
	CALCULATED	ACTUAL		
961Y	7037 ± 8	7280	243	3.3
962Y	5879 ± 7	6154	275	4.5

Sequence:	961Y	GGA CAG TTT GGT CTG TAC TTG G
	962Y	CCG CCA AGG GTA ACT ACC C

Melting temperature:	961Y	60.5 °C
	962Y	61.2 °C

GC content:	961Y	50 %
	962Y	63 %

Table 7: Properties of the oligonucleotide primers used in PCR product generation and sequencing.

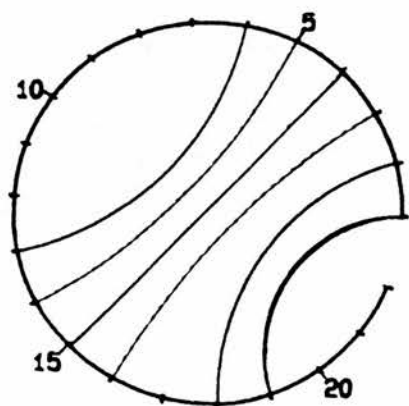
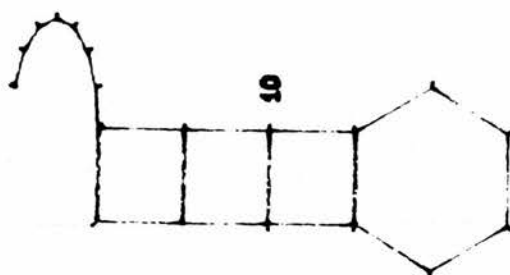
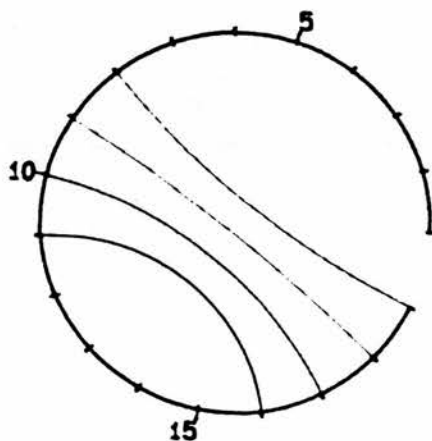
**A****B**

Figure 37: Primer self-complementarity calculated with the UWGCG programs CIRCLES and SQUIGGLES.  
 The primer sequence is represented as an arc and a potential stem loop respectively. Complementary base pairs are indicated by a connecting strand. Bases are numbered from the 5'-terminus.  
 A) 961Y, B) 962Y

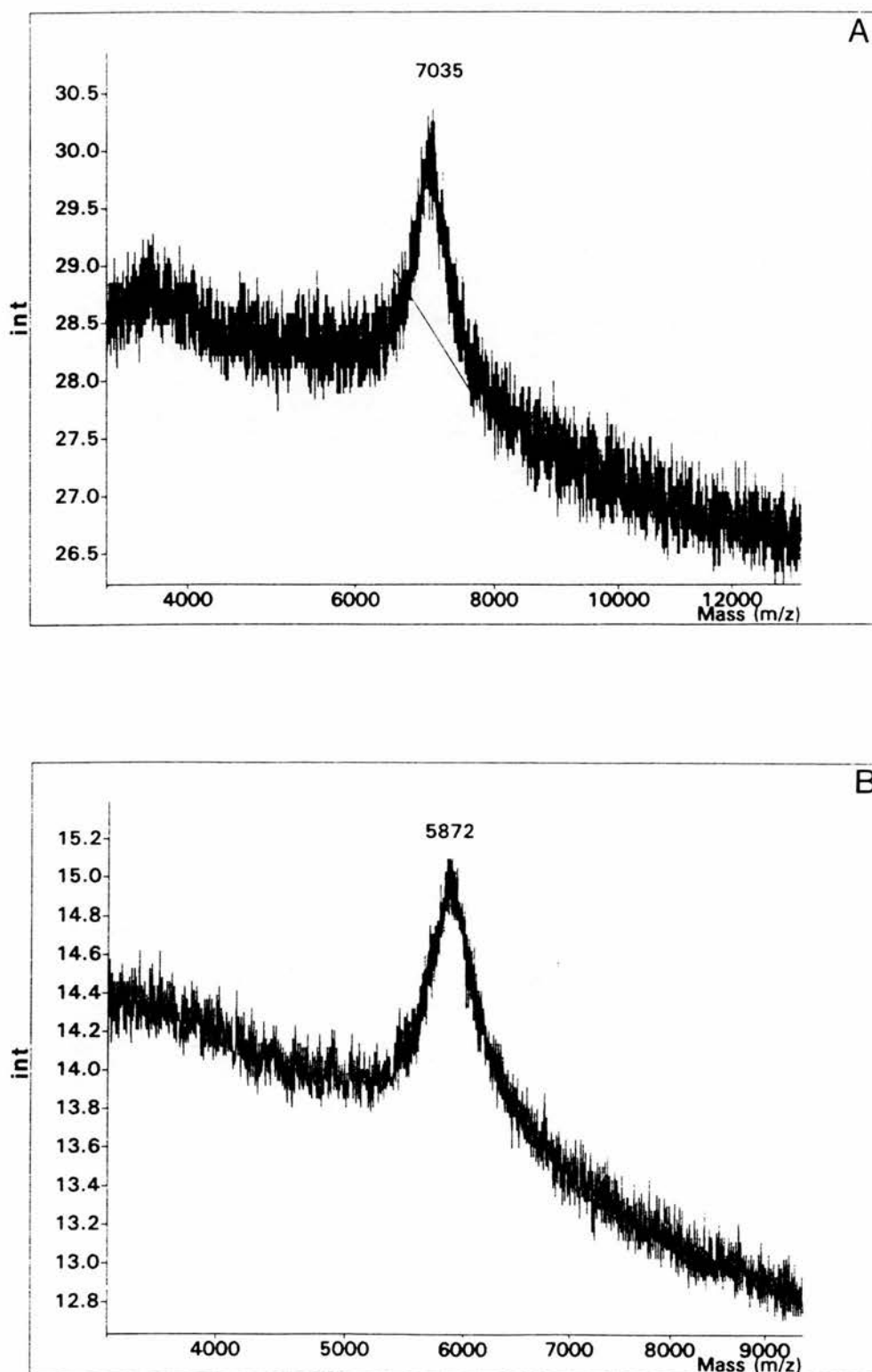


Figure 38: Laser desorption mass spectra of the oligonucleotide primers.  
 A) 961Y  
 B) 962Y  
 The signal shown is an average of 21 separate determinations.  
 Calculated mass is shown in daltons.  
 Int = signal intensity (arbitrary units)  
 Analyses were carried out by S.Cunningham (Welmet).

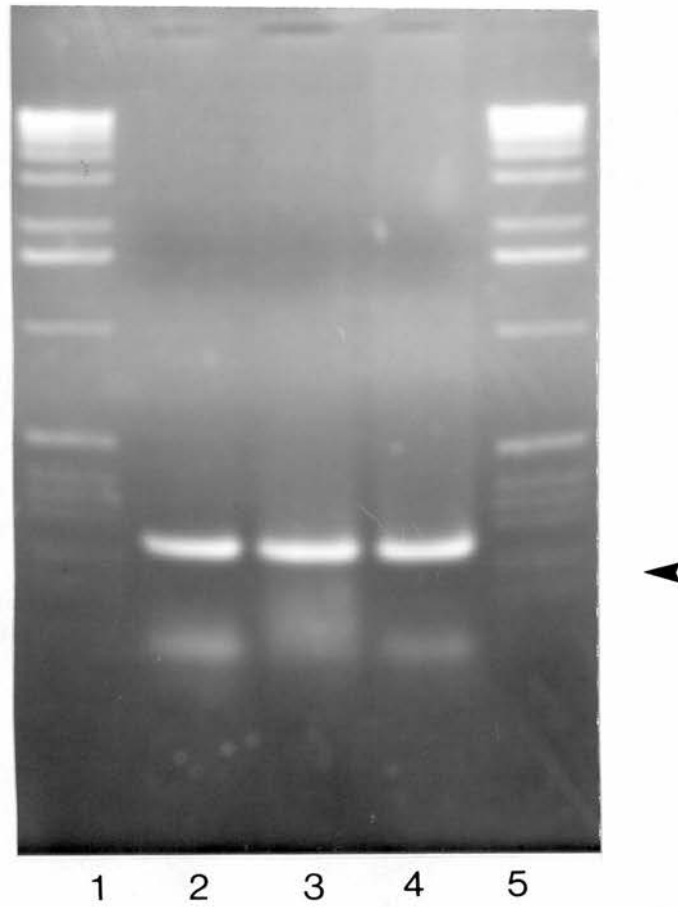


Figure 39: Amplification of *PYK1* DNA by the PCR from pK19-117. Different volumes of the reaction mix were mixed with 3µl loading buffer and analysed on a 1.5% agarose gel in the presence of ethidium bromide. Lane: 1) DNA size markers (Gibco 1kb ladder)  
 2) 1µl reaction mixture  
 3) 5µl reaction mixture  
 4) 10µl reaction mixture  
 5) DNA size markers (Gibco 1kb ladder)  
 Arrow indicates location of PCR product of interest.

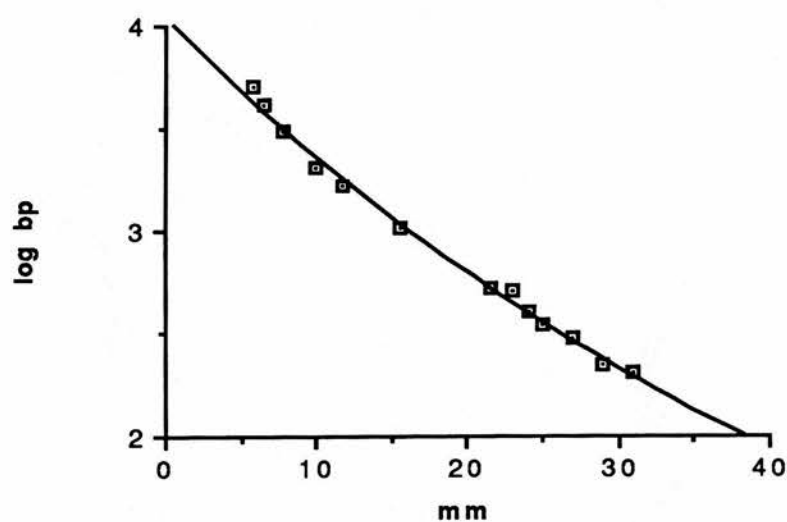


Figure 40: Calibration curve for calculating size of PCR product. Distance migrated in mm by each of the bands in the marker lane in figure 39 plotted against the  $\log_{10}$  of their length in bp.

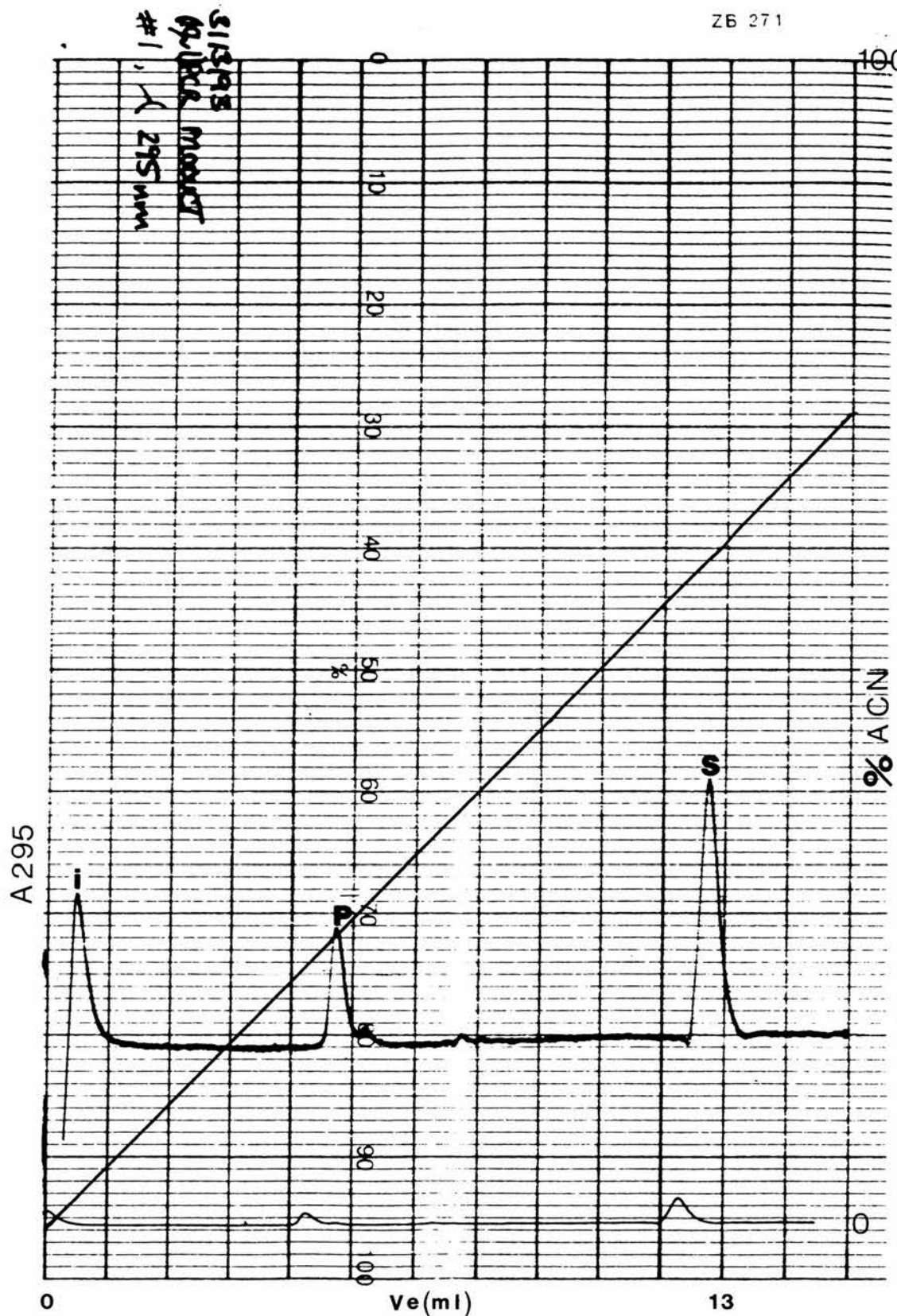


Figure 41: HPLC purification of the PCR product from pK19-117.  
 68 $\mu$ l of PCR reaction mixture loaded onto C18 reverse phase microbore HPLC system (Applied Biosystems).  
 uv detection at 295nm.  
 Product eluted with 0-70% (v/v) acetonitrile (ACN) gradient.  
 Chart speed 1.2mm/min.  
 i - injection spike, P - PCR product peak, S - solvent front,  
 Ve - elution volume (ml)



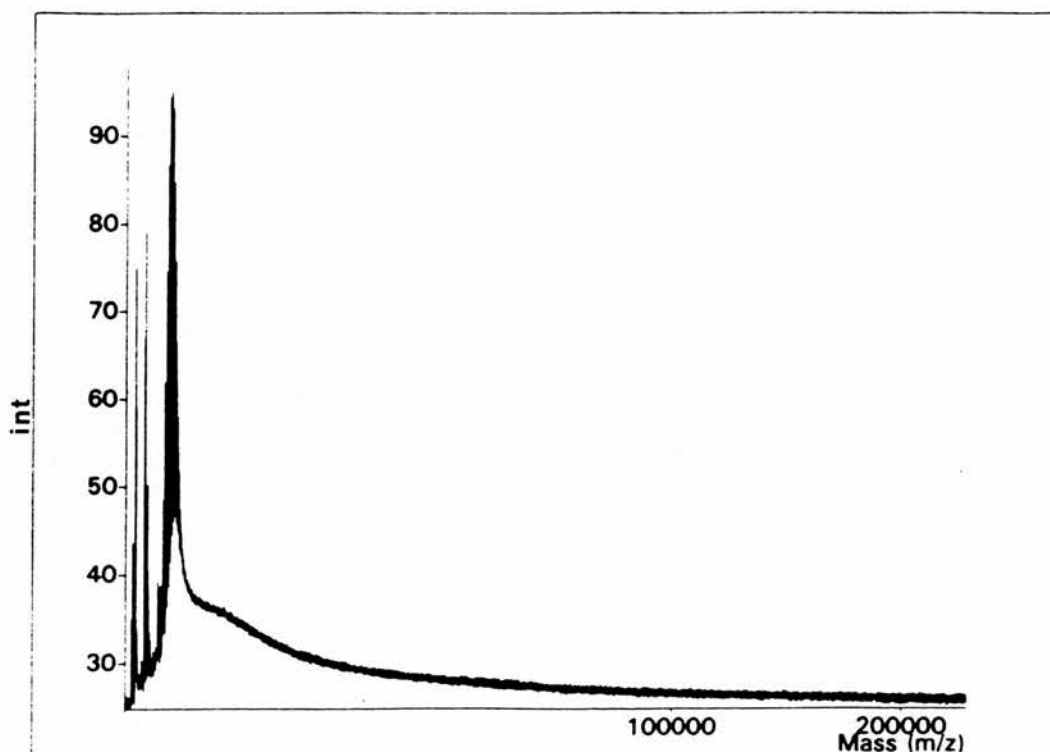
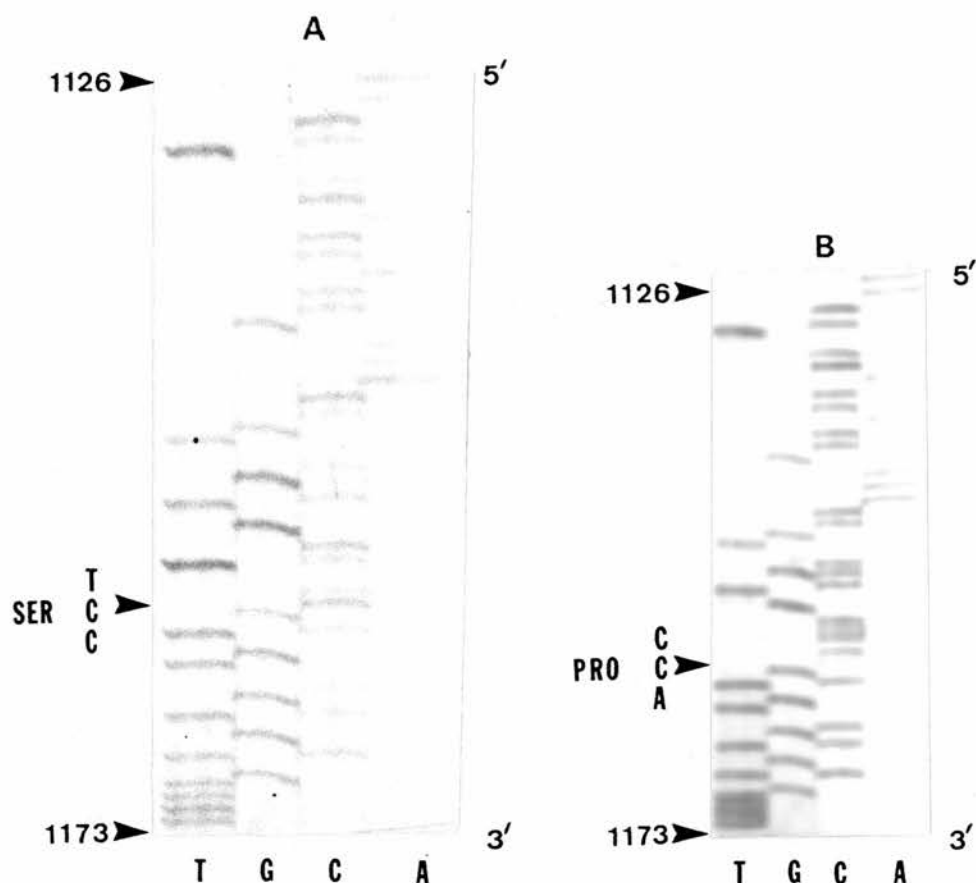


Figure 42: Laser desorption mass spectrum of the PCR product from pK19-117. HPLC purified product from Figure 40 subjected to LDMS. Signal generated is an average of 11 separate determinations. Int = signal intensity (arbitrary units) Analyses were carried out by S.Cunningham (Welmet). Although low molecular weight matrix material is observed, the PCR product itself cannot be detected.



1101 ACATGAGAAA CTGTACTCCA AAGCCAACCT CCACCACCGA AACCGTCGCT  
 1151 GCCTCCGCTG TCGCTGCTGT TTTCGAACAA AAGGCCAAGG CTATCATTGT

Fig. 43 Autoradiographs of the DNA sequence of *PYK1*  
 A) wild type, B) Ser 384 Pro mutant  
 The DNA sequence is from the expression vector pMA91pyk carrying the wild type or mutated *PYK1* gene respectively. In both figures the DNA sequence begins at base 1126 and ends at base 1173. The sequence runs in the 5'→3' direction from the top of the figure. The sequence is numbered according to McNally et al. (1989b). The serine 384 residue (sequence TCC) in the wild type gene and the proline 384 residue (sequence CCA) in the mutated gene are indicated. The underlined sequence below the figure shows the region indicated in the autoradiographs.

### **3.4 PURIFICATION OF THE WILD TYPE AND MUTANT ENZYMES**

The wild type and mutant pyruvate kinases were purified in exactly the same manner using identical equipment and reagents (Scheme 2).

The elution profile of the wild type pyruvate kinase from the Sephacryl S200 column is shown in Fig. 44A. It is identical in all major respects to the elution profile of the mutant enzyme (Fig. 44B). Similarly, the elution profile of the wild type enzyme from the DEAE ion-exchange column (Fig. 45A) is identical to that of the mutant enzyme (Fig. 45B).

The purified enzymes were subjected to analysis by SDS-PAGE (Fig. 46). From the resultant gel it can be seen that the enzyme is essentially homogeneous and free of contaminating proteins after the final ion-exchange chromatography step.

Both enzymes demonstrated a linear relationship between initial velocity and enzyme concentration (Fig. 47).

The purification process is summarised in Tables 8 and 9.

### **KINETIC CHARACTERISATION OF THE WILD TYPE AND MUTANT ENZYMES**

#### **1) The effect of fructose-1,6-bisphosphate**

It was discovered during the purification process that the mutant enzyme was essentially inactive in the absence of the allosteric activator Fru-1,6-P<sub>2</sub>. In contrast, the wild type enzyme is only slightly affected by the effector over the same concentration range (Fig.48). Throughout this thesis the mutant form of the enzyme was assayed in the presence of 5mM Fru-1,6-P<sub>2</sub> unless otherwise stated.

#### **2) The effect of phosphoenolpyruvate**

The purified wild type and mutant enzymes were assayed with varying amounts of the substrate PEP. Plots of velocity against substrate concentration are shown in Fig 49. The data from these experiments can be analysed via a Hill plot (Fig. 50) From such a transformation, the  $S_{0.5}$  for PEP can be calculated

easily. The degree of cooperativity between binding sites is given by  $n_H$ , the Hill coefficient, and is equal to the slope of the line produced.

### **3) The effect of ADP**

The pure wild type and mutant enzymes were assayed with varying amounts of the other substrate ADP. A plot of velocity against substrate concentration for each enzyme is shown in Fig. 51. Estimates of  $S_{0.5}$  and  $n_H$  can also be calculated from Hill plots of these data (Fig. 52).

### **4) The effect of potassium**

The effect of potassium (as the chloride salt) on the wild type and mutant enzyme activity is shown in a plot of velocity against KCl concentration in Fig. 53. As can be seen for both enzymes, the plot is weakly sigmoidal between 0-100mM KCl. Above 100mM, KCl is inhibitory. Estimates of  $S_{0.5}$  and  $n_H$ , obtained from Hill plots, are shown in Fig.54.

### **5) The effect of monovalent cations**

The wild type and mutant enzymes were assayed in the presence and absence of Fru-1,6-P<sub>2</sub> with 100mM various monovalent chlorides in a buffer containing tetrapropylammonium as the counter ion. The data are normalised with respect to potassium, the usual physiological ion bound to the enzyme. The monovalent cations tested did not significantly affect the activity of the coupling enzyme (Fig. 55).

### **6) The effect of divalent cations**

The wild type and mutant enzymes were assayed in the presence and absence of Fru-1,6-P<sub>2</sub> with 15mM various divalent cations (Fig. 56). The cations were present as the chloride salt except barium, which was used as the acetate salt. The results are normalised with respect to magnesium, the usual physiological cation bound to the enzyme. Zinc inhibited the coupling enzyme and could not be tested. Apart from zinc, none of the other divalent cations significantly affected the activity of the coupling enzyme (Fig. 57).

### **7) The effect of pH**

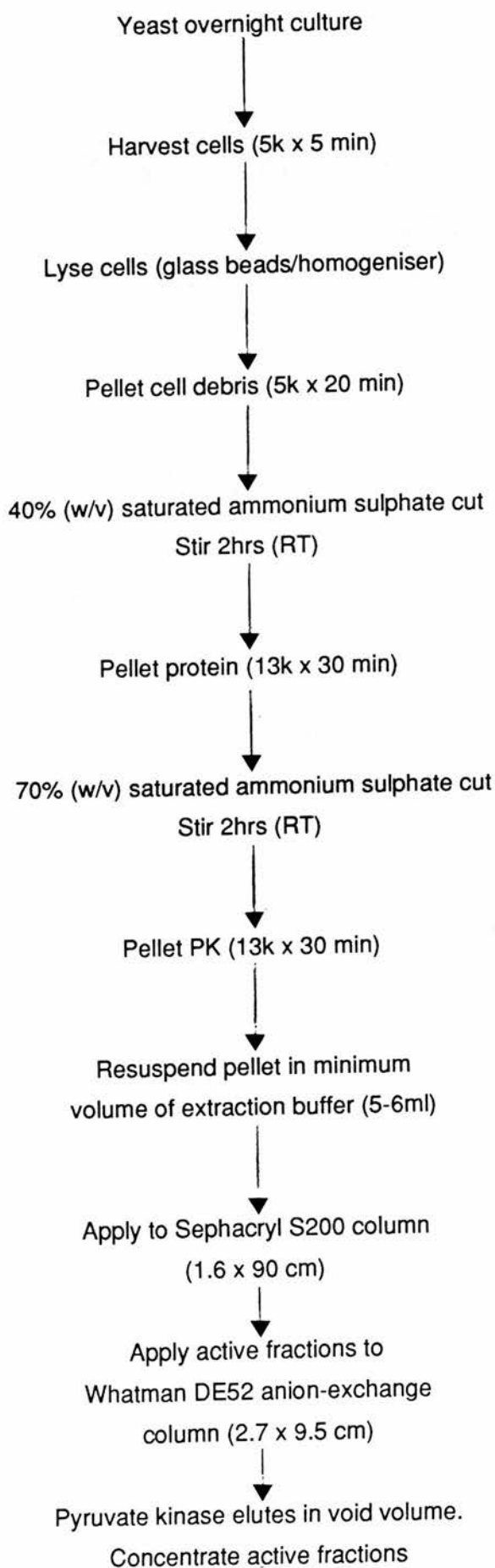
The effect of varying the pH of the buffer on the activity of the wild type and mutant enzymes is shown in Fig. 58. In the presence of the allosteric activator Fru-1,6-P<sub>2</sub>, the pH optimum of the wild type and mutant enzymes is

6.5. In the absence of the effector, the wild type enzyme activity profile is unaltered whilst the mutant enzyme is virtually inactive except at pH 8.5 and 9.5. The activity of the mutant enzyme at high pH is much lower than in the presence of effector. The pH profile of the mutant enzyme is much narrower than the wild-type enzyme.

### **8) Determination of $k_{cat}$**

The catalytic constant  $k_{cat}$  gives an indication of the efficiency of the enzyme in terms of the rate of breakdown of the enzyme-substrate complex to products and free enzyme. For enzymes displaying hyperbolic kinetics, the calculation of  $k_{cat}$  is simply  $V_m/[e]$ , where  $V_m$  is the maximum calculated velocity for the reaction and  $[e]$  is the concentration of enzyme. Note that for pyruvate kinase there are four active sites participating in the reaction and so  $[e]$  is effectively four times the determined enzyme concentration. The protein preparation needs to be free from contaminants and its concentration known to a high degree of accuracy for  $k_{cat}$  values to be accurately calculated. Table 10 gives a summary of the  $k_{cat}$  values, and the other kinetic parameters determined for both the wild type and mutant enzymes.

## SCHEME 2: PYRUVATE KINASE PURIFICATION PROTOCOL



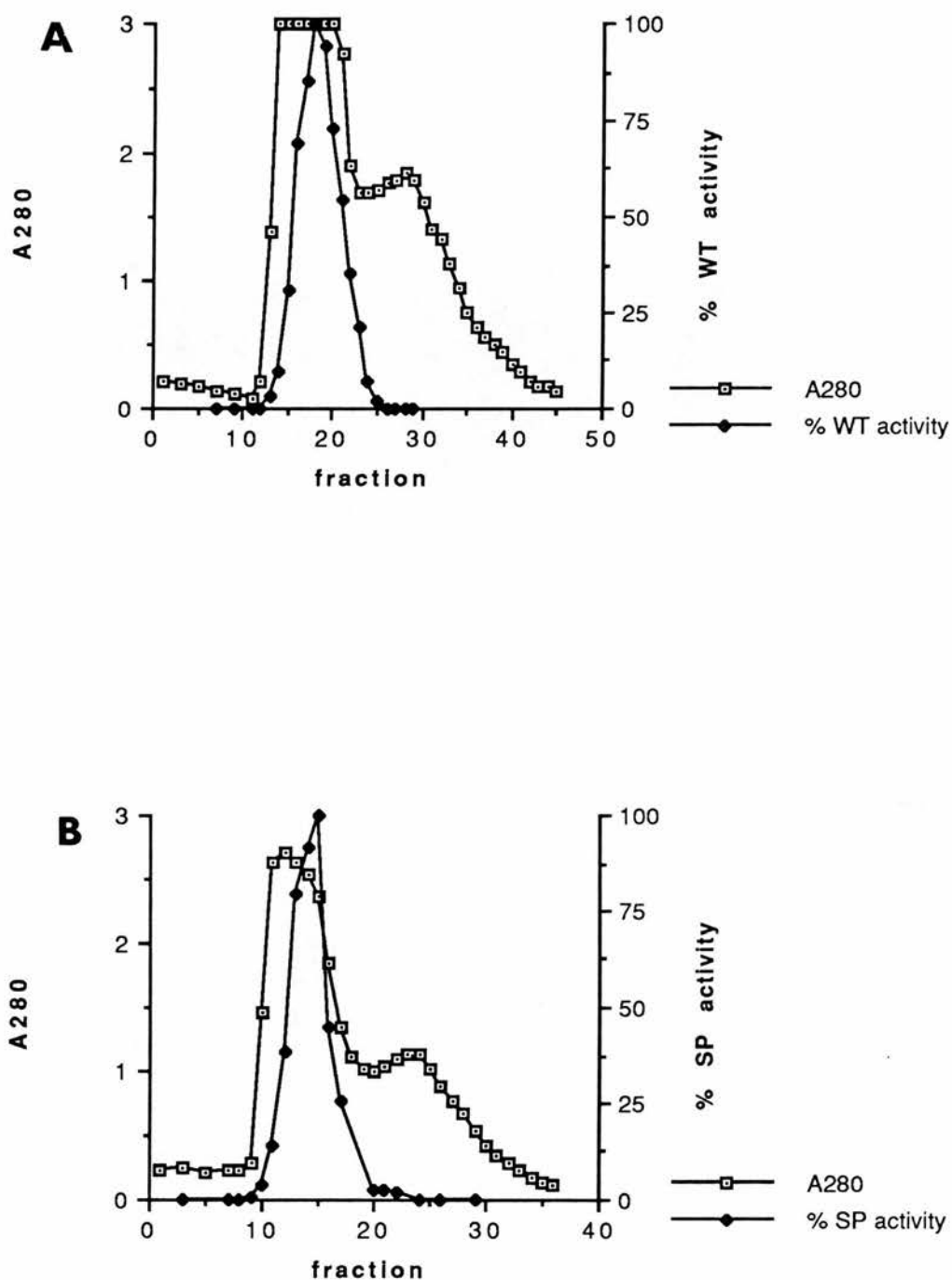


Figure 44: Elution of: A) wild type and B) S384P mutant pyruvate kinase from Sephacryl S200 gel filtration column. Fractions (5ml) were eluted and their absorbance at 280nm measured. Some fractions were assayed for enzyme activity according to the method described earlier (Section 2.3). The elution buffer comprised: 50mM Tris-HCl, pH 7.5, 20% (v/v) glycerol, 3mM  $MgCl_2$ , 1mM DTT, 0.04% (w/v) sodium azide. The flow rate was 20ml/hr.



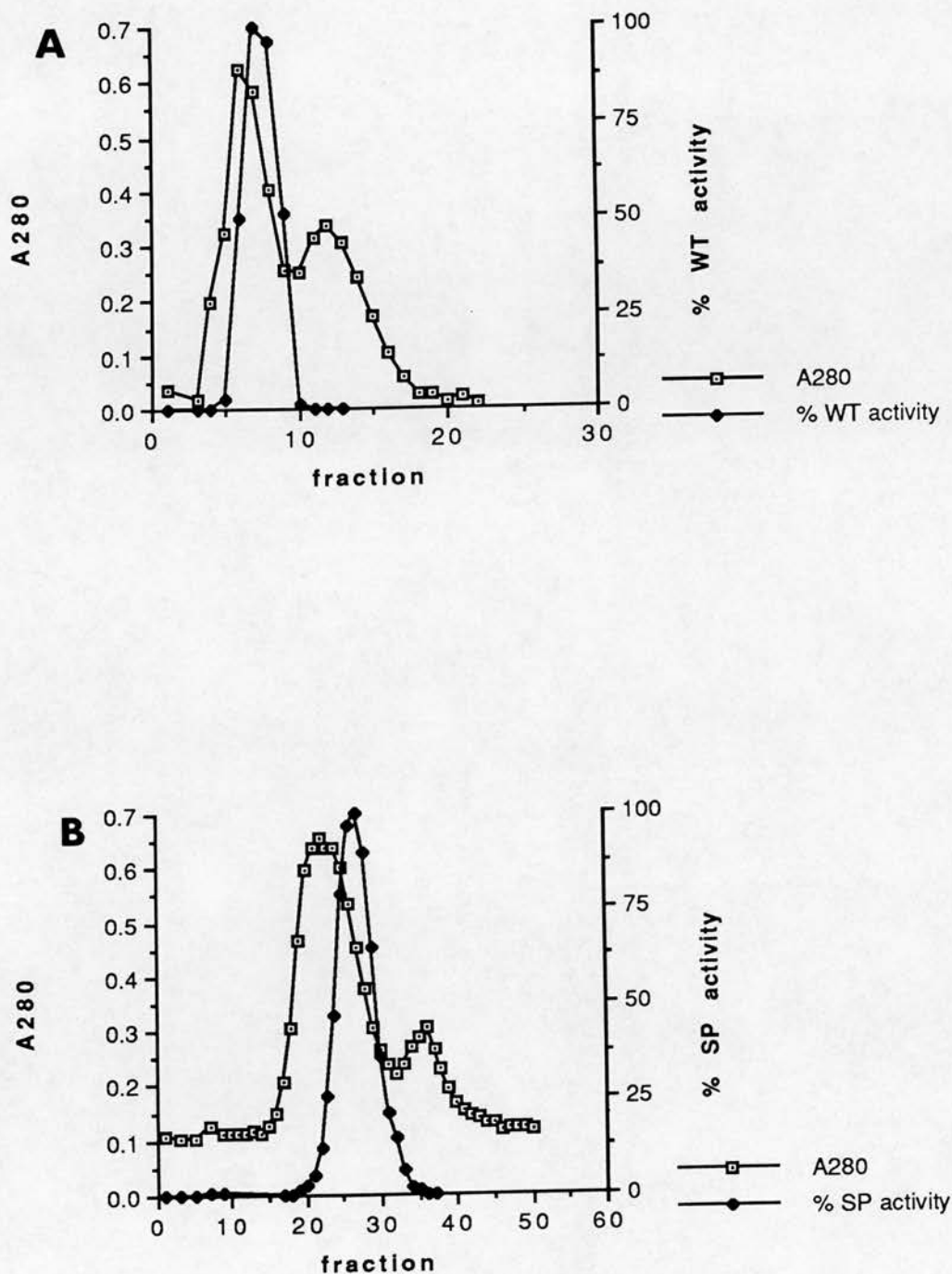


Figure 45: Elution of: A) wild type and B) S384P mutant pyruvate kinase from DEAE-cellulose anion-exchange column. Fractions (2.5ml) were eluted and their absorbance at 280nm measured. Some fractions were assayed for enzyme activity according to the method described earlier (Section 2.1.3). The elution buffer comprised: 20mM Tris-HCl, pH 8.5, 20% (v/v) glycerol 3mM  $MgCl_2$ , 1mMDTT. The flow rate was 30ml/hr. N.B. The first ten fractions from the wild-type enzyme preparation were discarded. The elution profile should therefore be shifted to the right, where it matches the profile of the mutant enzyme preparation.

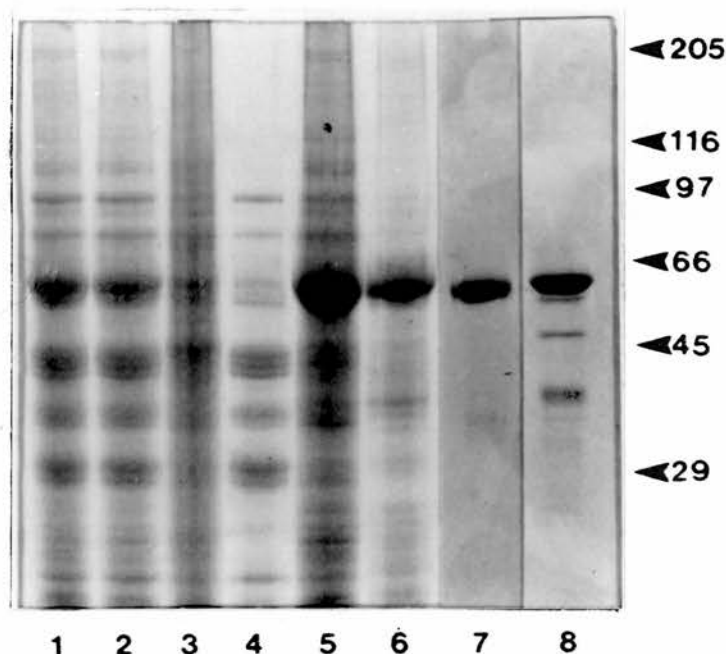


Figure 46: Stages of purification of wild type pyruvate kinase. Samples treated and analysed by SDS-PAGE as described in Section 2.7. Lanes 1) cell-free yeast extract; 2) supernatant from 40% (w/v) ammonium sulphate precipitation; 3) pellet from 40% (w/v) ammonium sulphate precipitation; 4) supernatant from 70% (w/v) ammonium sulphate precipitation; 5) pellet from 70% (w/v) ammonium sulphate precipitation; 6) fraction from gel filtration step showing highest pyruvate kinase activity; 7) fraction from ion-exchange step showing highest pyruvate kinase activity; 8) sample of commercially available rabbit muscle pyruvate kinase (Sigma). Arrows indicate size (kDa) and position of molecular weight standards analysed under identical conditions. 205 - rabbit muscle myosin; 116 - *E.coli*  $\beta$ -galactosidase; 97 - rabbit muscle phosphorylase B; 66 - bovine plasma albumin; 45 - egg ovalbumin; 29 - bovine carbonic anhydrase.

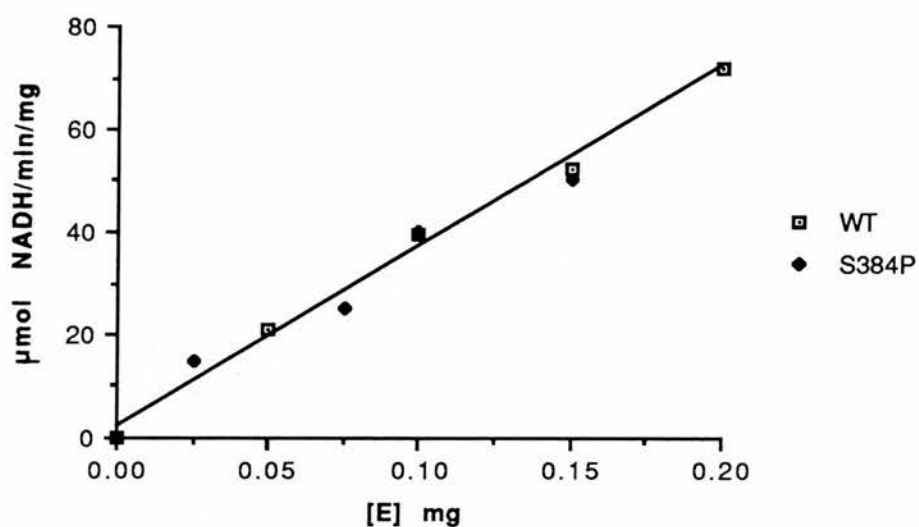


Figure 47: Rate of reaction as a function of enzyme concentration.  
 A) wild type and B) S384P mutant pyruvate kinase  
 from ion-exchange step was assayed according to the method described earlier  
 (Section 2.3).  
 Standard assay mixture was used.  
 S384P mutant enzyme was assayed in the presence of 5mM Fru-1,6-P<sub>2</sub>.  
 Protein concentration was determined by measuring the absorbance at 280nm  
 and using a value of 0.51 for a 1mg/ml solution (Yun et al., 1976).

**TABLE 8: PURIFICATION OF WILD TYPE PYRUVATE KINASE**

FRACTION	VOLUME (ml)	PROTEIN (mg/ml)	TOTAL PROTEIN (mg)	SPECIFIC ACTIVITY (U/mg)	TOTAL ACTIVITY (U)	YIELD (%)	FOLD
C.E.	192	1.8	346	51	17650	100	1.0
40S	213	1.5	320	56	17920	100	1.1
70P	7.5	10	75	94	7050	40	1.8
S200	6	3	18	245	4410	25	4.8
IEX	5.5	1.5	8.3	325	2670	15	6.4

**TABLE 9: PURIFICATION OF S384P MUTANT PYRUVATE KINASE**

FRACTION	VOLUME (ml)	PROTEIN (mg/ml)	TOTAL PROTEIN (mg)	SPECIFIC ACTIVITY (U/mg)	TOTAL ACTIVITY (U)	YIELD (%)	FOLD
C.E.	172	1.5	260	44	11400	100	1.0
40S	194	1.3	250	49	12300	100	1.1
70P	7	11.5	81	85	6890	60	1.9
S200	6	2.75	16.5	225	3720	32	5.1
IEX	5.5	1.75	9.6	275	2640	23	6.25

C.E. - cell-free extract, 40S - supernatant from 40% saturated ammonium sulphate precipitation, 70P - pellet from 70% saturated ammonium sulphate precipitation, S200- pooled gel-filtration fractions, IEX - pooled anion-exchange fractions.

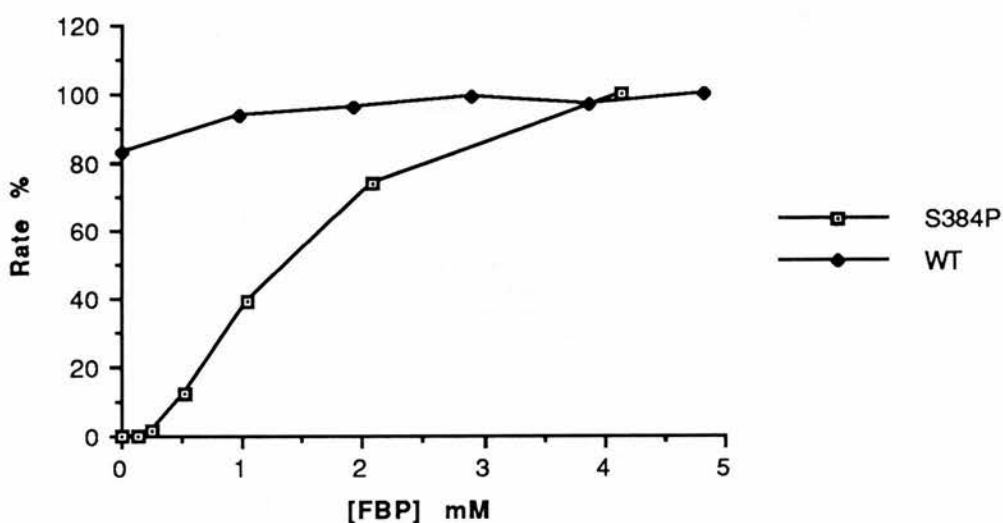


Figure 48: Activity of: A) wild type and B) S384P mutant pyruvate kinase as a function of fructose-1,6-bisphosphate concentration. The enzyme from the ion-exchange step was assayed according to the method described earlier (Section 2.3). The activity is expressed as a percentage of the maximal rate observed at the highest effector concentration used. Fru-1,6-P<sub>2</sub> was present as the trisodium salt.

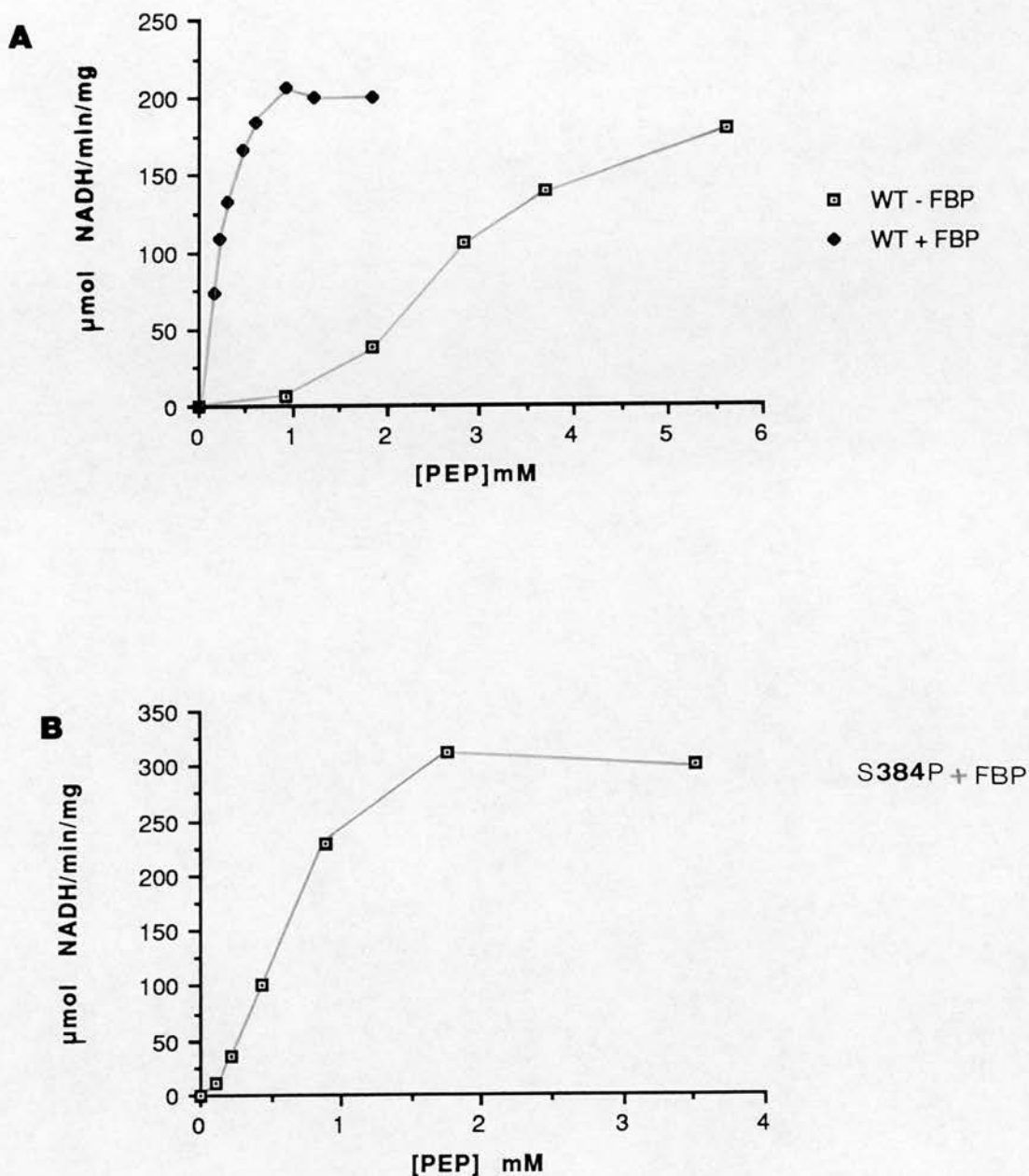


Figure 49: Rate of reaction as a function of the substrate PEP.  
 A) wild-type and B) S384P mutant pyruvate kinase.  
 Assay conditions: 50mM MES-TPA, pH 6.5, 100mM KCl, 15mM  $\text{MgCl}_2$ , 2.4mM ADP, 1.1 units lactate dehydrogenase, 0.15mM NADH.  
 PEP was present as the mono(cyclohexylammonium salt).  
 Fru-1,6- $\text{P}_2$  (where present) was 5mM.  
 A full description of how the assay was performed is given in Section 2.3.

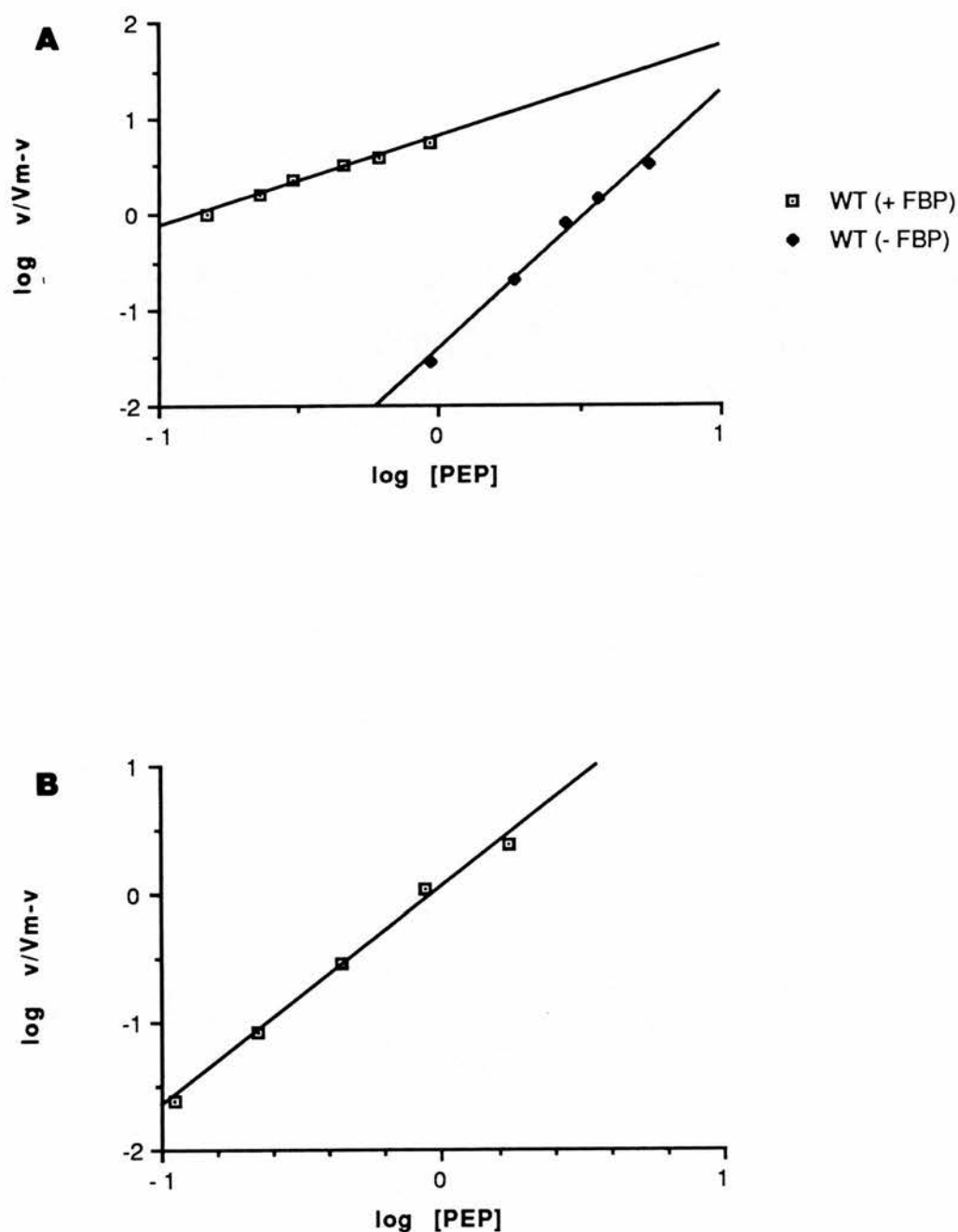


Figure 50: Hill plot of the data presented in Figure 49.  $V_m$  was calculated from a Hanes plot of the same data (not shown). A) wild type and B) S384P mutant pyruvate kinase.



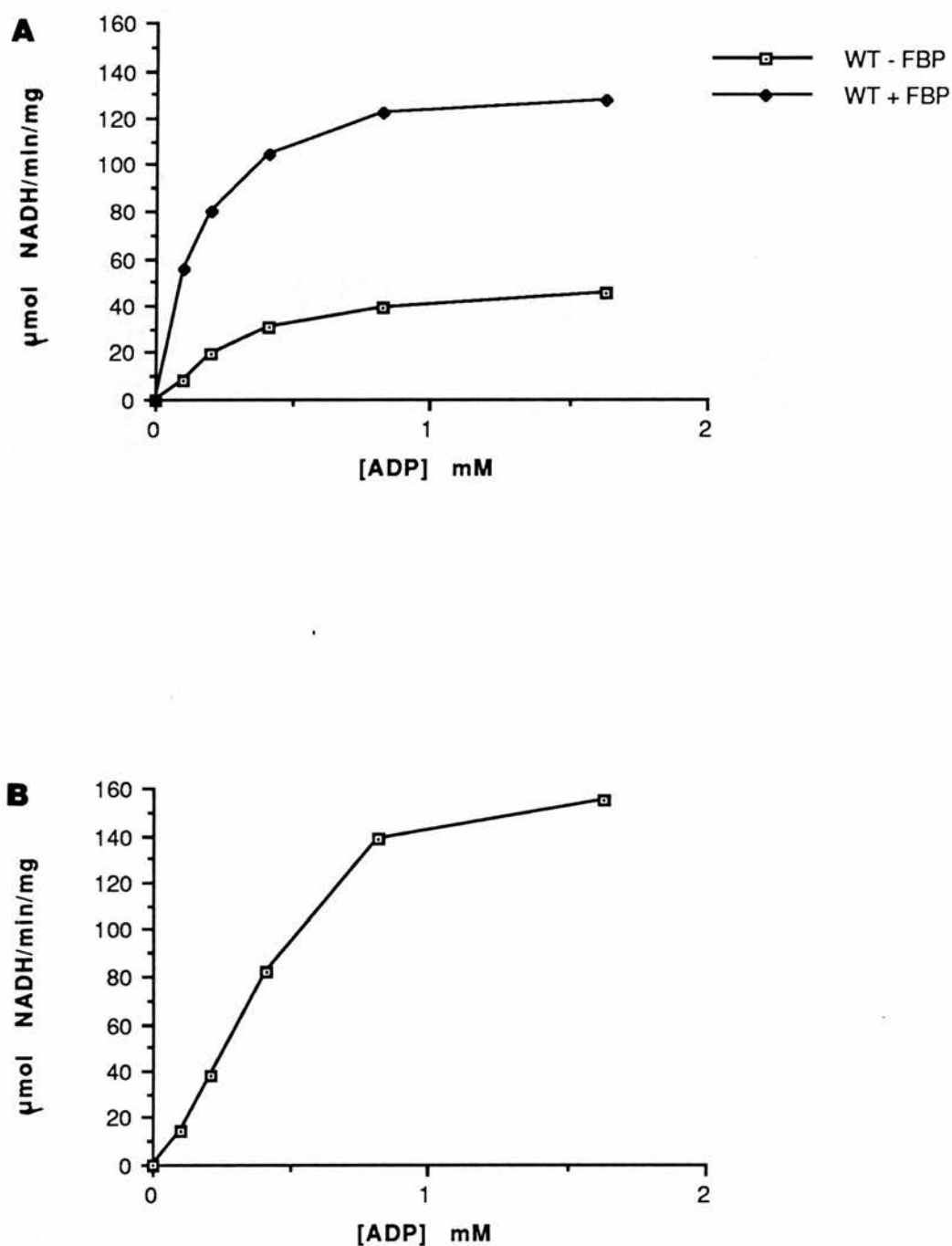


Figure 51: Rate of reaction as a function of the concentration of the substrate ADP. A) wild type and B) S384P mutant pyruvate kinase from ion-exchange step was assayed according to the method described earlier (Section 2.3). ADP was present as the di(monocyclohexylammonium) salt.

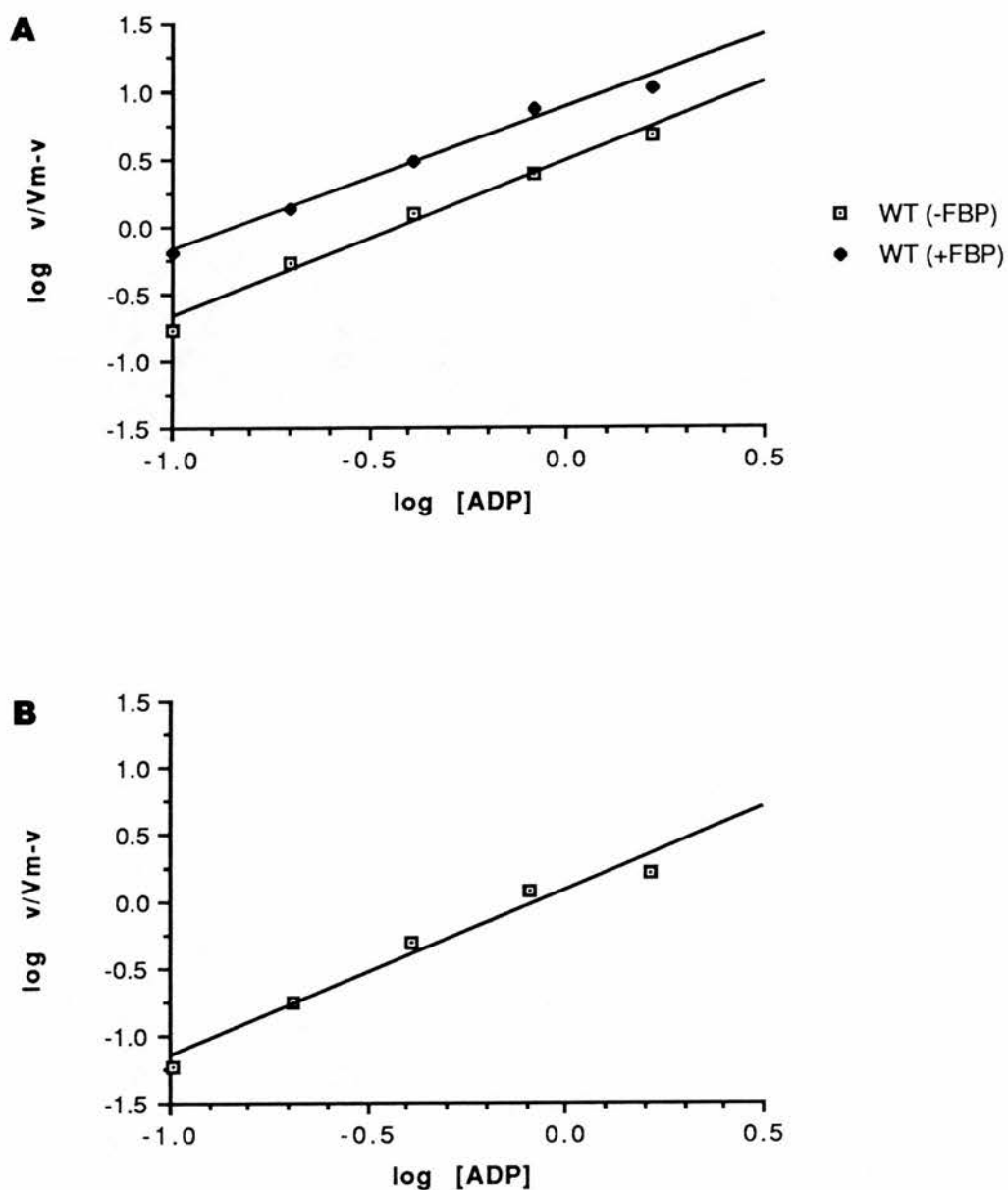


Figure 52: Hill plot of the data presented in Figure 51.  $V_m$  was calculated from a Hanes plot (not shown). A) wild type and B) S384P mutant pyruvate kinase.

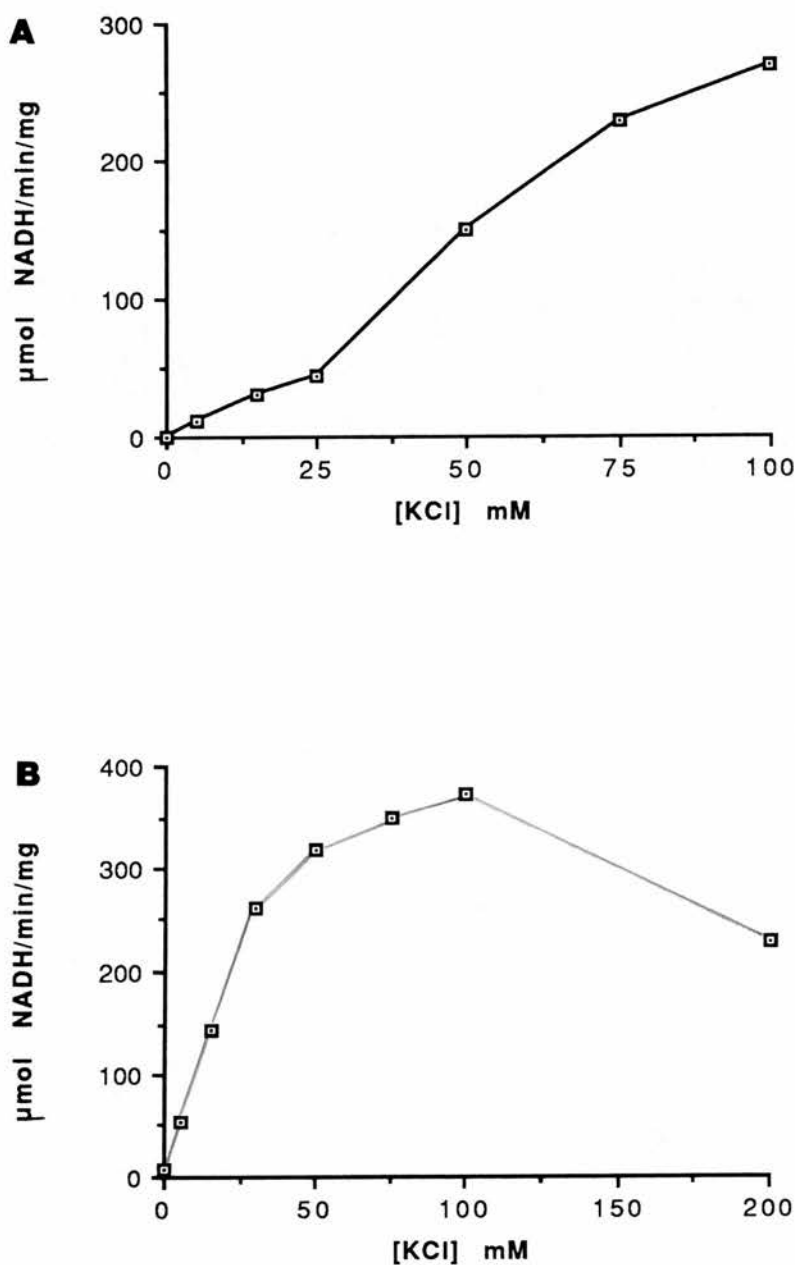


Figure 53: Rate of reaction as a function of the concentration of potassium.  
 A) wild type and B) S384P mutant pyruvate kinase from ion-exchange step was assayed according to the method described earlier (Section 2.3).  
 Potassium was present as the chloride salt.  
 Wild type enzyme assayed in the absence of Fru-1,6-P<sub>2</sub>.  
 S384P mutant pyruvate kinase was assayed in the presence of 5mM Fru-1,6-P<sub>2</sub>.

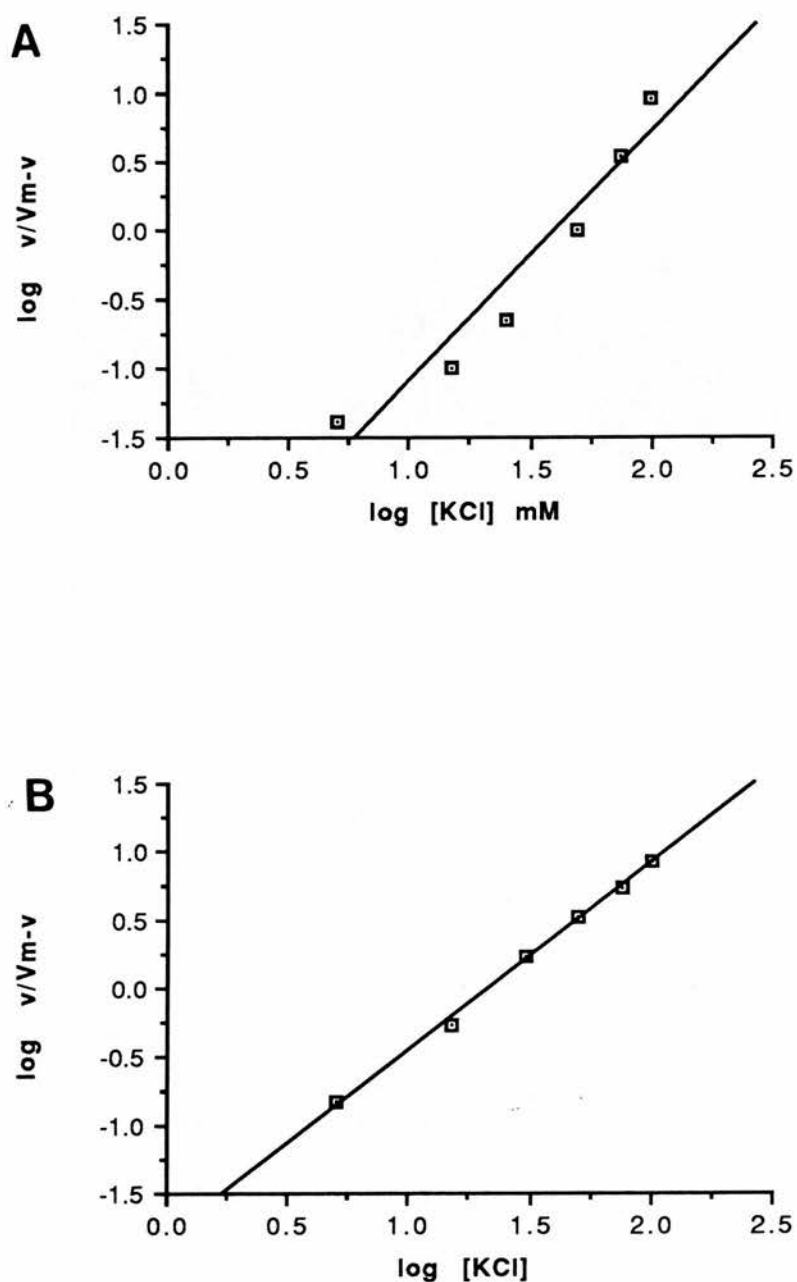


Figure 54: Hill plot of the data presented in Figure 53.  $V_m$  was calculated from a Hanes plot (not shown). A) wild type and B) S384P mutant pyruvate kinase.

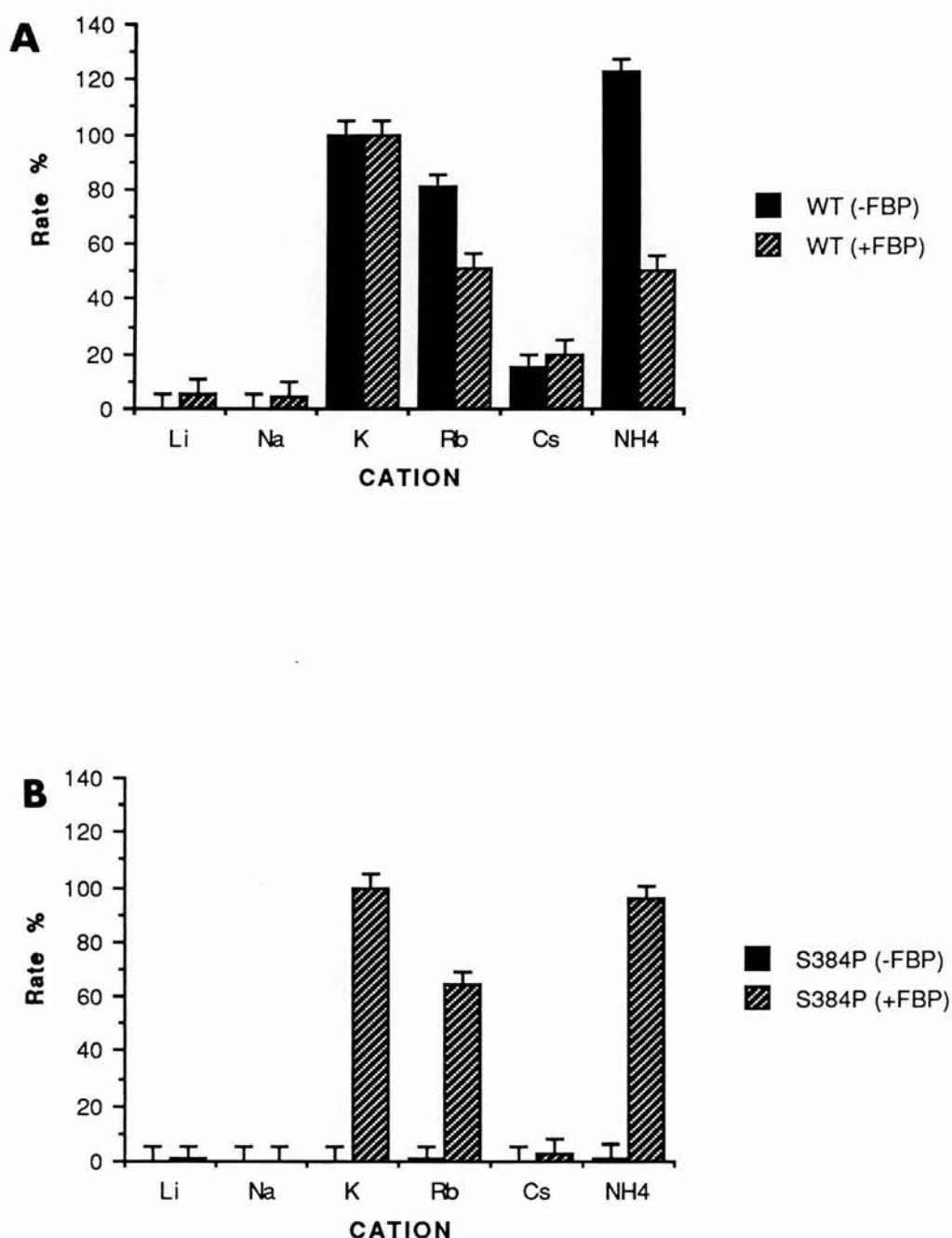


Figure 55: Monovalent cation specificity of: A) wild type and B) S384P mutant pyruvate kinase in the presence and absence of Fru-1,6-P<sub>2</sub>. Enzymes from the ion-exchange step were assayed according to the method described earlier (Section 2.3) except that 0.1ml 1M MCl was added separately. Assay buffer comprised: 50mM MES-TPA, pH 6.5, 100mM MCl, 15mM MgCl<sub>2</sub>. Values are expressed relative to K<sup>+</sup>, the usual physiological cation, which was designated as giving 100% activity. Fru-1,6-P<sub>2</sub>, where present, was 5mM.

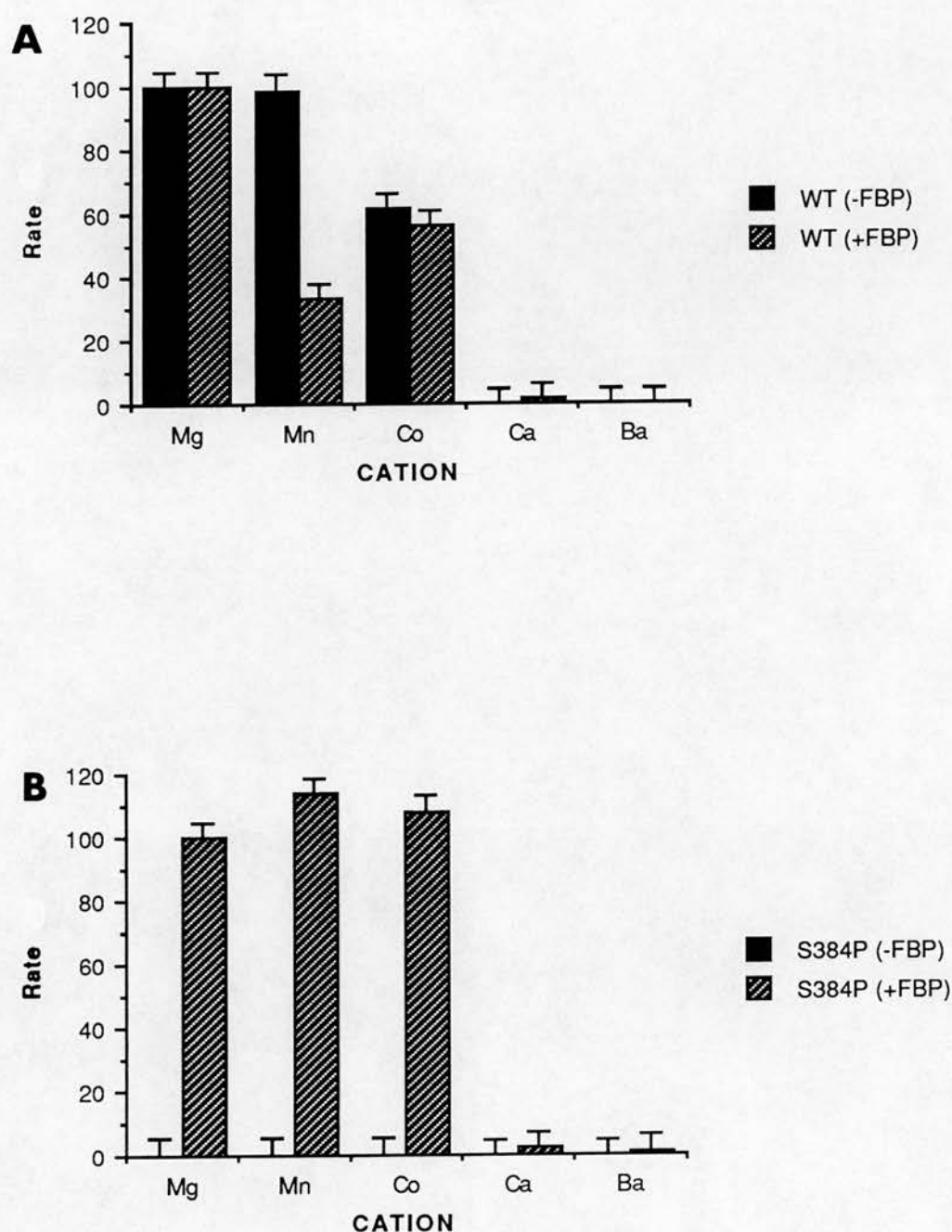


Figure 56: Divalent cation specificity of A) wild-type and B) S384P mutant pyruvate kinase. Assay conditions: 50mM MES-TPA, pH 6.5, 100mM KCl, 15mM  $M^{2+}$ , 2.4mM ADP, 5.6mM PEP, 0.15mM NADH, 1.1 units lactate dehydrogenase. Cations were added as the chloride salts, except barium, which was added as the acetate salt. FBP (where present) was 5mM. Rates are expressed in arbitrary units relative to magnesium, which was designated as giving 100 units of activity. A full description of how the assays were performed is given in Section 2.3.

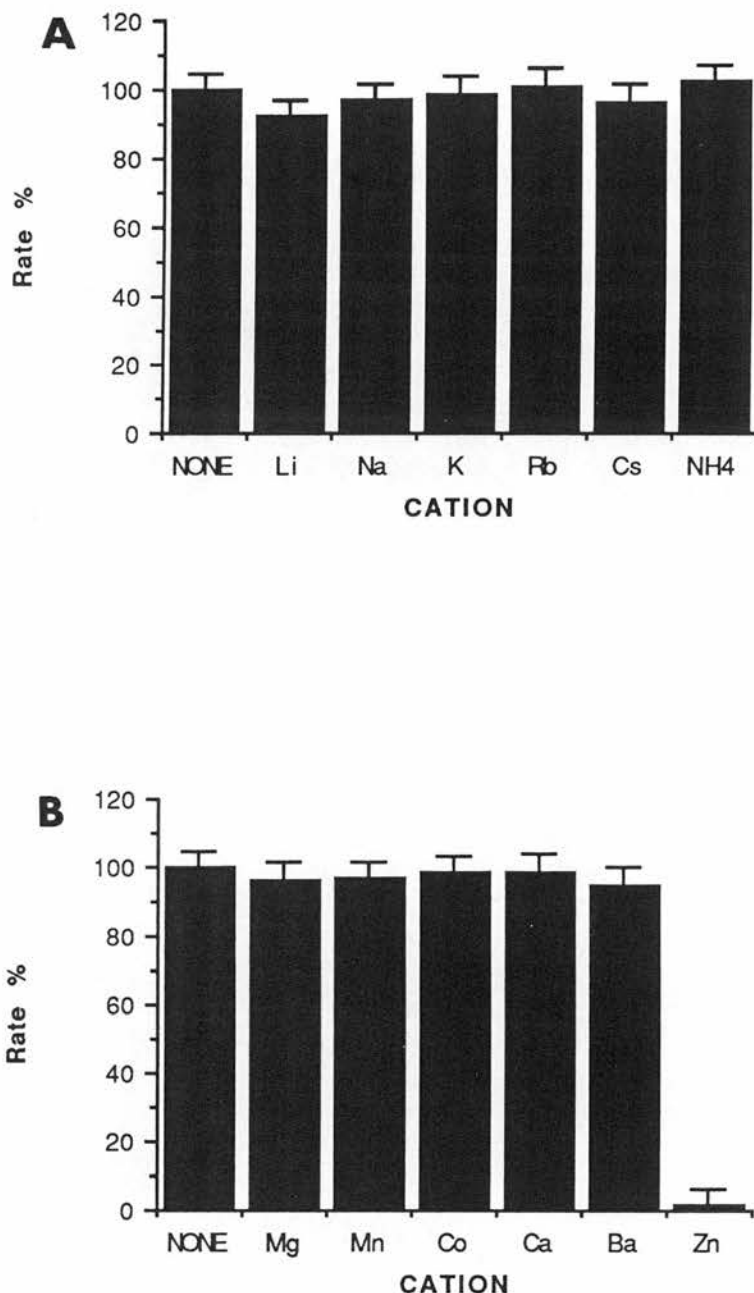


Fig. 57 Effect of divalent and monovalent cations on lactate dehydrogenase. A) Lactate dehydrogenase (0.02 Units) was incubated in the presence of 15mM of the indicated divalent cations (present as the chloride salt, except barium, which was present as the acetate salt). Other components: 0.14mM NADH- $\text{Na}_2$ , 13.7mM NaPyruvate. B) Lactate dehydrogenase (0.09 Units) was incubated in the presence of 100mM of the indicated monovalent cations (present as the chloride salt). Other components: 0.14mM NADH- $\text{Na}_2$ , 18.2mM NaPyruvate. Buffer comprised: 50mM MES-TPA. Assay temperature: 30°C.



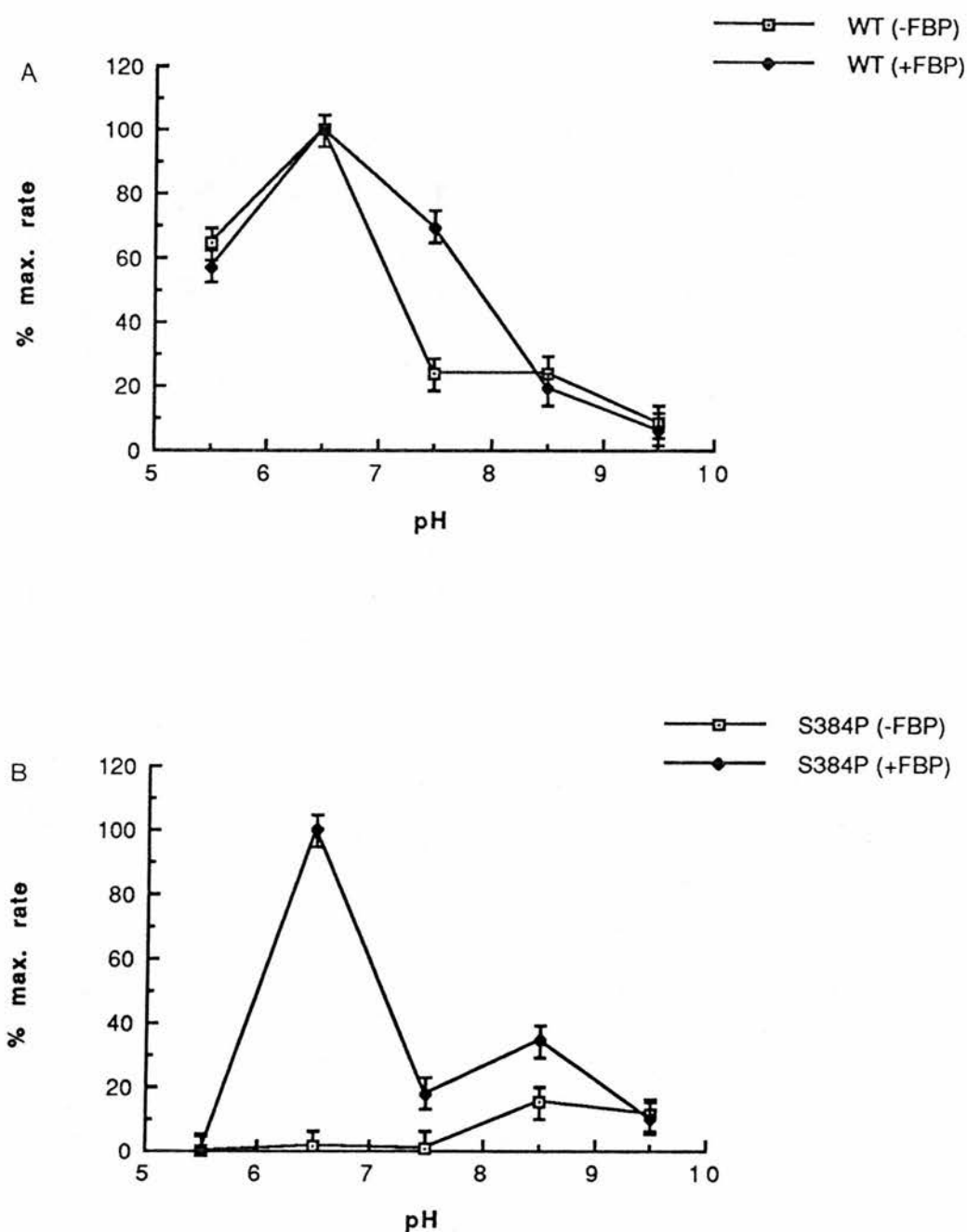


Figure 58: Activity of: A) wild type and B) S384P mutant pyruvate kinase as a function of pH in the presence and absence of Fru-1,6-P<sub>2</sub>.

Enzymes from the ion-exchange step were assayed according to the method described earlier (Section 2.3) except that different pH buffers were used.

At pH values below 7.0, MES-TPA buffers were used.

Above pH 7.0, Tris-HCl buffers were used.

Assay buffer comprised: 50mM buffer, 100mM KCl, 15mM MgCl<sub>2</sub>.

Fru-1,6-P<sub>2</sub>, where present, was 5mM.

**TABLE 10 KINETIC PARAMETERS OF THE WILD TYPE AND S384P MUTANT PYRUVATE KINASES DETERMINED BY ENZYME ASSAY**

PARAMETER	WILD TYPE	MUTANT
$S_{0.5}$ PEP (-FBP)	3.34mM	-
$n_H$	2.67	-
$S_{0.5}$ PEP (+FBP)	0.16mM	0.94mM
$n_H$	1.00	1.69
$S_{0.5}$ ADP (-FBP)	0.39mM	-
$n_H$	1.16	-
$S_{0.5}$ ADP (+FBP)	0.15mM	0.69mM
$n_H$	1.04	1.46
$S_{0.5}$ KCl (-FBP)	41.5mM	-
$n_H$	1.80	-
$S_{0.5}$ KCl (+FBP)	-	21.4mM
$n_H$	-	1.36
pH optimum	6.5	6.5
$k_{cat}$ (-FBP)	258s <sup>-1</sup>	1 s <sup>-1</sup>
$k_{cat}$ (+FBP)	299s <sup>-1</sup>	204s <sup>-1</sup>

### 3.5 FLUORESCENCE AND CIRCULAR DICHROISM SPECTROSCOPY STUDIES

#### 1) Fluorescence studies

The effect of saturating concentrations of the substrates PEP (5mM) and ADP (2mM) on the fluorescence emission spectrum of both the wild type and mutant enzyme emission spectra are shown in Figs. 59 and 60 respectively. .

The effect of varying the concentration of the effector Fru-1,6-P<sub>2</sub> on the emission spectra of the wild type and mutant enzymes is shown in Figs. 61. The data from these titrations were analysed in a variety of ways to obtain estimates of the dissociation constant of the effector with the enzymes. A number of other fluorimetric titrations with a variety of ligands were also performed. The data from these experiments are summarised in Table 11.

The CD and fluorescence experiments were carried out in 20mM Tris-HCl, pH 8.5, 20% glycerol, 3mM MgCl<sub>2</sub> and 1mM DTT.

#### 2) Circular dichroism (CD) spectroscopy

The CD spectra of the wild type and mutant enzymes are shown in Fig. 62 . The data obtained from these spectra were analysed by the CONTIN program (Provencher, 1981) to obtain values for the various secondary structural elements (alpha helix, beta sheet and random coil). The values obtained for both the wild type and mutant enzyme are shown in Table 12.

The effect of saturating concentrations of substrates PEP (5mM) and ADP (2mM) and of the effector Fru-1,6-P<sub>2</sub> (1mM) on the CD spectra of the wild type and mutant enzymes are shown in Figs. 63, 64 and 65 (wild type) and Figs. 66, 67 and 68 (mutant) respectively.

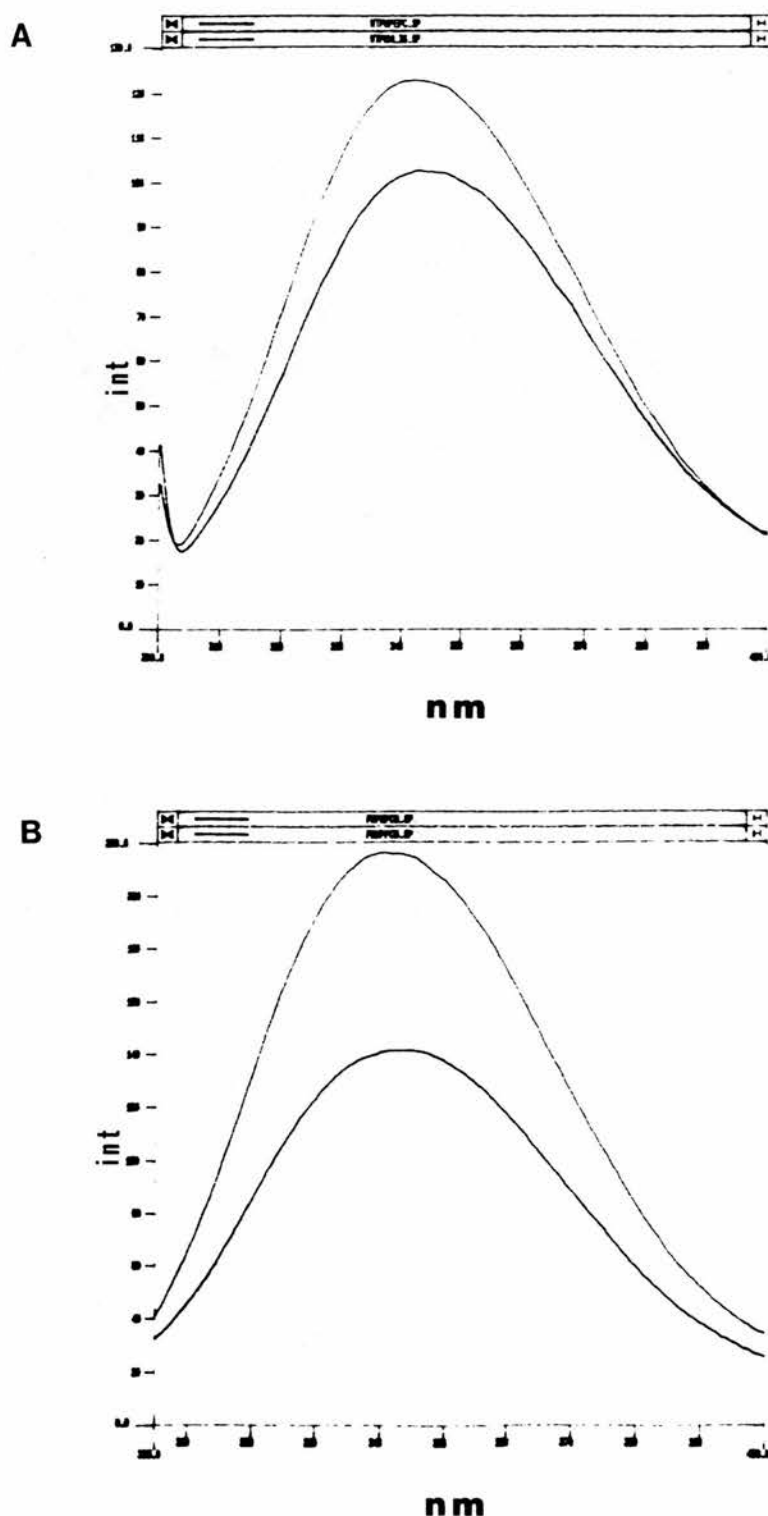


Fig. 59 Effect of 5mM PEP on the fluorescence emission spectra of yeast pyruvate kinase.  
 A) wild type (0.137mg/ml), B) S384P mutant enzyme.  
 Upper trace in each figure - spectrum in absence of ligand.  
 Lower trace in each figure - spectrum in presence of ligand.  
 Excitation 295nm, emission 300-400nm.  
 Buffer: 20mM Tris-HCl, pH 8.5, 20% (v/v) glycerol, 3mM  $\text{MgCl}_2$ , 1mM DTT.  
 int = fluorescence emission intensity (arbitrary units)

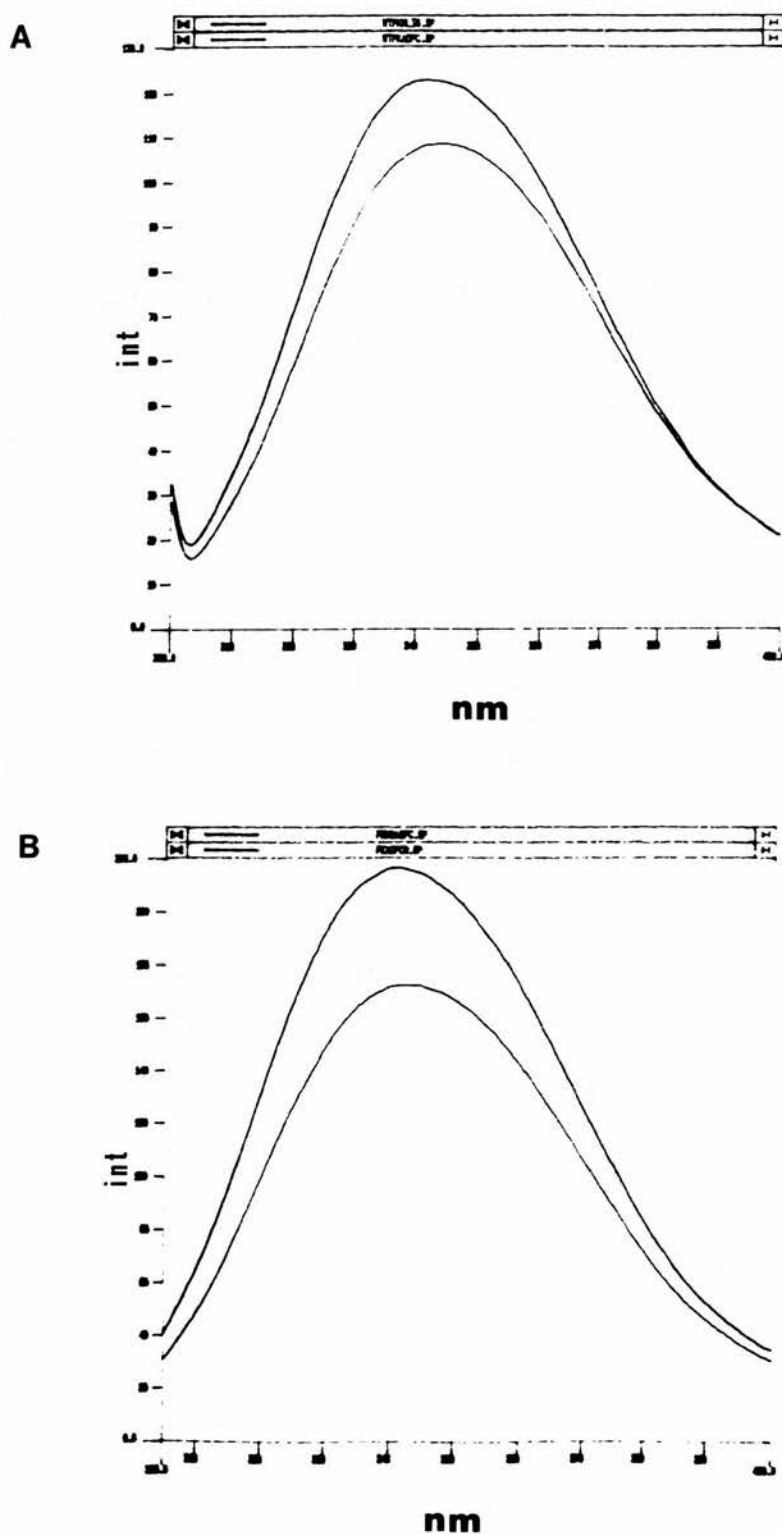


Fig. 60 Effect of 2mM ADP on the fluorescence emission spectra of yeast pyruvate kinase.  
 A) wild type (0.137mg/ml), B) S384P mutant enzyme (0.2mg/ml)  
 Other conditions exactly as described in Fig. 59.

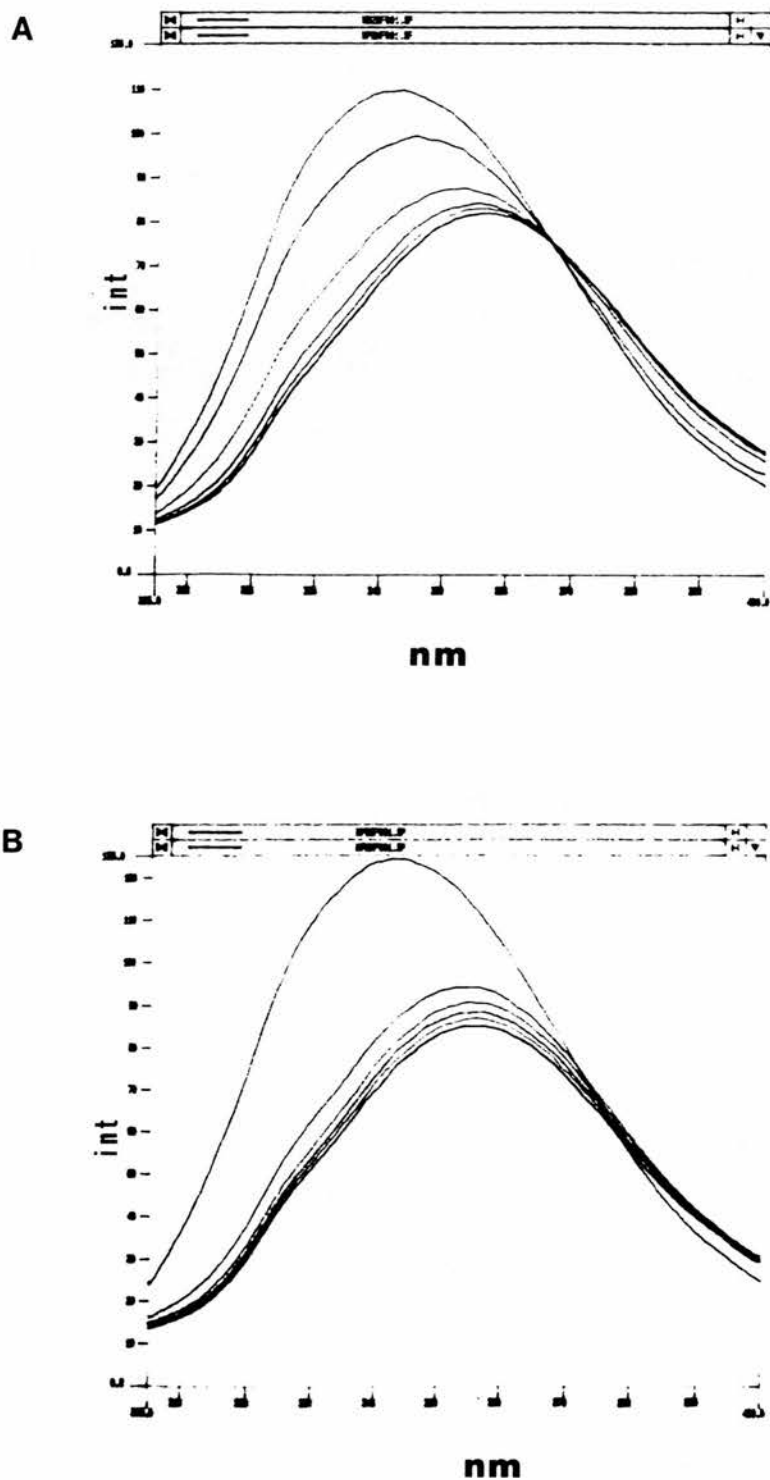


Fig. 61 Effect of increasing concentrations of Fru-1,6-P<sub>2</sub> on the fluorescence emission spectra of yeast pyruvate kinase. A) wild type enzyme (0.137mg/ml), B) S384P mutant enzyme (0.2mg/ml). A decrease in signal intensity upon each addition of ligand is observed. Total ligand concentration at each measurement is: i) 0μM, ii) 27μM, iii) 54μM, iv) 78μM, v) 110μM, vi) 133μM. Other conditions as described in Fig. 59.

**TABLE 11**  
**BINDING PARAMETERS OF THE WILD TYPE AND S384P MUTANT PYRUVATE KINASES**  
**DETERMINED BY FLUORIMETRY**

PARAMETER	WILD TYPE	MUTANT
S <sub>0.5</sub> Fru-1,6-P <sub>2</sub>	49.3μM	15.6μM
n <sub>H</sub>	1.23	1.80
S <sub>0.5</sub> Fru-1,6-P <sub>2</sub> (ADP)	269.3μM	56.8μM
n <sub>H</sub>	1.08	1.40
S <sub>0.5</sub> Fru-1,6-P <sub>2</sub> (PEP)	55.2μM	15.3μM
n <sub>H</sub>	1.76	0.95
S <sub>0.5</sub> ADP	3.02mM	2.49mM
n <sub>H</sub>	1.06	0.96
S <sub>0.5</sub> PEP	93.0μM	170μM
n <sub>H</sub>	1.06	1.00

**TABLE 12**  
**SECONDARY STRUCTURE CONTENT (%) OF THE WILD TYPE, S384P MUTANT AND CAT**  
**MUSCLE PYRUVATE KINASES.**

ENZYME	ALPHA HELIX	BETA SHEET	RANDOM
WILD TYPE	29 ± 0.51	29 ± 0.74	42 ± 0.9
S384P	20 ± 1.0	45 ± 1.0	35 ± 1.8
CAT	40	22	38

Wild type and S384P mutant enzymes were determined by CONTIN analysis of data collected by CD spectroscopy.  
Cat muscle values were derived by analysing X-ray crystallographic data and summing those structures that had been assigned as forming alpha helices or beta strands.



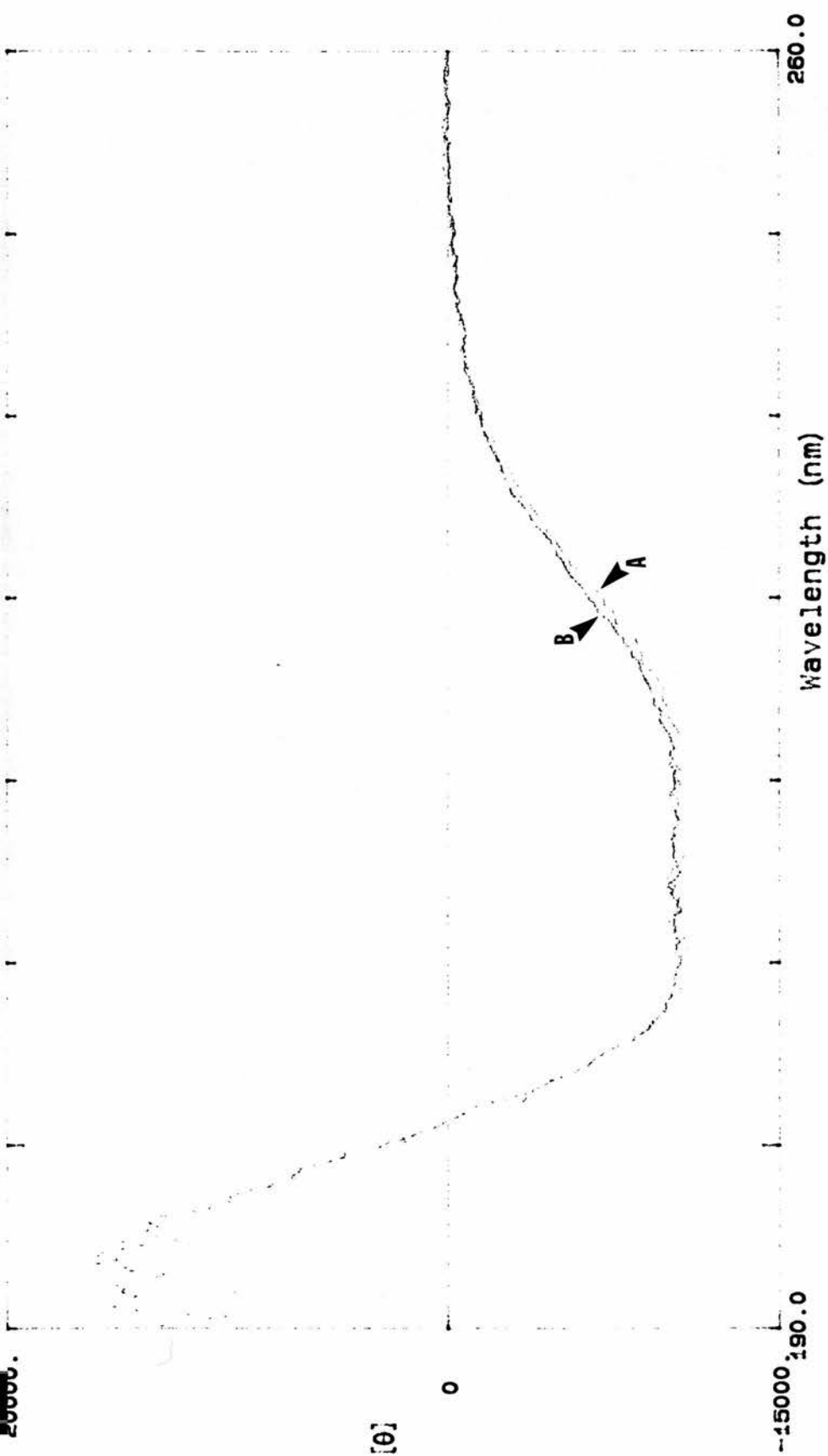


Fig.62 Far uv circular dichroism spectra of wild type and S384P mutant pyruvate kinase.  
 Cuvette contained: 0.137 mg/ml (wild type) or 0.2 mg/ml (S384P) protein in 20mM Tris-HCl, pH 8.5, 20% (v/v) glycerol, 3mM  $\text{MgCl}_2$ , 1mM DTT.  
 The mean residue ellipticity  $[\theta]$  ( $\text{degrees cm}^2 \text{dmol}^{-1}$ ) as a function of wavelength (nm) is recorded.

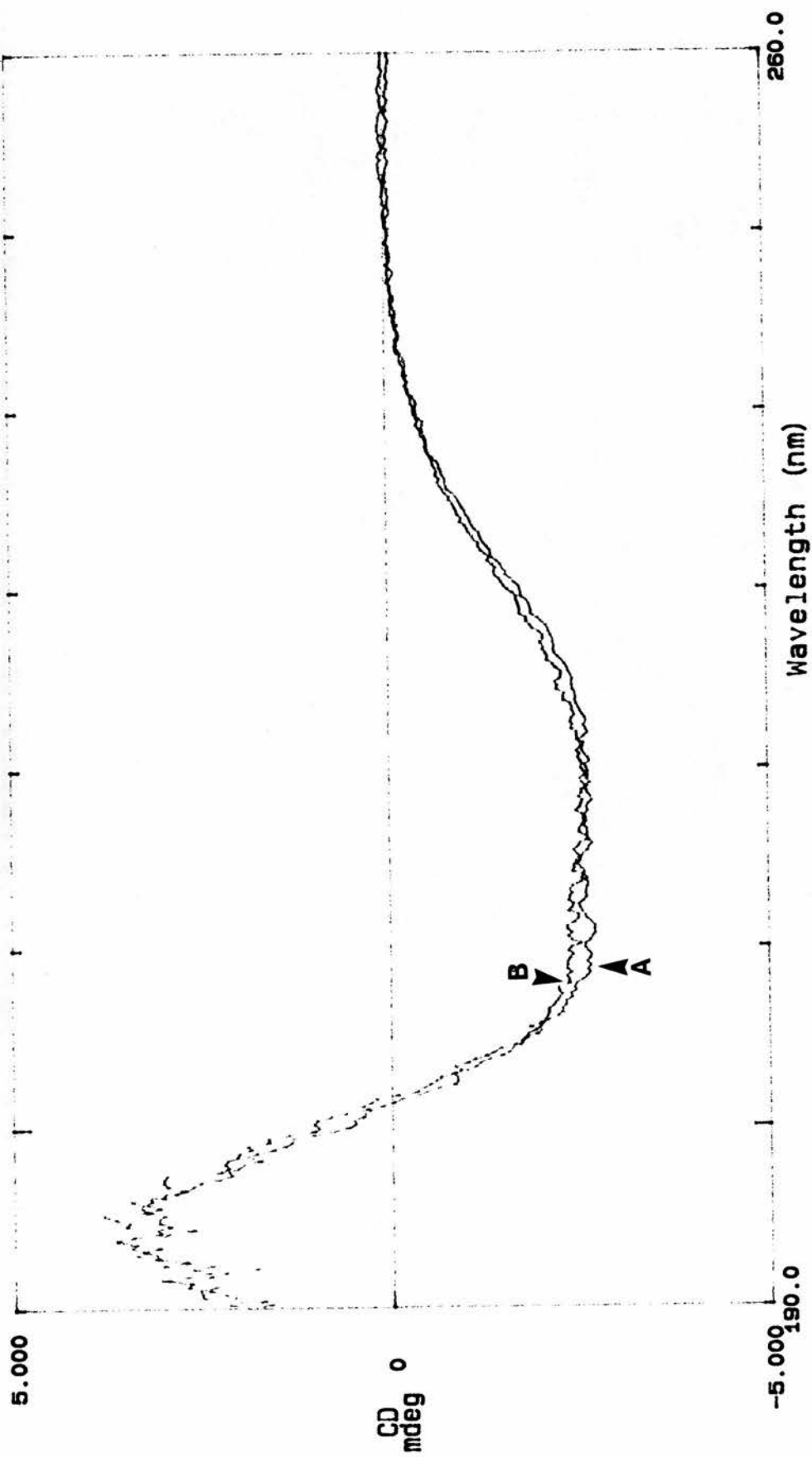


Fig. 63 Far uv circular dichroism spectra of wild type pyruvate kinase  
 A) in the presence, and B) absence of 5mM PEP.  
 Conditions as described for Fig. 62.

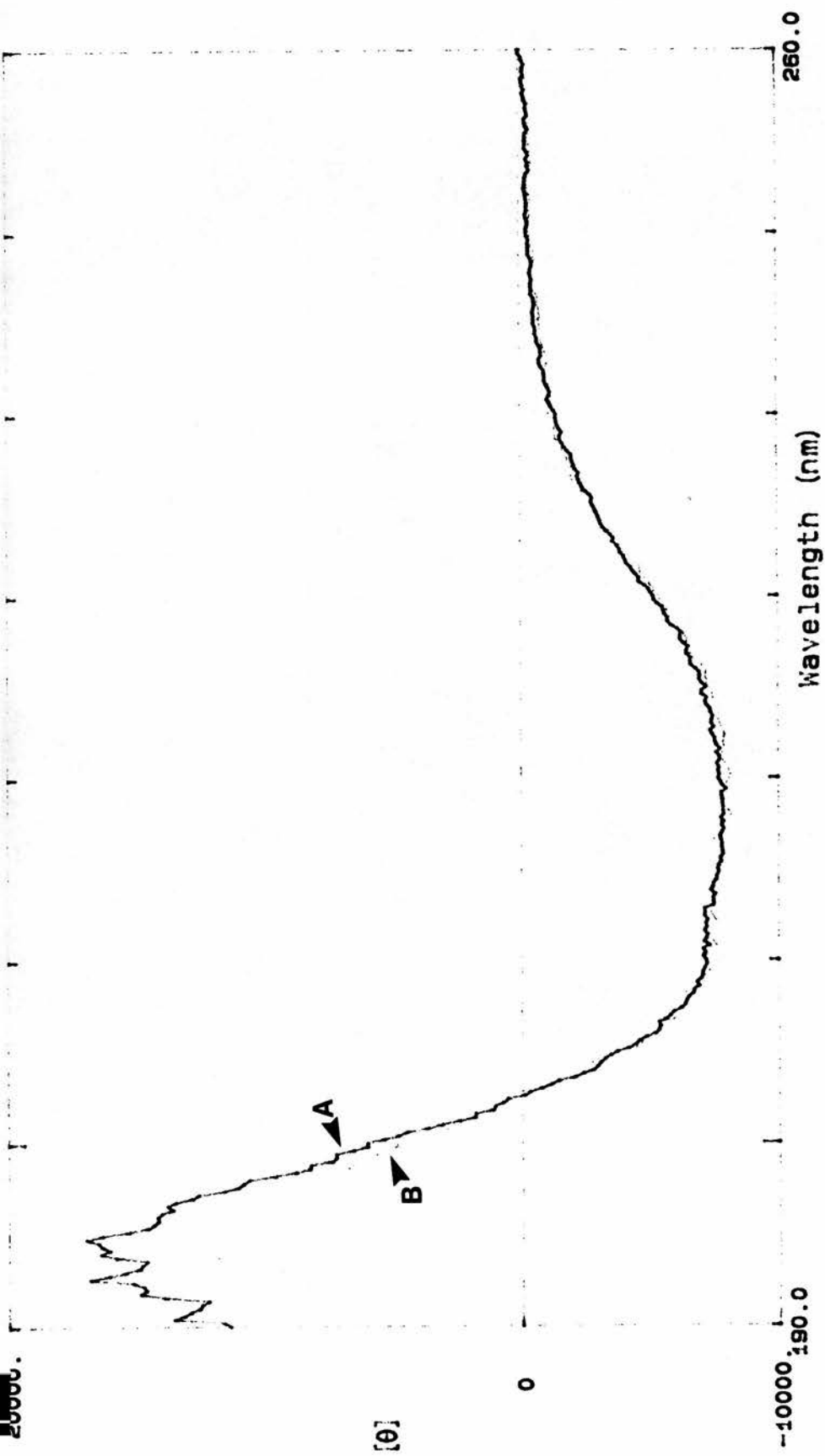


Fig. 64 Far uv circular dichroism spectra of wild type pyruvate kinase  
A) in the presence, and B) absence of 2mM ADP.  
Conditions as described for Fig. 62.

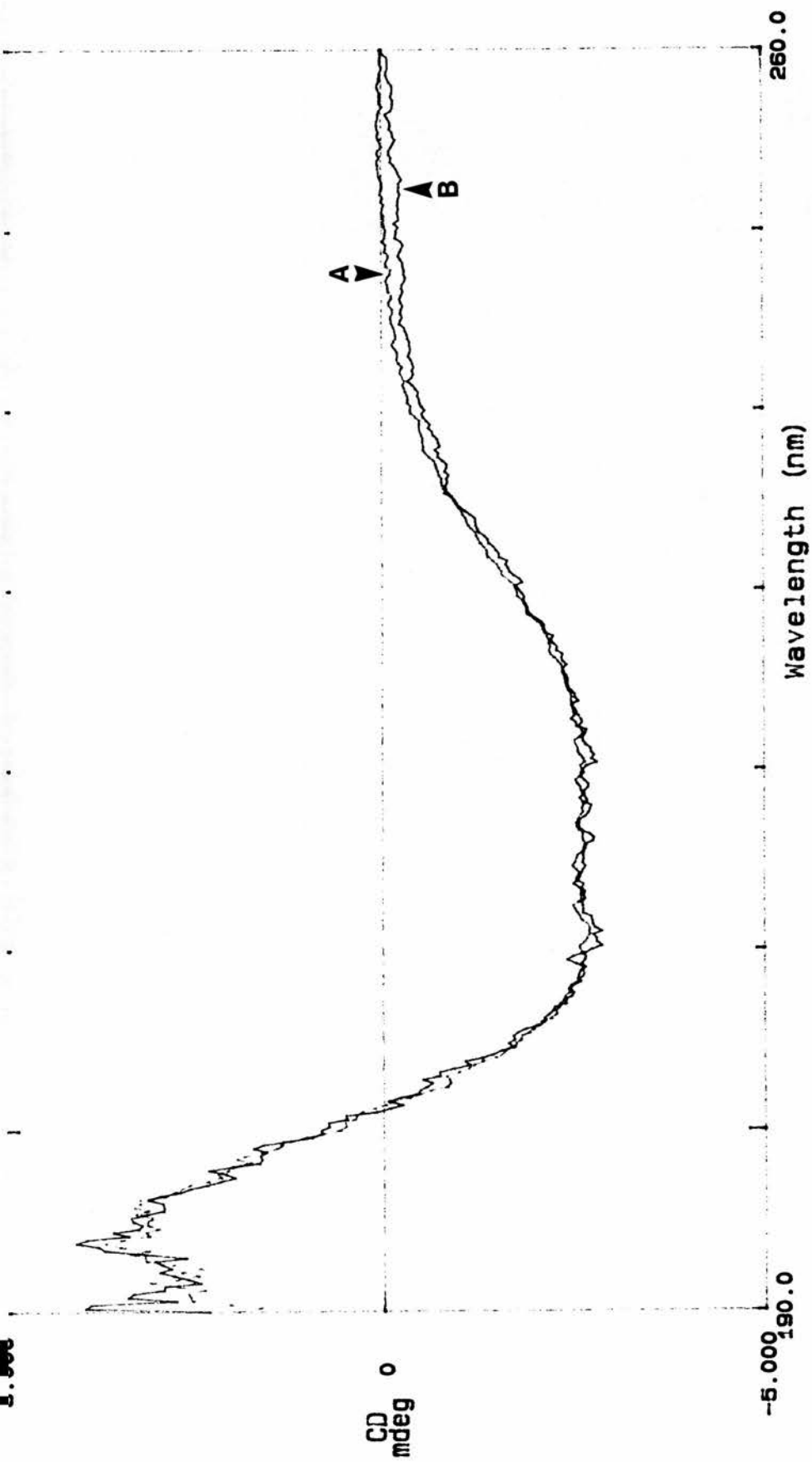


Fig. 65 Far uv circular dichroism spectra of wild type pyruvate kinase  
 A) in the presence and, B) absence of 1mM fructose-1,6-  
 bisphosphate.  
 Conditions as described for Fig. 62.

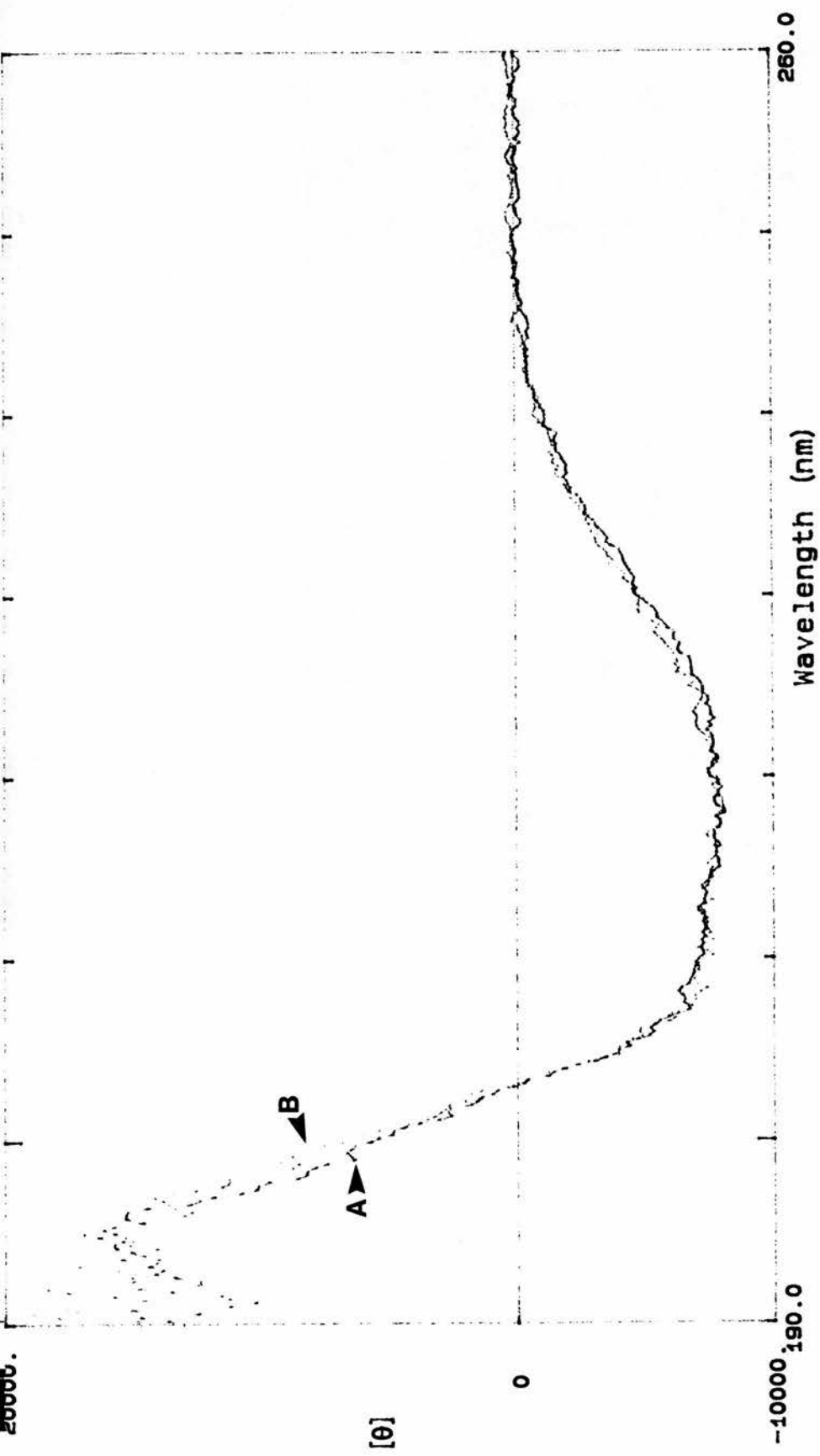


Fig. 66 Far uv circular dichroism spectra of S384P mutant pyruvate kinase A) in the presence, and B) absence of 5mM PEP. Conditions as described for Fig. 62.

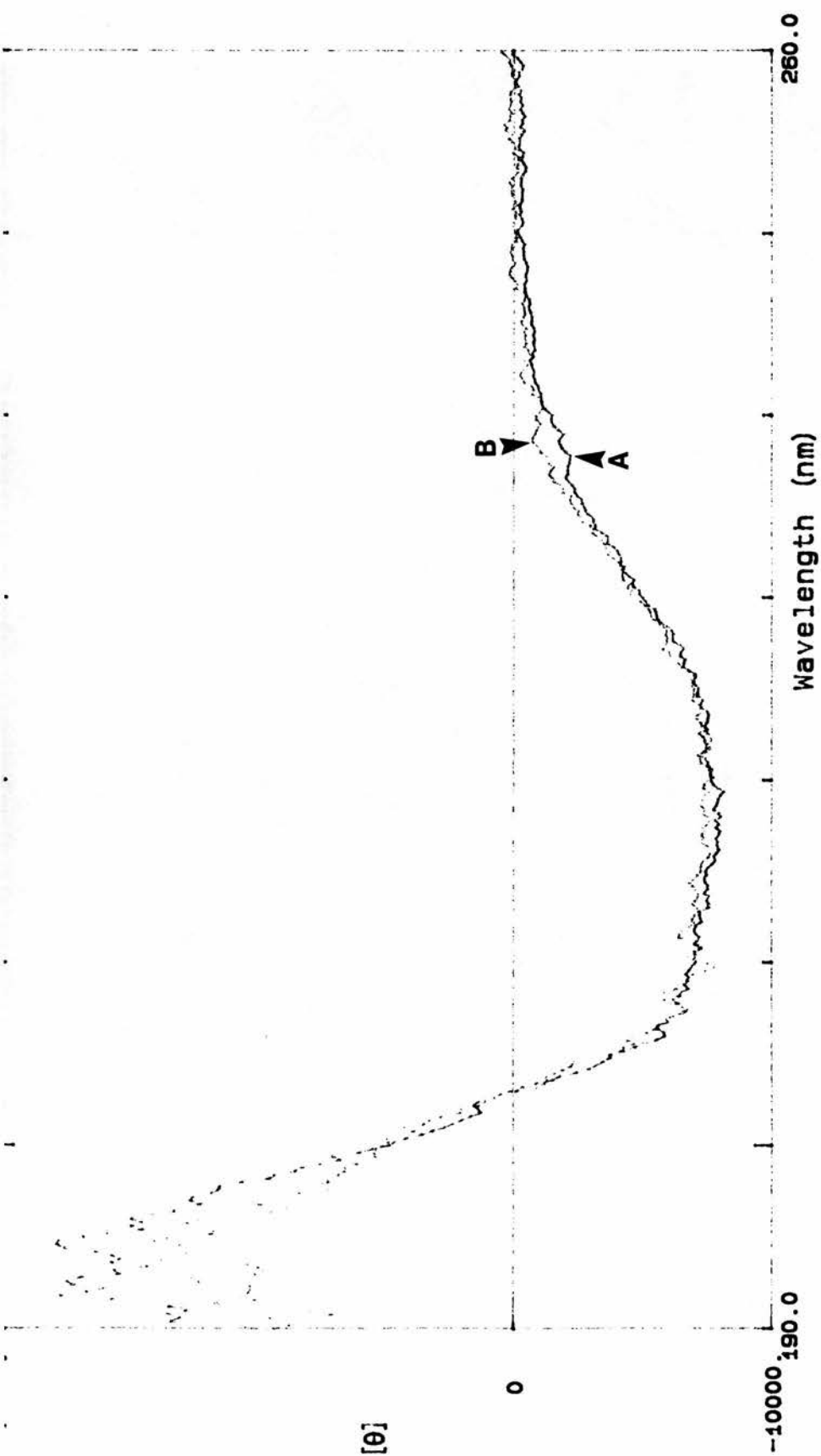


Fig. 67 Far uv circular dichroism spectra of S384P mutant pyruvate kinase A) in the presence, and B) absence of 2mM ADP. Conditions as described for Fig. 62.

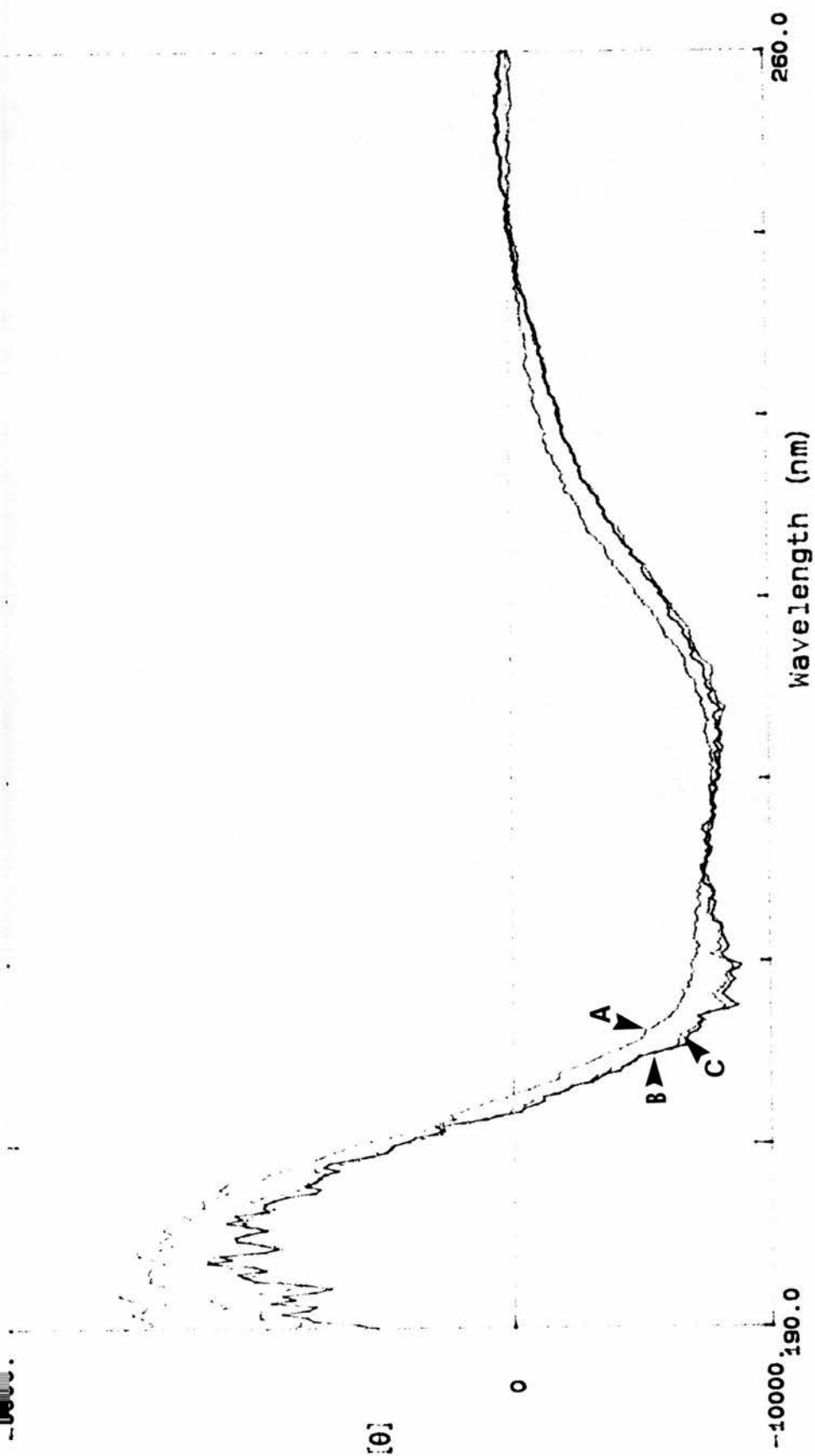


Fig. 68 Far uv circular dichroism spectra of S384P mutant pyruvate kinase in the presence and absence of Fru-1,6-P<sub>2</sub>.

- A) no added effector
- B) 1mM Fru-1,6-P<sub>2</sub>
- C) 5mM Fru-1,6-P<sub>2</sub>

Conditions as described for Fig. 62.

### **3.6 TRYPSIN DIGESTION OF WILD TYPE AND MUTANT PYRUVATE KINASE**

The effect of incubating samples of purified wild type and mutant pyruvate kinase with trypsin, in the presence and absence of various substrates and effectors, was examined. The protective effect of the various ligands on the susceptibility of the wild type and mutant enzymes to trypsin is shown in Figures 69 and 70 respectively. The time taken for the enzymes to lose 50% of their activity ( $T_{50}$ ) in the presence of each ligand is given in Table 13.

### **3.7 NEM INHIBITION OF WILD TYPE AND MUTANT PYRUVATE KINASE**

The effect of incubating purified samples of wild type and mutant pyruvate kinase with 2mM NEM, in the presence and absence of various ligands, was examined. The protective effect of the ligands on the two enzymes is shown in Figures 71 and 72 respectively. The time taken for the enzymes to lose 50% of their activity ( $T_{50}$ ) under the various conditions is displayed in Table 14.



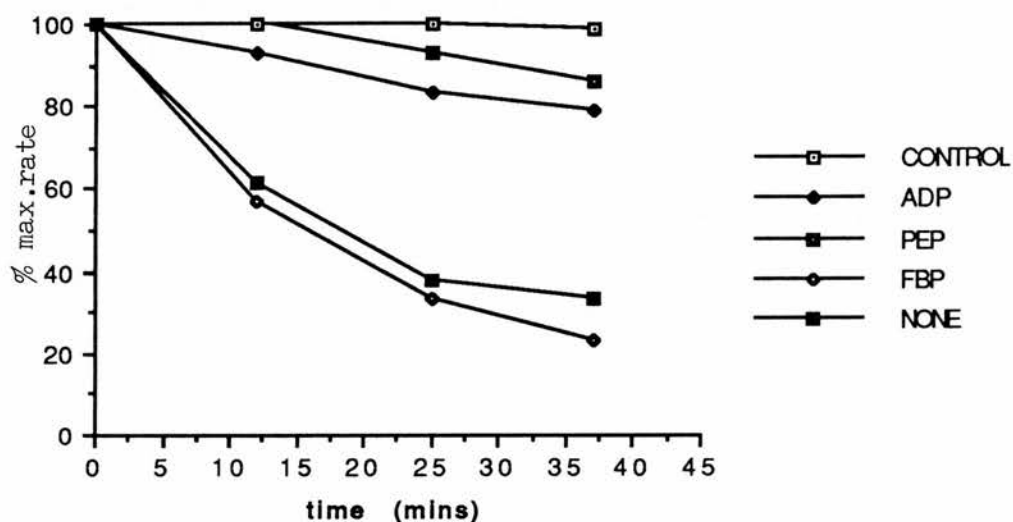


Fig. 69 Effect of ligands on the susceptibility of wild type pyruvate kinase to digestion by trypsin. Pyruvate kinase and trypsin (1:1 w:w) were incubated in standard assay buffer to which had been added the following ligands:

PEP	9.8mM
ADP	8.0mM
FBP	1.1mM

Aliquots (5 $\mu$ l) were removed and incubated in standard assay buffer to which had been added 1mM PMSF.

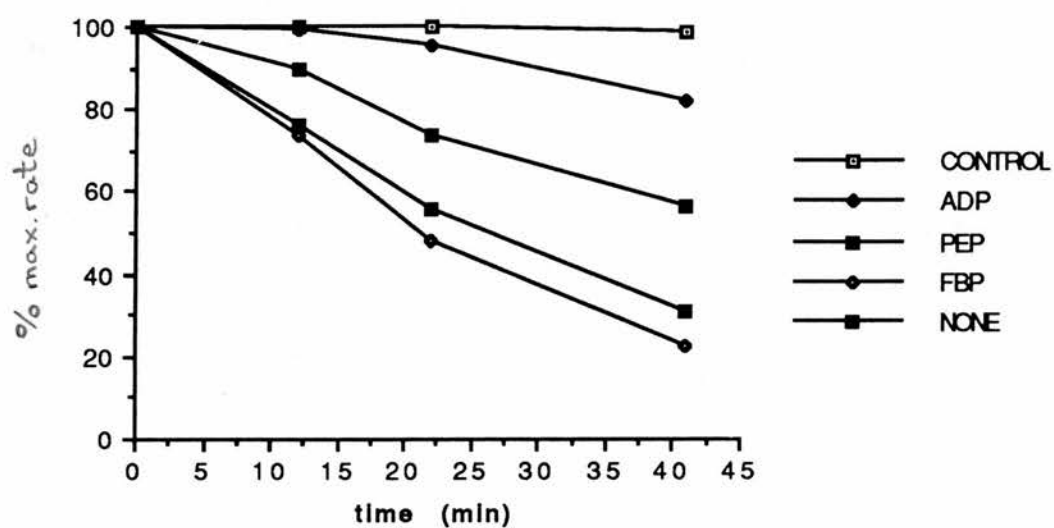


Fig.70 Effect of ligands on the susceptibility of S384P mutant pyruvate kinase to digestion by trypsin. Incubation and reaction conditions were exactly as described in Fig.69

**TABLE 13**  
**THE EFFECT OF LIGANDS ON THE SUSCEPTIBILITY OF WILD TYPE AND**  
**MUTANT PYRUVATE KINASE TO DIGESTION BY TRYPSIN.**

ADDITION	WT		S384P	
	T <sub>50</sub> (min)	FOLD	T <sub>50</sub> (min)	FOLD
NONE	19.4	1.0	23.5	1.0
ADP	99.1	5.1	84.8	3.6
FBP	16.5	0.85	18.3	0.78
PEP	120.8	6.2	47.6	2.0

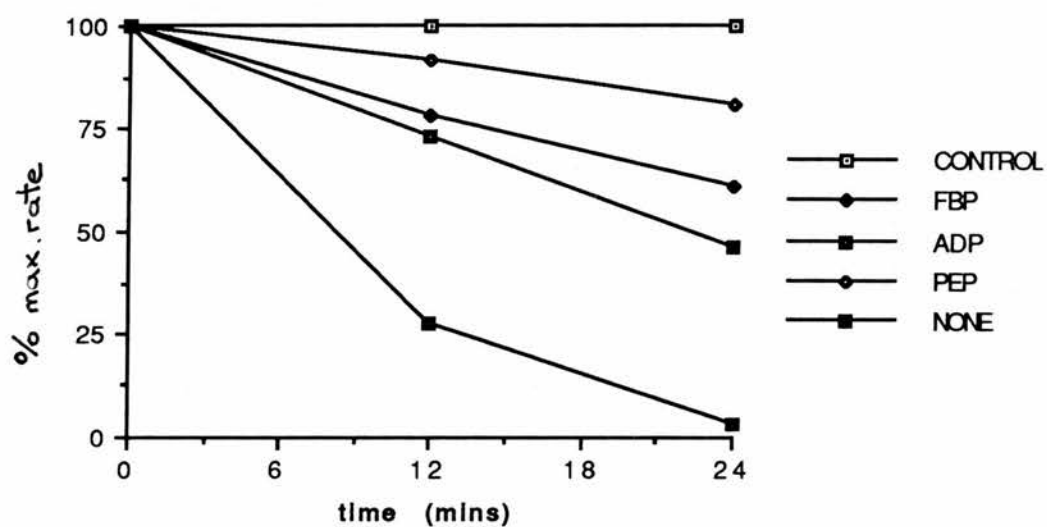


Fig. 71 Effect of ligands on the susceptibility of wild type pyruvate kinase to inhibition by NEM.  
 Enzyme was incubated in the presence of 2mM NEM in standard assay buffer to which had been added the following ligands:

PEP	9.8mM
ADP	8.0mM
FBP	1.1mM

Aliquots (5 $\mu$ l) were removed and incubated in standard assay buffer.

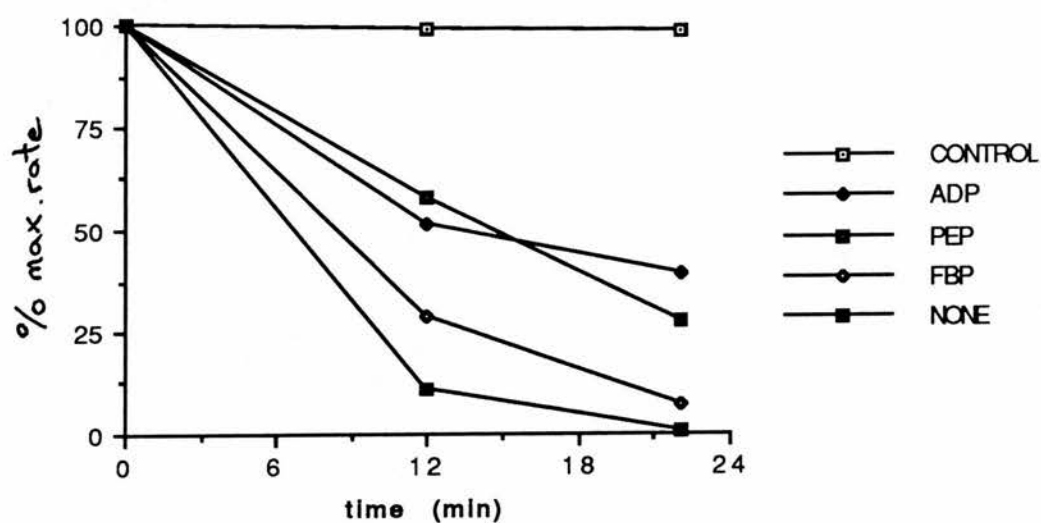


Fig. 72 Effect of ligands on the susceptibility of S384P mutant pyruvate kinase to inhibition by NEM. Incubation and reaction conditions were exactly as described in Fig.71

**TABLE 14:**  
**THE EFFECT OF LIGANDS ON THE SUSCEPTIBILITY OF**  
**WILD TYPE AND MUTANT PYRUVATE KINASE TO**  
**INHIBITION BY NEM.**

ADDITION	WT		S384P	
	T <sub>50</sub> (min)	FOLD	T <sub>50</sub> (min)	FOLD
NONE	8.8	1.0	6.9	1.0
ADP	23.1	2.6	14.8	2.1
FBP	32.3	3.7	8.0	1.2
PEP	60.0	6.8	15.5	2.2

### 3.8 THERMAL STABILITY STUDIES

The resistance of the wild type and mutant enzymes to thermal denaturation are shown in Fig. 73. The enzymes were incubated in assay buffer at the indicated temperature for three minutes. They were then cooled on ice for five minutes before being centrifuged to remove denatured enzyme. Aliquots of the supernatant were then assayed to determine residual activity.

The unfolding of the wild type and mutant enzymes as a function of temperature were studied by incubating the enzymes in assay buffer at various temperatures in a thermostatically controlled spectrophotometer and monitoring the change in absorbance at 280nm (Fig. 74). The influence exerted by the effector Fru-1,6-P<sub>2</sub> on unfolding was also studied. The absorbance of any protein at 280nm is due primarily to the presence of tyrosine and tryptophan residues and any increase in this value would indicate the exposure to the solvent of previously buried residues.

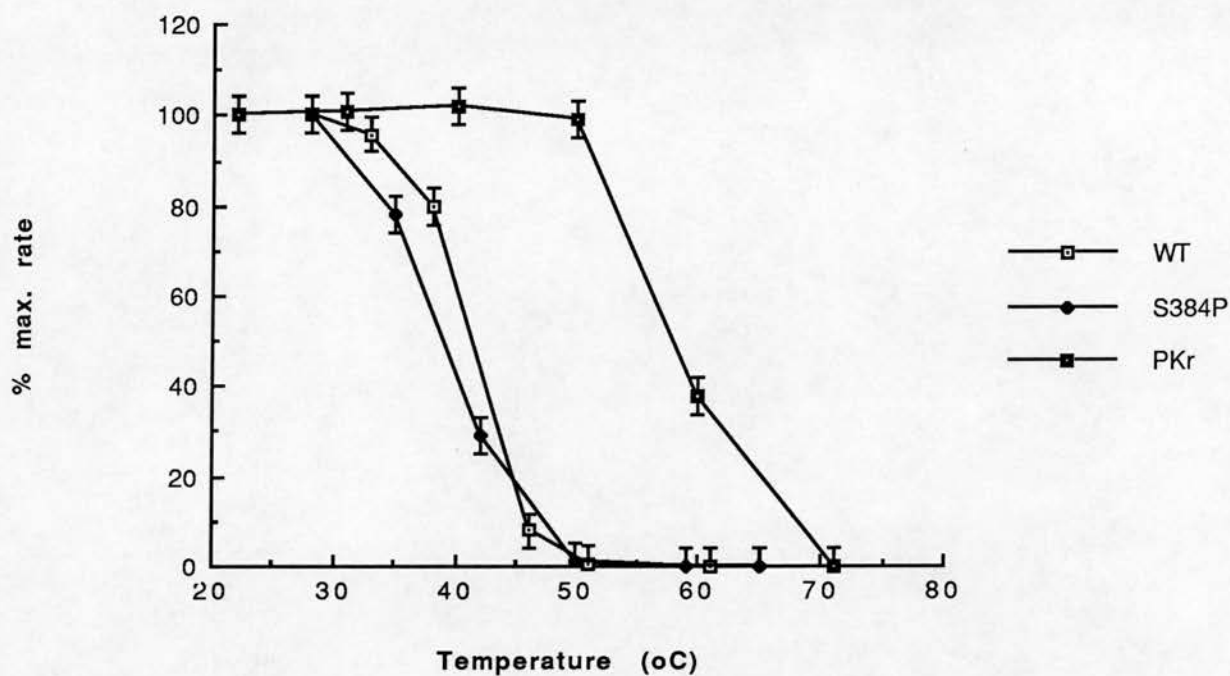


Figure 73: Thermostability of wild-type (WT), mutant (S384P), and rabbit muscle (PKr) pyruvate kinase enzymes.

Aliquots of enzyme were incubated at the indicated temperatures for 3 min, followed by incubation on ice for 5 min. Samples were then centrifuged (13,000 rpm x 5 min) and the supernatants assayed for activity as described in Section 2.3. The enzymes were assayed in the presence of 5mM Fru-1,6-P<sub>2</sub>.

The residual enzyme activities are expressed as % of the rate observed at 25°C.



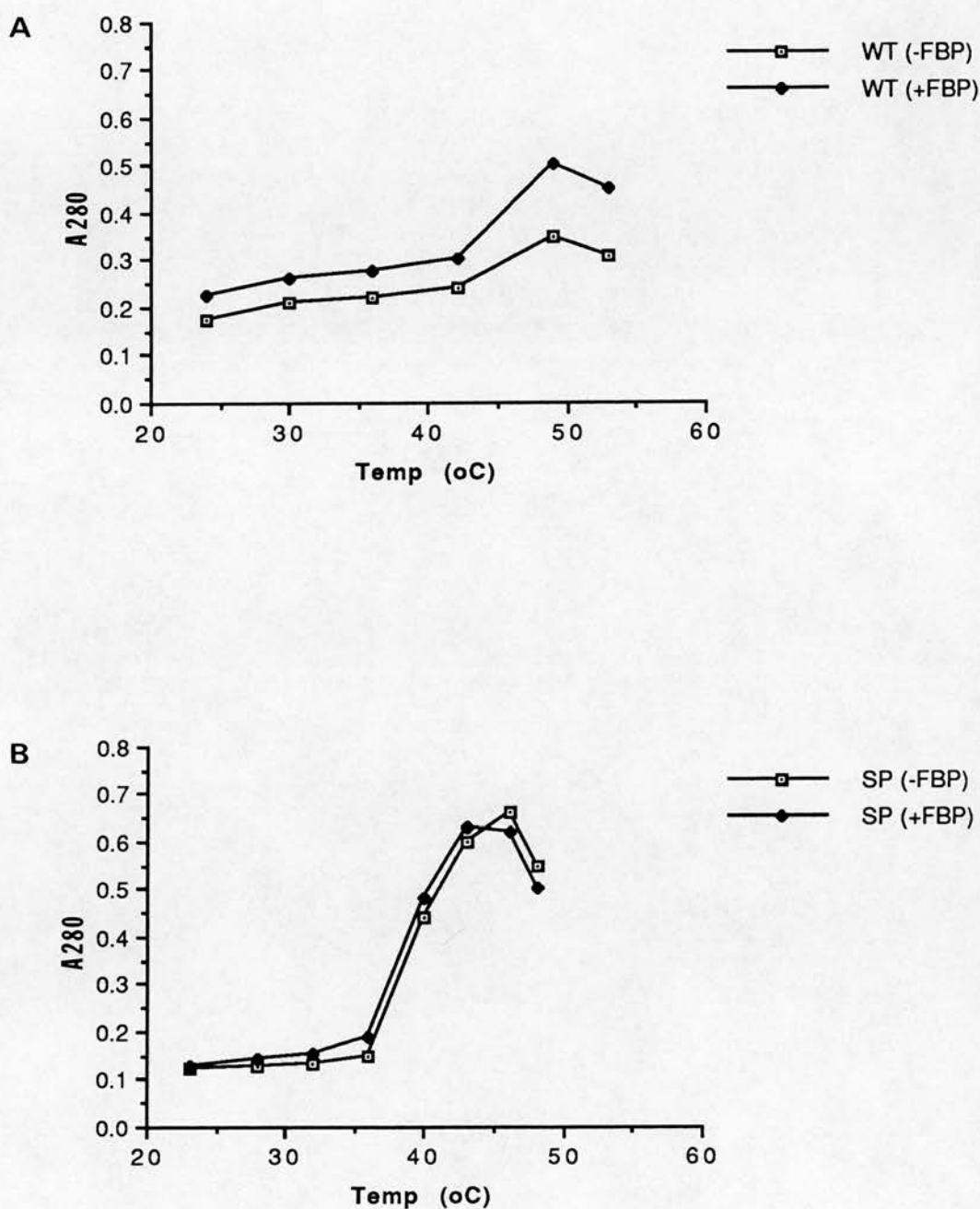


Figure 74: Unfolding of: A) wild type and B) S384P mutant pyruvate kinase. Aliquots of enzymes from ion-exchange step were incubated in a 1ml quartz cuvette placed in a thermostatically controlled heating block inside a uv spectrophotometer. The change in absorbance at 280nm was monitored. The enzyme was incubated in assay buffer in the presence and absence of 1mM Fru-1,6-P<sub>2</sub>.

### 3.9 ANTIBODY STUDIES

The polyclonal antiserum used in the following experiments was raised by immunising two female New Zealand White rabbits with an emulsion of antigen and Freund's Complete Adjuvant. The animals were housed in the Faculty Animal Area (Department of Biochemistry, University of Edinburgh). All the injections and blood sampling were performed by trained staff and not by the author himself. I would like to thank Mr.D.Henderson in particular for his help and advice during this period.

The full protocol for the raising of antiserum is described in Table 15. The antiserum was used in Western blotting experiments to determine the affinity of the preparation, in terms of the optimum dilution of antiserum to use, and the extent of cross-reactivity with other antigens. A typical Western blot is shown in Fig.75. The antiserum was also used in an attempt to precipitate wild type pyruvate kinase from solution. A comparison of the efficacy of the polyclonal antiserum and the pre-immune control serum in causing the precipitation of antigen is shown in Fig.76.

TABLE 15  
IMMUNISATION PROTOCOL

DAY	DETAILS	AMOUNT OF ANTIGEN (mg) PER ANIMAL	VOLUME OF ANTIGEN (ml) PER ANIMAL	FORM OF INJECTION
1	Pre-immunisation trial bleed 5ml per animal	-	-	-
8	1st immunisation	1	0.5	50:50 FCA : Ag emulsion
22	2nd immunisation	0.1	0.2	50:50 FCA : Ag emulsion
77	3rd immunisation	0.1	0.15	50:50 FIA : Ag emulsion
108	Post-immunisation trial bleed 5ml per animal			
FCA	Freund's complete adjuvant			
FIA	Freund's incomplete adjuvant			
Ag	antigen (desalted, post-ion exchange, pyruvate kinase solution)			

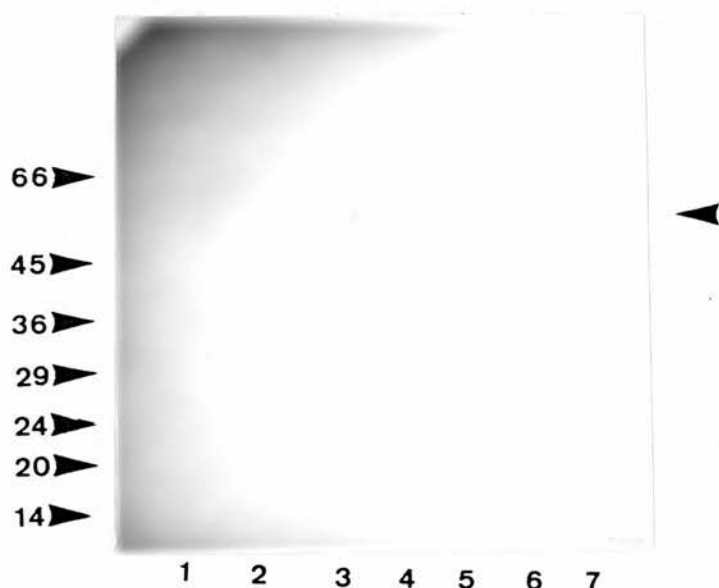


Fig.75 Western blot.  
 Protein samples were separated by electrophoresis on a 10% polyacrylamide gel in the presence of SDS and transferred to a nylon membrane. The membrane was probed with a solution of anti-wild type yeast pyruvate kinase antiserum diluted 1:400 in TBS. Lanes: 1) molecular weight standards, 2) rabbit muscle pyruvate kinase, 3) yeast wild type pyruvate kinase, 4) *T.acidophilum* cell-free extract, 5) *B.subtilis* cell-free extract, 6) *E.coli* cell-free extract, 7) *S.aureus* cell-free extract.  
 Arrows on left indicate position and size (kDa) of molecular weight markers.  
 66 = bovine plasma albumin, 45 = egg ovalbumin, 36 = rabbit muscle glyceraldehyde-3-phosphate dehydrogenase, 29 = bovine carbonic anhydrase, 24 = bovine trypsinogen, 20 = soybean trypsin inhibitor, 14 = bovine lactalbumin.  
 Arrow on right indicates position of yeast pyruvate kinase.

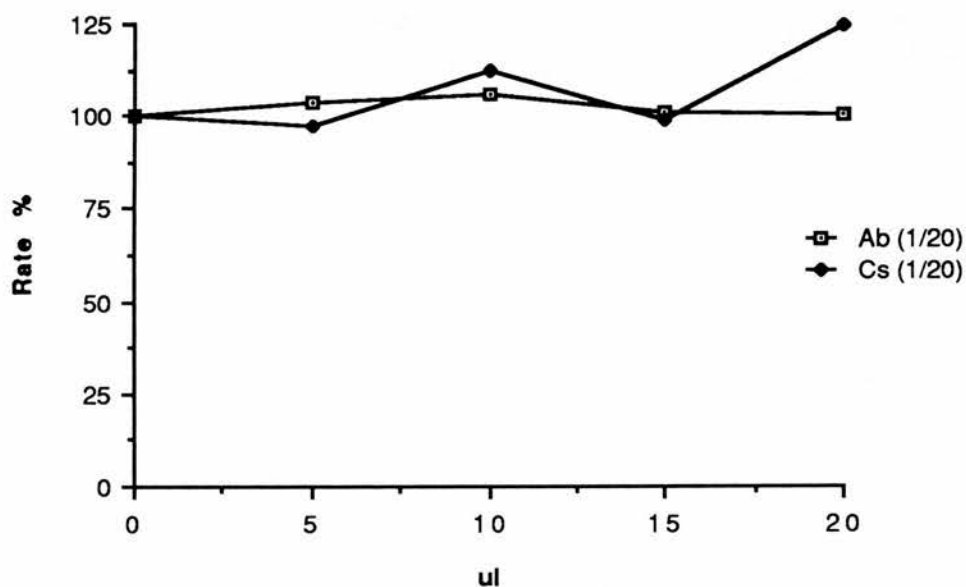


Fig. 76 Immunoprecipitation of wild type yeast pyruvate kinase. Wild type pyruvate kinase solution was incubated with either 1:20 diluted pre-immune serum (Cs) or immune serum (Ab) according to the protocol given in Section 2.8. After precipitation of Ab-Ag complexes, the activity of an aliquot of the supernatant was determined according to the protocol in Section 2.3. Activity of the samples is expressed as a % of the initial rate of a control sample. As can be seen, no precipitation of wild type pyruvate kinase is observed, perhaps due to non-optimal incubation conditions.

### 3.10 COMPUTER PREDICTIONS OF SECONDARY STRUCTURE

Several programs are available for the determination of protein secondary structure. The most accessible are those issued by the University of Wisconsin Genetics Computer Group (UWGCG). Portions of the sequences of the wild type and the mutant enzyme were compared by several well-known secondary structure prediction programs.

Figure 77 shows a plot for a 30 residue stretch of the wild type enzyme. The sequence is centred on serine 384. The upper section shows the sequence with an indication of the nature of the amino acid residue present i.e. whether they are acidic/basic or hydrophobic/hydrophilic. The upper panel shows a Chou and Fasman secondary structure prediction. The middle panel shows a hydrophobic moment plot and the lower panel shows a hydropathy prediction. Figure 78 shows an identical set of panels based on the same stretch of sequence but containing the proline 384 point mutation.

Figure 79 shows the Chou and Fasman secondary structure plot overlaid with the hydropathy profile for a 51 residue portion of the wild type enzyme. The sequence is centred on serine 384. Highly hydrophilic and hydrophobic segments are indicated with different symbols. A distinction can be made between beta coils, beta strands and alpha helical regions. Figure 80 shows an identical plot for the mutant enzyme containing the serine 384 to proline point mutation.

Figure 81 shows a plot from the program PREDICT for a 51 residue stretch of the wild type pyruvate kinase surrounding the mutagenesis target residue, serine 384. This program shows a consensus plot from eight different methods of predicting the secondary structure of a polypeptide. As a result, greater confidence can be placed in the output from these multiple plots than on the output from a single method like PEPLOT or PLOTSTRUCTURE. Figure 82 shows an identical type of plot for the mutant protein, where proline has replaced serine 384.

PEPPLOT of: Pkwt.Txt ck: 4683, 1 to 30 January 25, 1993 17:42  
 pyruvate kinase

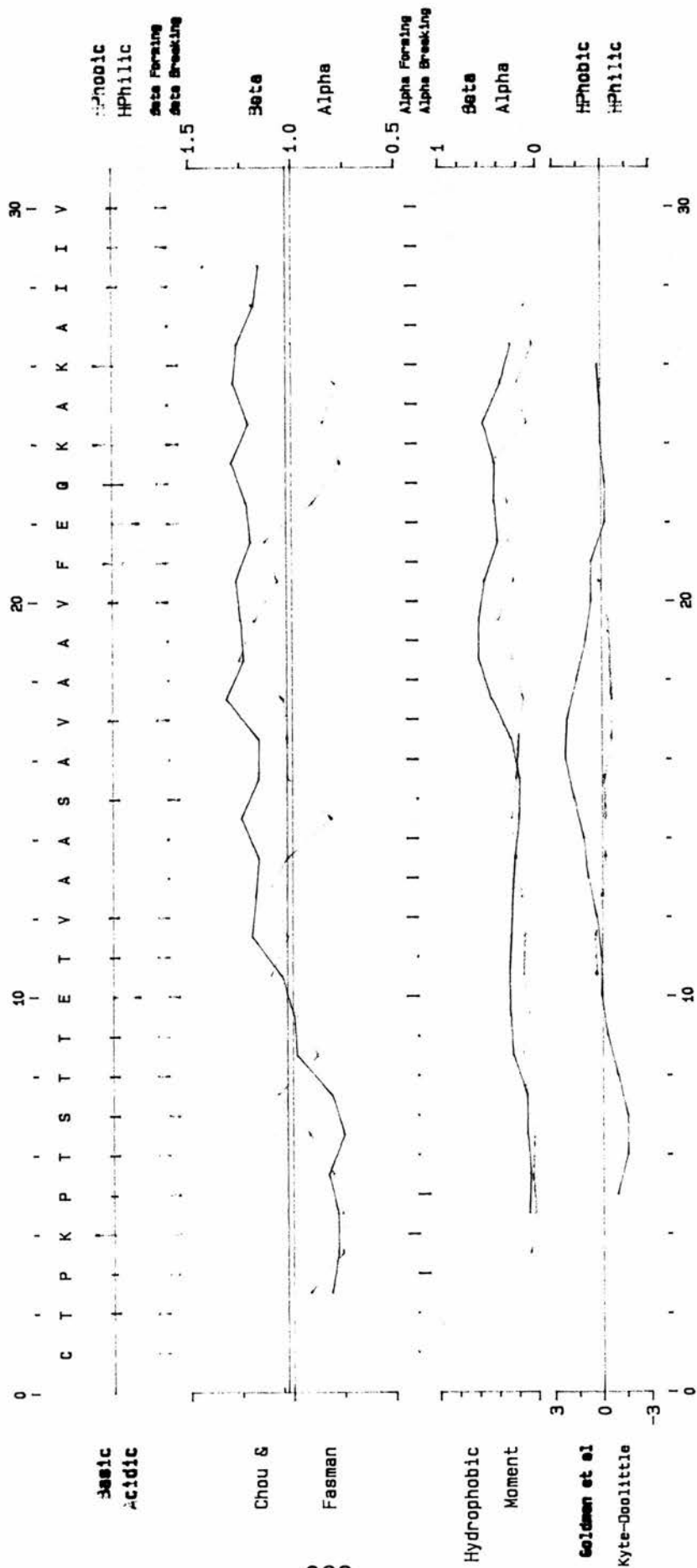


Fig. 77 Output from UWGGC program PEPPLOT for wild type pyruvate kinase.  
 Plot shows sequence, Chou and Fasman secondary structure prediction, hydrophobic moment and hydrophobicity predictions for a 30 residue portion (residues 370-399 inclusive) of the wild type enzyme.

PEPPLOT of: Pks384p.Txt ck: 4638, 1 to 30 January 25, 1993 17:47  
 PYRUVATE KINASE

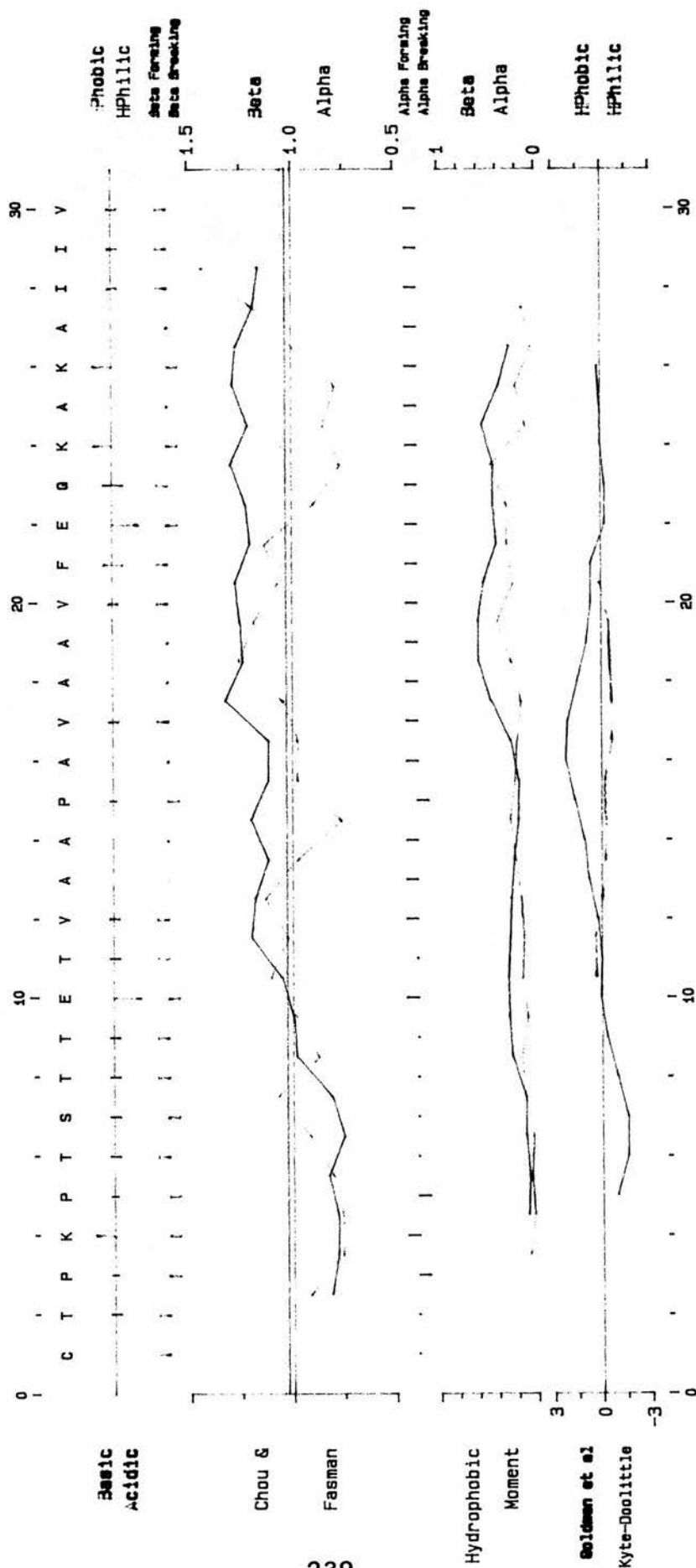


Fig. 78 Output from UWGCG program PEPPLOT for S384P mutant pyruvate kinase.  
 Plot shows identical output to Fig. 77.



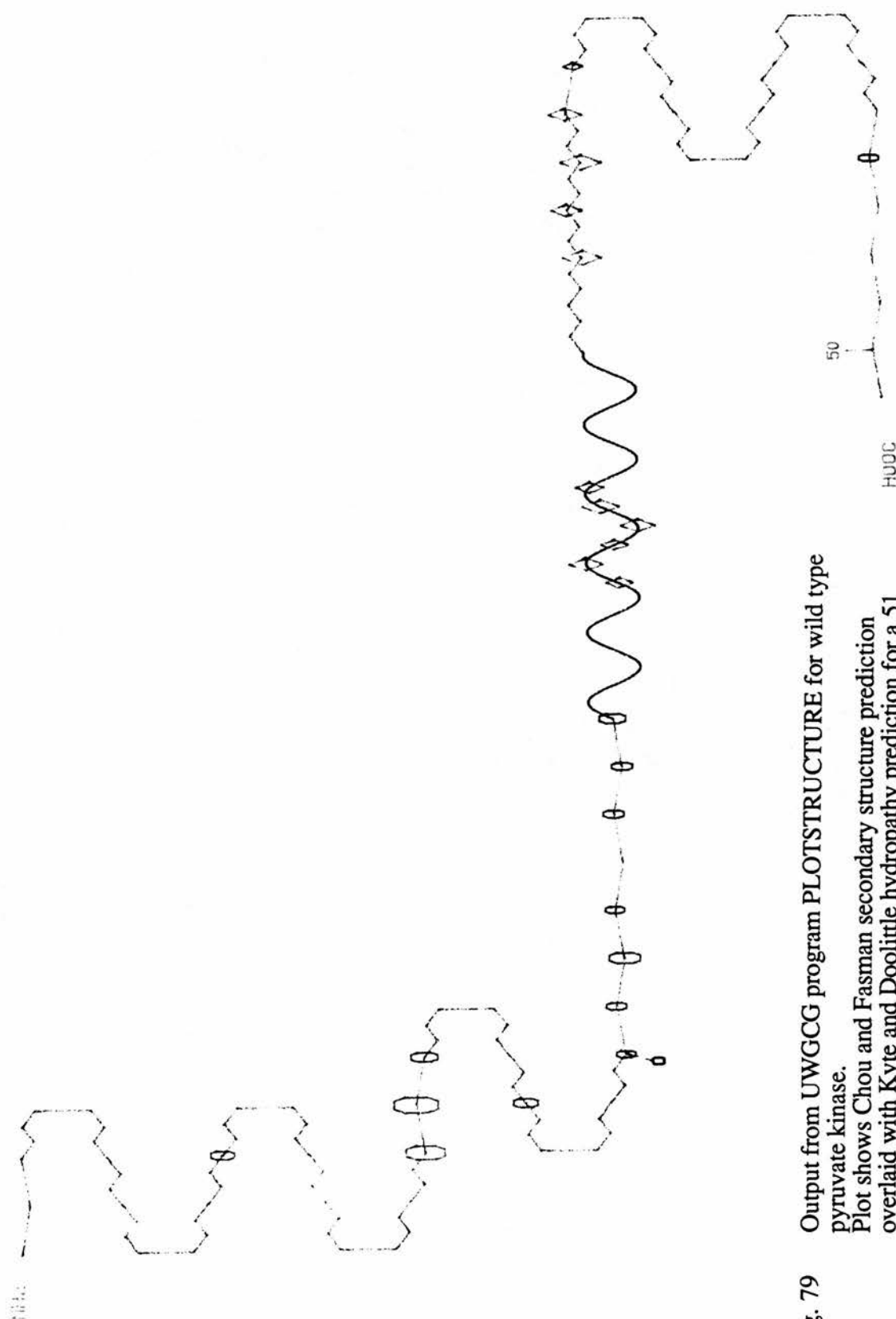


Fig. 79 Output from UWGCG program PLOTSTRUCTURE for wild type pyruvate kinase.  
Plot shows Chou and Fasman secondary structure prediction overlaid with Kyte and Doolittle hydropathy prediction for a 51 residue portion (residues 360-410 inclusive) of the wild type enzyme.

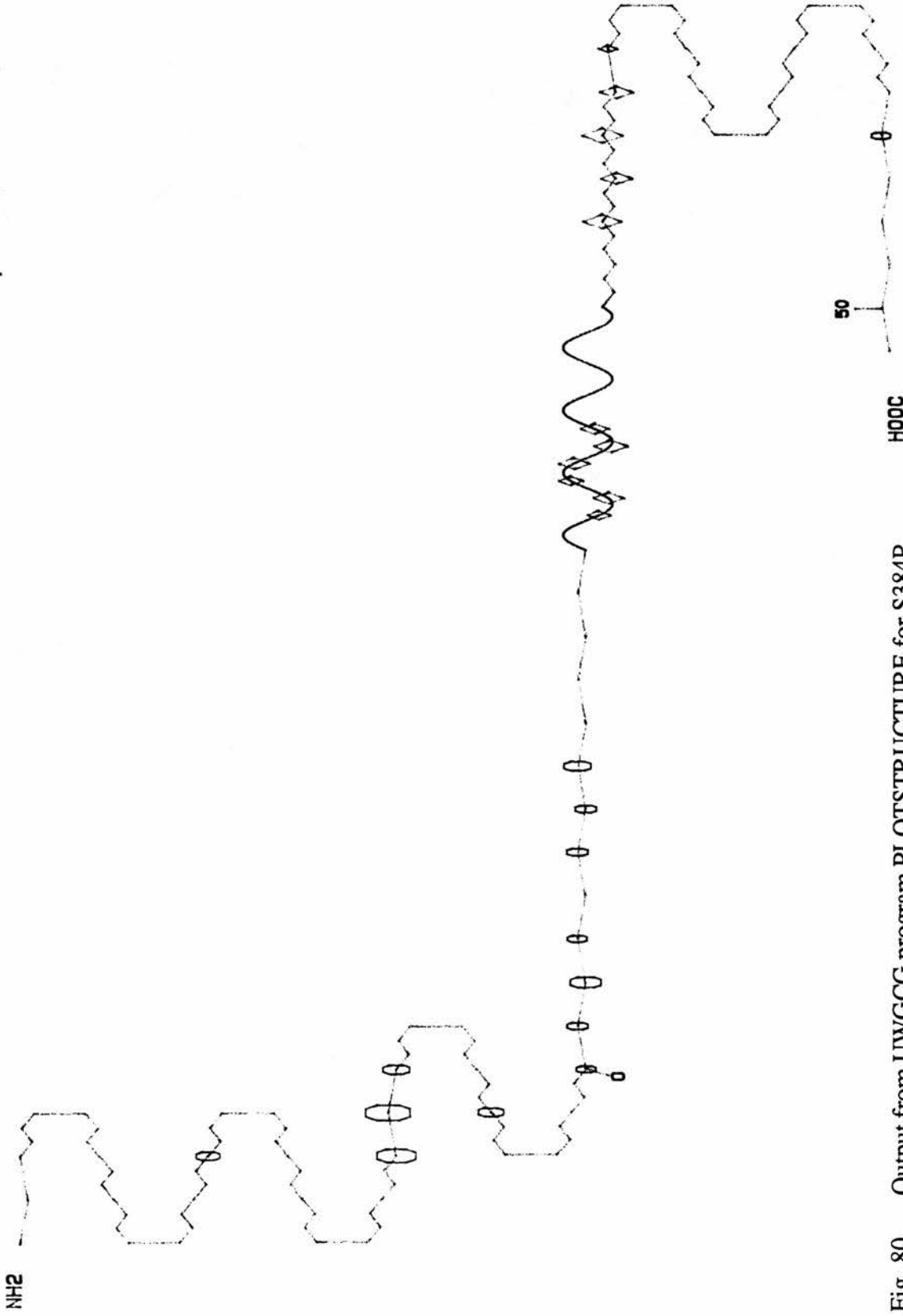


Fig. 80 Output from UWGCG program PLOTSTRUCTURE for S384P mutant pyruvate kinase.  
Plot shows identical output to Fig. 79.

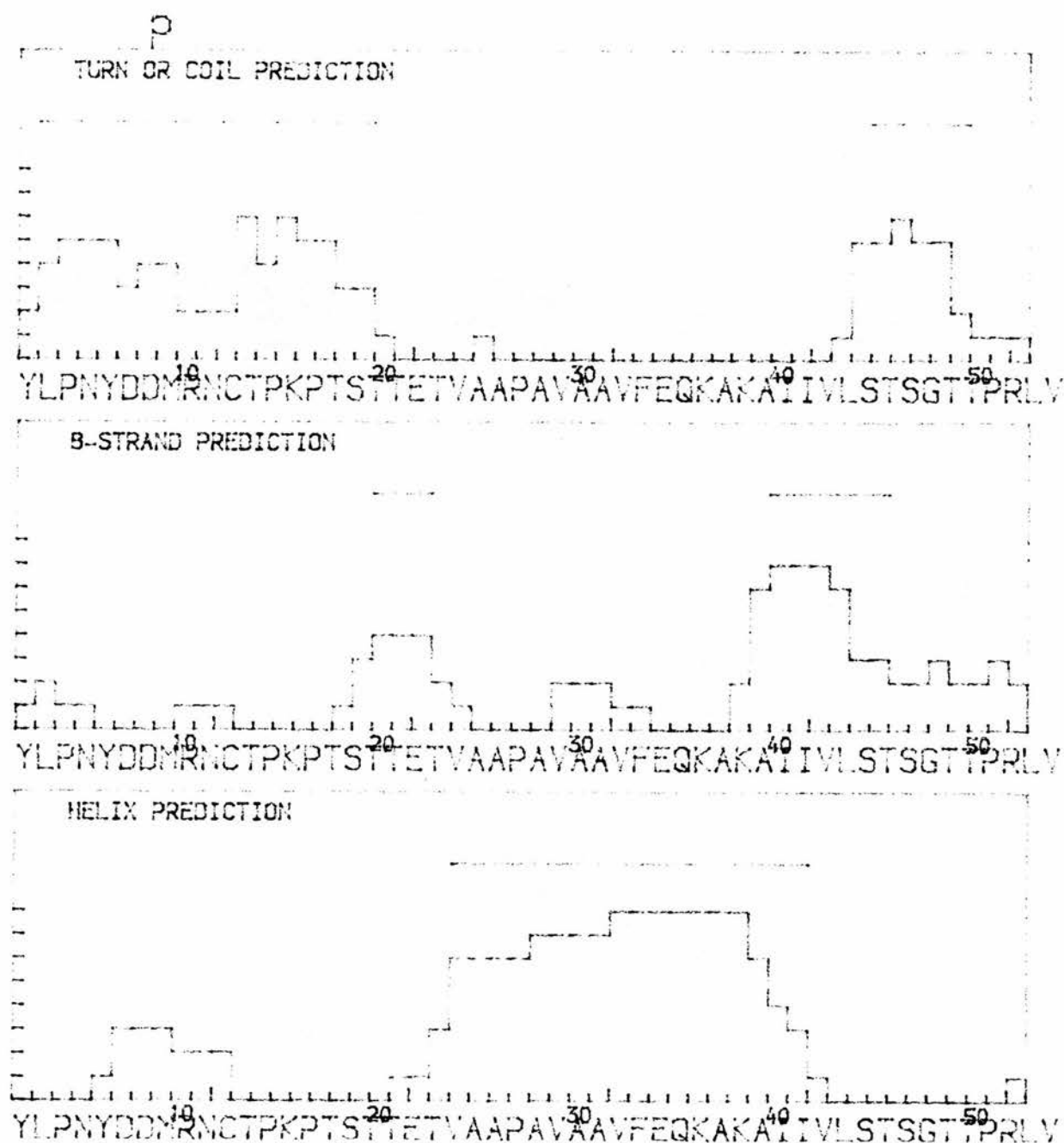


Fig. 81 Output from program PREDICT for wild type pyruvate kinase.  
A 51 residue portion of the wild type sequence surrounding serine  
384 was analysed.

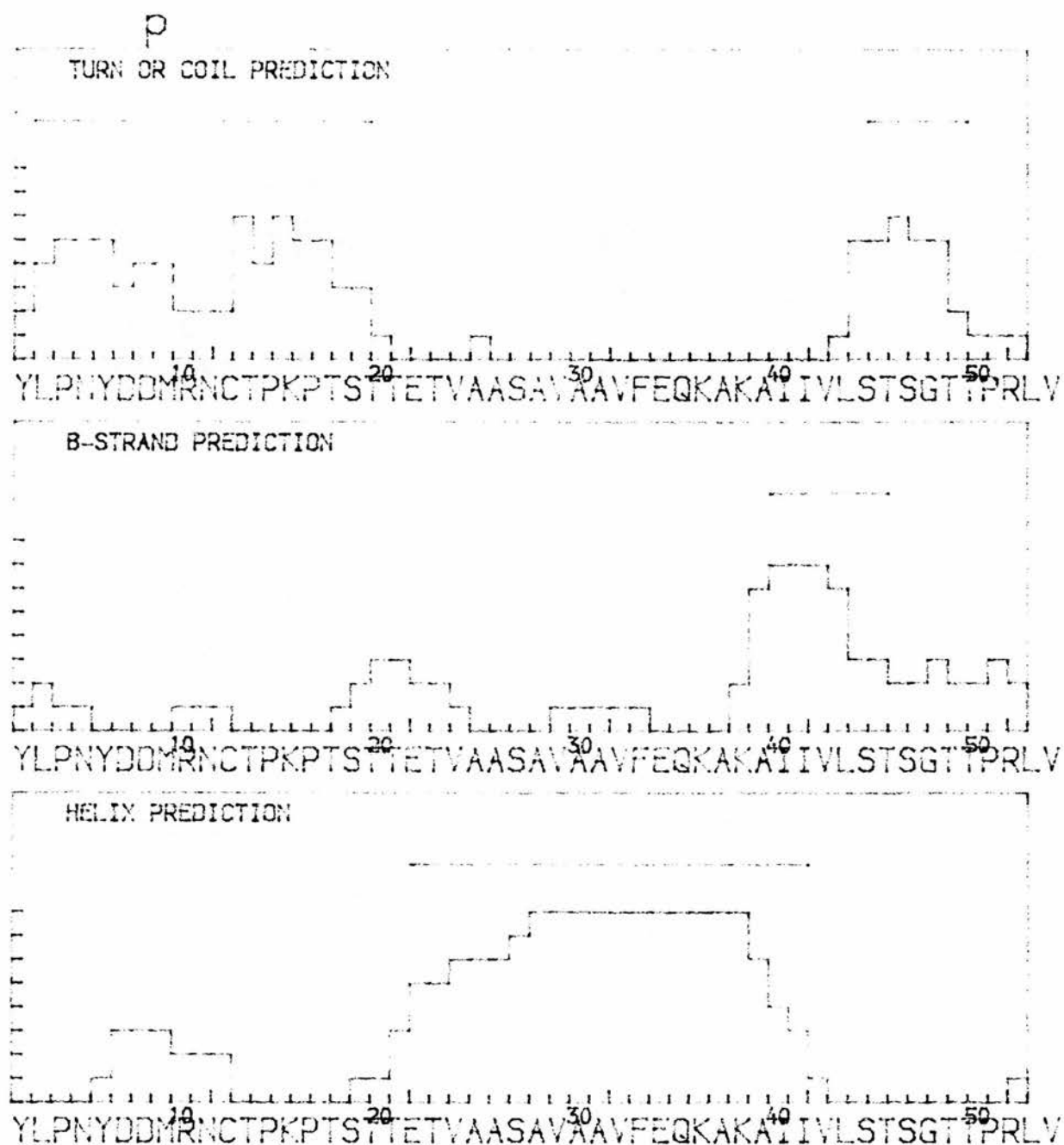


Fig. 82 Output from program PREDICT for S384P mutant pyruvate kinase. A portion of the polypeptide sequence identical in length and position to the wild type sequence was analysed.

### **3.11 ALIGNMENT AND PHYLOGENETIC ANALYSIS OF PYRUVATE KINASE SEQUENCES**

The primary amino acid sequences listed in Table 1 were compared using the program SeqAli. The percentage identities between sequences are shown in Table 16.

A phylogenetic tree based on a calculated distance matrix was constructed using the program FITCH (Fig. 83). A consensus phylogenetic tree was constructed after bootstrap analysis using the program SEQBOUT (Fig. 84).

All computer analyses were performed by I.Ernest at the International Institute of Cellular and Molecular Pathology, Research Unit for Tropical Diseases, Brussels, Belgium.

TABLE I 6

PERCENTAGE OF IDENTITY BETWEEN SEQUENCES:

	casta	castb	tobaa	brasg	tobag	colil	bacst	lacto	bras1	bras2	soltu	tobac	emeni	trire	yeast	yarli	trybb
casta	100.0																
castb	94.1	100.0															
tobaa	79.9	84.8	100.0														
brasg	39.6	43.1	39.7	100.0													
tobag	40.4	42.4	38.8	67.6	100.0												
colil	33.6	31.6	32.9	39.5	39.4	100.0											
bacst	36.2	34.3	35.3	37.7	41.2	51.5	100.0										
lacto	29.2	28.1	28.5	32.5	33.5	41.5	46.3	100.0									
bras1	31.9	30.8	31.1	34.5	36.3	44.7	44.7	38.6	100.0								
bras2	30.9	29.7	29.4	33.9	36.8	45.8	44.7	37.1	89.2	100.0							
soltu	31.4	30.1	30.0	34.5	36.5	47.5	44.9	37.6	85.3	83.3	100.0						
tobac	31.8	30.8	30.5	34.3	36.1	46.3	45.7	36.3	75.1	74.4	75.3	100.0					
emeni	32.2	30.5	31.6	34.6	34.5	45.0	45.0	37.1	43.5	44.1	43.6	44.5	100.0				
trire	31.2	29.9	31.0	33.7	33.8	44.3	40.5	36.7	43.1	43.1	42.8	42.2	68.8	100.0			
yeast	31.8	30.1	30.9	34.0	32.9	43.1	41.5	36.9	41.2	41.6	40.3	40.7	66.8	63.4	100.0		
yarli	31.4	31.3	30.1	33.5	35.0	44.2	41.3	37.2	43.3	43.8	43.2	42.5	65.2	60.9	67.6	100.0	
trybb	32.7	31.3	31.2	34.4	35.3	44.5	41.0	36.7	42.7	41.5	42.1	43.3	47.0	46.8	47.3	48.5	100.0
tryb2	32.9	31.5	31.4	34.2	34.9	44.5	41.2	36.5	42.3	41.5	42.1	43.3	47.4	47.0	47.8	49.0	99.0
leish	31.2	29.6	30.8	33.8	33.6	43.8	42.1	36.9	43.5	41.7	42.5	42.5	47.8	48.2	48.0	48.8	73.7
ratli	30.9	31.6	30.9	31.7	31.6	45.0	46.1	36.3	44.1	42.9	43.0	42.9	50.7	47.9	49.8	50.7	47.2
ratre	29.7	31.6	29.6	30.0	30.7	44.7	45.8	36.1	43.9	42.7	42.8	42.7	50.5	47.9	49.6	50.5	47.0
humli	31.5	32.0	31.3	32.3	32.6	46.3	47.1	36.5	45.1	43.7	44.4	43.6	51.3	47.9	50.0	51.1	49.0
humre	30.0	32.0	30.3	30.8	31.7	46.3	47.1	36.5	45.1	43.7	44.2	43.6	51.3	47.9	50.0	51.1	48.8
humml	31.9	31.8	31.2	34.3	35.7	48.2	47.3	37.1	45.9	45.1	45.2	46.8	53.8	49.4	51.0	50.9	50.6
humm2	31.9	31.8	31.2	34.1	35.5	48.5	47.3	37.3	46.1	45.3	45.2	47.0	54.0	49.4	51.2	50.9	50.8
catml	32.3	32.2	31.7	34.3	35.3	48.5	47.5	36.7	44.9	44.9	44.2	45.6	52.6	48.7	49.0	49.9	50.2
ratml	32.3	32.4	31.7	34.1	34.9	48.7	47.3	36.7	45.7	45.3	44.8	46.4	53.2	49.4	49.8	50.5	50.6
ratm2	31.0	31.0	30.0	33.1	33.7	45.8	45.8	35.0	44.1	43.7	43.6	45.6	51.1	47.9	48.2	48.3	49.2
chick	32.4	32.6	32.0	34.1	34.9	48.0	48.0	36.5	44.3	43.1	43.8	44.4	52.0	49.0	49.2	51.1	50.8
coli2	34.6	33.0	33.0	33.8	36.1	36.3	40.0	33.0	36.2	36.2	35.7	37.3	38.4	37.3	37.7	36.8	36.4

TABLE 16 continued

	tryb2	leish	ratli	ratre	humli	humre	humml	humml2	catml	ratml	ratml2	chick	coli2
casta	32.9	31.2	30.9	29.7	31.5	30.0	31.9	31.9	32.3	32.3	31.0	32.4	34.6
castb	31.5	29.6	31.6	31.6	32.0	32.0	31.8	31.8	32.2	32.4	31.0	32.6	33.0
tobaa	31.4	30.8	30.9	29.6	31.3	30.3	31.2	31.2	31.7	31.7	30.0	32.0	33.0
brasg	34.2	33.8	31.7	30.0	32.3	30.8	34.3	34.1	34.3	34.1	33.1	34.1	33.8
tobag	34.9	33.6	31.6	30.7	32.6	31.7	35.7	35.5	35.3	34.9	33.7	34.9	36.1
colil	44.5	43.8	45.0	44.7	46.3	46.3	48.2	48.5	48.5	48.7	45.8	48.0	36.3
bacst	41.2	42.1	46.1	45.8	47.1	47.1	47.3	47.3	47.5	47.3	45.8	48.0	40.0
lacto	36.5	36.9	36.3	36.1	36.5	36.5	37.1	37.3	36.7	36.7	35.0	36.5	33.0
bras1	42.3	43.5	44.1	43.9	45.1	45.1	45.9	46.1	44.9	45.7	44.1	44.3	36.2
bras2	41.5	41.7	42.9	42.7	43.7	43.7	45.1	45.3	44.9	45.3	43.7	43.1	36.2
soltu	42.1	42.5	43.0	42.8	44.4	44.2	45.2	45.2	44.2	44.8	43.6	43.8	35.7
tobac	43.3	42.5	42.9	42.7	43.6	43.6	46.8	47.0	45.6	46.4	45.6	44.4	37.3
emeni	47.4	47.8	50.7	50.5	51.3	51.3	53.8	54.0	52.6	53.2	51.1	52.0	38.4
trire	47.0	48.2	47.9	47.9	47.9	47.9	49.4	49.4	48.7	49.4	47.9	49.0	37.3
yeast	47.8	48.0	49.8	49.6	50.0	50.0	51.0	51.2	49.0	49.8	48.2	49.2	37.7
yarli	49.0	48.8	50.7	50.5	51.1	51.1	50.9	50.9	49.9	50.5	48.3	51.1	36.8
trybb	99.0	73.7	47.2	47.0	49.0	48.8	50.6	50.8	50.2	50.6	49.2	50.8	36.4
tryb2	100.0	73.5	47.4	47.2	49.4	49.2	51.0	51.2	50.6	51.0	49.6	51.2	36.4
leish	73.5	100.0	46.6	46.4	48.2	48.0	49.6	49.8	49.2	49.6	48.0	49.2	36.6
ratli	47.4	46.6	100.0	99.4	92.4	92.3	69.6	69.6	67.4	68.1	64.5	68.6	35.6
ratre	47.2	46.4	99.4	100.0	91.9	90.6	69.4	69.4	67.2	67.9	64.3	68.4	35.4
humli	49.4	48.2	92.4	91.9	100.0	99.4	70.8	70.8	68.7	69.4	66.0	69.6	36.7
humre	49.2	48.0	92.3	90.6	99.4	100.0	70.8	70.8	68.7	69.4	66.0	69.8	36.5
humml	51.0	49.6	69.6	69.4	70.8	70.8	100.0	99.6	93.2	93.6	91.1	86.0	37.8
humml2	51.2	49.8	69.6	69.4	70.8	70.8	99.6	100.0	93.2	93.6	91.1	86.0	37.8
catml	50.6	49.2	67.4	67.2	68.7	68.7	93.2	93.2	100.0	95.3	89.1	87.9	37.8
ratml	51.0	49.6	68.1	67.9	69.4	69.4	93.6	93.6	100.0	100.0	92.8	87.5	38.0
ratml2	49.6	48.0	64.5	64.3	66.0	66.0	91.1	91.1	89.1	92.8	100.0	83.2	35.2
chick	51.2	49.2	68.6	68.4	69.6	69.8	86.0	86.0	87.9	87.5	83.2	100.0	38.8
coli2	36.4	36.6	35.6	35.4	36.7	36.5	37.8	37.8	37.8	38.0	35.2	38.8	100.0





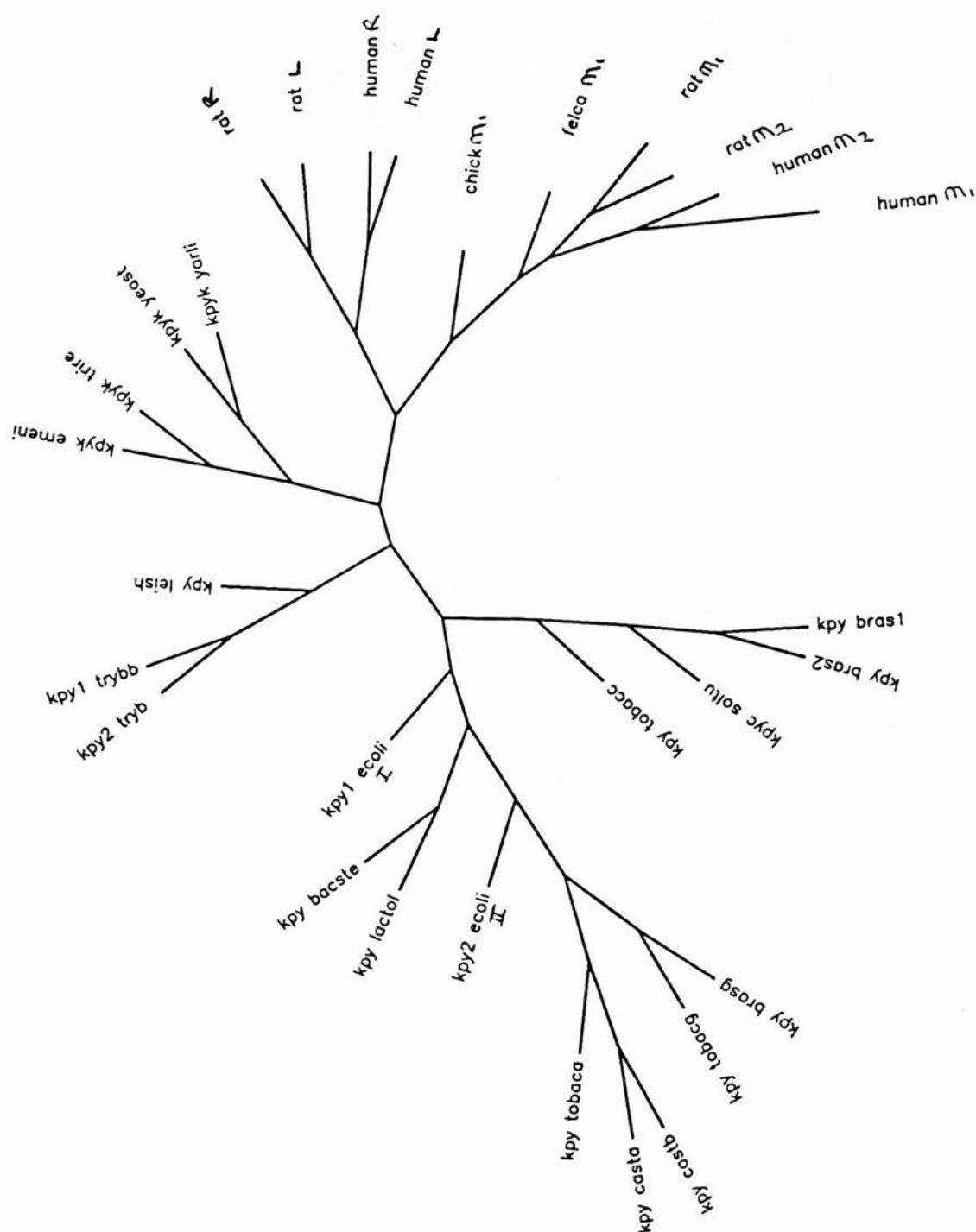


Fig. 84 Consensus phylogenetic tree for pyruvate kinase.  
The tree was constructed after 100 bootstrap analyses  
according to the method described in Materials and Methods.

## **4.0 DISCUSSION**

- 4.1 Purification of pyruvate kinase.
- 4.2 Enzyme assay conditions.
- 4.3 Morphological and biochemical studies of the parent and transformed cells.
- 4.4 Peptide sequencing.
- 4.5 DNA sequencing.
- 4.6 Purification and kinetic characterisation of wild type and mutant forms of pyruvate kinase.
- 4.7 Fluorescence and circular dichroism studies.
- 4.8 Trypsin digestion of wild type and mutant enzymes.
- 4.9 The effect of NEM on pyruvate kinase activity.
- 4.10 Thermal stability studies.
- 4.11 Antibody studies.
- 4.12 Computer predictions of secondary structure.
- 4.13 Sequence comparison of pyruvate kinases.
- 4.14 Alignment and phylogenetic analysis of pyruvate kinase sequences.

## 4.0 DISCUSSION

### 4.1 PURIFICATION OF PYRUVATE KINASE

A large number of methods for the purification of pyruvate kinase, from a number of species and tissues, to apparent homogeneity can be obtained from a search of the literature.

Advances in our knowledge of yeast biochemistry and physiology and the introduction of new techniques in molecular biology have identified several areas leading directly to improved yields of enzymes during purification. For example, several endogenous yeast proteases have been characterised (Jones, 1991) and specific inhibitors of them have been identified (Barrett et al., 1982; Harper et al., 1985). Genetic engineering allows the overexpression of large quantities of enzymes (or any other proteins) allowing smaller quantities of starting material to be used with subsequent savings in time and reagents. Prior to genetic engineering in yeast, the earlier methods of pyruvate kinase purification were noted for their requirement for large quantities of yeast cells (up to 4.5kg, Hunsley & Suelter, 1969) and the length of time necessary to obtain an homogeneous enzyme preparation (up to 10 days). Often the enzyme had degraded significantly or had reduced specific activities in these preparations. Consequently, the determination of the characteristics of the enzyme were strongly dependent upon the nature of the method used to isolate the protein. As a result properties such as subunit molecular mass, native molecular mass and  $K_M$  values for the various substrates were often subject to large errors and irreproducibility.

This project describes an improved purification of pyruvate kinase from yeast in terms of speed, convenience, reproducibility, yield and specific activity. The overexpression, purification and characterisation of a site-directed mutant form of the enzyme and its comparison with a wild-type counterpart isolated by the same methods are described. The results in Section 3.4, culminating in the purification tables (Tables 8 and 9), demonstrate the convenience and high yield of the new method. From cell lysis to use of the fractions obtained from the ion-exchange step took approximately 36 hours and was readily reproducible

over the course of the project.

#### **4.1.1 ISOLATION OF CELLS AND CELL LYSIS**

The first stage in all preparations is the isolation of tissue from the host organism and its lysis or rupturing to produce a cell-free homogenate. For yeast, this first step is simple. Centrifugation of large volumes (1L) of growth media at low speeds (5000rpm x 5min) results in the pelleting of sufficient cells for most studies. However, the choice of method of cell lysis is much more varied. A number of different methods have been described. A popular method in early studies was autolysis or plasmolysis of the cells by incubation in toluene at temperatures ranging from -20°C to 45°C for periods up to six hours (Roschlau & Hess, 1972; Fell et al., 1974). This process resulted in the solubilisation of the cell wall and the release of the intracellular contents. The effects of this treatment on the enzyme being purified were not specifically mentioned. Other methods of yeast cell lysis included high pressure homogenisation (Aust et al., 1975), sonication (Hirai et al., 1975), incubation with ammonium hydroxide (De La Morena et al., 1968) and homogenisation by a suspension of glass beads (Murcott et al., 1991). Intracellular components have also been extracted directly from dried cells with a 25% (v/v) glycerol solution (Hess et al., 1966). Often the simplest and most direct methods are the most successful and glass bead lysis was the method of choice during this work.

#### **4.1.2 AMMONIUM SULPHATE PRECIPITATION**

In *S.cerevisiae* the main substances that contaminate the soluble proteins are cell debris and other solid material (45% dry weight of cells), lipid (10%), RNA (5%) and DNA (0.4%). A variety of methods are available for the removal of such contamination prior to the selective purification of the desired protein. Protamine sulphate or polyethyleneimine have been used to complex nucleic acid allowing their removal by filtration or precipitation. Clarification of cell lysate solutions with sodium tetraborate (borax) has also been used, although this is largely done on preparations of an industrial scale (Milburn et al., 1990).

Centrifugation in the presence of relatively low concentrations of ammonium sulphate (25-40% saturated w/v) is generally considered adequate to remove the majority of the insoluble protein and cell debris. Ammonium sulphate also serves to stabilize enzymes and to prevent proteolysis and bacterial action (Scopes, 1987).

As can be seen from lanes 1 and 2 in Figure 46, the supernatant from a 40% saturated (w/v) ammonium sulphate precipitation (40S) does not have a significantly different profile from that of the cell-free extract (CE). This suggests that very few soluble proteins have been removed by this procedure. However, a large pellet was precipitated by this treatment (40P) and this is suggestive of the fact that insoluble matter, including cell wall fragments and intracellular organelles, have been removed. The 40P profile (lane3, Figure 46) shows a high background staining but few specific bands and, most importantly, very little protein in the region corresponding to the position of pyruvate kinase. This suggests that this precipitation step results in a general removal of protein but which includes very little pyruvate kinase itself.

The further addition of ammonium sulphate to the 40S fraction to bring it to 70% (w/v) saturation results in the efficient removal of the majority of pyruvate kinase. A comparison of lanes 4 and 5 in Figure 46 demonstrates that the majority of the protein that migrates close to authentic rabbit muscle pyruvate kinase is removed by this precipitation step. A large proportion of the other proteins remain in the supernatant (70S). In preliminary experiments it was found that significant pyruvate kinase activity remained in the supernatant from a 60% saturated (w/v) ammonium sulphate precipitation.

#### **4.1.3 GEL FILTRATION CHROMATOGRAPHY**

The problem facing the experimenter at this stage is the quite high proportion of remaining protein contaminants in the pellet from the second ammonium sulphate precipitation (70P) and the residual salt concentration. Both aspects can be addressed simultaneously by the use of gel filtration chromatography. By judicious use of matrix a group separation of salt from

protein can be effected combined with a significant resolution of individual proteins.

The majority of the denatured contaminants in the 70P fraction (Figure 46, lane 5) have a molecular mass less than that of the individual pyruvate kinase subunits. Thus, even in an oligomeric state, a large proportion of the native protein contaminants will be smaller in size than pyruvate kinase. As a result, addition of the 70P fraction to a chromatography column containing a gel filtration matrix whose exclusion size is in the region of the native molecular size of pyruvate kinase will result in the enzyme eluting at, or near, the void volume for this type of column. Contaminating proteins will be retarded sufficiently to allow separation. Lane 6 in Figure 46 shows that most of the contaminating proteins both larger and smaller than the pyruvate kinase subunit have been removed. A few contaminating bands are seen and these may be due to degradation products of the enzyme or, more likely, to subunits of oligomeric proteins of a size similar to, or larger than pyruvate kinase, which would elute with the enzyme in the void volume of the column.

The matrix used in this study for the gel filtration step was Sephacryl S200HR (High Resolution) (Pharmacia). Sephacryl is a cross-linked copolymer of dextran and bisacrylamide. The fine particles of the HR grade (25-75mm) pack better than coarse particles, giving less zone broadening and therefore better resolution. The resolution of two separated zones in gel filtration increases as the square root of column length. Long columns should, therefore, be used to obtain the best resolution. In general the length of column is decided by the resolution required and the diameter by the sample capacity. Where maximum resolution is required the starting zone must be narrow relative to the length of the column. A sample volume of 0.5-5% of the bed volume is recommended.

For the gel filtration step in this study, a 90cm x 1.6cm (id) column of matrix was used, corresponding to a bed volume of  $180\text{cm}^3$ . The redissolved pellet from the second ammonium sulphate precipitation step was usually of the order of  $6-10\text{cm}^3$  corresponding to 3-6% of the bed volume.

Maximum resolution in gel filtration is obtained with long columns and



low flow rates. A flow rate of  $5\text{-}25\text{ ml.cm}^2.\text{hr}^{-1}$  is suggested for such columns.

In this study a flow rate of  $10\text{ ml.cm}^2.\text{hr}^{-1}$  was used.

#### 4.1.4 ION-EXCHANGE CHROMATOGRAPHY

The isoelectric point (pI) of yeast pyruvate kinase has been determined as 6.6 (Hunsley & Suelter, 1969). This property, as well as the large size of the enzyme, can be exploited to further purify the enzyme by ion-exchange chromatography.

At pH values above the pI proteins will have a net negative charge due to ionisation of acidic side groups. An anion-exchange matrix equilibrated to a pH well above the pI for pyruvate kinase is unusual in that it does not significantly bind the enzyme but will bind many contaminating proteins that are negatively charged at this pH. Preliminary experiments showed that at pH 8.5, very little pyruvate kinase binds to the matrix (DEAE-cellulose), whereas a high proportion of the remaining contaminants are removed. At pH values above 8.5, pyruvate kinase binding to the column was unacceptably high and below pH 8.5 the contaminating proteins did not bind efficiently.

The size of the native pyruvate kinase enzyme also facilitates its purification from the anion-exchange matrix chosen as it elutes close to the void volume of the column whilst other proteins are hindered to some degree.

Ion-exchange chromatography is usually performed on short broad columns. The sample volume should be limited to 1-5% of the bed volume if the required protein is to be eluted with the starting buffer. However, if contaminants are to be adsorbed and the sample of interest allowed to pass straight through, the sample size is less important than the amount of contaminant which is present. As with gel filtration chromatography, maximum resolution is obtained at rather low flow rates. Flow rates of  $10\text{ ml.cm}^2.\text{hr}^{-1}$  are usually suitable for the resolution of protein mixtures.

In this study a  $10\text{cm} \times 2.7\text{cm}$  (id) column of matrix (DEAE-cellulose) was prepared, corresponding to a bed volume of  $60\text{cm}^3$ . The sample volume

was in the range  $3\text{-}6\text{cm}^3$ , corresponding to 5-10% of the bed volume. The sample was eluted by buffer flowing under gravity, corresponding to a flow rate of  $5\text{ ml.cm}^2.\text{hr}^{-1}$ .

The unusual binding properties of pyruvate kinase to ion-exchange columns is not an isolated phenomenon. Under normal conditions proteins in a buffer whose pH is greater than the pI of the protein would adsorb to an anion-exchange column. Conversely, proteins in a buffer of pH less than the pI would adsorb to a cation-exchange column. There are also "sticky" proteins that will bind to both types of column in the same buffer, and "slippery" proteins that are difficult to get to bind to any adsorbent within a stable pH range. These effects are partly due to non-electrostatic interactions e.g. hydrophobic and van der Waals forces and partly to uneven distribution of charges over the protein surfaces.

The calculated pI for yeast pyruvate kinase determined using the ISOELECTRIC POINT program (Devereux et al., 1984) is 7.66. The large difference between this value and that observed in the purified enzyme may indicate that several normally charged residues are obscured and are not available to undergo charge interactions with the ion-exchange matrix, leading to the anomalous binding behaviour observed. In this sense, yeast pyruvate kinase can be categorised as an example of a "slippery" protein.

An examination of the computer model of yeast pyruvate kinase indicates that several charged residues appear to be buried deep in the polypeptide structure and would presumably be unable to participate in charge interaction with the column matrix. Although apparently incompatible with the expectation that all charged hydrophilic residues ought to be in contact with the solvent, this finding is compatible with the observed pI difference and the anomalous behaviour of pyruvate kinase on anion-exchange columns. Of particular interest in this regard are residues Arg 18, 40 and 436 and Lys 412 (yeast numbering).



#### 4.1.5 COMPOSITION OF BUFFER

Another advantage of the modified purification scheme described here is the possibility of using similar buffers throughout the entire procedure. Thus, the same buffer was used for resuspending the cells after pelleting, washing the glass beads after cell lysis and resuspending the protein pellet obtained from the second ammonium sulphate precipitation. This buffer consisted of 50mM Tris-HCl, pH 7.5, 3mM MgCl<sub>2</sub>, 1mM DTT, 20% (v/v) glycerol and 0.04% (w/v) sodium azide. All purification steps were carried out at room temperature. The samples obtained from the gel filtration step were applied directly to an anion-exchange column equilibrated with 50mM Tris-HCl, pH 8.5, 3mM MgCl<sub>2</sub>, 1mM DTT, and 20% (v/v) glycerol. The pyruvate kinase was eluted with an identical buffer.

The slightly alkaline pH of the initial buffer prevents acid proteases released upon cell lysis from being activated and maintains the enzyme in a less active conformation. The enzyme is further protected from denaturation and inactivation by the inclusion of magnesium ions and DTT. The magnesium ions are essential for enzyme activity and help the enzyme keep an active conformation during purification. The DTT maintains the cysteine thiol groups in a fully reduced state during purification, in an attempt to mimic the conditions experienced by the protein in the cytosol. The sodium azide protects the gel matrix and the eluted fractions from bacterial contamination. It does not affect the enzyme in any way. The operations are carried out at room temperature to help prevent inactivation of the enzyme which is cold-labile. Stabilization of labile enzymes can be assisted by attempting to mimic the conditions of low water activity. The most widely used method is to use glycerol in the buffer solutions. Glycerol forms strong hydrogen bonds with the water, effectively slowing down the motion of the water molecules and so reducing the water activity. It has been suggested that protein molecules preferentially bind water, and the structure so formed is less able to unfold against the structured glycerol solvent than it would be able to in water alone (Scopes, 1987).

#### **4.1.6 PROTEASE INHIBITORS**

In order to prevent as much as possible the degradation of the pyruvate kinase by proteolysis from enzymes released during yeast cell lysis, a variety of protease inhibitors were used. These were added together to the pellet immediately prior to lysis in order to maximise their effectiveness. Six broad groups of proteases are known. The serine proteases can be inhibited by 3,4-dichloroisocoumarin (DCIC) and phenylmethanesulphonylfluoride (PMSF). The thiol proteases are inhibited by E64 (and to some extent by PMSF). The acid proteases are best inhibited by working in alkaline conditions as much as possible. Metalloproteases can be inhibited by 1,10-phenanthroline. Carboxypeptidases are inhibited by benzamidinium hydrochloride (and by PMSF). Other proteases are also inhibited by benzamidinium. The inhibition is due primarily to covalent modification and active site competition of the indicated enzymes and so once inhibited further addition is not usually required. The concentration of each inhibitor was in the range 0.1-1mM, although benzamidinium was added up to 50mM (see Section 2.6 for details).

## 4.2 ENZYME ASSAY CONDITIONS

Many different methods are available for analysing the catalytic activity of pyruvate kinase. These include monitoring the loss of pyruvate from the reaction media spectrophotometrically (Pon & Bondar, 1967), determining the amount of  $^{14}\text{C}$ -pyruvate as it is formed from  $^{14}\text{C}$ -phosphoenolpyruvate (Kaslow & Garrison, 1983), reacting the carbonyl groups of generated pyruvate with 2,4-dinitrophenylhydrazine to produce a coloured product (Imamura & Tanaka, 1982) and recording the loss of NADH as it is converted to  $\text{NAD}^+$  in a coupled enzyme assay with lactate dehydrogenase (Bucher & Pfeleiderer, 1955). By far the most commonly used technique is the latter, i.e. coupling the reaction:



to the simultaneous reaction:



Conditions are chosen such that the pyruvate is converted to lactate as soon as it is produced via the first reaction. The stoichiometry is such that the rate of the second reaction, determined by the rate of decrease of absorbance at 340nm, is equivalent to the rate of the first reaction.

### 4.2.1 GENERAL CONSIDERATIONS

Enzyme activity is affected by the concentrations of its substrates, activators and inhibitors specific for the enzyme, non-specific effects of compounds such as salts and buffers, pH, ionic strength, temperature and in some cases interactions with other proteins or material that might be present.

Activity is nearly always greatest at the highest feasible substrate concentration. For enzymes obeying Michaelis-Menten kinetics a substrate concentration at least ten times the  $K_m$  should be used. This ensures that zero order kinetics for the reaction will be observed. At  $10K_m$ , the rate is 91% of the theoretical rate at infinite concentration. There are two reasons for operating well above the  $K_m$  value. First, slight variation of concentration from one set of

assays to another makes very little difference to the observed rate. Second, consumption of substrate during the assay will make little difference to the rate and, if products are accumulating, any inhibitory effect they may have is less if the substrate concentration is high.

When dealing with multiply charged substrates such as ADP and PEP, their effect on ionic strength should be considered. Physiological ionic strengths are normally in the range 0.1-0.2M. As salt concentration increases above 0.2M, activity is often depressed. Temperature is also important. Enzyme reaction rates, like almost every other chemical process, increase with temperature, typically by a factor of between 1.5-2.2 for every 10°C rise. At a mean value of 1.8, activity increases by 6% per degree Celsius rise in temperature. As a result, accurate control of temperature to within  $\pm 0.5^{\circ}\text{C}$  is important.

Coupled enzyme assays require a large amount of coupling enzyme to be sure that it is the enzyme being measured that is limiting. The basic principle is that a steady state should be set up in which the rate of reaction of the coupling enzyme is equal to that of the enzyme being measured. Theoretically this can not be achieved; it will only be approached asymptotically. One must first define how closely we wish this condition to be achieved and in what period of time. A typical spectrophotometric assay will run for a few minutes, and the accuracy of the pipetting and instrumentation is unlikely to be better than  $\pm 2\%$ . If we set our restrictions as 98% of the true rate one minute after the start of the reaction, then the amount of the coupling enzyme needed is not so great. The minimum amount of coupling enzyme required (in units) is five times the  $K_M$  of the substrate of the coupling enzyme, measured under the conditions of the assay in which it is to be used.

#### 4.2.2. OPTIMISING THE ENZYME ASSAY

A variety of different assay conditions for the rabbit skeletal muscle and *S.cerevisiae* enzyme are listed in Table 15. From a study of the literature, it can

TABLE 17 PREVIOUS PYRUVATE KINASE ASSAY CONDITIONS

SOURCE	BUFFER/pH	PEP (mM)	ADP (mM)	Mg <sup>2+</sup> (mM)	KCl (mM)	NADH (mM)	LDH	REFERENCE
Rabbit muscle	triethanolamine 50mM, pH7.5	0.78	0.23	8.0 (SO <sub>4</sub> )	75	0.15	35µgml <sup>-1</sup> 630 units	Bucher & Pfeleiderer 1955
Rabbit muscle	imidazole 100mM, pH7.0	1.0	2.0	4.0 (Cl)	100	0.16	? an excess	Tietz & Ochoa 1958
Yeast	TMA-cacodylate 100mM, pH6.2	5.0	10.0	24.0 (Cl)	100	0.15	33µgml <sup>-1</sup>	Hunsley & Suelter 1969
Yeast	Tris-HCl 50mM, pH?	0.78	0.23	8.0 (SO <sub>4</sub> )	75	0.15	37µgml <sup>-1</sup>	Barbalace et al 1974
Yeast	triethanolamine 50mM, pH7.4	1.0	1.0	10.0 (Cl)	100	0.10	4 units	Hirai et al 1975
Yeast	MES 100mM, pH6.2	10.0	10.0	15.0 (Cl)	150	0.25	3µgml <sup>-1</sup>	Ford & Robinson 1976
Yeast	sodium phosphate 50mM, pH6.5	5.0	10.0	20.0 (Cl)	100	0.10	7 units	Sprague 1976
Yeast	MES 100mM, pH6.2	10.0	10.0	24 (Cl)	100	0.15	33µgml <sup>-1</sup>	Aust et al 1975
Yeast	imidazole 50mM, pH7.3	0.10	0.10	10.0 (Cl)	50	2.0	4 units	Burke et al 1983
Yeast	TPA-cacodylate 100mM, pH6.2	5.0	10.0	10.0 (SO <sub>4</sub> )	100	0.15	14 units	Morris et al 1984

be seen that the properties of the yeast and the muscle enzyme are clearly different with regard to their pH optima and kinetic constants for substrates and cofactors. It is evident therefore, that the optimum assay conditions for the yeast enzyme will be different from those for the muscle enzyme. The assay conditions so far described in the literature for the yeast enzyme, and summarised in Table 16, are unsuitable for a variety of reasons that are outlined below.

#### **4.2.2.1 BUFFER COMPONENTS**

Cacodylate is unsuitable due primarily to its extreme toxicity. Less toxic alternatives are readily available. Tris and triethanolamine are unsuitable as their usable pH ranges lie outside the pH optimum of the yeast enzyme. Imidazole can be used. However, pure imidazole is relatively expensive and the less pure forms may contain compounds that interfere with the enzyme itself, the coupling enzyme, or any of the other components of the assay. These impurities may also affect the performance of other experiments e.g. fluorescence measurements. Sodium phosphate is unsuitable as sodium cations compete with potassium for binding to the enzyme and phosphate anions interfere with the binding of PEP and ADP to the active site of the enzyme. MES is suitable as it has low toxicity and has maximum buffering capacity in the region around the pH optimum of the enzyme. It is also relatively inexpensive in a pure form. For these reasons MES was chosen as the buffering component in the enzyme assay system used in this thesis. The buffer counterion was tetrapropylammonium to allow modification of the monovalent metal cation content in other experiments. The pH was 6.5 which is close to the pH optimum for the yeast enzyme.

#### **4.2.2.2. SUBSTRATE CONCENTRATION**

##### **A) PHOSPHOENOLPYRUVATE**

The range of PEP used in the previous assays was 0.1mM to 10mM. A suitable concentration to use was 5.6mM as this was mid-way between the previous values and was still several times the  $K_M$  for this substrate ensuring that the enzyme was saturated at all times. It was also a convenient and



economic amount of the salt used to measure out repeatedly (100mg/ml) and avoided contributing excessively to the ionic strength of the assay media.

#### **B) ADP**

The range of ADP used in the previous assays was 0.1mM to 10mM. A suitable concentration to use in these assays was 2.4mM as this is several times the  $K_M$  for this substrate ensuring that the enzyme was fully saturated throughout the assay. High concentrations of ADP are known to be inhibitory to yeast pyruvate kinase and so lower concentrations are preferable. There is also an economic consideration. A convenient amount of the ADP salt to use was 100mg/ml. A lower concentration of ADP also resulted in a lower contribution to the ionic strength of the assay media.

#### **C) MAGNESIUM**

Pyruvate kinase has a requirement for divalent cations, usually magnesium. The most convenient salts to use are the chloride or sulphate. The sulphate anions inhibit the enzyme, possibly by mimicking the  $\gamma$ -phospho group of ATP and thus interfering with the binding of PEP and ADP at the active site. The chloride anion has not been reported to have any significant effect on enzyme activity. However, magnesium chloride is very hygroscopic and tends to absorb water vapour and so care must be taken when storing this compound for long periods. The range of concentrations used in previous assays was 8-25mM. A value of 15mM was chosen as being clearly in excess of the  $K_M$  for this cation and to reduce its contribution to the ionic strength of the assay media.

#### **D) POTASSIUM**

The yeast pyruvate kinase also has a requirement for monovalent cations, usually potassium. Previous assays used potassium chloride in the range 50-150mM. A concentration of 100mM was chosen as being intermediate in value and yet sufficient to saturate the enzyme

##### **4.2.2.3 NADH**

Throughout most of the assays described previously, a concentration of 0.15mM NADH was used. This gives an absorbance at 340nm of 0.93. This is sufficient for the sensitivity of most spectrophotometers to detect a change in

signal due to enzymic oxidation of NADH by lactate dehydrogenase.

#### **4.2.2.4. LACTATE DEHYDROGENASE**

In early assays the coupling enzyme had to be prepared fresh whenever it was required and so specific activities varied from preparation to preparation. From examination of Table 16 it can be seen that a large excess of lactate dehydrogenase was usually used corresponding to 20-37mg/ml. This would have been equivalent to several hundred units per assay. This is a vast excess to what is actually required and later workers used 4-14 units. Stable preparations of lactate dehydrogenase are commercially available. The enzyme is stabilised in 3.6M ammonium sulphate. Unless desalted, where activity is rapidly lost, the effect of the salt on pyruvate kinase activity must be considered. Ammonium cations are a known activator of the enzyme and sulphate anions are a potential inhibitor. In the assays used in this thesis, one unit of lactate dehydrogenase was present. Not only is this sufficient for the reaction but it also minimises the contamination of the assay with ammonium sulphate to 1mM, which would not have any significant effect on activity.



### 4.3 MORPHOLOGICAL AND BIOCHEMICAL STUDIES OF THE PARENT AND TRANSFORMED YEAST CELLS

The fact that an essential glycolytic enzyme has been mutated may manifest itself as differences in some of the fundamental properties of the cells expressing the mutant enzyme. Properties such as cell morphology and growth rate can be investigated simply.

The cells overexpressing mutant protein are slower growing (doubling time 3.6 hrs) than the same strain overexpressing wild-type enzyme (doubling time 2.5 hrs), although both grow more quickly than the parental strain containing the *PYK1* disruption (doubling time 5.8 hrs). The slow growth of the mutant enzyme expressing cells may be due to the deleterious effects of a less efficient pyruvate kinase enzyme. One might postulate that a cell expressing a mutant glycolytic enzyme but able to grow on glucose as the sole carbon source was unaffected by the introduced mutation. However, this is not necessarily the case. A cell expressing a completely non-functional pyruvate kinase could grow on glucose if an alternative pathway to glycolysis existed. Such an alternative pathway is present in yeast and is depicted in Scheme 1.

If sufficient DHAP is converted to glycerol-3-phosphate this could be transported into the mitochondria and be reconverted to DHAP with the concomitant production of reduced flavine adenine dinucleotide ( $\text{FADH}_2$ ). The  $\text{FADH}_2$  can be oxidised via the oxidative phosphorylation pathway on the inner mitochondrial membrane to generate ATP. If this pathway were the sole or major route by which the cells expressing mutant protein were growing then inhibition of oxidative phosphorylation by cyanide would result in a marked decrease in the rate of growth of these cells compared to wild-type cells. Fig. 30 shows the growth rates of the parental strain and the wild type and mutant-expressing strains in the presence and absence of  $10\mu\text{M}$  KCN. The growth of the parental strain is severely inhibited by cyanide. There is no decrease in growth rate of the wild type or the mutant cells. This implies that there is sufficient active mutant pyruvate kinase present in the cells to allow adequate growth on glucose. By

implication there is also sufficient intracellular Fru-1,6-P<sub>2</sub> to maintain the activity of the effector-dependent mutant enzyme. A reduction in growth rate due to an inefficient pyruvate kinase may manifest itself as a build-up of the intracellular levels of the substrates PEP and Fru-1,6-P<sub>2</sub>. It was not possible to measure the intracellular levels of PEP. This may be due to several factors. PEP is labile in acid or alkaline conditions and so attempts to isolate enzyme-free cellular extracts by acid or alkaline precipitation methods may have resulted in the destruction of the PEP. Also, the levels of PEP may be below those detectable with simple enzyme assays, especially as PEP is an important intermediary metabolite in numerous biochemical pathways and as such would not accumulate to any appreciable degree even in a cell where the pyruvate kinase was not present.

Fig. 31 compares the intracellular levels of Fru-1,6-P<sub>2</sub> between the parent strain and the wild type and mutant overexpressing cells. Clearly there is a significant difference in the levels of Fru-1,6-P<sub>2</sub> between the different cells. A build up of Fru-1,6-P<sub>2</sub> in the parent strain is observed. This is probably due to the reduced flux through the glycolytic pathway caused by the absence of pyruvate kinase. The amount of Fru-1,6-P<sub>2</sub> is nearly double that of the wild type cells (except at early stages of growth) and nearly four times that of the mutant expressing cells. The amount of Fru-1,6-P<sub>2</sub> in the wild type expressing cell is nearly twice that in the mutant enzyme expressing cell assayed under identical conditions. The pattern of production of the effector molecule is the same in all strains i.e. a peak of production in mid-log phase growth followed by a decline to a basal level in late-log and stationary phases of growth. The overexpression of an active pyruvate kinase may well be sufficient to explain the large increase in the growth rates of the transformed strains over the parent strain. Whether the difference in activity of the overexpressed enzymes is sufficient to explain the differential production of Fru-1,6-P<sub>2</sub> within those cells is a subject for further investigation. In reality there are probably many factors that contribute to this observed difference in the pool of intracellular Fru-1,6-P<sub>2</sub> and the difference in the activity of the overexpressed pyruvate kinases is but one facet of this problem.

The intracellular and extracellular morphology of the parent and transformed cells are strikingly different (Fig. 29). The cells overexpressing wild type and mutant pyruvate kinase appear normal in all respects. The parent cells however, are smaller and irregularly shaped. The cell wall appears to be more densely stained than the transformed cells. The intracellular regions are less densely stained than either of the two transformed cells and also appear to have a large number of vesicle-like inclusions. The disruption of *PYK1* by the insertion of *URA3* might be expected to severely affect the growth of the resultant cells. This is because *PYK1* has also been identified as *cdc19* and is therefore involved in the regulation of cell growth and division in some manner.

Many glycolytic enzymes have been found to bind DNA (Ronai, 1993). Examples include lactate dehydrogenase, phosphoglycerate kinase, aldolase, and glyceraldehyde-3-phosphate dehydrogenase. Although none of these enzymes interact with a specific target DNA sequence, their association with DNA may play a role in transcription and replication of DNA through general stabilization of the nuclear matrix or chromatin structure. Although pyruvate kinase was not specifically examined in this system, it is an intriguing thought that this enzyme may also have a similar DNA binding function which would help explain the severe deleterious effects observed in cells in which it is absent.

Many glycolytic enzymes have also been found to interact with tubulin and microtubules *in vitro* (Walsh et al., 1989). Interactions between tubulin and microtubules and the enzymes lactate dehydrogenase, glyceraldehyde-3-phosphate dehydrogenase and pyruvate kinase probably occur *in vivo* (based on calculated affinity constants for these components). These enzymes may, therefore, play a structural role in the formation of the microtrabecular lattice. A disruption of *PYK1*, leading to the complete absence of pyruvate kinase, may interfere with cell division due to the involvement of microtubules in chromosomal separation. As tubulin is involved in the formation of components of the cytoskeleton, cell morphology may also be disrupted. Pyruvate kinase has also been found to associate with actin in separate studies, increasing the likelihood of an important role for this enzyme in maintaining cell structure (Walsh & Knull, 1988).



## 4.4 PEPTIDE SEQUENCING

The mutant enzyme was purified and digested with cyanogen bromide. This compound cleaves proteins on the C-terminal side of methionine residues. It was expected, from an analysis of the amino acid sequence, that 11 peptides would be produced by this procedure (Table 4). The peptides were dissolved in 4M guanidine hydrochloride and applied to a microbore reverse phase HPLC column in order to separate them. The chromatogram produced is shown in Fig.32. Clearly, several distinct peaks are visible. Some peaks were better resolved than others. The peptides were detected by their absorbance at 220nm. Absorbance in this region of the uv spectrum is due to the peptide bond and so can be used to give an approximate measure of the amount of material present in each peak. The peptide containing the serine 384 to proline mutation is the largest (14.4kD) and most hydrophobic, as determined by a computer program that analyses the properties of possible protein digestion products (PEPTIDESORT; Devereux et al., 1984). The peak numbered 17 in the chromatogram in Fig.32 was chosen as the likliest candidate considering the suspected properties of the peptide and its resolution compared to the rest of the peaks present. The peptide was isolated and subjected to 16 rounds of N-terminal Edman degradation on an automated peptide sequencer. The degradation products were separated by HPLC and compared to a standard chromatogram containing all possible PTH-amino acid residues and reaction products. The retention times of these products on the HPLC column are shown in Fig.33. The chromatogram produced for the first round of Edman degradation is shown in Fig.34. It shows an excess of aspartate, which is often a characteristic of the first round of degradation, and also a clear excess of valine. Unfortunately, other amino acids are also present in surprisingly large amounts, notably tyrosine, isoleucine, leucine and alanine. This suggests that contaminating peptides are also present in peak 17. A more comprehensive analysis of the data performed by D.Lamont (Welmet) suggested the presence of up to seven contaminating peptides (Table 6). A positive identification of the point mutation was not possible by this method because the sequencing did not extend far enough into

the peptide. The serine 384 to proline mutation is present 18 residues from the N-terminus of peptide 11. As sequencing was suspended after 16 cycles, due to multiple contaminating signals, the mutation could not have been detected. It is sometimes possible to follow the sequence of a known protein when contaminating peptides are also present. However, as the peptide containing the mutation of interest was not well represented in the sample this procedure was also impossible (Table 6). No other peptides from this separation were considered as suitable for sequencing. Only one peptide gave a clear signal that could be identified unambiguously. That was peptide 5. A comparison of this peptide with a computer database revealed a 100% match with yeast pyruvate kinase (Fig.35). A better method for separating the peptides was not readily available. The reverse phase microbore HPLC system is widely used and has a range of preset elution programs for the purposes of peptide separation. It was not economic in terms of time or expense to optimise elution conditions for this particular digest or to purchase a column with a different matrix in order to try and improve the separation. It may well be that the optimum separation had indeed been effected by the system used and that time spent trying to improve the separation would have been futile. As has been observed earlier, yeast pyruvate kinase is an unusual protein in terms of its behaviour on ion-exchange matrices. It may be that the unusual behaviour also extends to the individual peptides on reverse phase matrices, resulting in poor resolution and a different order of elution when compared to the predicted behaviour of the peptides using the PEPTIDESORT program.

Due to the expense of the sequencing reaction, and the low likelihood of obtaining an improved resolution of fragments from a repeat digestion and HPLC purification, this approach was abandoned in favour of sequencing the plasmid DNA used to overexpress the mutant protein.

## 4.5 DNA SEQUENCING

To confirm that the overexpressed pyruvate kinase under study contained the desired serine to proline mutation, a portion of the plasmid DNA containing the site of the point mutation was sequenced. Two oligonucleotide primers were designed to be exactly complementary to a short region 80-100bp either side of the mutagenised region. The potential secondary structure of the oligonucleotides was checked using the UWGCG programs CIRCLES and SQUIGGLES. From Fig. 37 it can be seen that both oligonucleotides have the potential to self-anneal and form stem-loop structures. The stability of these structures is calculated to be about 2kJ/mol. Under the conditions in which these oligonucleotides are used i.e. in PCR and sequencing reactions, it is unlikely that such structures would exist, as the presence of an exactly complementary template sequence would make oligonucleotide-template pairing much more favourable thermodynamically.

The size of the oligonucleotides was confirmed by LDMS. This is a relatively new technique and is used primarily for the determination of the molecular mass of peptides and small proteins. It is not routinely used for determining the size of DNA molecules. As a result, the lack of appropriate DNA mass standards makes the error in DNA mass determination greater than for protein work. However, an acceptable agreement (3.3-4.5%) between the expected mass and that determined by LDMS was obtained. As can be seen from Fig. 38, both oligonucleotides are substantially free from contaminants, either precursor nucleoside triphosphates or prematurely terminated oligonucleotides.

The oligonucleotides were used to amplify a stretch of DNA from double-stranded plasmid DNA by the polymerase chain reaction. From agarose gel electrophoretic analysis, it can be seen that the PCR product is about 275bp in size (Fig.39). This is a little larger than the expected size of 253bp. The increase in apparent size is probably due to anomalous running of the PCR product compared to the marker DNA. The markers used (1kb ladder, Gibco BRL, UK) are polymers of a small repeating unit used to generate a nested set of fragments of varying size (Fig. 40). As such their mobility in an agarose gel

may well be different from that of a natural DNA sequence. An attempt to confirm the mass of the PCR product by LDMS was not successful. The estimated size of a 253bp ds DNA fragment is of the order of 160kD. This is beyond the detection range of the LDMS equipment. This procedure however, was able to confirm the absence of smaller DNA fragments. The PCR product was purified by reverse phase HPLC prior to sequencing. As can be seen from Fig.41, the DNA fragment is essentially free of any contaminants.

The PCR sequencing technique was not successful. In all attempts to sequence by this method premature stops were observed in all four sequencing lanes. This is usually indicative of a contaminated DNA template. After purifying the template by a commercial ion-exchange method (PCR magicprep, Promega) and repeating the process, still no sequence information was obtainable. The PCR template, Taq polymerase, oligonucleotides and other components were either used fresh or specially purified for each sequencing reaction, and so the failure for readable sequence to be produced is even more disturbing.

Other disadvantages of PCR sequencing include the random introduction of incorrect nucleotides at a frequency greater than for other sequencing strategies, the magnesium-dependent nature of the Taq polymerase reaction requiring accurate titration of DNA template with  $MgCl_2$  and the need to use glycerol-tolerant sequencing gels due to the formation of glycerol-boric acid adducts in traditional sequencing gels. The latter problem is especially tiresome as it means that small numbers of sequencing reactions must be run separately from other reactions performed using the non-PCR sequencing method, adding to the expense and inconvenience of this system. Another sequencing method was therefore tried. Double-stranded sequencing using a genetically modified form of T7 DNA polymerase (Sequenase, USB) was successful at the first attempt. With slight modifications it allowed readable sequence up to 100 bp either side of the point mutation to be produced.

The DNA sequence in the region of the serine to proline mutation is shown adjacent to the wild-type sequence (Section 3.3, Fig.43). Although only a portion of the *PYK1* sequence was analysed in this way no spurious mutations

were observed. The entire *PYK1* sequence was determined when the mutagenesis reactions were performed (McNally, 1989a; McNally et al., 1989b) and there is no reason to believe that any spurious mutations have been introduced into either sequence during propagation of the plasmids since that time.



## 4.6 PURIFICATION AND KINETIC CHARACTERISATION OF WILD TYPE AND MUTANT FORMS OF PYRUVATE KINASE

The purification protocol for pyruvate kinase is shown in Scheme 2. The wild type and mutant enzymes were purified in an identical manner. The elution profile from the Sephacryl S200 gel filtration column for the wild type and mutant enzymes are shown in Fig. 44. In both cases the activity peak is located in the first protein peak to be eluted from the column. This peak elutes in the void volume of the column, as determined by prior calibration with Dextran Blue 2000. It is possible to estimate the minimum size of the enzyme at this stage. The column matrix excludes proteins greater than 200kDa in size. As a result proteins larger than this are eluted in the void volume. The active enzyme, therefore, must be larger than 200kDa. This is consistent with the idea that pyruvate kinase is a tetramer of identical subunits each approximately 55kDa in size (McNally, 1989).

The elution profile from the ion-exchange column is shown in Fig. 45. A large peak elutes in the void volume of the column. The pyruvate kinase activity is found to elute slightly behind this protein peak, indicating that the enzyme does not bind significantly to the column matrix under the conditions used. This is consistent with the enzyme being of a large size (and hence excluded from the matrix) and having an isoelectric point (pI) significantly below 8.5. This is consistent with previous findings. A pI of 6.6 for the wild type enzyme has been reported (Yun et al., 1976).

The rate of reaction against the amount of enzyme was found to be linear for both the wild type and mutant enzymes (Fig. 47). This demonstrates that no significant inhibition of either enzyme occurs at high or low protein concentrations, as has been recorded for other enzyme preparations (Cornish-Bowden, 1981). Protein aggregation or dissociation could be responsible for these phenomena but do not appear to be relevant to the pyruvate kinase preparations produced here, when assayed under the stated conditions.

The effect of the positive allosteric effector fructose-1,6-bisphosphate on the rate of the reaction catalysed by the wild type and mutant pyruvate kinases

is shown in Fig. 48. The wild type enzyme shows a slight increase in rate in the presence of the effector compared to the rate in its absence. The concentration of effector does not influence the rate between 1-5mM.

The effect of Fru-1,6-P<sub>2</sub> on the mutant enzyme is more profound. The relationship between reaction velocity and effector concentration shows an apparent saturation effect over the range 0-5mM. The conclusion is that the mutant enzyme is fully active only in the presence of high (5mM) concentrations of effector, and is effectively inactive in its absence. The serine to proline mutation seems to exert an effect on either the efficacy of effector binding or on the mechanism by which the effector brings about a more active conformation of the enzyme. As the mutation is thought to interfere in the transmission of the allosteric effect across intersubunit contacts, the pronounced disturbance in the mode of action of the effector is, perhaps, not surprising. The concentration of Fru-1,6-P<sub>2</sub> where the mutant displays half maximal activity was calculated as 1.9mM  $\pm$  0.1mM. It has been reported that the pyruvate kinase from *S.carlsbergensis* requires Fru-1,6-P<sub>2</sub> in order to achieve optimum V<sub>m</sub> values (Hess & Haekel, 1967). This phenomenon may be related to that observed with the mutant enzyme from *S.cerevisiae*. Unfortunately, the amino acid sequence of the *S.carlsbergensis* enzyme is not known and so comments on its ability to bind the effector, and the mechanism by which it adopts an active conformation in the presence of the effector, are limited.

A plot of reaction velocity against PEP concentration for the wild type enzyme is shown in Fig. 49. In the absence of the effector, the plot is strongly sigmoidal. In the presence of 1mM Fru-1,6-P<sub>2</sub> the plot is better represented by an hyperbola. Transformation of these data into a Hill plot indicates that in the absence of effector the S<sub>0.5</sub> PEP is 3.34mM. The value for the Hill coefficient ( $n_H = 2.67$ ) suggests that a strong, positive homotropic interaction between PEP binding sites occurs. This confirms data obtained by other workers (e.g. Murcott, 1992). In the presence of 1mM Fru-1,6-P<sub>2</sub> the S<sub>0.5</sub> PEP is reduced to 0.17mM and the Hill coefficient to 1.0. This indicates that the binding of the effector to the enzyme increases the affinity of the enzyme for substrate by a factor of 20, and abolishes cooperativity between PEP binding sites.

A plot of reaction velocity against PEP concentration, in the presence of 5mM effector, for the mutant enzyme was also sigmoidal. Note that in the absence of effector the enzyme was inactive and so kinetic data for this case were unobtainable by traditional enzyme assay methods. The data were transformed into a Hill plot. In the presence of the effector, the  $S_{0.5}$  PEP was calculated to be 0.94mM with a Hill coefficient of 1.69. Thus the mutant enzyme displayed a five-fold lower affinity for PEP than the wild type enzyme under the same conditions, and the cooperativity between PEP binding sites was increased.

A plot of the reaction velocity against ADP concentration for the wild type enzyme is shown in Fig. 51A. In the absence of effector, the plot is clearly sigmoidal. Also, the maximum velocity appears only to be about one-third of that observed in the presence of effector. In the presence of effector, the plot becomes hyperbolic and the maximum observed velocity increases markedly. This may indicate that the conformation of the active site, in the absence of effector, is considerably different to that in the presence of effector, such that ligands necessary for catalysis are not optimally orientated. When the  $S_{0.5}$  ADP is being determined kinetically, the reactions are started by the addition of an excess of PEP. Conversely, when the  $S_{0.5}$  PEP is being determined, the reactions are started by an excess of ADP. The variation in maximum velocity in the presence and absence of Fru-1,6-P<sub>2</sub> is not observed when the  $S_{0.5}$  PEP determinations were performed. This suggests that, in the absence of effector, an ordered addition of substrates to the enzyme is required for the formation of the catalytically active complex, with ADP binding before PEP. The addition of effector overcomes this requirement and, along with the increase in affinity and abolition of cooperativity, may be one of the ways in which the effector activates the enzyme. An ordered addition of substrates to yeast pyruvate kinase has been claimed by other workers, although they determined that the order of substrate binding was PEP first, followed by ADP then magnesium (Morris et al., 1984). The data were transformed into a Hill plot (Fig.52). The  $S_{0.5}$  ADP was calculated as 0.39mM. The Hill coefficient was 1.16. This indicates that a slight positive homotropic interaction between ADP binding sites occurs. This is

consistent with data from other sources in which ADP appears to exhibit only a small degree of cooperativity between binding sites (Hunsley & Suelter, 1969). In the presence of effector the plot becomes hyperbolic, with  $S_{0.5}$  reduced to 0.15mM and  $n_H$  reduced to 1.04. Thus, what little cooperativity existed is abolished by the addition of effector, and further supports the claim that the effector brings about a conformational change in the enzyme molecule upon binding.

A plot of reaction velocity against ADP concentration for the mutant enzyme is shown in Fig. 51B. Note that these data are obtained in the presence of 5mM Fru-1,6-P<sub>2</sub>. As the mutant enzyme was observed to be inactive in the absence of effector, kinetic data were not obtainable. The data were transformed into a Hill plot (Fig. 52B). The  $S_{0.5}$  ADP was calculated to be 0.69mM and  $n_H$  was 1.46. This suggests that the point mutation causes a four-fold decrease in affinity for ADP and a marked increase in cooperativity between ADP binding sites.

A plot of reaction velocity against monovalent cation concentration for the wild type enzyme, in the absence of the effector, is shown in Fig. 53A. The enzyme is known to require monovalent cations for activity (Tietz & Ochoa, 1958). The data were transformed into a Hill plot (Fig. 54A). The  $S_{0.5}$  K<sup>+</sup> was calculated to be 41.5mM with  $n_H$  1.8. This is indicative of a strong, positive homotropic interaction between potassium binding sites and supports the findings of other workers (Rhodes et al., 1986).

A plot of reaction velocity against monovalent cation concentration for the mutant enzyme, in the presence of effector, is shown in Fig. 53B. The plot is weakly sigmoidal upto 100mM. Above 100mM the cation appears to inhibit the enzyme. The data were transformed into a Hill plot (excluding the points above 100mM). The  $S_{0.5}$  K<sup>+</sup> was calculated to be 21.4mM with  $n_H$  1.37. Thus, even in the presence of effector, there is observed to be a significant positive homotropic interaction between potassium binding sites in the mutant enzyme.

The effect of varying the monovalent cation on the activity of the wild

type and the mutant enzymes, in the presence and absence of Fru-1,6-P<sub>2</sub>, was determined (Fig. 55).

In the absence of effector, maximum activity in the wild type enzyme is observed when ammonium ions are present as the activating monovalent cation (Fig. 55A). Potassium and rubidium ions also strongly activate the enzyme. Caesium barely activates the enzyme at all, and lithium and sodium do not have any stimulatory effect whatsoever.

In the presence of the effector, potassium is observed to be the most potent activator of the wild type enzyme. Rubidium and ammonium ions activate equally well but produce only 50% of the activity as potassium. Caesium, lithium and sodium all produce some activation but only extremely poorly. The effect of ammonium to produce such a great activation in the absence of the effector may be due to the stabilising effect of ammonium sulphate solutions seen in many other systems (Scopes, 1987). The toxic effect of ammonium compounds in cells means that these species never accumulate to any significant extent and that this form of activation probably never occurs *in vivo*. The effect of Fru-1,6-P<sub>2</sub> is to select against ions other than potassium, possibly by producing a conformation in which potassium binding is enhanced. The ability of potassium to produce significant changes in conformation of *S.cerevisiae* pyruvate kinase has already been noted (Kuczenski & Suelter, 1970).

The effect of monovalent cations on the mutant enzyme in the presence and absence of Fru-1,6-P<sub>2</sub> was also studied (Fig. 55B). In the absence of the effector, none of the monovalent cations studied caused an activation of the enzyme. In the presence of the effector, potassium and ammonium appeared to produce about the same level of activation. Rubidium produced about two-thirds of the activation as either potassium or ammonium. Lithium, sodium and caesium were not able to activate the enzyme in the presence of the effector. These results suggest that the conformational change induced in the wild type enzyme by potassium and ammonium is not being produced in the mutant enzyme, or, that the conformational change is insufficient to cause activation. The conformational change induced by the effector allows potassium to function and activate the enzyme. Thus the two species produce two different types of



conformational change. The observed activation by ammonium is again probably an experimental artefact and would not occur *in vivo*. The conformation of the active site of the mutant enzyme in the presence of effector is probably slightly different to that of the wild type enzyme under the same conditions. This is seen in the different activation profiles of the two enzymes and reflects real differences in the geometry of the active site and in particular ligands associated with the binding of the monovalent cation.

The effect of divalent cations on the activity of the wild type enzyme was studied. The results are displayed in Fig. 56A. In the absence of Fru-1,6-P<sub>2</sub> magnesium and manganese ions activated the enzyme to the same extent. Cobalt produced about two-thirds of the activity observed with magnesium. Calcium and barium did not activate at all. In the presence of the effector, maximum activation was observed with magnesium. Cobalt activation was unaltered, whilst the effect of manganese was dramatically reduced. Calcium and barium again had no effect on enzyme activation. Thus, Fru-1,6-P<sub>2</sub> appears to select against ions other than magnesium from activating the enzyme. Manganese and cobalt have often been used to activate the wild type enzyme in NMR experiments due to their paramagnetic properties (Nowak & Mildvan, 1972). However, it may be that these cations do not fully mimic the effects of magnesium. The conformational changes observed to occur upon effector binding probably serve to affect the binding of all components in the reaction, including the metal cations. If the divalent cation is required to form a substrate-enzyme bridge complex, then the disposition of ligands and the dimensions of the active site must necessarily be altered upon effector binding. Cations able to bind ligands in the absence of effector may not be able to do so in the presence of effector.

The effect of divalent cations on the activity of the mutant pyruvate kinase was also determined (Fig. 56B). In the absence of Fru-1,6-P<sub>2</sub> none of the divalent cations studied were capable of activating the enzyme. In the presence of the effector, magnesium, manganese and cobalt all produced about the same degree of activation. The selection against cations other than magnesium in the wild type enzyme is not apparent in the mutant enzyme. This

may indicate that the conformation of the active site of the mutant enzyme, in the presence of effector, is different from that of the wild type enzyme. Ligands that bind magnesium may not be as flexible in the effector-activated mutant as they are in the wild type enzyme, leading to the ability of manganese and cobalt to activate the mutant as potently as magnesium. Calcium and barium had no effect on enzyme activation. The effect of calcium (and possibly also barium) may be to produce an inactive enzyme-substrate- $M^{2+}$  complex. The binding of calcium may allow one catalytic cycle but then the prevention of the enzyme to release product, or to relax sufficiently to bind further substrate molecules, produces an inactive inhibited enzyme (Boiteux et al., 1983).

That these metal cation effects were not due simply to differential levels of inhibition or activation of the coupling enzyme, lactate dehydrogenase, was examined by assaying the coupling enzyme alone in the presence of the various cations under investigation (Fig. 57). Apart from zinc, which completely inhibited the coupling enzyme and which was not used in the resultant pyruvate kinase assays, none of the metal cations studied had any significant effect on the activity of the coupling enzyme. The inhibition of lactate dehydrogenase by zinc may be due to the accessibility of the active site cysteine residue. Sulphydryl groups have a high affinity for metal cations such as zinc. A similar effect might be expected from cations such as  $Cu^{2+}$ ,  $Cd^{2+}$  or  $Hg^{2+}$  were they to be tested. Some authors have reported the effect of zinc on pyruvate kinase as being strongly inhibitory. In each case the pyruvate kinase was assayed with the coupled enzyme method using lactate dehydrogenase. The result obtained is not surprising if it is the coupling enzyme that is being inhibited and not the pyruvate kinase. The authors do not specifically report the effect of the metal cation additions on the coupling enzyme in separate control experiments e.g. Murcott, 1992.

The effect of pH on the activity of the wild type and mutant enzymes was examined (Fig. 58). In the absence of Fru-1,6- $P_2$  the wild type enzyme shows a narrow pH profile, with maximum activity being displayed at pH 6.5. This is in agreement with the data from a number of workers (e.g. Hunsley &

Suelter, 1969). A rapid decrease in activity at higher pH values is observed. A less dramatic decrease in activity is observed as the pH falls below 6.5. In the presence of the effector, a broader pH profile is observed. The wild type enzyme still has a pH optimum at 6.5 but becomes more active at higher pH values. Thus, the effector may produce a conformational change at the active site that allows the enzyme to retain activity as the pH increases. This may suggest a more confined active site with a decreased accessibility of solvent. Such a conformational change could favour catalytic activity as this would reduce the possibility of phospho transfer to water by providing a more hydrophobic environment for the substrates. Any observed effect on the pH profile would therefore be coincidental and of no particular benefit to the enzyme. Indeed, the physiological benefit of a broader pH profile is unclear. Pyruvate kinase would become more active under conditions of metabolic stress, where feedforward activation by Fru-1,6-P<sub>2</sub> would be possible. Under these conditions, intracellular pH is often observed to decrease. The possibility remains, therefore, that the observed broadening of the pH profile is an experimental artefact with no physiological basis.

In the absence of Fru-1,6-P<sub>2</sub> the mutant enzyme is very much less active than in the presence of the effector (Fig. 58B). At pH 6.5, the  $k_{\text{cat}}$  of the mutant enzyme is 250-fold lower in the absence of effector than in its presence. The enzyme is more active at pH values greater than 8.5. However, even under these conditions it only displays 15% of the activity of the fully activated mutant enzyme. In the presence of the effector, the mutant enzyme shows a pH profile broadly similar to the wild type enzyme. The pH optimum is 6.5. The activity of the mutant enzyme at pH 5.5 is virtually zero, unlike the wild type enzyme. The effect of pH on the mutant enzyme is difficult to explain. At pH 5.5, and in the presence of effector, the conformation of the enzyme is clearly different to that of the wild type enzyme. This either allows protonation of the residues essential for catalysis rendering the enzyme inactive (Morris et al., 1984), or results in a conformational change so severe that the binding of substrates either cannot occur or does not induce further conformational changes leading to activation. It has been suggested that salt bridges play an important



role in stabilising the conformation of pyruvate kinase (Walker et al., 1992). The drop in pH would be expected to severely disrupt the component residues of salt bridges by affecting the size and distribution of charge on their sidegroups.

N.B. It is possible that the differences in catalytic activity observed upon changing the pH of the assay medium may be due to loss of enzyme by denaturation rather than to any inferred conformational changes at the active site or elsewhere on the enzyme. As the appropriate control experiments to determine more fully this possibility were not performed in this study, it must remain highly speculative whether the conformational changes suggested actually occur.

## 4.7 FLUORESCENCE AND CIRCULAR DICHROISM STUDIES

The fluorescence emission spectra of the wild type and the mutant enzymes were obtained in the region 305-400nm. The excitation wavelength was 295nm, ensuring that the predominantly absorbing residue was the single tryptophan present in each subunit. The emission spectra obtained in the absence and presence of substrates and effectors are identical for both the wild type and mutant enzymes. The fluorescence emission in each case is seen as a broad peak with a maximum at 340nm. This is indicative of a tryptophan residue that is quite exposed to the solvent. Upon the addition of the substrates PEP and ADP to saturating concentrations, the intensity of emission decreases indicating that a conformational change has taken place in the vicinity of the tryptophan residue. As the emission maximum has not been altered by substrate binding, this indicates that the quenching has occurred "internally" i.e. by residues adjacent to the tryptophan. This effect is observed in both the wild type and mutant enzymes (Fig. 59 and 60). The emission spectra obtained in the presence of the effector Fru-1,6-P<sub>2</sub> are quite different. Addition of Fru-1,6-P<sub>2</sub> results in a decrease in fluorescence intensity and a shift of the emission maximum to a longer wavelength. The emission maximum is altered from 340nm to 360nm, indicating that the tryptophan residue has become almost completely exposed to the solvent. This indicates that a greater conformational change has occurred in the environment of the tryptophan, in the presence of the effector, than in the presence of either of the two substrates. This conformational change is observed in both the wild type and mutant enzymes and is complete at effector concentrations of 0.1mM (Fig. 61). This seems to indicate that the change in conformation affecting the tryptophan residue occurs at lower concentrations of effector than is observed to be the case from analysing the data from the enzyme assays. This could arise from the effects of other ligands on Fru-1,6-P<sub>2</sub> affinity, or possibly, from the fact that Fru-1,6-P<sub>2</sub> affects some other feature of the enzyme (or enzyme-substrate complex) which is important for its effects on activity. The exposure of the tryptophan may be an unimportant indicator of the state of enzyme activation but is suggestive of the fact that Fru-1,6-P<sub>2</sub> exerts a

profound influence on the enzyme. Certain minor conformational changes are complete at a very low concentration of effector. Other conformational changes, leading to the full activation of both the wild type and the mutant enzymes, require much larger concentrations before they are complete.

Titration of the enzymes with Fru-1,6-P<sub>2</sub> and measurement of the fluorescence change allows the determination of the dissociation constant (K<sub>d</sub>) of the effector for the enzyme. The K<sub>d</sub> for the wild type enzyme is 49.3 μM (at pH 8.5 and in the absence of other substrates) and that for the mutant enzyme under identical conditions is 15.6 μM. The values for both enzymes suggests that a very tight association of effector and protein occurs. The point mutation at the subunit interface appears to increase the affinity of the mutant enzyme for effector by a factor of more than three. The binding kinetics also change from weakly sigmoidal in the wild type to strongly sigmoidal in the mutant. A maximum fluorescence quench of about 40% is seen in both enzymes indicating that the tryptophan has been exposed to about the same degree in both enzymes.

Other factors may influence the change in the mutant enzyme from an inactive to an active conformation apart from the concentration of effector.

Possibilities may be:

- 1) A time-dependent conformational change.
- 2) An association/dissociation of subunits in the presence of effector.
- 3) An ionic strength-induced conformational change.
- 4) A contaminant of the effector solution causing the conformational change.
- 5) Fru-1,6-P<sub>2</sub> is not the true effector and the conformational change is brought about by similar but different compounds.

If the differential activity of the mutant enzyme observed to occur at various effector concentrations were actually produced in a time-dependent manner, then it should be possible to incubate the enzyme with a low concentration of effector for a longer period and observe the same increase in activity as was observed at higher effector concentrations. This was found not to be the case. Mutant enzyme incubated in the presence of 1mM effector for 10 minutes always showed lower activity than enzyme incubated with 5mM effector

for one minute. Thus, although there may well be a minimum time for the completion of the conformational change, it is the concentration of effector that is the critical component in the observed transition.

It has been shown in mammalian cell cultures that Fru-1,6-P<sub>2</sub> causes the association of monomeric M2 pyruvate kinase (identified as a cytosolic thyroid hormone binding protein) to a tetrameric form (Ashizawa et al., 1991). If this were also true for the mutant enzyme, then various forms of the enzyme in different stages of association between monomer and tetramer should be detectable by cross-linking experiments using glutaraldehyde in the presence and absence of effectors. The tetrameric, dimeric and monomeric forms would be observed when analysed by SDS-PAGE. There was insufficient time to perform these types of experiments under fully controlled conditions. The detection of dimeric and tetrameric forms of pyruvate kinase by SDS-PAGE would be difficult due to the high molecular mass of these forms (110kD and 220kD respectively) leading to their poor penetration and low resolution in even low percentage polyacrylamide gels. This method of analysing the degree of association of subunits has been successfully used with lactate dehydrogenase and phosphoglycerate mutase (Hermann et al., 1981; White et al., 1993). However, both of these enzymes are considerably smaller than pyruvate kinase (subunit molecular mass 35kD and 27kD respectively) allowing easy discrimination between tetrameric, dimeric and monomeric forms of these enzymes.

The evidence from other sources is contrary to the hypothesis that the effector promotes the assembly of inactive monomers of the mutant enzyme to active tetramers. Mutant enzyme artificially denatured into its constituent monomers is completely inactive. Also, the mutant enzyme is isolated in an identical fashion to the wild type enzyme in a procedure where the concentration of effector is negligible. The enzyme under these conditions is tetrameric with no evidence of dimeric or monomeric forms existing in any significant amounts. Thus the hypothesis that the effector functions by causing the association or dissociation of subunits to activate the mutant enzyme is likely to be false.

The highly charged nature of the effector might lead one to believe that

an ionic strength-induced conformational change could be produced. It has been shown that the ionic strength of the media affects the interaction of the effector with the enzyme (Speranza et al., 1990). However, as the combined ionic strength of the components of the assay mixture is little altered by the contribution of 5mM effector, it can be supposed that this hypothesis is not correct.

A contaminant of the effector might be the true cause of the observed conformational change. An examination of a sample of the effector by HPLC failed to identify any contaminants. The effector was used as the trisodium salt. It can be seen from the results of the monovalent cation activation experiments (Section 3.4) that sodium fails to activate the mutant enzyme to any extent.

If Fru-1,6-P<sub>2</sub> were not the true effector it should be possible to activate the enzyme with likely breakdown products or similar compounds that could have contaminated the effector preparation. Fructose-1-phosphate, fructose-6-phosphate and fructose-2,6-bisphosphate did not activate either the wild type or the mutant enzyme. Fructose-2,6-bisphosphate is not likely to be an activator of the yeast enzyme despite being a potent activator in the highly similar trypanosome enzymes (Oppenheimer, 1987). Trypanosome glycolysis is largely confined to a subcellular organelle, the glycosome, where the majority of the glycolytic enzymes are sequestered. Phosphofructokinase, the enzyme that produces Fru-1,6-P<sub>2</sub>, is one of these enzymes, whereas pyruvate kinase (which is not) is found in the cytoplasm. Access of Fru-1,6-P<sub>2</sub> to the cytoplasm is limited by the impermeability of the glycosomal membrane. Thus, regulation of pyruvate kinase in trypanosomes is performed by the related compound Fru-2,6-P<sub>2</sub>, which is produced in the cytoplasm by 6-phosphofructo-2-kinase. Other eukaryotes that regulate their pyruvate kinases often do so via Fru-1,6-P<sub>2</sub> over other hexose-phosphates.

The remaining idea, that a concentration-dependent conformational change is produced by the effector remains the most obvious and convenient way of explaining the data. Despite saturation of the effector site at very low concentrations there may be another low affinity site that must be saturated to complete the conformational change. The point mutation may have left the



primary site relatively unaltered but may have decreased the affinity of a secondary site for the effector. Evidence against this hypothesis is that a secondary site ought to be identifiable through the analysis of Fru-1,6-P<sub>2</sub> binding data e.g. a Scatchard analysis. This would only be true, however, if binding at the second site also produced a change in the property being detected - in this case fluorescence emission. If not, one would need some other method for detecting binding at the second site e.g. <sup>14</sup>C-Fru-1,6-P<sub>2</sub>. Also, no candidates for a secondary effector site have been proposed from analysis of X-ray crystallography data. However, the only model for pyruvate kinase so far available is from the non-allosterically regulated cat muscle enzyme and so this does not necessarily exclude the possible existence of such a secondary site. Recently, the effector site in the pyruvate kinase from *Bacillus stearothermophilus* has been suggested to lie in a different position to that of the cat muscle enzyme (Walker et al., 1992). The proposed new site is a pocket deep between domains A and C, separated from the other pocket by close interdomain contacts and accessed via an alternative channel in the protein structure. It ought to be noted at this point that the most potent effector of the *B.stearothermophilus* enzyme is ribose-5-phosphate, and not Fru-1,6-P<sub>2</sub> and that the various forms of pyruvate kinase have probably evolved mechanisms of allosteric regulation precisely tailored to their regulatory requirements.

The conclusion that a concentration-dependent activation of the mutant enzyme exists can be supported by proposing that the conformational change observed, i.e. a change in tryptophan fluorescence that is complete at an effector concentration of 0.1mM, is not reflecting the full activation of the enzyme. The tryptophan residue is already quite well exposed to solvent in the absence of effector and only a small change in conformation, elicited by a low concentration of effector, would be required to make it fully exposed. This low concentration of effector is, however, insufficient to bring about full enzyme activation, which requires a much greater effector concentration. Also, it is likely that the geometry of the active site is highly ordered and that the correct orientation of ligands is only obtained in the presence of all the substrates and cofactors. This may make

it appear that the kinetics of binding of the various substrates studied by fluorescence techniques were not in accord with those determined during enzyme assays.

## ANALYSIS OF FLUORIMETRY BINDING DATA

A number of experiments were performed on both the wild type and mutant enzymes, where the fluorescence emission at 340nm was monitored as a function of ligand concentration. From these experiments, typical sigmoid and hyperbolic ligand saturation curves were obtained. The data from these plots could be used to produce Hill-type plots, from which  $S_{0.5}$  and Hill coefficient values ( $n_H$ ) could be determined for the various ligands. The data from these experiments is summarised in Table 11.

### 1) BINDING OF Fru-1,6-P<sub>2</sub> TO THE WILD TYPE ENZYME

At pH 8.5, and in the absence of other substrates and cofactors (except magnesium), the binding of the effector Fru-1,6-P<sub>2</sub> to the enzyme appears to be weakly sigmoidal. The  $S_{0.5}$  Fru-1,6-P<sub>2</sub> under these circumstances is 49.3 $\mu$ M, which agrees well with the value obtained by other workers e.g. Murcott et al., 1991. The degree of cooperativity of binding between effector sites appears to be very much reduced. The Hill coefficient was calculated as 1.23. Previous work indicates a much greater cooperative effect with a Hill coefficient of 2.25. This indicates that the pH difference, the absence of potassium, or the absence of any of the other substrates, all of which are known to affect the conformation of the enzyme, are affecting the ability of the effector to modulate its own binding to the enzyme.

### 2) BINDING OF Fru-1,6-P<sub>2</sub> TO THE MUTANT ENZYME

The binding of Fru-1,6-P<sub>2</sub> to the mutant enzyme was investigated under exactly the same conditions as for the wild type enzyme. The  $S_{0.5}$  Fru-1,6-P<sub>2</sub> for the mutant enzyme was determined to be 15.6 $\mu$ M with a Hill coefficient of 1.8. These values are significantly different to those for the wild type enzyme. The introduction of the point mutation therefore appears to affect the binding of effector, apparently tripling the affinity of the enzyme for effector and increasing the cooperativity between effector binding sites. Apart from the significant



changes in conformation due to the different buffer conditions, in terms of the high pH and the lack of other substrates, the mutant enzyme appears to adopt a conformation different to that of the wild type. This allows a tighter effector binding, due perhaps to a different orientation of ligands in the effector site. The increase in cooperativity indicates a difference in the way in which subunits interact with each other. The mutation may cause stabilising salt bridges to form that are not possible in the wild type enzyme or protect other contact regions from being disrupted.

The great difference in the binding properties of the effector to both the wild type and mutant enzymes is probably due more to the different buffer conditions than on vast differences in conformation between the two enzymes. The geometry of the active site in the absence of so many compounds essential for catalytic activity may be reflected in the unusual fluorescence signals produced. Assessing the binding properties of the effector in the presence of substrates may produce different conclusions.

### **3) BINDING OF Fru-1,6-P<sub>2</sub> TO THE WILD TYPE ENZYME IN THE PRESENCE OF ADP**

Before effector was added, the wild type enzyme was incubated with saturating concentrations of the substrate ADP. As a result, the  $S_{0.5}$  Fru-1,6-P<sub>2</sub> was calculated to be 269.3  $\mu$ M with a Hill coefficient of 1.08. Thus, the addition of ADP has caused a five-fold reduction in affinity for the effector and converted the weakly sigmoidal binding kinetics into an hyperbola compared to the enzyme in the absence of ADP. This indicates that the effector site conformation is significantly different in the presence of one of substrates. It also indicates that the addition of substrate appears to abolish cooperativity between effector sites on different subunits.

#### **4) BINDING OF Fru-1,6-P<sub>2</sub> TO THE MUTANT ENZYME IN THE PRESENCE OF ADP**

The determination of the effect of ADP on the binding of the effector to the mutant enzyme was carried out under exactly the same conditions as for the wild type enzyme. The  $S_{0.5}$  Fru-1,6-P<sub>2</sub> was calculated to be 56.8  $\mu$ M with a Hill coefficient of 1.40. Thus, in the mutant enzyme, the affinity for the effector has been reduced three-fold compared to the result in the absence of substrate, and the cooperativity between effector sites has also been reduced slightly. This broadly matches the effects seen in the wild type enzyme. The small decrease in cooperativity indicates a slight disruption of intersubunit communication between effector sites and may be attributed to a small conformational change upon substrate binding.

#### **5) BINDING OF Fru-1,6-P<sub>2</sub> TO THE WILD TYPE ENZYME IN THE PRESENCE OF PEP**

The binding of Fru-1,6-P<sub>2</sub> to the wild type enzyme was determined in the presence of saturating concentrations of the other substrate, PEP. The  $S_{0.5}$  Fru-1,6-P<sub>2</sub> under these circumstances was 55.2  $\mu$ M with a Hill coefficient of 1.76. Thus, in the presence of PEP, the effector appears to bind the wild type enzyme with about the same affinity as in its absence. The cooperativity between effector sites increases significantly from 1.23 to 1.76. This indicates that the addition of PEP causes a significant change in enzyme conformation. The conformational change affects the communication between effector sites rather than the ability of the enzyme to bind the effector molecule. The change in conformation elicited by PEP is different to that produced by ADP.

#### **6) BINDING OF Fru-1,6-P<sub>2</sub> TO THE MUTANT ENZYME IN THE PRESENCE OF PEP**

The determination of the effect of PEP on the binding of the effector to the mutant enzyme was carried out under identical conditions to that of the wild type enzyme. The  $S_{0.5}$  Fru-1,6-P<sub>2</sub> in the presence of PEP was found to be

15.3 $\mu$ M with a Hill coefficient of 0.95. This indicates that the enzyme binds the effector with about the same affinity as in the absence of substrate, but with a much decreased degree of cooperativity between effector sites. This suggests that the effect of substrate binding is to reduce communication between effector binding sites. The effect in the mutant enzyme is different to that observed in the wild type enzyme. Thus, the conformational change elicited by PEP is different in the two enzymes.

## **7) BINDING OF ADP TO THE WILD TYPE ENZYME**

The ability of the wild type enzyme to bind the substrate ADP was followed by fluorimetric means. The conditions were the same as have been described for the determination of Fru-1,6-P<sub>2</sub> binding to the wild type enzyme. The S<sub>0.5</sub> ADP was found to be 3.02mM with a Hill coefficient of 1.06. This compares with the kinetically determined values of 0.39mM and 1.16 respectively. This indicates that the wild type enzyme can bind ADP under the conditions used but with a much reduced affinity. This suggests that the difference in pH, the absence of potassium and PEP produce a different enzyme conformation that is not able to bind ADP very effectively. The cooperativity between ADP binding sites is only slightly reduced. The ADP sites have been found not to interact to any great extent by a number of workers (e.g. Hunsley & Suelter, 1969).

## **8) BINDING OF ADP TO THE MUTANT ENZYME**

The binding of ADP to the mutant enzyme was measured in exactly the same way as for the wild type enzyme. The S<sub>0.5</sub> ADP was found to be 2.49mM with a Hill coefficient of 0.96. A comparison with the values determined from enzyme assays is not appropriate here due to the difference in conditions, especially the presence of high concentrations of Fru-1,6-P<sub>2</sub> required for activation of the mutant enzyme. However, the results suggest that the conformation of the mutant enzyme under the conditions used for assay and in the absence of the other reaction components leads to the production of an

enzyme conformation that is not conducive to the optimum binding of ADP. It may be that the disposition of ligands at the active site are not well placed to allow efficient substrate binding. The inflexibility of the active site may lead to the reduction in the degree of cooperativity observed between ADP binding sites.

#### **9) BINDING OF PEP TO THE WILD TYPE ENZYME**

The binding of PEP to the wild type enzyme was assessed by fluorimetric means as described above. The  $S_{0.5}$  PEP was determined as  $93.0\mu\text{M}$  with a Hill coefficient of 1.06. This compares to the kinetically determined values of  $3.34\text{mM}$  and 2.67 respectively. Thus, the affinity of the enzyme for PEP has increased by a factor of 35 and the cooperativity between PEP binding sites has been virtually abolished. This suggests that the change in pH, or the lack of potassium or ADP, has altered the conformation of the enzyme allowing much tighter binding of substrate and reducing the degree of communication between binding sites on different subunits.

#### **10) BINDING OF PEP TO THE MUTANT ENZYME**

The binding of PEP to the mutant enzyme was determined by exactly the same means as for the wild type enzyme. The  $S_{0.5}$  PEP was found to be  $0.17\text{mM}$  with a Hill coefficient of 1.0. Thus, despite the different assay conditions, the point mutation results in a two-fold reduction in binding affinity compared to the wild type enzyme. The cooperativity between PEP binding sites has not been affected relative to the situation seen in the wild type enzyme. This suggests that the conformation of the mutant enzyme is slightly different to the wild type enzyme assayed under the same conditions and greatly different to either the wild type or the mutant enzyme determined under optimum assay conditions.

## CONCLUSIONS

The data from the experiments described above is summarised in Table 11.

The conformation of the wild type and mutant enzyme, determined via the fluorimetric method, are different to each other in many respects. Each substrate affects the binding of the effector to different degrees, reflecting the unique conformation adopted by the enzymes in their presence, and the subtle influences this will have on the binding sites of the other components and the ability of one subunit to communicate changes to the other binding sites on different subunits. The conformations of the wild type and mutant enzymes in the buffer used for the fluorimetric titrations are different from those adopted in the standard assay buffer. The higher pH, the absence of potassium, and the lack of the other substrates and effectors, all contribute to the final geometry of the active site and the effector sites. This also affects the ability of one subunit to communicate with the other subunits. There is little wonder therefore, that the results obtained from the fluorimetric titrations are different from those obtained by traditional enzyme assay. The different results serve to reinforce the concept of the importance of different conformations in enzyme activity and the role of individual compounds to affect, either subtly, or quite dramatically, the ability of the enzyme to bind compounds or to communicate change to other subunits in the enzyme.

A point mutation in the active site of *E.coli* phosphofructokinase has been observed to alter the cooperativity of the enzyme for substrates (Berger & Evans, 1990). Cooperativity has also been induced in *E.coli* glutathione reductase by a single point mutation located at the subunit interface (Scrutton et al., 1992). It is possible that a mutation affecting intersubunit communication, as has been produced here in the yeast pyruvate kinase, may interfere with substrate binding at the active site. The great difference in the assay conditions employed prevents a more precise discussion of the influence of the point mutation on the various properties studied.



## CIRCULAR DICHROISM STUDIES

Circular dichroism (CD) is a sensitive technique that can be used to determine the secondary structure of proteins and peptides in solution. Circular dichroism spectra for the wild type and mutant forms of pyruvate kinase were collected in the region 260-190nm in the presence and absence of a number of different ligands. To get reliable results it is important to understand the limitations of the technique. Circular dichroism spectra of proteins may look complicated, but the the long wavelength regions are dominated by the CD due to any alpha helical structures present. As a result, the information content of a protein CD spectrum is often lower than one might guess. In reality, CD data can give statistically significant estimates of multiple classes of secondary structure only if the data extend down to 184nm. If data extending only to 200nm are used, alpha helix is the only secondary structure that can be determined with confidence The situation is not much improved if data extending to 190nm are used (Johnson, 1990).

The CD of proteins is primarily the CD of the amide chromophore. Secondary structure, as measured by CD, counts amide-amide interactions. The amide chromophore begins absorbing far into the uv region with the first prominent peak at about 220nm. Absorption by alpha helix dominates in the region 240-190nm, with an intense negative peak at about 222nm, another reasonably intense negative peak at 208nm and an intense positive peak at 192nm. The beta sheet also has a fairly intense peak at 198nm, and random coil has an intense negative peak at 198nm. Despite this, CD spectra measured to 190nm do not usually contain enough information to reliably allow calculation of the secondary structural content other than the alpha helix content, which can normally be predicted accurately with spectra truncated at 200nm.

Circular dichroism instruments can not make accurate measurements on samples with an absorbance greater than 1.0. Solvent transparency is usually the major problem requiring the use of low concentrations of buffer. Note that, in an attempt to overcome the problems of solvent transparency in this work, the CD ( and fluorescence) measurements were performed with a buffer concentration of

20mM Tris-HCl, rather than the 50mM used in the enzyme assays. Solvent transparency problems can be partially overcome by using short pathlength (0.02cm) cuvettes. At a scan speed of 10nm/min a single spectrum takes seven minutes to produce. In order to increase the signal-to-noise ratio multiple scans can be collected and averaged automatically. Another important factor for the correct interpretation of CD spectra is the requirement for an accurate estimation of the protein content of the sample. The protein content of the ion-exchange purified fractions was determined by measuring the absorbance at 280nm ( $A_{280}$ ) compared to a suitable reference blank. The  $A_{280}$  for a 1mg/ml solution of yeast pyruvate kinase has been calculated as 0.51 (Yun et al., 1976). It should be noted that Lowry determinations are not sufficiently accurate to be used with CD measurements (Johnson, 1990).

Figure 62 shows the CD spectra of the wild type and mutant enzymes. It can be seen that there is no significant difference in the spectra in the regions important for estimating secondary structure.

The interpretation of CD spectra is not straightforward and the calculation of secondary structure is prone to many sources of error. The usual method is to determine the CD spectra for polypeptides that are assumed to adopt a single secondary structure in solution and then fit them to the CD spectra of the protein being analysed. The fraction of each secondary structure is taken to be the fraction of the corresponding polypeptide CD spectrum that is contained in the protein spectrum. There are a number of problems with this approach:

- 1) The CD spectrum of an alpha helical polypeptide is for the infinitely long structure, and only short helices are found in proteins.
- 2) Beta sheets come in parallel and antiparallel varieties, and it is not usually known which variety the polypeptide assumes in solution.
- 3) There are various types of beta turn and their CD spectra have not been well characterised.
- 4) There is disagreement over what conditions produce a true random coil in solution and the CD spectra have not been well determined. Moreover, it is not clear that "random" should be used for the residues that do not fall into the other secondary structure classifications since they are not really "randomly"



orientated.

The CD spectra in this work were analysed by the program CONTIN (Provencher & Glockner, 1981). This program was developed by using reference protein spectra measured 190nm. It has been stated that the best fit with this program is for proteins containing a high alpha helical content, and this is probably due to the general inadequacy of spectra truncated at 190nm for determining other elements of secondary structure, as outlined earlier.

Circular dichroism can be used to follow changes in secondary structure upon the binding of ligands. It is unusual for such dramatic changes in protein conformation to be elicited by ligand binding. This is reflected in the spectra presented in this work. The addition of the substrates PEP and ADP, and the effector Fru-1,6-P<sub>2</sub>, to the wild type and mutant enzymes, do not appear to cause any significant changes in the CD spectra produced, and hence no difference in the secondary structure of these enzymes (Figures 63 to 68 inclusive).

The other data presented (fluorimetric, trypsin digestion, chemical modification and thermal stability) all suggest that tertiary structural changes occur readily upon ligand binding. The apparent significant change in secondary structure content of the mutant enzyme over the wild type enzyme (Table 12) may be an artefact due to difficulty fitting the CD spectra with the CONTIN algorithm or inaccuracies in protein determination which are critical to the final secondary structure estimation.

#### 4.8 TRYPSIN DIGESTION OF WILD TYPE AND MUTANT ENZYMES

The analysis of conformational transitions using limited proteolysis has been used successfully in a number of enzyme systems for assessing the extent of conformational change induced in proteins by the binding of various substrates and effectors (Arnone et al., 1992). A number of proteolytic enzymes have been used in such studies. For this study trypsin was used as it has broad substrate specificity, does not require any special incubation conditions that might compromise the activity of the target enzyme, is relatively inexpensive and can be completely and rapidly inhibited when required. The effect of trypsin digestion on wild-type and S384P mutant pyruvate kinase activity was investigated. The role of substrates and effectors in protecting the enzyme against digestion was also studied. The results are summarised in Table 13.

The enzymes were incubated in standard assay buffer. Additions were 9.4mM PEP, 8.0mM ADP and 1.1mM Fru-1,6-P<sub>2</sub>. Aliquots of the digestion mix were taken at specific time points and incubated in the reaction mix to which had been added 1mM PMSF to inhibit the added trypsin. PMSF was observed to have no significant effect on either pyruvate kinase or lactate dehydrogenase. The PMSF was extremely labile and only poorly soluble in water, and so was dissolved in methanol immediately prior to use and stored on ice until required.

The substrates PEP and ADP significantly protect the wild-type enzyme from trypsin digestion compared with the enzyme in the absence of substrates (Fig.69). It should be noted that the assay buffer contains the essential metal cations K<sup>+</sup> and Mg<sup>2+</sup> which, by themselves, do not appear to protect the enzyme. The allosteric effector Fru-1,6-P<sub>2</sub> offers little or no protection of the wild-type enzyme and actually appears to enhance the destruction of the enzyme at longer incubation times.

The same pattern of protection was observed with the mutant enzyme (Fig. 70). Here, ADP appeared to offer more protection from trypsin digestion than PEP. However, both ADP and PEP were significantly more effective in

protecting the mutant enzyme than Fru-1,6-P<sub>2</sub> which did not prevent trypsin digestion to any extent.

The time taken for the enzymes to lose 50% of their activity can be measured and used to compare the effect of the additions in protecting the enzymes from trypsin digestion. When no additions were made, the wild type enzyme lost 50% of its activity after 19.4 minutes. When PEP was present, this time was extended to 120.8 minutes, a six-fold increase. ADP extended the inactivation time to 99.1 minutes, over a five-fold increase. Conversely, the presence of Fru-1,6-P<sub>2</sub> decreased the inactivation time to 16.5 minutes.

For the mutant enzyme, the time taken for the enzyme to lose 50% of its activity in the absence of substrates and effectors was 23.5 minutes. Addition of ADP extended this time to 84.8 minutes, nearly a four-fold increase. Addition of PEP resulted in a two-fold increase in the inactivation time to 47.5 minutes. The effector, Fru-1,6-P<sub>2</sub>, caused a decrease in the observed inactivation time to 18.3 minutes. These data are summarised in Table 13.

These data can be taken to indicate that substrates and effectors induce different conformations in the wild type and mutant pyruvate kinase enzymes that are differentially susceptible to digestion with trypsin. PEP and ADP significantly protect the enzymes from digestion indicating that a "closed" conformation exists that prevents trypsin from gaining access to susceptible bonds. It is important to note that the degree of extrapolation required to obtain a 50% inactivation time for PEP and ADP may exaggerate the degree of protection actually offered by these compounds. Fru-1,6-P<sub>2</sub> appears to offer very little protection from trypsin digestion. This indicates that the enzyme is in a more "open" or "relaxed" conformation where access by trypsin to susceptible bonds is easier. PEP and ADP bind at effectively the same site and might be expected to produce similar conformations of the enzyme. The allosteric activator binds at an altogether different site from the two substrates and so might be expected to produce an entirely different conformation in its presence. In fact, several different studies suggest that Fru-1,6-P<sub>2</sub> binding promotes a "looser" conformation which would make accessibility of trypsin to cleavage sites easier (Kapoor, 1976; Speranza et al., 1990). PEP and ADP may provoke a more

closed conformation in order to produce an environment in which the exclusion of water from the active site is essential to allow an efficient phospho transfer reaction to proceed.

An examination of the primary sequence of yeast pyruvate kinase in conjunction with the computer model of the subunit tertiary structure, reveals the location of a vast number of potential trypsin cleavage sites (61 in total). The distribution of lysine and arginine residues in a single subunit is shown in Fig. 85. Of these residues, several appear at interdomain regions, where polypeptide flexibility would be greater and accessibility by trypsin easier than in more compact regions of the domain. A number of charged residues are suspected as being important in ADP binding. In particular Arg 48, 90 and 263 and Lys 85 are thought to be among those residues involved in binding the phospho groups of ADP. The fact that ADP significantly protects both the wild type and mutant enzyme from trypsin digestion suggests that these residues may be important cleavage sites in the unprotected enzymes. ADP appears to protect the mutant enzyme more than the wild type enzyme. This suggests that the conformation of the mutant enzyme after binding ADP is significantly different to that of the wild type enzyme. This conformational change may protect more lysine and/or arginine residues that are near to the ADP binding site. Of particular interest in this regard are residues Arg 215 and Lys 193 and 195, which are very close to those charged residues at the active site and could be perturbed sufficiently on binding ADP to be protected from trypsin cleavage.

Binding of the effector Fru-1,6-P<sub>2</sub> to both the wild type and mutant enzymes significantly increases the susceptibility of the enzymes to trypsin digestion. The effector binding site has been identified in the *E.coli* enzyme by the covalent attachment of pyridoxal-5'-phosphate to lysine residues (Speranza et al., 1990). The equivalent residues in the yeast enzyme are 394-409. In this region there are several charged residues, notably Arg 407 and Lys 392 and 394. They could fulfill the same function as those positively charged residues at the active site i.e. binding the negatively charged phospho groups of the effector. Upon effector binding a significant conformational change occurs, resulting in the exposure of more arginine and lysine residues than are exposed in the native

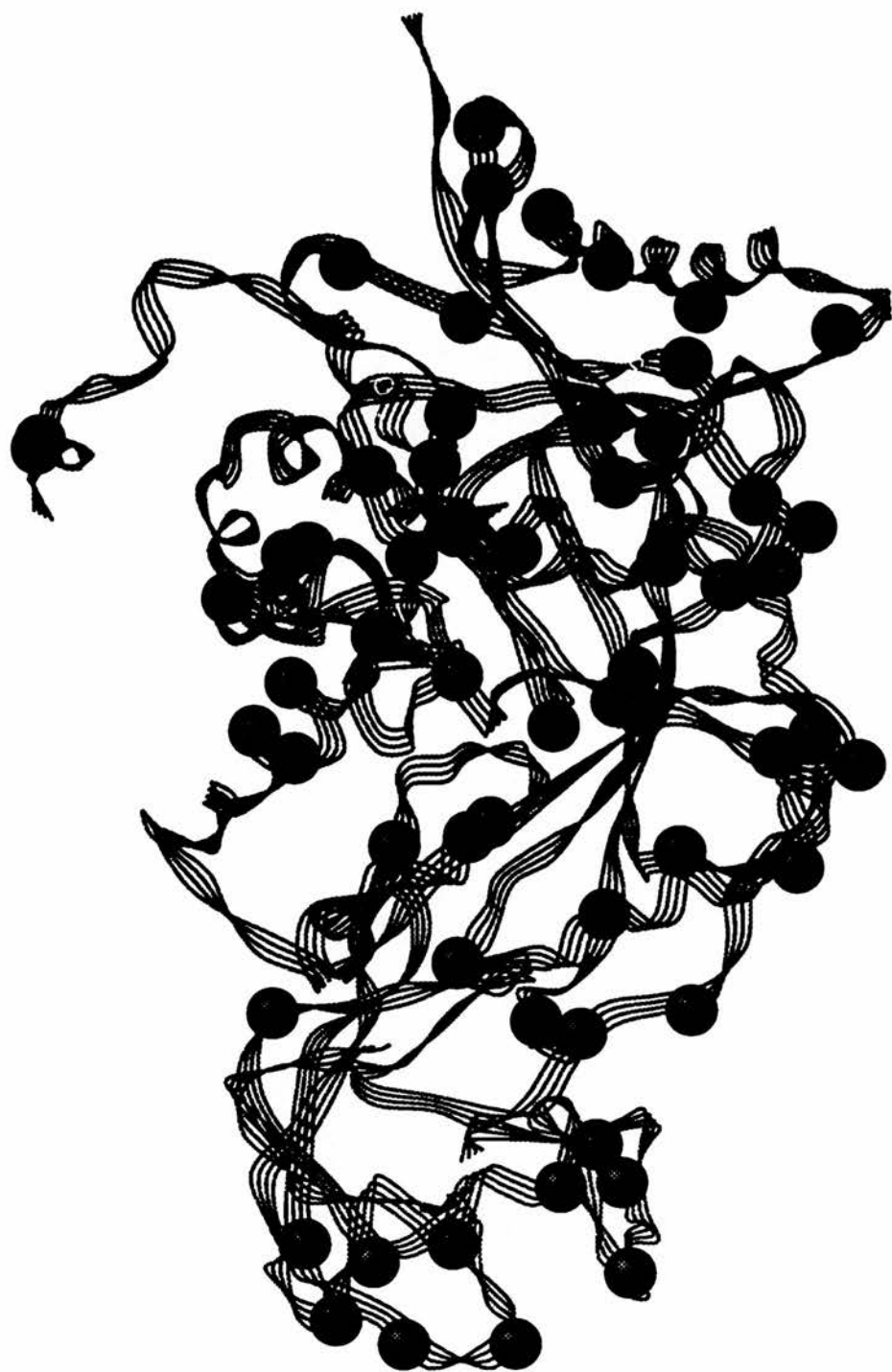


Fig. 85 Potential trypsin cleavage sites in a single yeast pyruvate kinase subunit.  
Polypeptide chain shown as a ribbon.  
Lysine and arginine residues shown as spheres.



unligated conformation. A small local perturbation might result in residues such as Arg 424 and 458 and Lys 412 becoming exposed. A larger, global conformational change could expose any number of charged residues. Of particular significance would be residues located in the interdomain regions. Such residues include Arg 408, 427, and 430 and Lys 235, 280 and 281, found between domains B and C, and Lys 193, 195, 336 and 387, found between domains A and B, which would be more prone to exposure than other charged residues partly shielded in the more compact regions of the various domains.

The trypsin digestion data are more suggestive of altered conformations of pyruvate kinase than the NEM inhibition studies because there are more trypsin cleavage sites potentially accessible to trypsin than there are thiol groups accessible to NEM. Hence, any observed difference in pyruvate kinase activity during the trypsin experiments is more indicative of a global conformational change induced by substrate or effector binding. Local perturbations caused by a small number of NEM modifications may not be the primary cause of the observed enzyme inactivation.

## 4.9 THE EFFECT OF NEM ON PYRUVATE KINASE ACTIVITY

The effect of the reagent N-ethylmaleimide on pyruvate kinase activity was determined for both the wild-type enzyme and the S384P mutant enzyme. NEM reacts specifically with the sulphhydryl groups of cysteine residues in enzymes often leading to their inactivation (Wieker & Hess, 1972; Plaxton et al., 1990). The inactivation may be due to the prevention of substrates binding to the active site of the enzyme by steric hindrance caused by the covalent modification. Alternatively, NEM treatment may prevent the enzyme adopting an active conformation by affecting the flexibility of the protein molecule.

The effect of 2mM NEM on enzyme inactivation was studied and the role of substrates and effectors in preventing the covalent modification of the enzyme was also investigated. The enzymes were incubated in standard assay buffer. Additions included 9.4mM PEP, 8.0mM ADP and 1.1mM Fru-1,6-P<sub>2</sub>. The enzymes were allowed to react with the added substrates and effectors for three minutes prior to NEM addition. The enzymes were assayed immediately after NEM addition and at regular intervals up to 24 minutes later. The results are summarised in Table 14. NEM addition did not immediately affect the enzyme activity of either the wild type or the mutant enzyme. However, after the incubation with NEM was allowed to continue, a significant difference in the activity of both enzymes was observed.

A useful measure of the extent of protection offered by compounds against this type of inhibition is the length of time required for the enzyme to lose 50% of its activity (T<sub>50</sub>). The effect of NEM on the wild type enzyme, in the presence and absence of various ligands is shown in Fig. 71. In the absence of any substrates or effectors, the wild-type enzyme lost approximately 50% of its activity after 8.1 minutes. Note that the essential cations K<sup>+</sup> and Mg<sup>2+</sup> present in the assay buffer did not prevent inactivation of the enzyme. The presence of the substrates PEP and ADP protected the wild-type enzyme with calculated T<sub>50</sub> values of 58.7 minutes and 22.3 minutes respectively. The allosteric effector Fru-1,6-P<sub>2</sub> offered limited protection to the wild-type enzyme



with a  $T_{50}$  of 31.9 minutes. The results with the mutant enzyme showed a similar difference in the ability of substrates and effectors to protect against NEM inhibition (Fig. 72). In the absence of substrates and effectors, the mutant enzyme had a  $T_{50}$  of 6.7 minutes. The substrates PEP and ADP offered significant protection of the enzyme, increasing the  $T_{50}$  to 14.7 and 13.8 minutes respectively. The allosteric effector Fru-1,6- $P_2$  conferred limited protection and increased the  $T_{50}$  to 8.6 minutes. The biphasic nature of the observed inhibition with both enzymes may be indicative of the rapid reaction of highly exposed cysteines followed by the slower reaction of less accessible residues.

These results are consistent with the existence of different conformations of the enzyme existing in the presence and absence of various substrates and effectors. When the substrates PEP and ADP are present the enzyme adopts a stable conformation markedly resistant to the presence of the thiol group modifier NEM. This is indicative of a "closed" conformation where cysteine sidegroups are not exposed to the solvent or are protected by nearby residues preventing NEM from reacting with them. The conformation adopted in the absence of substrates (but in the presence of the essential metal cations) is more "relaxed" with cysteine sidegroups readily accessible to the solvent and hence to NEM reaction. The allosteric activator Fru-1,6- $P_2$  induces a conformational change in which some of the thiol groups are exposed and some are protected, thus accounting for the intermediate level of protection afforded in the presence of NEM. The fact that the substrates PEP and ADP bind at essentially the same place could explain why they protect the enzyme to the same degree. The conformation in the presence of either substrate is likely to be very similar. Conversely Fru-1,6- $P_2$ , by binding at a site distinct from either of the substrates, induces a different conformation where different cysteine residues are exposed or protected. Cysteine residues important in enzyme activity are more readily exposed in the presence of the allosteric activator than they are in the presence of the substrates.

The distribution of cysteine residues in the yeast pyruvate kinase monomer was examined by reference to the computer model of the yeast enzyme

based on the coordinates of the cat skeletal muscle enzyme (Clayden, 1987; Murcott, 1990). There are seven cysteine residues per monomer, although none appear to be well-placed to participate in substrate or effector binding (Fig. 86). The proposed effector binding site, identified in the *E.coli* enzyme, and corresponding to residues 394-409 in the yeast enzyme is quite close to only one cysteine residue, Cys 425. A local conformational change induced by the binding of the effector might expose this residue, leading to covalent modification by NEM. A more extensive conformational change might allow other cysteine residues to be exposed. The fact that this is indeed the experimental observation supports this conclusion. In contrast, the large degree of protection from NEM modification afforded by the substrates PEP and ADP indicates that the cysteine residues are less exposed to the solvent and, as all the cysteines are quite distant from the active site, a conformational change must have occurred upon substrate binding to offer this protective effect. This supports the trypsin digestion studies where PEP and ADP were seen to protect the enzyme, perhaps by producing a more compact structure, and the effector was seen to offer very little protection, indicating a looser overall structure for the enzyme. It may be that in the tetrameric enzyme the disposition of the cysteines may be different to that observed in the monomeric model. In particular, cysteines nearer to intersubunit contacts might be more exposed when the effector molecule is bound to the enzyme than when substrates are present. However, it should be noted that the computer model of the monomer is based on its disposition in the tetramer.

It has been observed on many occasions and with many different pyruvate kinase enzymes that compounds known to react with cysteines and other reactive side-chains can be prevented from doing so by substrates, substrate analogues and effectors (Section 1.5). Assuming that the primary sequence for the pyruvate kinase from the yeast *Saccharomyces carlsbergensis* is very similar to that of *S.cerevisiae*, it may be possible to identify some of the cysteine residues postulated in earlier work (Wieker & Hess, 1972 and Fig 12). These authors reported that the pyruvate kinase from *S.carlsbergensis* contained six cysteine residues per subunit as opposed to seven in the *S.cerevisiae*

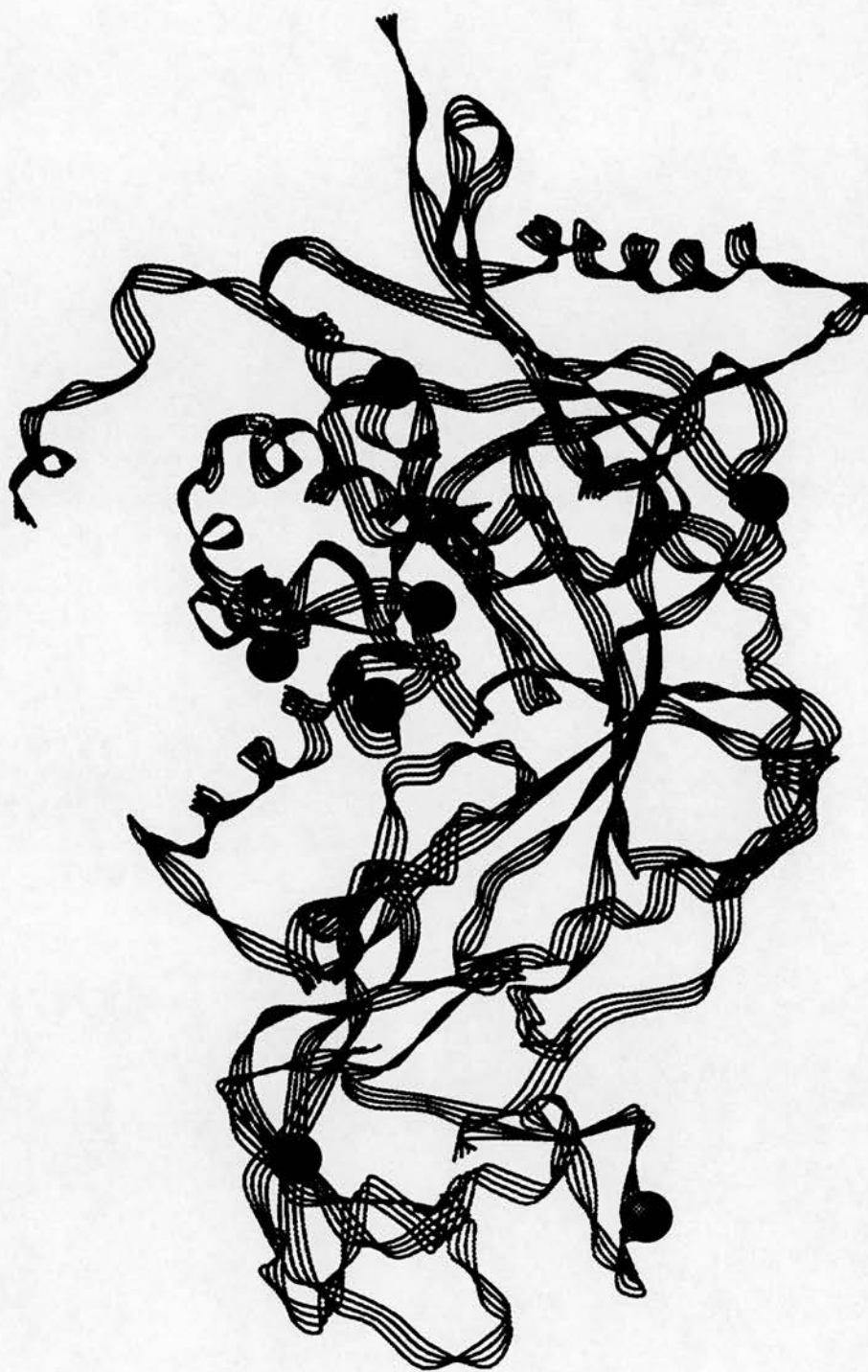


Fig. 86      Yeast pyruvate kinase subunit showing location of cysteine residues.  
Polypeptide shown as a ribbon.  
Cysteine residues shown as spheres.

enzyme. Three of these cysteines were located on the surface of the protein, and could be distinguished from one another by their reactivity towards DTNB. The other three cysteines were less reactive and are probably buried in the hydrophobic core of the enzyme. The most reactive cysteine was not part of the active site or the allosteric effector site and may correspond to residue 370 of the *S.cerevisiae* enzyme. The second most reactive cysteine was deemed to be part of the active site and may correspond to residue 120 in the *S.cerevisiae* enzyme, which is apparently located at the opening of the active site cleft. The third most reactive cysteine was part of the allosteric site and, in the *S.cerevisiae* enzyme, may be equivalent to Cys 425. Until the gene encoding the pyruvate kinase from *S.carlsbergensis* is cloned and sequenced the location of the cysteines, and their comparative position with respect to the *S.cerevisiae* enzyme, must remain speculative.

#### 4.10 THERMAL STABILITY STUDIES

Many proteins are progressively inactivated by heating. This thermal inactivation is often accompanied by denaturation and precipitation of the protein. The introduction of point mutations into features of secondary structure within a protein are often found to affect the ability of the protein to resist thermal denaturation. Mutations can make the protein more or less resistant to such treatment. One way to measure the effect of heating on an enzyme is to determine the temperature at which 50% of the enzyme activity is lost ( $T_{50}$ ). This was done for the wild type and the S384P mutant pyruvate kinases and also for the rabbit muscle enzyme. The results are shown in Fig. 73.

The rabbit muscle enzyme was found to be highly resistant to thermal denaturation ( $T_{50} = 58^{\circ}\text{C}$ ). This result is in accordance with data previously recorded (Potter, 1993). The wild type yeast enzyme had a  $T_{50}$  of  $42^{\circ}\text{C}$ , much lower than the rabbit muscle enzyme. This reflects the different tertiary and quaternary structures adopted by the two enzymes and is a consequence of their different amino acid sequences. The S384P mutant pyruvate kinase had a  $T_{50}$  of  $39^{\circ}\text{C}$ , 7% lower than the wild type enzyme. The effect of the point mutation is to disrupt the helix  $\text{C}\alpha 2$ . This may well affect the overall structure of the tetrameric enzyme. The mutation may expose residues to the solvent that are not normally exposed and so catalyse thermal denaturation to some extent. The secondary structure of the mutant enzyme, as measured by its CD spectrum, is not significantly different from that of the wild type enzyme (Fig. 62). It may not be possible to detect a small difference in alpha helical content between the wild type and mutant forms of the enzyme. The large difference actually detected (Table 12) may be an artefact due to inaccurate measurement or bias in the CONTIN algorithm used to calculate secondary structure content. This suggests that the point mutation has not had a great influence on the secondary structure of the enzyme. Thus, it is apparent that the altered response of the mutant enzyme to a rise in temperature is due to a change in the quaternary and tertiary



structure compared to the wild type enzyme. A “loosening” of intersubunit contacts, or an increase in subunit flexibility, due to the introduction of the helix-destabilising proline residue, might be sufficient to explain the reduced thermal stability observed in the mutant enzyme. It has been shown that a difference of 1°C in melting temperature between wild type and mutant forms of a protein corresponds to a difference in energetic stability of approximately 2.1kJ/mol. Thus, in this case, the Ser 384 to Pro mutation would lead to a destabilisation of the enzyme by 6.3kJ/mol.

The yeast enzyme is known to be cold-labile (Kuczenski & Suelter, 1970), indicating that associations between apolar groups (which are significantly weakened at low temperatures) are an important feature in the stabilization of the tetrameric enzyme. An increase in temperature, therefore, might be expected to stabilize hydrophobic contacts over other forms of intersubunit contact. Obviously, a point will be reached where prolonged exposure to a denaturing environment will result in the loss of enzyme activity. The point mutation in the mutant enzyme may have disrupted an important hydrophobic contact contributing to the observed loss of thermal stability. The alpha helix, C $\alpha$ 2, is a known intersubunit contact area and so the implication that the mutation may have affected some physical property as well as the kinetic properties is not surprising. The serine to proline mutation would have increased the hydrophobicity of the C $\alpha$ 2 helix. As a result, it may be that an increase in the strength of the hydrophobic contact region is sufficient to explain the observed changes in kinetic and physical properties. An analysis of a range of point mutations engineered into bacteriophage T4 lysozyme have shown that the most successful ways of producing a more thermostable enzyme are: a) reducing the difference in entropy between folded and unfolded protein, which in practice means reducing the number of conformations in the unfolded state; b) stabilising the alpha helices, and c) increasing the number of hydrophobic interactions in the interior core.

The most obvious way of decreasing the number of unfolded

conformations is to introduce novel disulphide bridges, based on a knowledge of the tertiary structure of the folded protein. Where this is not possible, a reduction in the conformational freedom of the unfolded states, and hence a stabilisation of the native protein, may be produced by the introduction of proline residues. Proline residues have less conformational freedom in unfolded structures than any other residue since the proline sidechain is fixed by a covalent bond to the main chain. Such mutations can only be made at positions that neither change the conformation of the main chain in the folded structure nor introduce unfavourable contacts with neighbouring side chains. The detrimental effects of the introduced proline at residue 384 imply, therefore, that there have been some main chain conformational changes, or effects on residues near the introduced proline. This supports the desired intention of this residue change, which was to alter intersubunit contacts sufficiently to produce measurable effects in the kinetic or physical properties of the mutant protein.

In support of the conclusions expressed above, a point mutation at a dimer interface (glycine 418 to tryptophan), analogous to that produced in the mutant pyruvate kinase, has been observed to cause a significant lowering of the thermal stability of the dimeric enzyme glutathione reductase from *E.coli* (Scrutton et al., 1992). A pronounced destabilisation of yeast phosphoglycerate mutase has also been produced by a lysine to proline substitution in a subunit interface region (White et al., 1993).

The absorbance of the wild type and S384P mutant enzymes at 280nm ( $A_{280}$ ) was monitored as a function of temperature, in the presence and absence of the effector Fru-1,6-P<sub>2</sub>. In the presence of effector, the  $A_{280}$  of both the wild type and mutant enzymes was greater than the corresponding unligated enzymes at all temperatures studied (Fig. 74). This indicates that the effector acts to alter the conformation of each enzyme to expose more uv absorbing sidegroups (e.g. Trp, Tyr and Phe) to the solvent. The absorbance at 280nm increased as a function of temperature whether or not effector was present. This indicates that rising temperature causes a progressive conformational change that also leads to the exposure of uv absorbing groups to the solvent. The absorbance at 280nm reached a maximum at higher temperatures for the wild type and the mutant



enzymes before falling sharply. The maximum absorbance was observed at a lower temperature for the mutant enzyme than for the wild type enzyme. The maximum absorbance at 280nm was observed at a lower temperature for each enzyme when Fru-1,6-P<sub>2</sub> was present than when no ligand was added. The sharp fall in absorbance at 280nm can be attributed to the denaturation, aggregation and precipitation of the enzymes which effectively removes chromophoric groups from solution. The exposure of hydrophobic regions to the solvent would facilitate the aggregation of proteins via these exposed areas. The decreased ordering of water molecules around hydrophobic regions as the temperature is increased may influence the rate and extent of aggregation. The participation of water in the inactivation of pyruvate kinase is further suggested by the stabilization of the enzyme in the presence of 20% (v/v) aqueous glycerol solutions. Burying hydrophobic sidechains in the interior of the protein molecule, thereby shielding them from contact with the solvent, is a major determinant in the folding of proteins. Any treatment that results in the exposure of hydrophobic residues to the solvent would be expected to increase protein instability. The introduction of the helix destabilising proline residue may have resulted in the increased exposure of previously buried stretches of hydrophobic residues, thus contributing to the observed instability of the mutant.

Thus, in the presence of effector, both enzymes are in a more open conformation in which chromophores are more exposed to the solvent than in the unligated state. This leads to their more rapid denaturation as temperature is increased. The wild type enzyme is more resistant to thermal denaturation than the mutant enzyme.

A similar phenomenon has been observed in several other systems. An increase in absorbance at 280nm has been recorded with glutamate dehydrogenase from *Pyrococcus furiosus* as a function of temperature (Klump et al., 1992). Also, addition of Fru-1,6-P<sub>2</sub> to the pyruvate kinase from *E.coli* was observed to significantly increase its susceptibility to thermal denaturation, indicating that a pronounced conformational change had occurred (Speranza et al., 1990).

#### 4.11 ANTIBODY STUDIES

A polyclonal antiserum against wild type pyruvate kinase from yeast was raised in, and purified from, rabbits. The antiserum was used in a variety of different experiments with varying degrees of success.

The antiserum was first used in Western blotting experiments to determine the specificity and affinity of the preparation. A mixture of proteins from a number of different sources were separated by electrophoresis on an SDS-polyacrylamide gel. The proteins were electro-blotted onto a nylon membrane and incubated with varying dilutions of the antiserum as described earlier (Section 2.8). The optimum dilution of antiserum to use was found to be 1:1500. The polyclonal antiserum was found to react only with wild type yeast pyruvate kinase (Fig. 75). It did not react with purified rabbit pyruvate kinase, or with any of the proteins in cell extracts from *E.coli*, *Bacillus subtilis*, *Staphylococcus aureus* or *Thermoplasma acidophilum*. Thus, it can be concluded that the polyclonal antiserum prepared from the rabbits was specific to the antigen it was raised against, did not cross-react with host enzyme, and displayed a high affinity for the target antigen. One of the problems confronting the producers of mutated enzymes is the effect of the mutation on catalysis. It is possible to interfere with the catalytic mechanism of the enzyme very easily, especially when the nature of the active site is not fully known. A procedure for identifying inactive mutant forms of yeast pyruvate kinase, that may be produced during site-directed mutagenesis experiments, is now available.

Immunodiffusion experiments were also attempted. The technique relies on the diffusion of antigen and antibody towards each other from separate wells cut into an agarose gel. When the two proteins meet, they combine and form a precipitate. The distance of the precipitate from the wells depends upon the concentration of the two components. Pyruvate kinase and other proteins were allowed to diffuse towards a sample of either polyclonal antiserum or a control well containing a sample of pre-immune serum. Under the conditions described in the experimental protocol (Section 2.8.1) no precipitation was observed with either the pre-immune serum or the polyclonal antiserum. There are several

possible reasons for this lack of precipitation. One, or both, of the proteins could have denatured during storage. The pyruvate kinase preparation was used fresh from the final stages of purification and was found, during standard enzyme assays, to be highly active. The antiserum was stored at  $-20^{\circ}\text{C}$ . It has been reported that impure samples of antiserum do not retain their activity for long unless stored at  $-70^{\circ}\text{C}$ . The antiserum used in this assay was purified using a rapid method that relied on the binding of impurities to an anion-exchange matrix. Hence, the possibility of residual contaminants eluting with the non-retained antiserum cannot be discounted. Thus, the denaturation, or proteolysis, of the antiserum during storage preventing the formation of an antibody-antigen precipitate would be possible. Another way in which the interaction of antibody and antigen could be disrupted is by the incubation of the components in non-optimal conditions. The matrix for the interaction consisted of pyruvate kinase assay buffer in which 1% (w/v) agarose had been dissolved. This may not have been suitable for the formation of precipitates due, possibly, to the high salt content interfering with the electrostatic interaction of antibody and antigen. It has also been reported that sodium azide, commonly used to prevent microbial contamination, interferes with the interaction of antibody with antigen. The preparations of antiserum used in these experiments were stored in the presence of 0.02% (w/v) sodium azide. It may also have been the case that the range of concentrations of antibody and antigen used in these experiments did not fall within the zone of maximum interaction that is commonly observed with antibody-antigen precipitation studies. Either too much or too little of one of the interacting components would result in the formation of soluble, rather than insoluble, aggregates. Thus, although an interaction between antigen and antibody had occurred, it would not have been observed.

A direct precipitation of pyruvate kinase from solution with varying concentrations of polyclonal antiserum was attempted (Fig. 76). This immunotitration experiment was also unsuccessful in that the activity of the samples incubated in the presence of the polyclonal antiserum was not significantly different from those incubated with the pre-immune serum. The

reasons for the failure of these experiments appear to be different from those for the failure of the immunodiffusion experiments. The denaturation of the polyclonal antiserum is the most likely explanation. However, the antiserum in this instance were stored at  $-70^{\circ}\text{C}$  in the absence of sodium azide. The incubation buffer was of sufficiently low ionic strength not to interfere with the antibody-antigen interaction. The range of dilutions of antibody used was much lower than that used in the immunoblotting experiments and so would have been sufficient to cause some interaction with the enzyme. Thus, it appears that the titre of anti-pyruvate kinase antibodies in the rabbit serum was extremely low due, perhaps, to poor immunogenic responses from the host animals or, more likely, to losses during purification and storage.



## 4.12 COMPUTER PREDICTIONS OF SECONDARY STRUCTURE

Several computer programs exist for analysing protein secondary structure. The programs most readily available are those produced by the University of Wisconsin Genetics Computer Group (UWGCG)(Devereux et al., 1984) and the program PREDICT (Sawyer et al., 1988). The wild type and mutant forms of yeast pyruvate kinase were analysed by a number of these programs.

The program PEPLOT displays a variety of data. The most useful are the alpha helix/beta strand prediction plot (Chou & Fasman, 1978), the hydrophobic moment plot (Eisenberg et al., 1984) and the hydropathy plot (Kyte & Doolittle, 1982).

When the wild type and mutant pyruvate kinase enzymes were analysed by these methods none of the plots drawn by this program showed any significant difference between any of the calculated parameters for either of the enzymes. i.e the secondary structure, the probability of certain residues being on the surface of the protein or buried, and the exposure of certain residues to the solvent were indistinguishable (Fig. 77 and 78).

The Chou and Fasman alpha and beta conformational potentials are plotted as running averages of four adjacent residues. The horizontal lines across the panel indicate the minimum levels for predicting alpha and beta structures. The small hashmarks at the top of the panel classify each residue as forming, breaking or indifferent for beta structures. Likewise the hashmarks at the bottom of the panel classify each residue as alpha-forming, breaking or indifferent. Maximum resolution of structures is best seen in small sections of the polypeptide of interest (40-60 residues). The hydrophobic moment is a measure of the "amphiphilicity" of a sequence that is helpful for identifying structures located at the interface between hydrophobic and hydrophilic regions of a protein. Thus, segments of secondary structure that are located so that one side faces the hydrophobic interior of the protein and the other faces the exterior or solvent have high hydrophobic moments (i.e. greater than 0.4). The

hydrophobic moment may also be useful for helping locate transmembrane segments which typically have low hydrophobic moments and high hydrophobicities. This plot therefore allows one to predict whether the secondary structures predicted by the Chou and Fasman method are located on the surface of the protein, are transmembrane segments, or are within the globular core of the protein. The hydropathy profile is frequently used to find intra-membrane regions of proteins. It is also commonly used to try to predict the positions of antigenic sites on proteins. The hydropathy profile is calculated using a window nine residues wide. Peaks in this panel indicate hydrophobic (interior) regions, and valleys hydrophilic (surface) regions. Globular proteins typically produce hydropathy plots with hydropathy values ranging from +2 to -2. Trans-membrane segments of proteins usually produce much higher hydropathy scores (typically in the +3 to +4 range).

Another program, PEPTIDESTRUCTURE, shows a very significant difference between the secondary structure of the wild type (Fig. 79) and mutant (Fig. 80) forms of the enzyme. The output from this program seems to indicate that the serine 384 to proline mutation disrupts the alpha helix in which it is situated compared to the structure seen in the wild type enzyme. This is supported by the experimental evidence of the different properties exhibited by the mutant enzyme and the known behaviour of proline as a helix disrupting amino acid. Further, a CONTIN analysis of the secondary structure of the wild type and mutant enzymes indicates that the mutant enzyme has lost some alpha helical structure and gained some beta sheet structure (Table 12).

The interpretation of these plots is often difficult. The plots themselves are often crude and simplistic and do not accurately reflect the real situation. The vast array of possible conformations available to a protein in solution can not realistically be represented by a computer program. The programs themselves are quite old, e.g. Chou and Fasman (1978), Kyte and Doolittle (1982), and although the algorithms on which they calculate the potential secondary structure are based on real data obtained from protein sequence databases, they cannot readily be updated or improved as our knowledge of protein secondary structure increases. As a result, the output from these plots is perhaps less sophisticated

than other, more recent, programs in terms of accuracy in calculating the secondary structural elements of proteins.

In an attempt to overcome any inaccuracy produced by analysing sequences by only one algorithm, the PREDICT program was also used to determine the secondary structure of the wild type and mutant enzymes (Fig. 81 and 82). This program is essentially a combination of eight different secondary structure prediction programs. The output from the program is a series of panels in which the helix, beta strand and coil elements are displayed against the number of programs that predict their occurrence within a particular sequence. As a result, an element of secondary structure scoring highly indicates a greater probability of that structure being present than if it had a lower score. A low score does not mean that that element of secondary structure would not form, just that the confidence limits of one being able to say that it does occur are lower. The PREDICT plot for the wild type enzyme shows a very strong probability of there being an alpha helix in the middle of the given sequence (Fig. 81). This region corresponds almost exactly to helix C $\alpha$ 2, and shows that the PREDICT algorithm is sufficiently sensitive to allow interpretation of secondary structural features associated with small sections of sequence. The PREDICT plot for the mutant enzyme however, is not much different to that of the wild type enzyme (Fig. 82). A small difference at the N-terminus of the alpha helix is observed. The substitution of the serine with a proline has caused a reduction in the number of programs attributing a helix structure to that part of the sequence. The difference however, is only small and is not what was expected. A much larger destabilising effect of proline was anticipated, resulting in a dramatic reduction in the attribution of a helical structure to the affected part of the sequence by the prediction programs. It is often the case however, that a single proline residue present within a strong helical region does not have the expected destabilising effect when assessed by a number of secondary structure prediction programs (MacArthur & Thornton, 1991). The most dramatic destabilising effect is observed when the residue(s) immediately prior to the proline are within beta strand structures. Proline residues within helices are



tolerated by the prediction programs when the residues immediately preceding the proline are hydrophobic and when the proline is close (within 3-4 residues) of the N-terminus of the helical region. From the given sequence it can be seen that the proline substitution is the sixth residue of a 13-residue helix and that the three residues preceding the proline are the hydrophobic residues valine and alanine. Thus, it is not surprising that the destabilising effects of proline are not observed with any of the computer prediction methods. This does not mean, of course, that the proline substitution does not have any effects on the enzyme *in vivo*.

In a sense these programs are not designed to provide accurate data, merely to act as an aid to interpretation. After all, there are very few examples of proteins where all that is known about them are their amino acid sequences, thus requiring computer programs to provide information not otherwise available. There are now accurate physical techniques for determining the secondary structure of proteins e.g. circular dichroism, and so reliance on these programs for this sort of information may soon no longer be necessary.

Having said that, plots of structural measurements like PEPLOT and PREDICT can be of significant value for detecting similarity between sequences. Similarity that is often difficult for the human or the computer to recognise in the primary sequence may generate patterns of secondary structure measurements that are recognisably similar when plotted.

#### 4.13 SEQUENCE COMPARISON OF PYRUVATE KINASES

The complete primary amino acid sequences of all pyruvate kinases known to date are shown in Table 1. In this respect it is the most comprehensive compilation of pyruvate kinase sequences yet prepared. Sequence information is available from most types of organisms found in nature-bacteria, fungi, protozoa, plant, bird and mammal. Various tissues within these organisms are also represented e.g. the sequences for mammalian blood, liver and muscle isoenzymes and plant cytosolic and plastidic isoenzymes are available. From the alignment it can be seen that the sequences are clearly related to each other.

The greatest variation in the sequences lies in the size and composition of the N-terminal region. This region forms a small flexible domain that is thought to interact with the other domains and contribute to intersubunit communication (Fig.3). The higher eukaryotes show the highest degree of similarity in this region. However, differences do exist-the most significant being in the presence of a phosphorylation site on a short N-terminal extension found in rat and human liver and rat erythrocyte forms but absent in the muscle forms. The only region of secondary structure in the N-terminus, identified from X-ray crystallographic studies on the cat muscle enzyme, are two short alpha helices. The great variation in sequences makes it impossible to positively attribute these features to the other enzymes. Undoubtedly secondary structural features exist but their identification must await more detailed analysis of the other enzymes. The flexibility of the N-terminal region in the cat muscle makes precise predictions of its behaviour difficult. Its contribution to intersubunit communication is supported by the great variation observed in this region across the enzymes so far sequenced. The implication is that sequence variability is in some way contributory to variety of function. The great length of the N-terminal region in the plant enzymes and information provided by Dr.S.Blakeley (Queen's University, Kingston, Canada) suggest that such sequences may be involved in transport across intracellular membranes e.g. the outer and inner chloroplast membranes. Evidence that such sequences are found in other enzymes comes from studies on pyruvate phosphate dikinase from maize (*Zea*

ways) (Matsuoka et al., 1988). These workers found that an N-terminal sequence composed of three separate modules functioned in transporting the enzyme across the chloroplast membrane. An alignment of the putative signal from maize with the plant N-terminal regions of pyruvate kinase shows only a poor correlation between sequences (Table 18). This may indicate that other, previously unidentified chloroplast translocating signals exist in these enzymes. A more convincing chloroplast signal peptide is found in the tobacco and castor seed isoenzyme A. These enzymes show partial identity to a signal peptide found in the small subunit of ribulose-1,5-bisphosphate from *Chlamydomonas* (Mishkind et al., 1985) (Table 18). The signal peptide from this enzyme is also comprised of three blocks or domains. An N-terminal block rich in serine and threonine residues comprises domain I. This is followed by a glycine/leucine/lysine-rich block in close proximity to several proline residues. Domain III consists of a region rich in serine residues. In tobacco and castor seed isoenzyme A all these elements can be found. The series of four asparagine residues in this sequence may form the signal peptide cleavage site (Blakeley et al., 1991). Three adjacent asparagine residues are also found in the tobacco G isoenzyme in a similar position and so may also indicate the site of cleavage of a signal peptide. It is worth commenting that the first 100 residues of all of the chloroplast sequences shown in Table 18 are rich in hydrophobic residues which would facilitate transport across intracellular membranes.

A remarkable number of residues are conserved across all the sequences. These are likely to be involved in substrate binding and orientation and in preserving essential interdomain and intersubunit contacts. Domains A and C appear to be the most conserved, with domains B and N being less well conserved respectively. The extreme C-terminal regions, forming part of domain C, are also highly variable. Like domain N, they may function in intersubunit communication and so contribute to the variety of kinetic properties displayed by the pyruvate kinases. It is interesting to note that an examination of the computer model of the yeast pyruvate kinase subunit reveals that portions of the last 50 residues of domain C are in very close proximity to domain N and so together might form the means of intersubunit interaction.

Tb.pA  
 Cs.pA  
 Cs.pB  
 Tb.pG  
 Bn.pG  
 PPKK

SQALNFFVSSSSRSPATFTISRPSVFPSTGSLRLLVKKSRLTLVVEASSAAASDIDEPQS  
 SQSLHF-SPNLTFAKQFPF-KLPLFPFTSNS-RYPVNN-YKSLSIKASTSPSSS-SDPQ-  
 A----VVVKDLEEAVRVVVLAVLRDMEVVVVLVTAVMGVVGDMNV-ARINMCHGTREWHK  
 A-TMN-LPTGLHVAAPASLNRLSSAKNVGDLFFSDSRHRKRVTNSQIMAVQSLEHIIH-  
 -----LSPNGGSAS-----TRSDKFLKPAFVRVVLGNEAKKSGRVSVRGGRKVDTTVR  
 MAA-----SVSRAICVQKPGS-----KCTRDREATSFARRSVAAPRPPHAKA

Tb.pA  
 Cs.pA  
 Cs.pB  
 Tb.pG  
 Bn.pG  
 PPKK

SPVLVSENGSG--GVLSSATQEYGRNAAPGTDSSSIEVDTVT-----  
 --VLVADNGTGNSGVLYNNNN----KSVTVSDPSSIEVDAVTETELKENGFR  
 SVIERVRR-----LNEEKGFVAIMMDTEGSEIHMGLGASSAKAEDGE  
 -----GVNNNVYANYVNFNVPSSGYSLGQESVYLNSPRKTXIVCTIGP  
 SARVETEVIPIVSPDV--PNREEQLERFLEMOKFSDTSVEMWSKPTVRRKTKI  
 AGVIRSDSGAGRGQHCSPLRAVVDAAPIQT-----

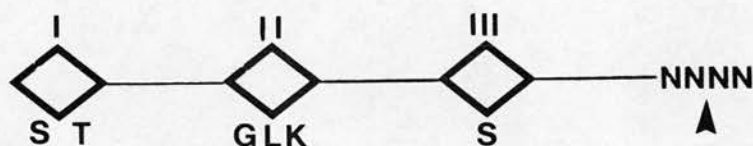


Table 18 N-terminal sequences of plant plastidic pyruvate kinase isoenzymes compared with maize pyruvate, phosphate dikinase (PPDK) signal sequence.  
 Underline = domains of maize PPDK signal sequence (Matsuoka et al., 1988).  
 Overline = blocks sharing similar motif to *Chlamydomonas* ribulose-1,6-bisphosphatase signal sequence (Mishkind et al., 1985).  
 Cs.pA/pB = castor seed pyruvate kinase plastid isoenzymes A and B  
 Tb.pA/pG = tobacco pyruvate kinase plastid isoenzymes A and G.  
 Bn.pG = *Brassica napus* pyruvate kinase plastic isoenzyme G.

Cartoon depicts domain structure of *Chlamydomonas* ribulose-1,6-bisphosphatase signal sequence. Arrow indicates putative signal sequence cleavage site.

The plant plastid sequences show some interesting features apart from the extreme length of the N-terminus. A deletion of some seven residues in the castor seed plastid isoenzyme B effectively removes the majority of an alpha helix ( $A\alpha 1$ ). The consequences of this on the behaviour of this enzyme with respect to the other plant enzymes cannot be predicted. It is worth noting at this point that a similar deletion is seen in the same region of the *Yarrowia lipolytica* enzyme, corresponding to the complete removal of the helix  $A\alpha 1$ . A detailed study of the X-ray crystal structure of the cat muscle enzyme did not suggest that  $A\alpha 1$  played any critical role in enzyme activity (Muirhead, 1987). However, any mutation that affects the integrity of a highly conserved structure such as the alpha/beta barrel of domain A is likely to have a pronounced effect on the kinetic properties of such an enzyme. A comparison of the X-ray structure and/or kinetic parameters of this enzyme with the otherwise highly similar enzyme from *S.cerevisiae* would be of interest.

The plastidic A and B isoenzymes from castor seed and tobacco all show a seven residue insertion in domain B corresponding to an extension of a beta strand ( $B\beta 7$ ) or, more likely, forming a flexible loop between two adjacent beta strands ( $B\beta 7$  and  $B\beta 8$ ) (Table 1). The beta strand  $B\beta 7$  has been implicated in forming a subunit interface. The plastidic G isoenzymes from *Brassica napus* and tobacco do not share this feature. Thus, there exists the possibility that the A and B isoenzymes have different regulatory properties compared with the G isoenzymes because of this structural difference. Unfortunately, no kinetic data are available for the three different isoenzymes to confirm this hypothesis. The G isoenzymes appear to be a quite distinct group and are as unrelated to the A and B isoenzymes as they are to other prokaryote and eukaryote enzymes.

The sequence LDTKGPEIRT (corresponding to residues 111-120 of the cat muscle enzyme) is well conserved across all the sequences and appears to be involved in binding the substrate ADP. In particular, residues Lys 114, Ile 118 and Arg 119 are important in this respect. This sequence has even been found in



a partial sequence from the archeabacterium *Thermophilus acidophilum* (Potter, 1993).

Other important regions conserved across most of the enzymes are the residues FASFIR (corresponding to residues 239-244 of the cat muscle enzyme), the conserved lysine 269 (presumed to be the proton-donating catalytic residue), residues MVARGDLG (corresponding to residues 290-297 of the cat muscle enzyme) and residues PTRAE (corresponding to residues 339-343 in the cat muscle enzyme) (Table 1).

The sequence FASFIR forms a beta strand ( $A\beta 4$ ) and a small loop. This region is in a critical part of the active site and is involved in providing ligands for the binding of both PEP and ADP. The PEP binding site is located in the loops that connect strands  $A\beta 3$  and  $A\beta 4-6$  to domain B and helices  $A\alpha 4-6$  respectively (Muirhead, 1985). In particular, Ser 242 serves in orientating PEP and Phe 243 provides a hydrophobic contact for the adenine ring of ADP. The sequence MVARGDLG forms a beta strand ( $A\beta 6$ ) and part of an alpha helix ( $A\alpha 6$ ). This region is essential for a number of reasons. First, the helix  $A\alpha 6$  is an important intersubunit contact. Second, this region also provides ligands for binding substrates at the active site, especially Arg 293 which is involved in ADP binding. Third, the  $A\beta 6/A\alpha 6$  region provides ligands for the enzyme-bound divalent cation. The sequence PTRAE forms part of the helix  $A\alpha 7$ . This helix is also an important intersubunit contact area.

The alpha helices  $C\alpha 1$  and  $C\alpha 2$ , thought to be critical in communicating the allosteric effect in the M2 isoenzyme, are not well conserved across the sequences. In fact, no single residue is absolutely conserved in these areas. In particular,  $C\alpha 1$  is quite poorly conserved with the plant plastid A and B isoenzymes having an insertion in this region and the G isoenzymes having a deletion. Indeed, a comparison of the yeast enzyme with the cat muscle enzyme reveals that the sequence corresponding to helix  $C\alpha 1$  is actually better

represented as a beta strand (Muirhead, 1987). This can clearly be seen in a secondary structure prediction plot of the relevant portion of the enzyme (Fig.79). The fact that these alpha helices are poorly conserved may indicate that they are capable of imposing a variety of properties on the enzymes that possess them, as opposed to the rigid conformations and limited flexibility of function imposed by having a large number of identical residues. The relevance of *differences* in the sequences of these alpha helices becomes apparent when it is noted that the only difference between the allosterically regulated M2 isoenzyme and the non-regulated M1 isoenzyme from rat muscle lies largely within these two alpha helices.

The effector site, identified in the *E.coli* enzyme (Speranza et al., 1990) and corresponding to the cat muscle residues 423-438, is more conserved across the sequences than either of the alpha helices C $\alpha$ 1 and C $\alpha$ 2.

It comprises a beta strand (C $\beta$ 1), an alpha helix (C $\alpha$ 3) and the sequence in between. The presence of such sequence similarity in this area may indicate the presence of a functional, or vestigial non-functional, effector site in many of the enzymes sequenced. Many are in fact known to be regulated by allosteric effectors. This site has been identified in the non-allosterically regulated cat muscle enzyme as a potential secondary nucleotide binding site (Muirhead, 198 ). It is impossible to predict the identity of potential ligands or the effect of their binding to the enzyme by simply comparing primary amino acid sequences. It is also dangerous to interpolate the potential structure of these regions from the known structure of the only enzyme so far crystallised, the non-regulated cat muscle enzyme. However, it is clear, from what has been said before about the composition of C $\alpha$ 1 and C $\alpha$ 2, that the primary sequence of these regions need not be similar for them to participate in ligand binding and contributing to transmitting an allosteric effect across the subunits. Other studies involving computer modelling of the effector site in the cat muscle enzyme suggests that totally different residues are involved in effector binding (Clayden, 1987). Hydrogen bonding between enzyme and effector could be facilitated by Val 468,



Pro 470, Arg 42, Leu 41 and Ser 66 (cat muscle numbering). Potential ligands for the two phospho groups of Fru-1,6-P<sub>2</sub> were identified as Arg 42 and Arg 105. However, not all of these residues are conserved in the yeast enzyme. The most important changes in the yeast enzyme involve Ser 66, which is changed to Ala, the absence of Arg 102 and the addition of a negative charge from Glu 498 (which is Ala in the cat enzyme).

It is far from certain that the site identified in the cat muscle enzyme as a second nucleotide binding site functions as a Fru-1,6-P<sub>2</sub> binding site in the yeast enzyme. There are substantially fewer potential ligands correctly orientated in the yeast enzyme that would be able to bind the effector. Crystals of an allosteric pyruvate kinase, formed in the presence of the effector, have never been prepared in a form suitable for high resolution X-ray diffraction studies. Also, it can not be stated with certainty that conformational changes originating in this region of the enzyme would be able to produce the observed changes in kinetics.

The effector site in the *E.coli* enzyme was identified by the labelling of a reactive lysine (residue 366) by pyridoxal 5'-phosphate in the presence of the effector. That this lysine is even close to the actual site of effector binding must also remain conjecture. A conformational change on effector binding could lead to the burying of a lysine sidechain, and hence its protection from reaction with pyridoxal 5'-phosphate, some distance from the effector site itself. A better way of identifying the ligands involved in the binding of the effector molecule, in the absence of X-ray crystallographic data, would be the preparation of a series of radioactively-labelled Fru-1,6-P<sub>2</sub> analogues with different reactive functional groups, that are capable of covalent attachment to the sidegroups of suspected ligands in the binding site. A similar series of experiments with a variety of ADP analogues has helped elucidate the ligands involved in nucleotide binding (Vollmer & Colman, 1990).

A comparison of the cat muscle and *B.stearothermophilus* sequences identified a region that was proposed to form a loop at the entrance of the allosteric site (Walker et al., 1992). This region, corresponding to residues 97-102 of the cat muscle sequence, was absent in the *B.stearothermophilus* and the other allosterically regulated enzymes then sequenced. The absence of the loop

from the allosteric forms suggested that the effector binding pocket was flexible and could adopt a variety of alternative conformations. The binding of the effector molecule was proposed to hold the pocket open resulting in the formation of the active conformation. Conversely, in the non-regulated forms, the presence of the loop was proposed to hold the pocket permanently open locking the enzyme in the active conformation. However, from the more extensive sequence records now available, this same loop region can be identified in the vertebrate M2, R and L isoenzymes. All of these isoenzymes are allosterically regulated. In the M2 isoenzymes from human and rat, the loop sequence is identical to that from the cat muscle enzyme. In the R and L isoenzymes the loop is highly similar. The presence of the loop sequence in these isoenzymes suggests a more complex behaviour and /or function for the loop structure. The ability of the R and L isoenzymes to be phosphorylated may negate or modulate the effect of the loop. The M2 isoenzymes are not phosphorylated yet still clearly display allosteric properties. The loop region may, therefore, be unimportant in determining the conformation of the effector site. It should be noted that the most potent effector of the *B.stearothermophilus* enzyme is not Fru-1,6-P<sub>2</sub> but ribose-5-phosphate. Thus, the loop may have a specific function in this enzyme but be redundant or ineffectual in the other enzymes.

An interdomain salt bridge between Asp 356 (located in Aβ8) and Arg 444 (located between Cα3 and Cβ2) has been identified (Walker et al., 1992). This feature is proposed to stabilize the active R conformation of the enzyme. It is interesting to note that these two residues are conserved in all the pyruvate kinase enzymes listed in Table 1, except the two *E.coli* isoenzymes. This suggests that the proposed salt bridge is very likely to be an important structural feature.

The C-terminal regions of the enzymes are almost as varied as the N-terminal regions. The longest C-terminal tail is found on the *B.stearothermophilus* enzyme. This may have something to do with the thermal stability exhibited by this enzyme. However, confirmation or refutation of this

hypothesis will have to await the sequencing of other pyruvate kinases from thermophilic organisms. The proximity of the N and C termini of the cat muscle pyruvate kinase suggests that the region occupied in the tetramer by the N-terminal domain might be substituted by the C-terminal extension. It is interesting to note that all the bacterial enzymes so far sequenced have short N-terminal domains and longer C-termini, thus adding weight to this hypothesis.

The plant cytosolic enzymes show a 13 residue insertion in the region between a beta strand ( $C\beta 2$ ) and an alpha helix ( $C\alpha 4$ ) that is absent in all the other sequences. This sequence could form a loop between these two elements of secondary structure. This potential loop is composed of residues with bulky, hydrophobic sidegroups e.g. phenylalanine, tryptophan and valine, and may thus have a role in maintaining hydrophobic contacts between subunits or domains, or in shielding some region from the solvent. The region is highly conserved amongst the cytosolic enzymes and so may well perform some essential function in these enzymes.

#### 4.14 ALIGNMENT AND PHYLOGENETIC ANALYSIS OF PYRUVATE KINASE SEQUENCES

Two phylogenetic trees are presented (Fig. 83 and 84). Both have been constructed by computer analysis of the primary sequences shown in Table 1. The first tree (Fig. 83) has variable branch lengths which gives evolutionary distances in PAM units. Evolutionary relationships between amino acid sequences are expressed as "accepted point mutations per 100 residues" (PAMs). This parameter, which was calculated according to Dayhoff (1978), takes into account the back mutations and multiple hits that may have occurred during evolution. This tree however, is only one of many possible trees that can be generated using the same data. Tree topologies may vary slightly with the order in which species are added to a tree (the order of the alignment). One way to get information about the tree topology is to do a bootstrap analysis. Here, columns in a multiple alignment are sampled at random and new nonsense alignments of identical length are created. If mutations occurred at random within a sequence, the tree topology should not change. The second (consensus) tree, with identical branch lengths, is the most probable tree after 100 bootstrap analyses (Fig. 84). It can only provide information about the likelihood of a specific branching point. It contains no information about evolutionary distances.

The clustering of sequences in the first tree corresponds to the taxonomic hierarchy of the organisms from which they originate. Thus, the vertebrates occupy one distinct branch along with the other eukaryotes represented in this tree - the fungi and protozoa. The plants and bacterial sequences occupy their own separate branches. This reflects the distinct Kingdoms of organisms found in nature. Among the eukaryotes, the vertebrate isoenzymes form a very tight cluster. The mammalian R and L isoenzymes are separate from the M1 and M2 isoenzymes. This indicates that they have only recently diverged from a common vertebrate ancestor. The fungal enzymes are all clearly related, being also only recently diverged from a common ancestor. The protozoan enzymes also cluster together. The tree indicates that the protozoa / vertebrate divergence occurred

after the protozoa / fungi divergence and accords well with our current knowledge of evolutionary relatedness.

Plant cells evolved from symbiotic associations that included (at least) a nucleocytoplasmic host cell, a mitochondrial ancestor, and a chloroplast ancestor (Woese, 1987). From protein and nucleic acid sequence studies it is now possible to identify with relative certainty the taxa from which these ancestors came. Mitochondria are descended from a group of purple sulphur bacteria, and chloroplasts from cyanobacteria. The origin of the nucleocytoplasmic host cell is less certain, but appears to be from sulphur metabolizing archaeobacteria. It has been proposed that the chloroplast ancestor oxidised  $H_2S$  by using it as an electron donor during photosynthesis (Searcy, 1992). Sulphur is particularly suitable for such symbiotic associations because, compared with oxygen, it is less toxic, more versatile in its chemistry and easily trapped and recycled within each association.

The plant cytosolic enzymes form another tight grouping and appear distinct from the plant plastidic enzymes. This indicates that the plant cytosolic / plastidic divergence occurred a very long time ago. However, the clustering of the plant cytosolic sequences may merely be an artefact of the way the tree is drawn. The angle of the plant cytosolic enzyme branch, and the precise location of its root, may bias its final position and give the false impression that it is more distantly related to the bacterial and fungal branches than it actually is.

The bacterial and plant plastidic enzymes form the most diffuse grouping. This may simply reflect the small range of organisms sampled. Although all the bacteria apparently share a common ancestor, the sequences shown appear to have diverged markedly. This is also true of the plant plastidic isoenzymes. The unusual and anomalous placing of the pyruvate kinase isoenzyme II from *E.coli* (kpy2 *ecoli*), on the plant plastidic branch, may give support to the theory that chloroplasts are derived from the descendants of endosymbiotic bacteria that invaded early eukaryotic cells. It should be noted that a lateral transfer of the pyruvate kinase gene from a cyanobacterium to *E.coli* may also account for the unusual position of this sequence in the tree.

The consensus tree (Fig. 84) only provides information about the point



of divergence of sequences, not on their evolutionary relatedness. The unrooted tree allows one to determine the order in which sequences appear to diverge from common ancestors. Again, a distinct clustering of sequences is observed. Vertebrate, fungi, protozoa, bacterial, plant cytosolic and plastidic zones can be clearly defined. An example of the usefulness of this kind of tree can be seen when one considers the vertebrate isoenzymes. In the vertebrate zone, the R and L isoenzymes and the M1 and M2 isoenzymes clearly share a common ancestor. Not surprisingly, the rat and human R and L isoenzymes appear to have diverged from an ancestral enzyme that is different from the ancestor from which the rat and human M1 and M2 isoenzymes have diverged. Although no estimates of the time of such a divergence can be calculated from this sort of tree in terms of millions of years, a temporal ordering of successive divergences can be inferred.

More interestingly perhaps, in this particular consensus tree, is the confirmation of the unusual position occupied by the isoenzyme II of *E.coli*. It appears that all the plastidic isoenzymes share a recent common ancestor with the *E.coli* isoenzyme II. The plant cytosolic / plastidic ancestor is very much older. Thus, it is more probable that the plant plastidic enzymes have descended from a bacterial endosymbiotic invader of a protoeukaryote than from a cytosolic enzyme that has subsequently been sequestered into an intracellular organelle.

There remains, however, a query over the construction of the tree itself. What parameters govern the direction and angle a particular branch makes with any other? This factor is presumably accounted for in the algorithm used in constructing the tree but its appropriateness is beyond the scope of this discussion. One should be aware that the position of a particular branch in close proximity to another may not necessarily imply evolutionary relatedness between the two.

## 5.0 CONCLUSIONS

This thesis has described the purification and characterisation of a novel form of the enzyme pyruvate kinase from the organism *S.cerevisiae* that was produced by site-directed mutagenesis. In an alpha helix considered as essential for the transmission of the allosteric effect across intersubunit contact zones, a serine residue (Ser 384) was mutated to a proline. The proximity of serine 384 in subunits 1 and 2 to the corresponding serine 384 in subunits 3 and 4 respectively, was likely to increase the helix-destabilising effects of the proline substitution. As a result, a variety of effects upon substrate binding properties, response to allosteric effectors, thermal stability and overall protein conformation were expected. Several studies to probe these, and other, aspects of the mutant protein and to compare them with the wild type protein were undertaken. From the results obtained, a number of conclusions can be drawn.

### 1) PURIFICATION

A revised purification protocol has been devised that improved upon previous methods in terms of:

- i) speed-pure protein, ready for a variety of kinetic studies, could be prepared in under 36 hours.
- ii) high yield-up to 15mg of pure enzyme could be produced from one litre of culture.
- iii) purity-an homogeneous enzyme preparation, greater than 98% pure, could be generated.
- iv) reproducibility-the procedure was highly robust and was reproducible over the course of the project.
- v) convenience-a minimum of purification steps ensured speed and high stability of the preparation.

### 2) KINETIC PROPERTIES OF THE MUTANT ENZYME

The mutant enzyme was active only in the presence of high concentrations of the positive allosteric effector fructose-1,6-bisphosphate. In the absence of this effector the enzyme had a  $k_{cat}$  250-fold lower than the wild



type enzyme. The fully activated mutant enzyme had a  $k_{\text{cat}}$  approximately 68% of the wild type enzyme. This indicates that the point mutation introduced into the enzyme has affected either the ability of the mutant protein to bind substrates and effectors, or to catalyse the kinase reaction as efficiently as the wild type enzyme, or both.

### **3) CHANGES IN CONFORMATION INDUCED BY LIGANDS**

Large conformational changes have been detected upon substrate and effector binding, in the wild type and the mutant enzymes, by a variety of techniques. The conformational change in the mutant enzyme is different to that undergone by the wild type enzyme. This is shown by the differential response of the two enzymes to digestion by trypsin, inhibition by NEM, thermal stability and changes in fluorescence emission. These changes can be quantified in terms of  $T_{50}$  values for the digestion, inhibition, and thermostability studies and  $S_{0.5}$  and  $n_H$  values for the kinetic and fluorescence studies.

### **4) ALTERED CONFORMATION OF THE MUTANT ENZYME**

It appears that in the absence of the effector, the mutant enzyme cannot adopt the conformation required for full catalytic activity. The effector changes the conformation of the enzyme, allowing residues important in catalysis to adopt the correct orientation, or to allow flexing of parts of the molecule involved in intersubunit communication. This interpretation is compatible with independent findings that point mutations are capable of disrupting catalysis, intersubunit communication and protein conformation.

### **5) SECONDARY STRUCTURE PREDICTIONS**

An attempt has been made to determine the extent of the disruption caused by the point mutation by reference to generally available secondary structure prediction programs. One method in particular indicated that the serine to proline mutation would reduce the length of the important alpha helix,  $\text{C}\alpha 2$ , at its N-terminal region and convert it to a length of beta strand. Changes in

secondary structure were monitored by circular dichroism spectroscopy. The results from these experiments indicated that, in the mutant enzyme, the amount of alpha helix was decreased relative to the wild type enzyme and the amount of beta strand was increased. However, the overall secondary structure was not significantly different between the two forms and so indicates that the two enzymes adopt a generally similar folded conformation. Greater changes in the quaternary and tertiary structure were observed with the fluorescence, trypsin digestion and NEM inhibition studies.

## **6) SEQUENCE ALIGNMENT**

The most comprehensive collection of pyruvate kinase sequence data yet assembled indicated that the most conserved residues were involved in substrate binding and maintaining the conformation of the active enzyme. Residues involved in effector binding or intersubunit communication were less well conserved. This indicates that the degree of interaction between subunits, and the overall conformation adopted by the enzymes listed, may vary considerably. There are more allosterically regulated enzyme sequences known than there are sequences from non-allosterically regulated enzymes. However, the only X-ray crystallographic data for the quaternary structure of the enzyme comes from the non-regulated cat muscle enzyme. This reflects the difficulty of isolating crystals of the allosterically regulated forms. The implication is that allosterically regulated enzymes are more flexible and have a more varied range of conformations than do the non-regulated forms. Thus, the model of the cat muscle enzyme may not be the most suitable for analysing the other enzymes considering their range of activity, the mode of their regulation, and the range of organisms from which they have been isolated.

## **7) IDENTIFICATION OF RESIDUES FOR FURTHER MUTAGENESIS STUDIES**

Several obvious targets for site-directed mutagenesis can be identified. Considering that so few residues are conserved across all the sequences analysed, those that are must contribute some essential function. It may be

possible to alter the specificity of the active site by changing the ligands involved in substrate binding e.g. Lys 269, Glu 271, Ser 242 and Phe 243. The precise location of the effector site is in doubt. The effect of point mutations in the suspected areas on the binding parameters and structural changes induced in the enzyme by such modifications may help to delineate the site further. Salt bridges have been identified as important for maintaining the conformation of the active enzyme. The introduction, or destruction, of salt bridges by site-directed mutagenesis may help to determine more precisely the contribution of these structures to the activity of the enzyme. Tryptophan residues could be introduced into parts of the protein and used as probes of the conformation of the enzyme under various conditions by monitoring the fluorescence emission of the mutated enzyme. Cysteine residues could be introduced and the effect of thiol modifying groups monitored by trypsin digestion or NEM-inhibition studies after exposing the enzyme to various ligand and effector molecules.

#### **8) PRODUCTION OF ANTI-PYRUVATE KINASE ANTISERA**

A high specificity, high affinity polyclonal antiserum against wild type yeast pyruvate kinase was produced. This would allow the identification of inactive forms of pyruvate kinase were they to be produced during further site-directed mutagenesis experiments. Analysis of the properties of the antisera against the mutant form of the enzyme produced during this work was hampered by the apparent instability of the antiserum preparations during storage.

#### **9) PHYLOGENETIC ANALYSIS**

An analysis of the 31 pyruvate kinase sequences was used to prepare a phylogenetic tree for the enzyme. This allows the identification of important branching points in the evolution of the enzyme and could be used to infer levels of similarity between the enzymes of organisms that have yet to be sequenced. It can also be used to identify unusual enzymes, such as the *E.coli* isoenzyme II which is apparently closely related to the plant plastidic enzymes. As a result, this seems to indicate that plant plastidic enzymes have evolved from a bacterial endosymbiotic invader rather than from a sequestered cytosolic enzyme.

## 6.0 REFERENCES

- Adair, G.S. (1925) *J. Biol. Chem.* 63, 529-545
- Ainsworth, S. & MacFarlane, N. (1973) *Biochem. J.* 131, 223-236
- Alberts, B., Bray, D., Lewis, J., Raff, M., Roberts, K. & Watson, J.D. (1983) "Molecular Biology of the Cell", Garland Publishing Inc, New York
- Allert, S., Ernest, I., Poliszczak, A., Oppendoes, F.R. & Michels, P.A. (1991) *Eur.J.Biochem.* 200, 19-27
- Arnone, M.I., Birolo, L., Giamberini, M., Cubellis, M.V., Nitti, G., Sannia, G. & Marino, G. (1992) *Eur. J. Biochem.* 204, 1183-1189
- Ashizawa, K., McPhie, P., Lin, K-H. & Cheng, S-Y. (1991a) *Biochem.* 30, 7105-7111
- Ashizawa, K., Willingham, M.C., Liang, C-M. & Cheng, S-Y. (1991b) *J.Biol.Chem.* 266, 16842-16846
- Atkinson, D.E. (1966) *Annu. Rev. Biochem.* 35, 85-124
- Aust, A., Yun, S.L. & Suelter, C.H. (1975) *Methods Enzymol.* 42, 176-182
- Barbalace, D.S., Chambliss, G.H. & Brady, R.J. (1971) *Biochem.Biophys.Res.Comm.* 42, 287-291
- Barrett, A.J., Kembhavi, A.A., Brown, M.A., Kirschke, H., Knight, C.G., Tamai, M. & Hanada, K. (1982) *Biochem. J.* 201, 189-198
- Beggs, J.D. Alfred Benzon Symp. 16, 383-389
- Bennet, W.S. & Steitz, T.A. (1980) *J. Mol. Biol.* 140, 211-230
- Bennetzen, J.L. & Hall, B.D. (1982) *J. Biol. Chem* 257, 3026-3031
- Benzimen, M. (1969) *Biochem. J.* 112, 631-636
- Berger, S.A. & Evans, P.R. (1990) *Nature* 343, 575-576
- Bezares, G., Eyzaguirre, J., Hinrichs, M.V., Heinrikson, R.L., Reardon, I., Kemp, R.G., Latshaw, S.P. & Bezaes, S. (1987) *Arch. Biochem. Biophys.* 253, 133-137
- Blakeley, S.D., Plaxton, W.C. & Dennis, D.T. (1990) *Plant. Mol. Biol.* 15, 665-669
- Blakeley, S.D., Plaxton, W.C. & Dennis, D.T. (1991) *Plant Physiol.* 96, 1283-1288
- Blattler, W. & Knowles, J.R. (1979) *Biochem.* 18, 3927-3933
- Bledig, S.A., Fotheringham, I.G. & Hunter, A.G. (1991) EMBL database,

accession number M63703

- Boiteux, A., Markus, M., Plessner, T., Hess, B. & Malcovati, M. (1983) *Biochem. J.* 211, 631-640
- Bornmann, L., Roschlau, P. & Hess, B. (1972) *Hoppe-Seyler's Z. Physiol. Chem.* 353, 696
- Boyer, P.D. (1954) *J. Am. Chem. Soc.* 76, 4331-4337
- Boyer, P.D., Lardy, H.A. & Phillips, P.H. (1942) *J. Biol. Chem.* 146, 673-682
- Boyer, P.D. (1962) "The Enzymes" 2nd Edition, 6, 95, Academic Press (New York)
- Bradford, M.M. (1976) *Anal. Biochem.* 72, 248-254
- Bucher, T. & Pfeleiderer, G. (1955) *Methods Enzymol.* 1, 435-440
- Burke, R.L., Tekamp-Olsen, P. & Najarian, R. (1983) *J. Biol. Chem.* 258, 2193-2201
- Cardenas, J.M., Hubbard, D.R. & Anderson, S. (1977) *Biochem.* 16, 191-197
- Chou, P.Y. & Fasman, G.D. (1978) *Adv. Enz.* 47, 45-147
- Chuang, D.T. & Utter, M.F. (1979) *J. Biol. Chem.* 254, 8434-8441
- Cigan, A. & Donahue, T.F. (1987) *Gene* 59, 1-18
- Clayden, D. (1987) PhD thesis, University of Bristol
- Consler, T.G. (1988) *J. Biol. Chem.* 263, 2794-2801
- Consler, T.G., Woodard, S.H. & Lee, J.C. (1989) *Biochem.* 28, 8756-8764
- Consler, T.G., Jennewein, M.J., Cai, G-Z. & Lee, J.C. (1992) *Biochem.* 31, 7870-7878
- Cooper, A. (1976) *Proc. Natl. Acad. Sci. USA* 73, 2740-2741
- Cooper, A. (1981) *Proc. Natl. Acad. Sci. USA* 78, 3551-3553
- Cooper, A. & Dryden, (1984) *Eur. Biophys. J.* 11, 103-109
- Cornish-Bowden, A. (1981) "Fundamentals of Enzyme Kinetics", Butterworth
- Cottam, G.L., Mildvan, A.S., Hunsley, J.R. & Suelter, C.H. (1972) *J. Biol. Chem.* 247, 3802-3809
- Creighton, D.J. & Rose, I.A. (1976) *J. Biol. Chem.* 240, 61-68
- Creighton, T.E. (1984) *Proteins: Structures and Molecular Properties*, New York, Freeman
- Dayhoff, M.O. (1978) *Atlas of protein sequence and structure*, Vol.5, Suppl. 3, National Biomedical Research Foundation, Silver Spring, MD, USA

- De Graaf, L.H. (1989) PhD thesis, University of Wageningen
- De Graaf, L.H. & Visser, J. (1988) *Curr. Genet.* 14, 553-560
- De La Morena, E., Santos, I. & Grisolia, S. (1968) *Biochem. Biophys. Acta* 151,
- Devereux, J., Haeberli, P. & Smithies, O. (1984) *Nucl. Acids Res.* 12, 387-395
- Dobson, M.J., Tuite, M.F., Roberts, N.A., Kingsman, A.J., Kingsman, S.M., Perkins, R.E., Conroy, S.C., Dunbar, B. & Fothergill, L.A. (1982) *Nucl. Acids Res.* 10, 2625-2637
- Dorit, R.L., Ohara, O. & Gilbert, W. (1989) *Proc. Natl. Acad. Sci. USA* 86, 6883-6887
- Dougherty, T.M. & Cleland, W.W. (1985) *Biochem.* 24, 5875
- Efron, B. (1982) "The jack-knife, the bootstrap and other resampling plans" The Society for Industrial and Applied Mathematics, Philadelphia
- Eigen, M. (1967) *Nobel Symp.* 5, 333
- Eisenberg, D., Sweet, R.M. & Terwillinger, T.C. (1984) *Proc. Natl. Acad. Sci USA*, 81, 140-144
- Engel, P. (1981) "Enzyme kinetics: The steady-state approach", 2nd Edition, Chapman Hall, London
- Engel, P.C. & Dalziel, K. (1969) *Biochem. J.* 115, 621-631
- Ernest, I., Callens, M., Opperdoes, F.R. & Michels, P.A.M. (1993) - in press
- Evans, P.R. (1992) "Proceedings of the Robert A. Welch Foundation Conference on Chemical Research", 26-27 October, XXXVI. Regulation of proteins by ligands, chapter III, 39-54
- Evans, H.J. & Sorger, G.J. (1966) *Ann. Rev. Plant Physiol.* 17, 47-52
- Faye, G., Leung, D.W., Tatchell, K., Hall, B.D. & Smith, M. (1981) *Proc. Natl. Acad. Sci. USA* 78, 2258-2262
- Fell, D.A., Liddle, P.F., Peacocke, A.R. & Dwek, R.A. (1974) *Biochem. J.* 139, 665-675
- Felsenstein, J. (1985) *Evolution* 39, 783-791
- Felsenstein, J. (1993) *PHYLIP manual*, version 3.5
- Ferdinand, W. (1966) *Biochem. J.* 98, 278-283
- Fersht, A. (1984) "Enzyme Structure and Mechanism", 2nd edition, W.H. Freeman & Co, New York



- Fitch, W.M. & Maroliash, E. (1967) *Science* 155, 279-284
- Flashner, M., Hollenberg, P.K. & Coon, M.J. (1972) *J. Biol. Chem.* 247, 8114-8121
- Ford, S.R. & Robinson, J.L. (1976) *Biochem. Biophys. Acta* 438, 119-130
- Foster, D.O., Lardy, H.A., Ray, P.D. & Johnston, J.B. (1967) *Biochem.* 6, 2120-2128
- Fothergill-Gilmore, L.A. (1986) *Multidomain Proteins: Structure and Evolution*, pp 85-174 (eds Hardie, D.G. & Coggins, J.R.) Elsevier Science Publications BV, Amsterdam
- Gilbert, D.G. (1993) *ReadSeq manual*
- Grinvald, A. & Steinberg, I.Z. (1974) *Biochem.* 13, 5170-5178
- Grosschedl, R. & Birnstiel, M.L. (1980) *Proc. Natl. Acad. Sci. USA* 77, 1432-1436
- Guppy, M. & Hochachka, P.W. (1979) *J. Comp. Physiol.* 129B, 185-191
- Gupta, R.J., Oesterling, R.M. & Mildvan, A.S. (1976) *Biochem.* 15, 2881-2887
- Haeckel, R., Hess, B., Lauterborn, W. & Wuster, K-H. (1968) *Hoppe-Seyler's Z. Physiol. Chem.* 349, 699-714
- Hammond, K.D. & Balinsky, D. (1978) *Cancer Res.* 38, 1323-1328
- Happold, F.C. & Beechey, R.B. (1958) *Biochem. Soc. Symp.* 15, 52-59
- Harper, J.W., Hemmi, K. & Powers, J.C. (1985) *Biochem.* 24, 1831-1841
- Harrison, W.H., Boyer, P.D. & Falcone, A.F. (1955) *J. Biol. Chem* 215, 303-308
- Hass, L.F. (1961) *J. Biol. Chem.* 236, 2284-2291
- Hassett, A., Blattler, W. & Knowles, J.R. (1982) *Biochem.* 21, 6335-6340
- Helmreich, E. & Cori, C.F. (1964) *Proc. Natl. Acad. Sci. USA* 52, 647-654
- Hermann, R., Jaenicke, R. & Rudolph, R. (1981) *Biochem.* 20, 5195-5201
- Hess, B., Haeckel, R. & Brand, K. (1966) *Biochem. Biophys. Res. Comm.* 24, 824-829
- Hess, B. & Haeckel, R. (1967) *Nature* 214, 848-851
- Heyduk, E., Heyduk, T. & Lee, J.C. (1992) *J. Biol. Chem.* 267, 3200-3204
- Higgins, D.G. & Sharp, P.M., (1988) *Gene* 73, 237-244
- Hill, A.V. (1910) *J. Physiol.* 40, 190-224
- Hill, R. *Proc. R. Soc.* (1925) B100, 419
- Hirai, M., Tanaka, A. & Fukui, S. (1975) *Biochim. Biophys. Acta* 391, 282-291



- Hollenberg, P.F., Flashner, M. & Coon, M.J. (1971) *J. Biol. Chem.* 246, 946-953
- Hunsley, J.R. & Suelter, C.H. (1969) *J. Biol. Chem.* 244, 4815-4822
- Imamura, K. & Tanaka, T. (1982) *Methods Enzymol.* 90, 150-165
- Imarai, M., Hinrichsen, P., Bazaes, S., Wilkens, M. & Eyzaguirre, J. (1988) *Int.J.Biochem.* 20, 1001-1008
- Inoue, H., Noguchi, T & Tanaka, T. (1986) *Eur. J. Biochem.* 154, 465-469
- Ito, H., Fukuda, Y., Murata, K. & Kimura, A. (1983) *J. Bact.* 153, 163-168
- Jacobsen, K.W. & Black, J.A. (1971) *J. Biol. Chem.* 246, 5504-5509
- Johnson, W.C. (1990) *Proteins: Structure, Function and Genetics* 7, 205-214
- Johnson, G.S. & Deal, W.C. (1970) *J. Biol. Chem.* 245, 238-245
- Johnson, G.S., Kayne, M.S. & Deal, W.C. (1969) *Biochem.* 8, 2455-2462
- Jones, E.W. (1991) *J. Biol. Chem.* 266, 7963-7966
- Kachmar, J.F. & Boyer, P.D. (1953) *J. Biol. Chem.* 200, 669-682
- Kanno, H., Fujii, H., Hirona, A. & Miwa, S. (1991) *Proc. Natl. Acad. Sci. USA* 88, 8218-8221
- Kapoor, M. (1976) *Int. J. Biochem.* 7, 439-443
- Kaslow, H.R. & Garrison, C.R. (1983) *Anal. Biochem.* 495-498
- Kato, H., Fukuda, T., Parkison, C., McPhie, P. & Cheng, S.Y. (1989) *Proc. Natl. Acad. Sci. USA* 86, 7861-7865
- Kauzmann, W. (1959) *Advan. Protein Chem.* 14, 1-63
- Kayne, F.J. (1973) "The Enzymes" 3rd Edition 8, 353-382
- Kayne, F.J. & Reuben, J. (1970) *J. Am. Chem. Soc.* 92, 220-222
- Kayne, F.J. & Suelter, C.H. (1968) *Biochem.* 7, 1678-1684
- Kimura, M. (1993) "The neutral theory of molecular evolution" Cambridge University Press, Cambridge
- Kinderlerer, J. (1986) *Biochem. J.* 234, 699-703
- Kiick, D.M. & Cleland, W.W. (1989) *Arch. Biochem. Biophys.* 270, 647-654
- Kingsman, S.M., Kingsman, A.J., Dobson, M.J., Mellor, J. & Roberts, N.A. (1985) *Biotech. & Genetic Engineering Rev.* 3, 377-416
- Klapper, M.H. (1977) *Biochim. Biophys. Res. Comm.* 78, 1018-1024
- Klump, H., Di Ruggiero, J., Kessel, M., Park, J-B., Adams, M.W.W. & Robb, F.T. (1992) *J. Biol. Chem.* 267, 22681-22685

- Koshland, D.E., Nemethy, G. & Filmer, D. (1966) *Biochem.* 5, 365-385
- Krebs, E.G. & Fischer, E.H. (1956) *Biochim. Biophys. Acta* 20, 150-157
- Kuczenski, R.T. & Suelter, C.H. (1970) *Biochem.* 9, 939-945
- Kuczenski, R.T. & Suelter, C.H. (1971) *Biochem.* 10, 2862-2866
- Kunkel, T.A. (1985) *Proc. Natl. Acad. Sci. USA* 84, 488-492
- Kuo, D.J. & Rose, I. (1978) *J. Am. Chem. Soc.* 100, 6288-6289
- Kwan, C.Y., Erhard, K. & Davis, R.C. (1975) *J. Biol. Chem.* 250, 5951-5959
- Kyte, J. & Doolittle, R.F. (1982) *J. Mol. Biol.* 157, 105-132
- Leblond, D.J. & Robinson, J.L. (1976) *Biochim. Biophys. Acta* 428, 108-118
- Lee, M.E. & Nowak, T. (1992) *Arch. Biochem. Biophys.* 293, 264-273
- Likos, J.J., Hess, B. & Colman, R.F. (1980) *J. Biol. Chem.* 255, 9388-9398
- Lin, M.L., Turpin, D.H. & Plaxton, W.C. (1989) *Arch. Biochem. Biophys.* 269, 228-238
- Llanos, R.M., Harris, C., Hillier, A.J. & Davidson, B.E. (1993) *J. Bact* 175, 2541-2551
- Lodato, D.T. & Reed, G.H. (1987) *Biochem.* 26, 2243-2250
- Lonberg, N. & Gilbert, W. (1983) *Proc. Natl. Acad. Sci USA* 80, 3661-3665
- Lone, Y-C., Simon, M-P., Kahn, A. & Marie, J. (1983) *FEBS Lett.* 195, 97-100
- Luche, R.M., Smart, W.C. & Cooper, T.G. (1992) *Proc. Natl. Acad. Sci. USA* 89, 7412-7416
- MacArthur, M.W. & Thornton, J.M. (1991) *J. Mol. Biol.* 218, 397-412
- MacFarlane, N. & Ainsworth, S. (1972) *Biochem. J.* 129, 1035-1047
- Maitra, P.K. & Lobo, Z. (1971) *J. Biol. Chem.* 475-488
- Malcovati, M. & Kornberg, H.L. (1969) *Biochim. Biophys. Acta* 178, 420-423
- Markus, M., Plessner, T., Boiteux, A., Hess, B. & Malcovati, M. (1980) *Biochem.J.* 189, 421-433
- Matsuoka, M., Ozeki, Y., Yamamoto, N., Hirano, H., Kanomurakami, Y. & Tanaka, Y. (1988) *J. Biol. Chem.* 263, 11080-11083
- McClelland, M., Hanish, J., Nelson, M. & Patel, Y. (1987) *Nucl. Acids. Res.* 16, 364
- McKnight, S.L. & Kingsbury, R. (1982) *Science* 217, 316-324
- McNally, T. (1989a) PhD thesis, University of Edinburgh

- McNally, T., Purvis, I.J., Fothergill-Gilmore, L.A. & Brown, A.J.P. (1989b) FEBS Lett. 247, 312-316
- Melamud, E. & Mildvan, A.S. (1975) J. Biol. Chem. 250, 8193-8201
- Mellor, J., Dobson, M.J., Roberts, N.A., Kingsman, A.J. & Kingsman, S.M. (1985) Gene 33, 215-226
- Milburn, P., Bonnerjea, J., Hoare, M. & Dunnill, P. (1990) Enzyme Microb. Technol. 12, 527-532
- Mildvan, A.S., Hunsley, J.R. & Suelter, C.H. (1974) "Probes of structure and function of macromolecules and membranes" (eds Chance, B., Yonetani, T. & Mildvan, A.S.) New York, NY, Academic Press, pp 131-146
- Mildvan, A.S. & Cohn, M. (1965) J. Biol. Chem. 240, 238-246
- Mildvan, A.S. & Cohn, M. (1966) J. Biol. Chem. 241, 1178-1193
- Mildvan, A.S., Sloan, D.L., Fung, C.H., Gupta, R.K. & Melamud, E. (1976) J. Biol. Chem. 251, 2431-2434
- Mishkind, M.L., Wessler, S. & Schmidt, G.W. (1985) J. Cell. Biol. 100, 226-234
- Monod, J., Wyman, J. & Changeux, J-P. (1965) J. Mol. Biol. 12, 88-118
- Monod, J., Changeux, J-P. & Jacob, F. (1963) J. Mol. Biol. 6, 306-329
- Morris, C.N., Ainsworth, S. & Kinderlerer, J. (1984) Biochem. J. 217, 641-647
- Morris, C.N., Ainsworth, S. & Kinderlerer, J. (1986) Biochem. J. 234, 691-698
- Muirhead, H. (1983) TIBS 8, 326-330
- Muirhead, H. (1987) "Biological macromolecules and assemblies", vol 3 pp 143-186, (Eds. Jurniak, F.A., & MacPherson, A.) Wiley, New York
- Muirhead, H., Clayden, D.A., Lorimer, C.G., Fothergill-Gilmore, L.A., Schiltz, E. & Schmitt, W. (1986) EMBO J. 5, 475-481
- Muirhead, H. (1990) Biochem. Soc. Trans. 18, 193-196
- Muirhead, H. (1991) EMBL/Genbank/DDJB Nucleotide Sequences Database, accession number X57859
- Murcott, T. (1990) PhD thesis, University of Bristol
- Murcott, T.M., McNally, T., Allen, S.C., Fothergill-Gilmore, L.A. & Muirhead, H. (1991) Eur. J. Biochem. 198, 513-519
- Murcott, T.M., Gutfreund, H. & Muirhead, H. (1992) EMBO J. 11, 3811-3814
- Neubauer, B., Lakomek, M., Winkler, H., Parke, M., Hofferbert, S. &

- Schroter, W. (1991) *Blood* 77, 1871-1875
- Nishizawa, M., Araki, R. & Teranishi, Y. (1989) *Mol. Cell. Biol.* 9, 442-451
- Noguchi, T., Inoue, H. & Tanaka, T. (1986) *J. Biol. Chem.* 261, 13807-13812
- Noguchi, T., Yamada, K., Inoue, H., Matsuda, T. & Tanaka, T. (1987) *J. Biol. Chem.* 262, 14366-14371
- Nowak, T. (1976) *J. Biol. Chem.* 251, 73-78
- Nowak, T. & Lee, J.C. (1977) *Biochem.* 16, 1343-1350
- Nowak, T. & Mildvan, A.S. (1970) *J. Biol. Chem.* 245, 6057-6062
- Nowak, T. & Mildvan, A.S. (1972) *Biochem.* 11, 2819-2828
- O'Brien, M.D. & Kapoor, M. (1975) *FEBS Lett.* 58, 336-369
- O'Leary, M.H., DeGooyer, W.J., Dougherty, T.M. & Anderson, V. (1981) *Biochem. Biophys. Res. Comm.* 100, 1320-1325
- Ohara, O., Dorit, R.L. & Gilbert, W. (1989) *Proc. Natl. Acad. Sci. USA* 86, 6883-6887
- Opperdoes, F.R. (1987) *Ann. Rev. Microbiol.* 41, 127-151
- Ozaki, H. & Shio, I. (1969) *J. Biochem. (Tokyo)* 66, 297-311
- Passerson, S. & Roselino, E. (1971) *FEBS Lett* 18, 9-12
- Pauling, L. (1935) *Proc. Natl. Acad. Sci. USA* 21, 186
- Perutz, M.F. (1960) *Nature* 228, 738-742
- Plaxton, W.C. (1989) *Eur. J. Biochem.* 181, 443-451
- Plaxton, W.C., Dennis, D.T. & Knowles, V. (1990) *Plant Physiol.* 94, 1528-1538
- Plowman, K. & Krall, A.R. (1965) *Biochem. J.* 4, 2809
- Pon, N.G. & Bondar, R.J.L. (1967) *Anal. Biochem.* 19, 272-279
- Ponte-Sucre, A., Alonso, G., Martinez, C., Hung, A., Rivas, L. & Ramirez, J.L. (1993) *Arch. Biochem. Biophys.* 300, 466-471
- Potter, S. (1993) PhD thesis, University of Edinburgh
- Pridmore, R.D. *Gene* (1987) 56, 309-312
- Proudfoot, N.J. & Brownlee, G.G. (1976) *Nature* 263, 211-214
- Provencher, S.W. & Glockner, J. (1981) *Biochem.* 20, 33-37
- Purvis, I.J., Loughlin, L., Bettany, A.J.E. & Brown, A.J.P. (1987) *Nucl. Acids Res.* 15, 7963-7973
- Rabin, B.R. (1967) *Biochem. J.* 102, 22c

- Raushel, F.M. & Villafrancha, J.J. (1980) *Biochem.* 19, 5481-5485
- Reed, & Cohn, (1972) *J. Biol. Chem.* 248, 6436-6442
- Reubens, J. & Kayne, F. (1971) *J. Biol. Chem.* 246, 6227-6231
- Reynard, A.M., Hass, L.F., Jacobsen, D.D. & Boyer, P.D. (1961) *J. Biol. Chem.* 236, 2277-2283
- Rhodes, N., Morris, C.N., Ainsworth, S. & Kinderlerer, J. (1986) *Biochem. J.* 234, 705-715
- Robinson, J.L. & Rose, I.A. (1972) *J. Biol. Chem.* 247, 1096-1105
- Ronai, Z. (1993) *Int. J. Biochem.* 25, 1073-1076
- Roschlau, P., & Hess, B. (1972) *Hoppe-Seyler's Z.Physiol.Chem.* 353, 944-948
- Rose, I. (1960) *J. Biol. Chem.* 235, 1170-1177
- Rose, I.A. (1970) *J. Biol. Chem.* 245, 6052-6056
- Rose, I. & Kuo, D.J. (1989) *Biochem.* 28, 9579-9585
- Rose, I., Kuo, D.J. & Warms, J.V.B. (1991) *Biochem.* 30, 722-726
- Sambrook, J., Fritsch, E.F. & Maniatis, T. (1989) "Molecular Cloning: A Laboratory Manual", Cold Spring Harbor Laboratory, Cold Spring Harbor, New York
- Sanger, F., Nicklen, S. & Coulson, A.R. (1977) *Proc. Natl. Acad. Sci. USA* 74, 5463-5467
- Sawyer, L., Fothergill-Gilmore, L.A. & Freemont, P.S. (1988) *Biochem. J.* 249, 789-793
- Scheiner-Bobis, G., Mertens, W., Willeke, M. & Schoner, W. (1992) *Biochem.* 31, 2107-2113
- Schindler, M., Mach, R.L., Vollenhofer, S., Hodits, R., Gruber, F., Visser, J., De Graaff, L. & Kubicek, C.P. (1993) GenEnbl/DDBJ data bank, accession number P31865
- Scopes, R.K. (1987) "Protein Purification, Principles and Practice" 2nd Ed., Springer-Verlag New York Inc.
- Scrutton, N.S., Deonarain, M.P., Berry, A. & Perham, R.N. (1992) *Science* 258, 1140-1143
- Searcy, D.G. (1992) "The Origin and Evolution of the Cell", Proceedings of the Conference on the Origin and Evolution of the Prokaryote and Eukaryote Cells

- (Hartman, H. & Matsuno, K. eds), World Scientific, Singapore, pp47-78
- Seeholzer, S.H., Jaworowski, A., & Rose, I. (1991) *Biochem.* 30, 727-732
- Setondji, J., Remy, P., Ebel, J.P. & Dirheimer, G. (1971) *Biochim. Biophys. Acta* 232, 585-594
- Sloan, D.L. & Mildvan, A.S. (1976) *J. Biol. Chem.* 251, 2412-2420
- Somero, G.N. & Hochachka, P.W. (1968) *Biochem. J.* 110, 395-399
- Sorger, G.J., Ford, R.E. & Evans, H.J. (1965) *Proc. Natl. Acad. Sci. USA* 54, 1614-1621
- Speranza, M.L., Valentini, G., Iadarola, P., Stoppini, M., Malcovati, M. & Ferri, G., (1989) *Biol. Chem. Hoppe-Seyler* 370, 211-216
- Speranza, M.L., Valentini, G. & Malcovati, M. (1990) *Eur. J. Biochem.* 191, 701-704
- Sprague, G.F. (1976) *J. Bact.* 130, 232-241
- Sprang, S. & Fletterick, R.J. (1979) *J. Mol. Biol.* 131, 523-551
- Stammers, D.K. & Muirhead, H. (1975) *J. Mol. Biol.* 85, 213-225
- Steinmetz, M.A. & Deal, W.C. (1966) *Biochem.* 5, 1399-1404
- Strick, C.A., James, L.C., O'Donnell, M.M., Gollaher, M.G. & Franke, A.E. (1992) *Gene* 118, 65-72
- Stuart, D.I., Levine, M., Muirhead, H. & Stammers, D.K. (1979) *J. Mol. Biol.* 134, 109-142
- Suelter, C.H. (1967) *Biochem.* 6, 418-423
- Suelter, C.H. (1970) *Science* 168, 789-797
- Suelter, C.H. & Melander, W. (1963) *J. Biol. Chem.* 238, PC4108
- Suelter, C.H., Singleton, R., Kayne, F.J., Arrington, S., Glass, J. & Mildvan, A.S. (1966) *Biochem.* 5, 131-139
- Sweeny, J.R. & Fisher, J.R. (1968) *Biochem.* 7, 665-675
- Takenaka, M., Noguchi, T., Inoue, H., Yamada, K., Matsuda, T. & Tanaka, T. (1989) *J. Biol. Chem.* 264, 2362-2367
- Tanaka, T., Sue, F. & Morimura, H. (1967) *Biochem. Biophys. Res. Comm.* 29, 444-449
- Tani, K., Yoshida, M.C., Satoh, H., Mitamura, K., Noguchi, T., Tanaka, T., Fujii, H. & Miwa, S. (1988a) *Gene* 73, 509-516

- Tani, K., Fujii, H., Nagata, S. & Miwa, S. (1988b) *Proc. Natl. Acad. Sci. USA* 85, 1792-1795
- Tietz, A. & Ochoa, S. (1958) *Arch. Biochem. Biophys.* 78, 477-493
- Tipton, P.A., McCracken, J., Cornelius, J.B. & Peisach, J. (1989) *Biochem.* 28, 5720-5728
- Titani, K., Cohen, P., Walsh, K.A. & Neurath, H. (1975) *FEBS Lett.* 55, 120-123
- Valentini, G., Stoppini, M., Speranza, M.L., Malcovati, M. & Ferri, G. (1991) *Biol. Chem. Hoppe-Seyler* 372, 91-93
- Vernet, T., Dignard, D. & Thomas, D.Y. (1987) *Gene* 52, 225-233
- Vollmer, S.H. & Colman, R.F. (1990) *Biochem.* 29, 2495-2501
- Wakita, M. & Hoshino, S. (1989) *Int. J. Biochem.* 21, 777-781
- Walker, D. (1987) PhD thesis, University of Bristol
- Walker, D., Chia, W.N. & Muirhead, H. (1992) *J. Mol. Biol.* 228, 265-276
- Walsh, J.L. & Knoll, H.R. (1988) *Biochim. Biophys. Acta* 952, 83-91
- Walsh, J.L., Keith, T.J. & Knoll, H.R. (1989) *Biochim. Biophys. Acta* 999, 64-70
- White, M.F., Fothergill-Gilmore, L.A., Kelly, S.M. & Price, N.C. (1993) *Biochem. J.* 295, 763-767
- Wieker, H-J. & Hess, B. (1972) *Hoppe-Seyler's Z. Physiol. Chem.* 353, 1877-1893
- Wildes, R.A., Evans, H.J. & Becker, R.R. (1971) *Biochim. Biophys. Acta* 229, 850-854
- Wittenberger, C.L; Palumbo, M. & Klein, I. (1973) *The 9th International Congress of Biochemistry, Stockholm, Abstract 2e*, 15, 62
- Woese, C. (1987) *Microbiol. Rev.* 51, 221-271
- Yun, S.L., Aust, A. & Suelter, C.H. (1976) *J. Biol. Chem.* 251, 124-128
- Zamora, J.M., Rosa, R., Rosa, C.D., Bianconcini, M.S.C. & Bacila, M. (1992) *Int.J.Biochem.* 24, 1833-1840
- Zaret, K.S. & Sherman, F. (1982) *Cell* 28, 563-573



# ALLOSTERIC PROPERTIES OF YEAST PYRUVATE KINASE STUDIED BY SITE-DIRECTED MUTAGENESIS

CHARL A. COLLINS, TERESA McNALLY\* and  
DAVID A. FOTHERGILL-GILMORE

Department of Biochemistry, University of Edinburgh, George  
Square, EDINBURGH EH8 9XD, UK  
Department of Genetics, University of Leeds, LEEDS LS2 9JT, UK

Pyruvate kinase (EC 2.7.1.40) is of particular importance in  
glycolysis for controlling the flux from fructose-1,6-bisphosphate  
through to pyruvate. It catalyses the essentially irreversible  
conversion of phosphoenolpyruvate to pyruvate by the addition of a  
phosphate and the loss of a phospho group which is transferred to ADP.

$\text{phosphoenolpyruvate} + \text{MgADP} + \text{H}^+ = \text{pyruvate} + \text{MgATP}$

The enzyme from most sources is a tetramer of identical subunits  
with about 500 residues in length. The enzyme has an absolute  
requirement for monovalent and divalent cations (usually  $\text{K}^+$  and  
 $\text{Mg}^{2+}$ ) which act to coordinate and orientate the substrates prior to  
catalysis. A number of isoenzymes of pyruvate kinase are found to  
exist in vertebrate tissues. Their kinetic and regulatory properties  
reflect the metabolic requirements of the tissues in which they are  
expressed. The L, M2 and R isoenzymes from liver, kidney and red  
blood cells respectively are all allosterically regulated by a number  
of effectors such as fructose-1,6-bisphosphate, ATP and  
concentrations of amino acids. These isoenzymes display a sigmoidal  
relationship of reaction rate with respect to substrate PEP. This  
control is essential to prevent futile cycling of substrates in tissues  
that can undergo glycolysis and gluconeogenesis. The M1 isoenzyme  
in skeletal muscle is not allosterically regulated and displays  
hyperbolic Michaelis-Menten type kinetics. The yeast *S. cerevisiae*  
has a single allosterically regulated form of the enzyme and has been  
sequenced in this lab (1). Intersubunit contact zones are thought to  
be important in mediating the allosteric transition. Two major types  
of intersubunit contact are present in pyruvate kinase. Interactions  
between subunits 1 and 2 and between subunits 3 and 4 do not  
contribute significantly to the enzyme's response to allosteric  
effectors. However, the interactions between subunits 1 and 3 and  
between subunits 2 and 4 are considered to be largely responsible  
for the enzyme's altered kinetic properties upon effector binding.  
The tetrameric enzyme could almost be considered to be a dimer of  
dimers (see Fig.1). The cat skeletal muscle enzyme has also been  
sequenced and crystallised, allowing its 3-dimensional structure to  
be resolved to 2.6Å (2). The main difference between the  
allosterically regulated cat muscle enzyme and the yeast enzyme have been  
attributed to two alpha helices ( $\text{Ca1}$  and  $\text{Ca2}$ ) that form the 1,3 (and  
2,4) intersubunit contacts. Work is under way on two aspects of the  
yeast pyruvate kinase activity. Examination of the crystal structure  
has led to the identification of lysine 239 as the ultimate proton  
donor during catalysis. The effect of altering the position of the  
positive charge on catalysis is being measured by mutating the  
lysine to both an arginine and a histidine by site-directed  
mutagenesis. Other mutations have been introduced into one of the  
alpha helices responsible for maintaining the intersubunit contacts  
described above. Serine 384 in subunits 1 and 2 lie directly  
opposite serine 384 in subunits 3 and 4 making this residue a  
favourable target for mutagenesis. Their proximity to one another can  
be exploited to maximise any alteration in kinetic properties. These  
serine residues have been mutated to the charged residues arginine  
and histidine and to the helix-destabilising residue proline. These  
mutations are expected to alter significantly the catalytic activity  
(Ser 239) and the response to allosteric effectors (Ser 384) of the  
enzyme. These effects can be detected and measured by standard  
biochemical techniques. Of particular importance are any conformational  
changes induced on binding the various effectors. These changes can  
be detected by methods such as tryptophan fluorescence, CD  
spectroscopy and equilibrium dialysis. The effect of these mutations

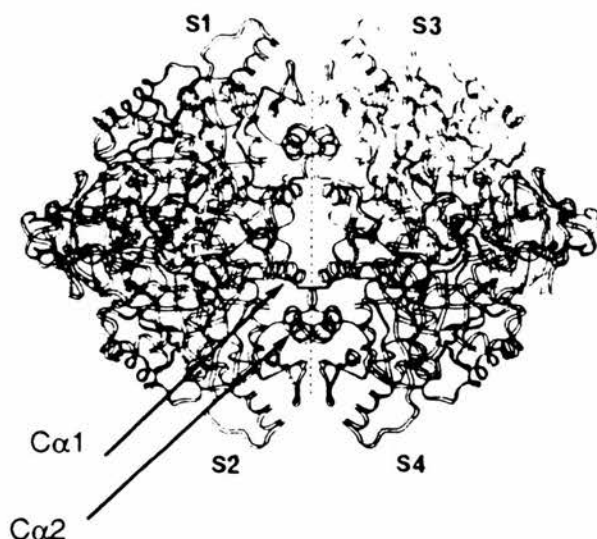


Fig. 1 A TETRAMER OF PYRUVATE KINASE

Individual subunits are labelled (S1-S4).  
The broken line shows the 1,3 (2,4) inter-  
subunit interface.  
The alpha helices  $\text{Ca1}$  and  $\text{Ca2}$  are indicated.

may be to inactivate completely or even to cause the dimerisation of  
the enzyme. If this is the case, purification of the mutants will be  
more difficult as enzymic activity can not be used to monitor the  
progress of the purification. A high affinity polyclonal antiserum  
against wild-type pyruvate kinase has been raised and purified from  
rabbits. This could prove very useful in aiding the identification and  
purification of mutant forms of the enzyme. An improved  
purification protocol has been devised that enables rapid  
purification of large amounts of protein for study.

An expression and mutagenesis system based on the pVT-L  
phagemid (3) is being developed to enhance the production and  
purification of mutant protein.

## REFERENCES

- 1) McNally, T., Purvis, I.J., Fothergill-Gilmore, L.A.  
& Brown, A.J.P. (1989) FEBS Lett. **247**, 312-316
- 2) Muirhead, H., Clayden, D.A., Barford, D., Lorimer, C.G.,  
Fothergill-Gilmore, L.A., Schitz, E. & Schmitt, W. (1986)  
EMBO J **5**, 475-481
- 3) Vernet, T., Dignard, D. & Thomas, D.Y. (1987) Gene **52**,  
225-233